Universitat Autònoma de Barcelona

Molecular characterization of the Ppz1 phosphatase and its regulatory subunit Hal3

CRISTINA MOLERO MERINERO

ADVERTIMENT. L'accés als continguts d'aquesta tesi queda condicionat a l'acceptació de les condicions d'ús establertes per la següent llicència Creative Commons: http://cat.creativecommons.org/?page_id=184

ADVERTENCIA. El acceso a los contenidos de esta tesis queda condicionado a la aceptación de las condiciones de uso establecidas por la siguiente licencia Creative Commons: http://es.creativecommons.org/blog/licencias/

WARNING. The access to the contents of this doctoral thesis it is limited to the acceptance of the use conditions set by the following Creative Commons license: https://creativecommons.org/licenses/?lang=en

Molecular characterization of the Ppz1 phosphatase and its regulatory subunit Hal3

Doctoral thesis presented by

CRISTINA MOLERO MERINERO

for the degree of PhD in Biochemistry, Molecular Biology and Biomedicine from the Universitat Autònoma de Barcelona.

Thesis performed at the Departament de Bioquímica i Biologia Molecular of the Universitat Autònoma de Barcelona and at the Institut de Biotecnologia i de Biomedicina.

Thesis supervised by Dr. Joaquín Ariño Carmona

Cristina Molero Merinero Dr. Joaquín Ariño Carmona

Cerdanyola del Vallès, June 2017

Look deep into nature, and then
you will understand everything better.
Albert Einstein

Llega el final de una gran etapa, ese momento que se veía tan lejos pero ya es hora de acabar el doctorado, al que logré sobrevivir (literalmente). Una etapa por la que he luchado, en la que más cosas he vivido y más me ha enseñado tanto de ciencia como de la vida... Desde que llegué a Barcelona para el máster, todos estos años han estado cargados de aventuras, rodeada de personas que me han apoyado a lo largo de todo este tiempo y ahora es el momento de agradecérselo.

En primer lugar, agradecer al Dr. Joaquín Ariño, por haberme aceptado, incluso siendo madrileña, en su laboratorio. Por toda la confianza que ha ido depositando en mí, y por todas las cosas que me ha enseñado. Además de la paciencia con la de veces que le puse de los nervios.

A mis padres, que gracias a ellos todo esto ha sido posible, que siempre confiaron en mí e intentaron darme lo mejor. Por su apoyo moral, afectivo y económico, sobre todo en las malas épocas para que todo fuese más fácil y consiguiese mis objetivos. Y tampoco me olvido de mi hermano, Álvaro, que él puede ser otro tipo de apoyo, pero también clave (Ahora ya tengo tiempo para ir de conciertos). A Wifly, que le ha tocado vivir entre tantos papers y siempre estuvo a mi lado durante días de escritura.

A mis chicos "Undiano", David: Guerra y Guima, Minchul y el once (Jose) porque han estado ahí día a día. Desde los comienzos con momentos en aquel piso de Muntaner, noches de Razz, muchos partidos de fútbol, viajes a Berlín... Y que ahora, a pesar de la distancia, consiguen ser un gran apoyo cada día.

Quiero destacar mi agradecimiento a toda la gente que ha formado parte del laboratorio del grupo de "Llevats", con los que más tiempo y horas he pasado durante este trabajo. Desde los comienzos, a Asier, por enseñarme a manejarme en este laboratorio y comenzar a conocer Hal3. A Carlos, por su buen gusto musical pero maldito legado del screen que me dejaste. A Silvia, por todos los trucos que me enseñó con las tétradas y DNA, así como temas de madurez. A Antonio, por todo lo que le molestamos preguntando, pero a pesar de ello siempre nos expone su conocimiento en todo detalle y por sus estrategias en los caterings. A la mami Montse, por todo lo que me ha aguantado, escuchado y ayudado no solo científicamente, si

no en lo personal, y la de litros de LB que me habrá preparado!!! Con los que más tiempo he pasado y he compartido momentos importantes en lab (y alguno fuera), Fondues, videos... A Jofre, por darle esa chispa menos inocente a los días. A David y Anna Bahí por enseñarme cosas de la Catalunya profunda. A Laura, por esa compañía cercana y que siempre me hacía plantearme las cosas con otros puntos de vista. A Albert por su serenidad y que siempre le veía haciendo famosos β-gal (al final me voy sin haber hecho ninguno). A los que han ido llegando más recientemente, que siempre que regresaba de Manchester había nuevas incorporaciones. A María, por ser la postdoc más molona en el grupo, y a ver si nos pasa el protocolo ese de la eternidad. A Ana Chun-Yi, que le deseo una buena etapa final y menos nervios para que pueda avanzar. A Diego, Santo, esos maños que escandalizan allá por donde van y se hacen destacar por el IBB. A Carlos por sus chapas. Y Marcel, quien espero que haya aprendido algo con las proteínas.

Gracias al Servei de Seqüenciació, que han ayudado gran parte en todo este trabajo. Por el estrés que les daba con las secuencias, y por la de horas que tuvieron que soportar el ruido del Bioruptor. En especial al Ministro (Roger) por sus visitas diarias para amenizar y capturar pokemon, que será un padrazo sin duda. Y a Guillem, por su buen rollo pasota y divertido que en días duros puso alguna sonrisa. A Lourdes por su ayuda con el papeleo y los esfuerzos en sofisticados envíos. A la gente de Veterinaria, sobre todo a Anna Vilalta por esa gran ayuda en prácticas.

Thanks to my labmates in Manchester!! Where I finally was feeling like at home... Good memories at Red Chilli, purification nights, rainy, snowy days... Since I arrived the first time, thanks to Deepankar for my beginnings with the AKTA and Graham, who was present throughout all my stays. Later, see how the group was growing... I remember when James and Eyong started their phD, also Simon as a postdoc, that added a fun part to the lab. And finally, girls in the group, Paulina and Petronela, with whom I spent the best time. Specially, to Efrain, with whom I shared the most time working and who taught me many things about purification and how to treat proteins, in addition to long personal conversations. And thanks so much to Dra. Lydia Tabernero, quien además de jefa, facilitó cada estancia que realicé en Manchester. Por toda su dedicación en este proyecto.

A mis amigos de Barcelona, que han hecho todo este tiempo sentirnos acogidos y ser como una familia. Incluyendo tantas historias durante los fines de semana, viajes, cumpleaños, conciertos, playa, cenas…

En especial Alba y Sofi, esos dos solecitos que hacen que Barcelona siempre brille. Esa buena vibra de la mexicana más especial de mi vida, y la paciencia más grande de esa bióloga gallega. Porque juntas hemos pasado tantos momentos, buenos, divertidos y malos, en los cuales siempre fuisteis mi apoyo para lograr estar donde estoy ahora. Proud of you girls!

A Phil, por muchos años de amistad, tantas veces que me ha ayudado y ha estado ahí para que siempre lograse seguir adelante. A Angy, porque a pesar de sus momentos juerguista es una de las personas más razonables y sensatas. A Maria, Michele, Alessandro, Marco, Nadia, Eliee… Y todo el grupo multicultural que formamos, porque llevais años oyéndome hablar de mis experimentos y a pesar de eso gracias a vuestra compañía ha sido más fácil pasar este tiempo. Porque sois clave para desconectar y pasar buenos momentos.

A mis compis de máster, donde comenzó este trayecto científico para conseguir un doctorado. Destacando a Manu, un gran científico y sufridor a la par durante todo este tiempo (ánimo que ya sólo te queda lo mejor… Escribir!), gracias por aguantarme con mis estreses y mis historietas (de campanilla). A Gerard, el niño del máster con el que hemos compartido más tiempo, además de algún secreto de genéticos.

A mi tierna Lau, aunque esté en Madrid hace posible que cada vez que nos vemos es como si no hubiera distancia.

A Seb, por aguantar mis idas y venidas de Manchester, aunque no las pudiese superar… Pero ahí estuvo gran parte de tiempo conviviendo con mis experimentos, en congresos, revisando escritos, y aguantando mis fines de semana de trabajo.

Puede que me olvide de gente, pero conociéndome, ya podéis imaginar que estoy escribiendo esto en el último momento… Por tanto, a todas las personas que de alguna manera han estado presentes durante este trabajo, muchísimas gracias.

TABLE OF CONTENTS

ABBREVIATIONS

Å	**Å**ngström
AMP	**A**denosine **m**ono**p**hosphate
AMPK	**AMP**-activated protein **k**inase
ATP	**A**denosine **t**ri**p**hosphate
BSA	**B**ovine **s**erum **a**lbumin
cAMP	**C**yclic **AMP**
CDK	**C**yclin-**d**ependent **k**inase
CoA	**Co**enzyme **A**
C-terminal	**C**arboxyl **terminal**
CWI	**C**ell **w**all **i**ntegrity
DNA	**D**eoxyribo**n**ucleic **a**cid
DTT	**D**i**th**thio**t**reitol
E. coli	*Escherichia Coli*
EDTA	**E**thylene**d**iamine**t**etraacetic **a**cid
g	**G**rams
GST	**G**lutathione **S**-**t**ransferase
GTP	**G**uanosine **t**ri**p**hosphate
H	**H**ours

HA	**H**em**a**gglutinin
IgG	**I**mmuno**g**lobulin **G**
IPTG	**I**so**p**ropyl-β-**t**hio**g**alactopyranoside
kbp	**k**ilo **b**ase **p**air
kDa	**K**ilo **da**ltons
LB	**L**ysogeny **b**roth/ Luria Bertani
M	**M**olar concentration
mM	**m**illi**m**olar concentration
MAP	**M**itogen-**a**ctivated **p**rotein
MAPK	**M**itogen-**a**ctivated **p**rotein **k**inase
Mbp	**M**ega **b**ase **p**airs
mg	**m**illi**g**ram
Min	**Min**ute
mm	**m**illi**m**etre
mRNA	**M**essenger **RNA**
ng	**n**ano**g**ram
nm	**n**ano**m**eter
Nt	**N**ucleo**t**ide

N-terminal	Amino **terminal**
OD	**O**ptical **d**ensity
ORF	**O**pen **R**eading **f**rame
PAGE	**P**oly**a**crylamide **g**el **e**lectrophoresis
PCR	**P**olymerase **c**hain **r**eaction
PEG	**P**oly**e**thylene **g**licol
P_i	**I**norganic **p**hosphate
pI	**I**soelectric **p**oint
PKA	**P**rotein **k**inase **A**
PMSF	**P**henyl**m**ethane**s**ulfonyl**f**luoride
PNPP	**P**-**N**itro**p**henyl **p**hosphate
PVDF	**P**oly**v**inili**d**ene **f**luoride
RNA	**R**ibo**n**ucleic **a**cid
rpm	**r**evolutions **p**er **m**inute
rRNA	**R**ibosomal **RNA**
S. cerevisae	*Saccharomyces cerevisiae*
S. pombe	*Schizosaccharomyces pombe*
SDS	**S**odium **d**odecyl **s**ulfate
SDS-PAGE	**SDS**-**P**olyacryl**a**mide **g**el **e**lectrophoresis

Sec	**Sec**ond
SEC	**S**ize **e**xclusion **c**hromatography
SEM	**S**tandard **E**rror of the **M**ean
TMA	**T**etramethylammonium
TBS	**T**ris-**b**uffered **s**aline
Tris	2-Amino-2-hydroxymethyl-propane-1,3-diol
Triton X-100	t-octylphenoxylpolyethoxy ethanol
tRNA	**T**ransfer **RNA**
WT	**W**ild **T**ype
µg	**m**icro**g**ram
µM	**m**icro**m**olar concentration
YNB	**Y**east **n**itrogen **b**ase
YPD	**Y**east extract **p**eptone **d**extrose

SUMMARIES

The *S. cerevisiae* Ser/Thr protein phosphatase Ppz1 is an important component in the maintenance of monovalent cation (K^+ and Na^+) homeostasis and, as such, impinges in multiple cellular processes, such as cell cycle progression, cell integrity maintenance. Cation homeostasis is a key factor for the survival of any single cell, particularly for microorganisms that, like yeasts, must confront environmental changes. Although Ppz1 is an enzyme related to the ubiquitous type-1 phosphatase (PP1c), Ppz-like enzymes are only found in fungi, including pathogenic ones. Two regulatory subunits of *S. cerevisiae* Ppz1 have been identified, Hal3 and Vhs3, which bind to the catalytic C-terminal half of Ppz1 and strongly inhibit its phosphatase activity. Modulation of PP1c by its many regulatory subunits has been extensively characterized, interestingly, Hal3 does not appear structurally similar to known PP1c inhibitors, with the exception of the presence of an RVxF related sequence, which is found in most PP1c regulators. This motif interacts with a hydrophobic groove of the phosphatase, whose structure is also conserved in Ppz1. However, Hal3 does not bind or inhibit *in vitro* yeast PP1c and this motif seems to not be relevant for its interaction with Ppz1. Therefore, Hal3 seems to be rather specific towards Ppz1, suggesting that the mechanism of Ppz1 regulation by Hal3 might differ from those found for PP1c regulatory subunits.

A major goal of this work was to gain insight into the specific regulatory mechanisms of Ppz1 by Hal3. To this end, two experimental approaches were undertaken. Firstly, a genetic screen was devised to identify Ppz1 mutations that would release Ppz1 from Hal3 regulation. A library of Ppz1 versions carrying random mutation in its C-terminal catalytic domain was generated and a functional screen in the *slt2* background carried out. This screen yielded 36 variants, of which 9 carried single and 4 double amino

acid changes. *In vivo* and *in vitro* characterization of these variants demonstrated that all of them affected the inhibitory capacity to be inhibited by, but not to interact with Hal3. Mapping the mutated residues in a Ppz1 model localized these residues in one of the region equivalent to that recognized on PP1c by Inhibitor-2. Secondly, we developed successful strategies to co-express in *E. coli* and to purify the protein complex formed by Ppz1 (C-terminal half) and Hal3. These preparations allowed the generation of diverse crystals. However, despite the many efforts to improve the obtained crystals, they were not of enough quality to obtain a high resolution data sets as to resolve the three-dimensional structure of the complex.

It was demonstrated years ago that Hal3 is a moonlighting protein, because in addition to its role in Ppz1 regulation, Hal3 contributes (together with Cab3 and Vhs3) to the generation of an atypical heterotrimeric PPCDC enzyme This essential and conserved enzyme exists as a homotrimeric flavoprotein in most eukaryotic species, and requires in the active site the presence of specific His and Cys residues, as well as a conserved Asn. The search of fungal genomes for the presence of putative PPCDC enzymes revealed that *Schizosaccharomyces pombe* contains a unique ORF (SPAC15E1.04, named here SpHal3)) that could encode a Hal3 homolog. We demonstrate that this gene has an unusual structure, being the result of a gene fusion event, containing a Hal3-like segment necessary for PPCDC activity (similar to ScHal3) in the N-terminal region and the sequence that encodes the thymidylate synthase enzyme in the C-terminus. Our results showed that SPAC15E1.04 is expressed as a single polypeptide and that the SpHal3 N-terminal half is sufficient to decide PPCDC activity, were the C-terminal half is able to provide TS function in *S. cerevisiae*. Our results confirmed the multifunctional nature of this fusion gene and demonstrated that it is an essential gene.

La proteína Ser / Thr fosfatasa Ppz1 de *S. cerevisiae* es un componente importante en el mantenimiento de la homeostasis de cationes monovalentes (K^+ y Na^+) y, como tal, incide en múltiples procesos celulares, tales como la progresión del ciclo celular y el mantenimiento de la integridad celular. La homeostasis de cationes es un factor clave para la supervivencia de cualquier célula, particularmente para los microorganismos que, como las levaduras, deben hacer frente a los cambios ambientales. Aunque Ppz1 es un enzima relacionado con la ubicua fosfatasa tipo 1 (PP1c), las enzimas tipo Ppz sólo se encuentran en hongos, incluyendo patógenos. Se han identificado dos subunidades reguladoras de *S. cerevisiae* Ppz1, Hal3 y Vhs3, que se unen a la mitad C-terminal catalítica de Ppz1 e inhiben fuertemente su actividad fosfatasa. La modulación de PP1c por sus muchas subunidades reguladoras ha sido ampliamente caracterizada, interesantemente, Hal3 no parece estructuralmente similar a los inhibidores de PP1c conocidos, con la excepción de la presencia de una secuencia relacionada con RVxF, que se encuentra en la mayoría de los reguladores de PP1c. Este motivo interactúa con un surco hidrofóbico de la fosfatasa, cuya estructura también se conserva en Ppz1. Sin embargo, Hal3 no se une o inhibe *in vitro* la PP1c de levadura y este motivo parece no ser relevante para su interacción con Ppz1. Por lo tanto, Hal3 parece ser bastante específico hacia Ppz1, lo que sugiere que el mecanismo de regulación de Ppz1 por Hal3 podría diferir de los encontrados para PP1c subunidades reguladoras.

Un objetivo principal de este trabajo fue obtener una visión de los mecanismos específicos de regulación de Ppz1 por Hal3. Con este fin, dos enfoques experimentales se llevaron a cabo. En primer lugar, se diseñó un cribado genético para identificar las mutaciones de Ppz1 que liberarían Ppz1 de la regulación de Hal3. Se generó una biblioteca

de las versiones de Ppz1 que portaban mutación aleatoria en su dominio catalítico C-terminal y se llevó a cabo un cribado funcional en el fondo *slt2*. Este cribado produjo 36 variantes, de las cuales 9 llevaron simple y 4 doble cambios de aminoácidos. La caracterización *in vivo* e *in vitro* de estas variantes demostró que todas ellas afectaron la capacidad inhibitoria de ser inhibida por, pero no para interactuar con Hal3. La asignación de los residuos mutados en un modelo de Ppz1 localizó estos residuos en una región equivalente a la reconocida en PP1c por el Inhibitor-2. Segundamente, desarrollamos estrategias exitosas para coexpresar en *E. coli* y purificar el complejo de proteínas formado por Ppz1 (mitad C-terminal) y Hal3. Estas preparaciones permitieron la generación de diversos cristales. Sin embargo, a pesar de los muchos esfuerzos para mejorar los cristales obtenidos, no fueron de suficiente calidad para obtener conjuntos de datos de alta resolución como para resolver la estructura tridimensional del complejo.

Hace años se demostró que Hal3 es una proteína multifuncional, porque además de su papel en la regulación de Ppz1, Hal3 contribuye (junto con Cab3 y Vhs3) a la generación de un enzima PPCDC heterotrimérico atípico. Este enzima esencial y conservado existe como una flavoproteína homotrimérica en la mayoría de las especies eucarióticas, y requiere en el centro activo la presencia de residuos His y Cys específicos, así como un Asn conservado. La búsqueda de genomas fúngicos para la presencia de enzimas putativo PPCDC reveló que *Schizosaccharomyces pombe* contiene un único ORF (SPAC15E1.04, llamado aquí SpHal3)) que podría codificar un Hal3 homólogo. Demostramos que este gen tiene una estructura inusual, siendo el resultado de un evento de fusión génica, que contiene un segmento de tipo Hal3 necesario para la actividad PPCDC (similar a ScHal3) en la región N-terminal y la secuencia que codifica la enzima timidilato sintasa en el extremo C-terminal. Nuestros resultados mostraron que

SPAC15E1.04 se expresa como un único polipéptido y que la mitad N-terminal de SpHal3 es suficiente para determinar la actividad de PPCDC, si la mitad C-terminal es capaz de proporcionar la función TS en *S. cerevisiae*. Nuestros resultados confirmaron la naturaleza multifuncional de este gen de fusión y demostró que es un gen esencial.

INTRODUCTION

1. Yeasts as model organisms: Saccharomyces cerevisiae and Schizosaccharomyces pombe

Yeasts are unicellular fungi included in the phylum Ascomycota, characterized by their ability to ferment sugars, which have been used by man for thousands of years for the production of food and alcoholic beverages (baking, brewing and wine fermentation). Nowadays, in addition to the practice in the food industry, they are extensively used in the field of biotechnology to generate multiple products with commercial interest such as biomass, organoleptic compounds, vaccines, etc.

Yeasts are very common in the environment, and are especially abundant in sugar-rich materials. In nature, they are found on the skin of mature fruits (such as apples and grapes) or berries, on plant surfaces, as well as in soils, with an optimal growth temperature of around 30 °C. Yeast cells may have asexual and sexual reproductive cycles, being the asexual reproduction by mitosis the predominant form of propagation in the Ascomycota. Thus, they can be found as haploid or diploid cells with different size and composition depending on the species, growth medium, and cell growth phase. Under severe stress conditions, such as nutrient starvation, haploid cells die. Nevertheless, diploid cells can undergo sporulation, entering into meiosis and producing haploid spores, which can eventually conjugate to reform diploids. These spores are formed inside sacs known as "asci", a microscopic reproductive structure from which the Ascomycota division is defined. Most of the members of Ascomycota can grow under both aerobic and anaerobic conditions, being facultative fermenters when oxygen is lacking or in the presence of excess sugar, taking their energy from glycolysis and converting the sugar to ethanol. Yeasts can use different sugars as carbon sources.

This phylum includes *Saccharomyces cerevisiae* (budding yeast) and *Schizosaccharomyces pombe* (fission yeast), both considered eukaryotic model organisms in molecular and cell biology. A major difference between them is the mode of asexual reproduction during vegetative growth. *S. cerevisiae* divides by budding, an asymmetric division process where a small bud (daughter cell) is formed on the parent cell. In contrast, *S. pombe* reproduces by fission, thereby creating two identically sized daughter cells. The *S. cerevisiae* genome became the first eukaryotic genome completely sequenced in 1996 (Goffeau *et al.*, 1996), and it is composed of 12,1 Mbp encoding around 6000 genes. Sequencing of the *S. pombe* genome was also completed (Wood *et al.*, 2002), and consist of approximately 13,8 Mbp containing around 5000 protein-coding genes. These organisms possess specific characteristics which make them a focus of study for researches. Some advantages are that they are single free-living cells, but with a cellular organization similar to higher organisms. The majority of yeast proteins have human homologs, which translates to similarities in their fundamental cellular processes such as cell division or DNA damage response. Another important characteristic of these yeasts is that they are considered non-pathogenic , are easy to cultivate in the laboratory, and have a short generation time. Also, their genetic manipulation is straightforward. These advantages make them good experimental systems to understand how cells work in more complex organisms such as humans.

2. Protein phosphorylation

Reversible phosphorylation of proteins is one of the most important and widespread regulatory mechanism for the control of intracellular events in eukaryotic cells. It is a universal post-translational modification with an ancient origin that plays a

key role in a wide range of cellular processes as in signaling pathways, gene transcription and metabolism. Protein phosphorylation is a dynamic process that results in a conformational change in the structure in many enzymes and receptors, causing them to modify their activity, protein interactions and/or localization. Alteration in the normal state of protein phosphorylation is one of the causes for various diseases such as cancer, diabetes, rheumatoid arthritis or hypertension. The importance of this mechanism is demonstrated by the fact that phosphoproteomic studies suggest that more than 70% of all eukaryotic cellular proteins are regulated by phosphorylation. *In vitro* studies have demonstrated that at least 30% of the *S. cerevisiae* proteome could be phosphorylated (Ptacek *et al.*, 2005). Diverse studies have defined the in vivo phosphoproteome of budding yeast and such data is available at the PhosphoGRID database (Sadowski *et al.*, 2013).

The state of phosphorylation of any protein depends on the balance between protein kinases (PKase), which catalyze the transfer of the γ-phosphate moiety of ATP to substrates, and phosphatases (PPase), which perform the reverse reaction (removing the phosphate from phosphorylated substrates). Proteins can be phosphorylated on nine amino acid residues: tyrosine, serine, threonine, cysteine, arginine, aspartate, glutamate and histidine, although in eukaryotic cells phosphorylation usually occurs on serine, threonine and tyrosine residues (86,4%, 11,8% and 1,8% respectively in human proteome) (Olsen *et al.*, 2006; Moorhead *et al.*, 2009). Notably, serine phosphorylation is predominant and, in that case, the covalent attached phosphate groups are removed by Serine/Threonine phosphatases (Cohen *et al.*, 1990; Choy, Page and Peti, 2012). The present work focuses on this kind of enzymes.

The detailed mechanisms of phosphatase function are less understood compared

to that of kinases. There are several reasons for this. For instance, phosphatases are often promiscuous, with broad substrate specificity and functional redundancy (one phosphatase may recognize many different substrates, and one substrate may be recognized by many different phosphatases). In addition, unlike kinases, phosphatases do not have recognizable primary sequence signatures, so it is not possible to predict which PPase can dephosphorylate a given phosphorylation site. As a rule, the number of protein kinases vastly exceeds that of PPases. Thus, *Saccharomyces cerevisiae* encodes 117 PKases and 32 PPases, based on sequence analysis of its genome (Sakumoto *et al.*, 1999).

2.1 Ser/Thr phosphatases

Serine/Threonine phosphatases were originally classified using biochemical assays as type 1 (PP1) or type 2 (PP2). An early classification, based on biochemical and functional differences, established criteria to subdivide them into four major classes (PP1, PP2A, PP2B and PP2C) according to substrate specificities, dependence on divalent cations, and sensitivity to certain inhibitors (Cohen, 1989). The members of the phosphatase protein type 1 (PP1) subfamily preferentially dephosphorylate the β subunit of phosphorylase kinase and they are inhibited by inhibitor-1 and inhibitor-2. Also, PP1 require the presence of Mn^{2+} to catalyze the dephosphorylation reaction. In contrast, the enzymes belonging to the protein phosphatase type 2 (PP2) group specifically dephosphorylate the α-subunit of phosphorylase kinase and are insensitive to inhibitor-1 and inhibitor-2. PP2 is subclassified into three distinct phosphatases by their dependence on divalent cations. PP2A subfamily could be active in the absence of divalent cations, PP2B is Ca^{2+} dependent and stimulated by calmodulin, and PP2C has an absolute requirement for Mg^{2+}. In addition, enzymes of the PPP family are often formed by a

catalytic subunit and one or more regulatory subunits. Remarkably, based on the degree of similarity, the catalytic subunits of Ser/Thr phosphatases are encoded by two distinct gene families: the PPP family, which comprises PP1, PP2A and PP2B; and the PPM family, which includes PP2C. The latter does not seem to be evolutionarily derived from the other major Ser/Thr PPs and has no sequence homology to ancient PPP enzymes, but converged during evolutionary development.

The catalytic subunits of the PPP family members are among the most highly conserved enzymes known, more than PP2C and PTPases (Ingebritsen and Cohen, 1983; Stralfors, Hiraga and Cohen, 1985; Barton, Cohen and Barford, 1994; Egloff *et al.*, 1995). Multiple alignments of the primary sequence of PPP family reveals shared blocks of identity, especially in a highly conserved central region of about 250-280 residues where they contain three signature motifs (-GDXHG-, -GDXVDRG- and – GNHE-) which define this family. These conserved sequences are lacking in PP2C (Shenolikar, 1994). PP2A and PP2B catalytic subunits share 49% and 40% sequence identity, respectively, with PP1 (Wang, Zhang and Wei, 2008). DNA cloning of PP1 and PP2A in eukaryotes has revealed extreme conservation of these enzymes throughout evolution, having a similar primary sequence. For that reason, they adopt a nearly identical and conserved three-dimensional structure. This includes the residues in the enzymatic center, and then the catalytic mechanism is common (Wozniak, Ołdziej and Ciarkowski, 2000; Ceulemans, Stalmans and Bollen, 2002). PP1, PP2A and PP2C enzymes are present in all eukaryotic organisms.

The advent of molecular cloning allowed the identification of novel protein serine/threonine phosphatase catalytic subunits related to, but distinct from, PP1 and PP2A. The genome of the budding yeast *S. cerevisiae* encodes not less than five of these

novel putative phosphatases, Sit4/Pph1 and Pph3, both related to PP2A, and Ppz1, Ppz2, and Ppq1, related to PP1 (Ariño, 2002).

2.2 The Ser/Thr Phosphatase Type 1

PP1 is a major protein Ser/Thr phosphatase and is ubiquitously expressed in all eukaryotic cells. PP1 catalyze over 90% of all eukaryotic protein dephosphorylation reactions, regulating many critical and diverse cellular processes such as glycogen metabolism, muscle contraction, cell cycle progression (exit from mitosis), neuronal signaling, protein synthesis (transcription and translation), splicing of RNA, cell growth and differentiation, etc. (Gibbons, Weiser and Shenolikar, 2005; Rebelo *et al.*, 2015).

The protein phosphatase 1 catalytic subunit (PP1c) is one of the most conserved eukaryotic proteins with a molecular mass ranging from 35 to 38 kDa. This phosphatase forms stable complexes with variable regulatory subunits. The association with distinct subunits converts PP1 into many different forms (holoenzymes), and is fundamental in targeting the enzyme to specific substrates or subcellular locations, and in modulating the activity of the phosphatase (Egloff *et al.*, 1995; Zhao and Lee, 1997; Cohen, 2002). Therefore, protein phosphatase type 1 is tightly regulated by these interactions, since overexpression or hyperactivation, as well as the absence of PP1 activity, are deleterious to the cell, given the broad cellular functions in which is involved. For this reason perturbation of PP1 activity is interesting in the development of novel therapeutics (Moorhead *et al.*, 2009; Bollen *et al.*, 2010; Chatterjee and Köhn, 2013).

Numerous crystallographic analyses of eukaryotic PP1 have revealed the structure of the catalytic site and indicated a number of residues involved in catalysis and/ or metal

ion binding (Ansai, Dupuy and Barik, 1996). The crystal structure of PP1c consists of a compact elliptical domain with a central β sandwich folded by 10 α-helices and 14 β-strands. The catalytic center is formed by two β-sheets that create a β-sandwich with a loop between β12 and β13 (Egloff *et al.*, 1995; Goldberg *et al.*, 1995; Griffith *et al.*, 1995; Wozniak, Ołdziej and Ciarkowski, 2000). The catalytic site contains six highly conserved residues for a binuclear binding metal site (Mn^{2+} and $Fe^{2+)}$ that are coordinated with a water molecule, which are essential for catalysis, and the phosphate group on the substrate (Egloff *et al.*, 1995; Barford, 1996; Stark, 1996; Peti, Nairn and Page, 2013). This catalytic site is at the intersection of three shallow grooves (Y-shape) (Figure 1), that are potential binding sites; the hydrophobic groove, a C-terminal groove, and the acidic groove (Kita *et al.*, 2002; Wang, Zhang and Wei, 2008). The COOH-terminal fragment of 30 residues is excluded from the globular structure and contains several phosphorylatable residues. Because of this, the extreme C-terminal of PP1c modulates its enzymatic activity. Meanwhile the hydrophobic groove plays a dominant role in binding inhibitors because recognition of subunits is mediated by these kind of interactions (Kita *et al.*, 2002; Gibbons, Weiser and Shenolikar, 2005).

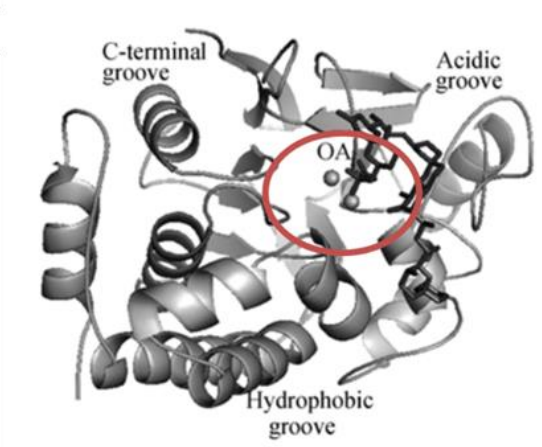

Figure 1. Structure of protein phosphatase-1. Frontal view of the three grooves radiating from the catalytic site (encircled). PP1c bound to okadaic acid (OA) (Wang, Zhang and Wei, 2008).

The catalytic domains of mammalian PP1s are 80-90% identical with those of fungi and the phenotypes derived from mutation of PP1 in fungi are partially complemented by the expression of mammalian PP1, indicating that the function is also conserved (Sangrador *et al.*, 1998). Molecular genetics has confirmed that both *S. cerevisiae* and *S. pombe* encode homologs of these major activities (Kinoshita, Ohkura and Yanagida, 1990; Stark, 1996). In *S. cerevisiae,* the catalytic subunit of PP1 is encoded by a single, essential gene termed *GLC7* (*DIS2S1*), which codes for a protein of 312 residues with a molecular mass of 36 kDa (Clotet *et al.*, 1991). Initially, *GLC7* was identified as a gene related to the metabolism of carbohydrates because it is necessary for the accumulation of glycogen (Peng, Trumbly and Reimann, 1990; Feng *et al.*, 1991) but, analogously to mammalian PP1c, it has also been implicated in the regulation of a wide variety of processes. For instance, *GLC7* is required for the control of mitosis, involved in the G2/M transition (Hisamoto, Sugimoto and Matsumoto, 1994; Stark, 1996), as well as essential in the development of meiosis (Zhang, Guha and Volkert, 1995; Tu, Song and Carlson, 1996).

Moreover, Glc7 plays a critical role in several functions related to the cytoskeleton, such as the kinetochore formation and control of spindle (Bloecher and Tatchell, 1999; Sassoon *et al.*, 1999), regulation of the endocytosis and reorganization of actin cytoskeleton (Chang *et al.*, 2002), or polarized and filamentous growth and response to pheromones (Cullen and Sprague, 2002). Glc7 is also involved in the formation of the ascus wall during sporulation (Tachikawa *et al.*, 2001). Additionally, this protein can participate in the maintenance of the cell integrity (Andrews and Stark, 2000) and in the maintenance of ionic homeostasis. Like its mammalian counterpart, Glc7 needs the binding of regulatory subunits to carry out all those functions.

2.2 Ser/Thr phosphatases type Z in *S. cerevisiae*: Ppz1 and Ppz2

Saccharomyces cerevisiae contains novel members of the Ser/Thr phosphatase family that are structurally related to PP1. Two of these enzymes are Ppz1 and Ppz2, which are closely related paralogs of 692 and 710 amino acids respectively, showing 67% identity over their full length (93% identical in its catalytic domain). *PPZ1* and *PPZ2*, in contrast to the single gene *GLC7*, are not essentials. Thus, these phosphatases do not perform the same functions that yeast PP1.

These phosphatases do not have any known homologues in higher eukaryotes, and are restricted to fungi. Thus, similar proteins have been found in other fungi such as *Schizosaccharomyces pombe* (Pzh1) (discussed in detail in section 4), *Neurospora crassa* (Pzl-1) or *Candida albicans* (CaPpz1), which share structural and functional characteristics (Balcells *et al.*, 1997, 1998; Szöor *et al.*, 1998; Vissi1 *et al.*, 2001; Adám et al, 2012; Leiter *et al.*, 2012).

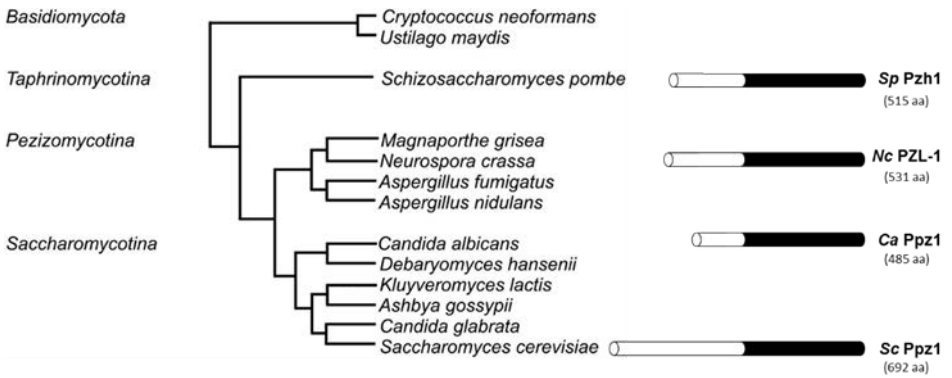

Figure 2. PPz-like phosphatases distribution in fungal species. Phylogenetic relationship and Ppz-like phosphatases conservation among fungi species. Right, schematic representation of previously characterized Ppz-like phosphatases with the number of residues between brackets. In black is represented the highly conserved catalytic domain. In white, the N-terminal extension, which is more variable between species.

Structurally, these phosphatases consist of two distinct domains. The C-terminal half (about 350 residues), comprises the catalytic domain and shows more than 60% sequence identity to the catalytic subunit of protein phosphatase-1 (PP1c) from a large variety of species, including mammals. The N-terminal half (from amino acid 1 to 319) is largely unstructured, rich in basic residues, as well as in Ser, Thr and Asn amino acids, and shows no similarities to other protein phosphatase sequences (Posas F, Casamayor A, Morral N, Ariño J, 1992; Hughes *et al.*, 1993). One of the most relevant aspects of the N-terminal region is the presence of a consensus sequence for N-myristoylation. The myristoyl group attached to the proteins appears to be important in mediating protein-membrane interaction or increasing its stability (Yonemoto, McGlone and Taylor, 1993). Specifically, Ppz1 has shown to be myristoylated *in vivo* at Gly-2 (Clotet *et al.*, 1996). Also, the N-terminal half contains multiple potential phosphorylation sites for a number of known protein kinases, including PK-A, PK-C and Ck-2 (Posas *et al.*, 1995). Phosphorylation might occur in vivo under certain conditions and, perhaps, regulate the

intracellular localization of the protein. However, it does not seem to be necessary for the enzyme activity, as deduced from the evaluation of the recombinant enzyme expressed in *E. coli* (Posas *et al.*, 1995). Although the function of the Ppz1 N-terminal extension is unknown, it has been reported that this half might be relevant for specificity, and contains some residues (241-317 region and Gly-2) that are required to perform some of the Ppz1 functions. In addition, it was suggested that the N-terminal domain may have a regulatory role for the C-terminal domain, protecting thereby the phosphatase activity (Clotet *et al.*, 1996). Despite the N-terminal is more variable between Ppz-phosphatases, a motif rich in serine and arginine residues is conserved in other orthologs from different fungal species. This observation suggested that this Ser/Arg-rich motif should be relevant for these phosphatases, although its role is still unclear (Minhas *et al.*, 2012).

Ppz1 is involved in the regulation of important processes of the *S. cerevisiae* biology. It plays an important role mainly in osmotic and saline homeostasis (Posas, Casamayor and Ariño, 1993; Posas, Camps and Arino, 1995). Thus, a *ppz1* mutant displays increased tolerance to toxic monovalent cations, such as sodium or lithium. These regulatory effects produce consequences in multiple cellular processes, such as maintenance of the cell wall integrity (Lee, Hines and Levin, 1993; Posas, Casamayor and Ariño, 1993). Also, this phosphatase has been related to protein translation (De Nadal *et al.*, 2001), and cell cycle progression at the G1/S transition (Clotet *et al.*, 1999). Ppz1 and its paralog Ppz2 have partially overlapping functions. However, the biological role of Ppz1 is more relevant than Ppz2, as exemplified by the fact that the single *ppz2* mutant has normal salt tolerance, but the double *ppz1 ppz2* strain displays higher halotolerance that the single *ppz1* one (Ariño, 2002).

The catalytic properties of Ppz1 are quite similar to that of protein phosphatases -1 and -2A. The Ppz1 C-terminal domain displays activity against several substrates, such as myelin basic protein, histone 2A, casein (Posas *et al.*, 1995) or myosin light chain (Petrenyi *et al.*, 2016), and it is also active towards *p*-nitrophenyl phosphate. This activity is dependent on the presence of Mn^{2+} ions, as it has been reported for PP1c. Ppz1 is also sensitive to some inhibitory toxins that bind to the PP1c active site (okadaic acid, microcystein-LR). This resemblance may be due to the sequence GEFD present in the C-terminal region of PP1, which is also found in residues 629-632 of Ppz1 (Posas *et al.*, 1995). A major difference with both PP1 and PP2A is that Ppz1 is unable to in vitro dephosphorylate glycogen phosphorylase. The phosphatase activity of Ppz1 is completely necessary for the function of this protein and the catalytic activity is largely lost by the mutation of Arg-451, a highly conserved residue in many eukaryotic Ser/Thr protein phosphatases that corresponds to Arg-96 in the catalytic subunit of PP1 (Clotet *et al.*, 1996).

As for PP1, the activity of Ppz1 must be tightly regulated, because overexpression of Ppz1 has been shown to be detrimental for yeast cell growth (Clotet *et al.*, 1996; De Nadal *et al.*, 1998). Furthermore, a recent genome-wide study in *S. cerevisiae*, in which the limit of gene overexpression from the strong inducible *GAL1* promoter is measured, has identified Ppz1 as one of the most toxic proteins (Makanae *et al.*, 2013). However, the molecular bases for this harmful effect are unknown.

3. The cellular roles of Ppz1 in *S. cerevisiae*

The phosphatase Ppz1 in *S. cerevisiae* was initially characterized by playing a role in the maintenance of cell integrity. However, the activity of this phosphatase is a key

determinant in cation homeostasis, a function that was postulated some years ago (Posas, Camps and Arino, 1995; Yenush *et al.*, 2002). It should be noted that this involvement in Na^+, K^+ and pH homeostasis could have important consequences for the determination of other cellular processes such as establishment of membrane potential, cell cycle regulation, cell wall integrity, or even protein translation.

3.1 Ppz1 and the regulation of cation homeostasis in *S. cerevisiae*

An important characteristic of the physiology of living cells is the maintenance of ionic homeostasis, on which depend a whole series of fundamental parameters, such as cellular size, turgor, concentration of intracellular cations, internal pH and membrane potential. To maintain the internal equilibrium, and in response to changes in the external environment, the cells carefully regulate the pass of ions across their plasma membrane. The intracellular concentrations of the major monovalent cations (H^+, K^+, and Na^+) must be tightly regulated to avoid an excess that could be damaging to the cell (Serrano, 1996). The toxicity depends on each specific cation; whereas potassium presents a wide range of tolerance, the intracellular concentration of sodium (and its analog lithium) must be kept as low as possible. Their toxicity is probably caused by antagonizing magnesium cations in the active site of some key enzymes (Murguía, Bellés and Serrano, 1995; Dichtl, Stevens and Tollervey, 1997; Yenush *et al.*, 2005). On the other hand, intracellular pH is strongly regulated because of its effect on proteins and biochemical reactions. To this end, cellular membranes contain diverse cation transport systems to ensure precise and safe intracellular ionic composition, retaining a large amount of internal K^+ and actively extruding sodium and lithium. The ejection of protons, together with the accumulation of K^+, allow maintaining an electrical membrane potential relevant for the transport of

nutrients and cations. Also, the ion gradient generated between the external medium and the cytoplasm determines the entry or exit of water across the membrane and, therefore, it is responsible for the size and cellular turgor (Serrano, 1996).

Yeasts are free living organisms that exhibit a rapid adaptation to the large variations in the external medium to which they are exposed. These organisms maintain a correct ion homeostasis because of the presence of cell wall and a membrane transport strategy different from mammals. In the yeast *Saccharomyces cerevisiae* many of these ion transporters have been identified and characterized (Arino, Ramos and Sychrova, 2010).

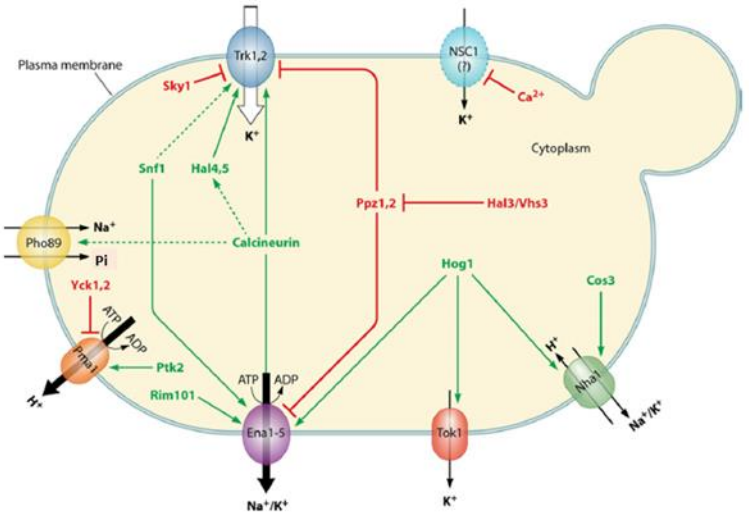

Figure 3. Principal transporters and their regulatory components involved in the homeostasis of monovalent cations in the yeast *Saccharomyces cerevisiae*. Only the main transporters located at the plasma membrane and their functional regulators are shown. Other elements involved in this process, such as vacuoles, are obviated for simplicity (Arino, Ramos and Sychrova, 2010).

S. cerevisiae has the ability to survive over a relatively wide pH range, but optimally proliferates at acidic environmental conditions. Intracellular pH regulation is partially

explained by the pH dependence of the plasma membrane H^+-pumping ATPase, Pma1, which ensures maintenance of such conditions by actively extruding protons out the cell. This movement generates an electrochemical proton gradient that finely regulates cytoplasmic pH between 6.2 and 6.8 and contributes to nutrient and cation uptake across the plasma membrane (Serrano, 1996).

Sodium is an abundant cation in the environment and can enters yeast cells through several low-affinity cation transport systems. The yeast *S. cerevisiae* is able to maintain a suitable intracellular concentration of Na^+, even in the presence of relatively high concentrations of this cation in the medium, through the coordinate regulation of uptake and efflux systems.

In addition to the Na^+/H^+ antiporter Nha1 in the plasma membrane, which plays an important role in the homeostatic regulation (Prior *et al.*, 1996; Kinclova-Zimmermannova, Gaskova and Sychrova, 2006), the P-type ATPase encoded by the gene *ENA1* constitutes the second significant system for sodium and lithium efflux in budding yeast cells. This pump is able to actively extrude sodium and lithium, but also potassium cations, in reactions coupled to ATP hydrolysis. In *S. cerevisiae* several (up to five) *ENA* genes are disposed in an unusual tandem repeat. Deletion of the entire *ENA* cluster results in a dramatic phenotype of sensitivity to high salinity environments as well as to alkaline pH (Haro, Garciadeblas and Rodriguez-Navarro, 1991; Garciadeblas *et al.*, 1993; Rodríguez-Navarro, Quintero and Garciadeblás, 1994; Wieland *et al.*, 1995). *ENA1* was the first member of this tandem to be identified and it is widely accepted to be the functionally relevant component of the cluster (Haro, Garciadeblas and Rodriguez-Navarro, 1991; Martinez, Latreille and Mirande, 1991; Wieland *et al.*, 1995; Benito, Garciadeblás and Rodríguez-Navarro, 2002; Ruiz, Yenush and Ariño, 2003).

Under standard growth conditions expression of *ENA* genes is very low, but when cells are exposed to elevated sodium and lithium levels, or to alkaline pH, the expression of *ENA1*, but not that of other members of the cluster, is potently induced (Garciadeblas *et al.*, 1993; Mendoza *et al.*, 1994). In addition, transcriptional response of *ENA1* is observed under glucose starvation conditions (Alepuz, Cunningham and Estruch, 1997), indicating that the expression could be repressed by the presence of glucose in the medium. The transcriptional regulation of *ENA1* to the diverse stimuli requires the intervention of multiple pathways that transmit signals to its promoter, which contains diverse regulatory elements recognized by specific transcription factors that activate or inhibit transcription according to the signal.

The yeast Ppz1 and Ppz2 are important determinants of salt tolerance in part because these Ser/Thr phosphatases affect the expression level of *ENA1* (Posas, Camps and Arino, 1995; Ariño, 2002; Ruiz, Yenush and Ariño, 2003). In *S. cerevisiae*, disruption of *PPZ1* confers a noticeable tolerance to sodium and lithium cations as a result of an increase in the efflux of these cations. Both cation efflux and *ENA1* expression are further enhanced upon additional deletion of *PPZ2* (Ruiz, Yenush and Ariño, 2003). This fact supports the notion that Ppz phosphatases regulate negatively the efflux of cations in yeast cells through the repression of the *ENA1* gene under basal conditions to avoid an excessive expression of the ATPase, which is detrimental to cell growth (Posas, Camps and Arino, 1995; Ariño, 2002). The mechanisms by which Ppz1 phosphatase influence *ENA1* expression is rather complex and appears to involve negative regulation of the calcineurin pathway (Ruiz, Yenush and Ariño, 2003).

Moreover, Ppz phosphatases are involved in the proper regulation of intracellular potassium concentration, which is important because K^+ is the major intracellular cation

responsible for cellular volume, turgor, electrical membrane potential and ionic strength. In yeast, potassium is the only alkali cation specifically transported under normal growth conditions. Through the uptake of potassium, the cell is able to reduce its membrane potential and thus prevents the entry of toxic cations such as sodium or lithium. *S. cerevisiae* has a dual mode of potassium transport, consisting of a high-affinity and a low-affinity potassium transport systems (Rodriguez-Navarro and Ramos, 1984). High-affinity potassium uptake is mediated by the transporters Trk1 and Trk2 (Gaber, Styles and Fink, 1988; Ko, Buckley and Gaber, 1990; Ko and Gaber, 1991), where Trk1 is the most physiologically relevant. Trk1 is a 180 kDa plasma membrane protein with an initially predicted structure of 12 transmembrane domains, exclusively present in plasma membrane lipids rafts (Yenush *et al.*, 2005). The deletion of both TRKs results in a significant defect in potassium transport and slow growth phenotype under limiting concentrations of potassium, which is restored by the addition of this cation to the media. The defect in K^+ transport produces a hyperpolarization of the plasma membrane and consequently, an increase in sensitivity to sodium, lithium, as well as other toxic cations such as spermine, hygromycin B or tetramethyl ammonium (TMA) (Ko, Buckley and Gaber, 1990; Ko and Gaber, 1991; Gómez, Luyten and Ramos, 1996; Madrid *et al.*, 1998; Mulet *et al.*, 1999).

The Trk transporters are perfectly regulated at the post-translational level by phosphorylation mechanism, and this regulation is crucial due to the effect that produce de entrance of potassium on the membrane potential. Several protein kinases and phosphatases controls the activity and/or stability of Trk1 and Trk2. For instance, the protein kinases Hal4 and Hal5 are required to stabilize the Trk transporters at the plasma membrane, specially under low potassium conditions. However, no direct

phosphorylation of Trks by Hal4 and Hal5 kinases has been reported. Despite that, Trk1 could be phosphorylated *in vitro* and *in vivo* by protein kinases and then, suggests activation of potassium transport (Mulet *et al.*, 1999; Yenush *et al.*, 2005; Holt *et al.*, 2009; Helbig *et al.*, 2010; Swaney *et al.*, 2013).

Ppz1 and Ppz2 play an important role in the regulation of Trk activity. Strains lacking Ppz phosphatases were characterized by presenting cytosolic alkalinization and reduction in the membrane potential that could be explained by the inhibitory role of the Ppz phosphatases on Trk potassium transporters. Thereby, the absence of Ppz1 and Ppz2 allows massive potassium uptake, and therefore the membrane potential is decreased. This avoids the entrance of toxic cations, which contributes to the hypertolerance to saline stress or toxic cations of Ppz-deficient cells. At the same time, the large accumulation of intracellular K^+ produces an increased cell size due to the higher turgor pressure (Yenush *et al.*, 2002; Merchan *et al.*, 2004; Ruiz *et al.*, 2004). It has been shown that Trk1 interacts physically with Ppz1 in plasma membrane rafts, and an increase in phosphorylated forms of Trk1 has been detected in *ppz* phosphatase mutants (Yenush *et al.*, 2005). This led to the hypothesis that Ppz1 might modulate Trk1 phosphorylation state, although a direct effect remains to be proved.

Therefore, an appropriate Trk regulation by Ppz phosphatases is essential to maintenance of K^+ and pH homeostasis. The deletion or overproduction of *PPZ1* and *PPZ2* lead to diverse Trk-mediated cellular effects caused by alterations of the internal potassium concentration. An increase in K^+ triggers proton efflux to maintain electrical balance and the consequent internal alkalinization. The increase of intracellular pH could signal on the *ENA1* promoter, which is responsive to high pH. Moreover, the turgor pressure increment causes constant stress on the cell wall, activating the Mpk1 pathway as is detailed below.

In fact, an increased activity of the Mpk1 pathway is observed in *ppz1 ppz2* mutant cells (Yenush *et al.*, 2002; Merchan *et al.*, 2004).

3.2 The Ppz phosphatases and the cell-wall integrity maintenance in *S. cerevisiae*

The principal function of the cell wall in *S. cerevisiae* is to maintain cell shape and act as a shield against physical or chemical external stresses, such as osmotic changes (Klis, Boorsma and De Groot, 2006). Thereby, the integrity of this structure is necessary for survival and, for this reason, it is under the thigh control of a regulatory mechanism known as the Cell Wall Integrity (CWI) Pathway. This pathway is composed by a group of cell wall sensors (Wsc1-3, Mid2, and Mtl1) coupled to a small GTPase (Rho1), which is a signal transducer that binds and activates the protein kinase C (Pkc1). The protein kinase Pkc1 is member of the Mitogen Activated Protein (MAP) kinase pathway that consists of several protein kinases (Bck1, Mkk1; Mkk2 and Mpk1), which in response to certain stimuli and through a phosphorylation cascade results in the final activation of the Slt2/Mpk1 (suppressor of the lytic phenotype) MAP kinase. Activation of Slt2 results in phosphorylation of several nuclear (as the transcriptional factor Rlm1) and cytosolic targets that activate specific transcription in response to aggressions to the cell wall (Levin, 2005).

The CWI pathway is active during vegetative growth and pheromone-induced morphogenesis on yeast cells, but also mediates the response triggered in case of cell wall damage provoked by chemical agents (e.g. Congo red, calcofluor white, zymolyase, caffeine) or environmental conditions (e.g. heat shock, hypoosmotic shock, or alkaline pH)

(Levin, 2005). Mutations in any of the elements that compose this pathway, such as deletion of the MAP kinase Slt2, result in cells prone to lysis under conditions that compromise cell wall integrity, such as salt exposure or high temperature (37 ºC). Moreover, *slt2* mutants are particularly sensitive to caffeine or calcofluor white. The lytic phenotype can be rescued by addition of 1 M sorbitol to the medium as osmotic stabilizer.

The Ppz phosphatases were initially related to the maintenance of cell integrity in *S. cerevisiae* because the *PPZ2* gene was isolated as a dosage dependent suppressor of the lytic defect associated with the disruption of *SLT2/MPK1* (Lee, Hines and Levin, 1993). Similar phenotypes to those observed in strains lacking either component of the Slt2/Mpk1 pathway (*bck1*, *mkk1*, *mkk2* or *mpk1* mutants) were described for *ppz* phosphatase mutants, such as increased size (elongated morphology), and temperature or caffeine sensitivity, leading to cell lysis. Moreover, the effects due to *PPZ1* and/or *PPZ2* deletion are additive to those caused by the absence of Slt2. Similarly to the *slt2* mutant, these defects can be suppressed in the presence of 1 M sorbitol (Hughes *et al.*, 1993; Posas, Casamayor and Ariño, 1993). The link between the Slt2/Mpk1 pathway and Ppz phosphatases can be explained by the relationship of these phosphatases with the regulation of potassium uptake. Since strains lacking Ppz activity display abnormally high accumulation of K^+ due to deregulated Trk activity, turgor pressure is increased causing a negative effect on cell wall. Therefore, these cells require a reinforcement of the cell wall mediated by the Pkc1–Slt2/Mpk1 pathway, and for that reason the activity of this pathway increases (Yenush *et al.*, 2002; Merchan *et al.*, 2004). In absence of Slt2, which leads to weakened cell wall, this situation produces a lytic phenotype.

3.3 The role of Ppz1 phosphatase in cell cycle progression

In *Saccharomyces cerevisiae,* as in any eukaryotic cell, the cell cycle consists in a succession of phases: DNA replication (phase S) and its separation into two complete genomes (mitosis, phase M), which are separated by the intervals G1 and G2. The regulation of the eukaryotic cell cycle is a complex process that involves two major control points (checkpoints); at G1/S, which determines DNA replication because it controls that external conditions are appropriate, that the size of the cell is adequate to start a new cycle, and ensures that any DNA damage caused by the previous replication is already repaired; and at G2/M, which regulates entry into mitosis after supervision that the DNA has been correctly duplicated during the S phase (Tyson, Csikasz-Nagy and Novak, 2002). In *S. cerevisiae* a new round of the cell cycle is committed at a control point called Start in the G1/S transition. It demands a sufficient level of G1 cyclin/Cdc28 protein kinase activity for the DNA synthesis, bud formation, and replication of the spindle pole body. CDC28 encodes a cyclin dependent kinase (CDK), which is the only CDK responsible for cell cycle control, in contrast to mammals. Thus, the activity of Cdc28 is regulated mainly by the binding of proteins denominated cyclins. Towards the end of mitosis, the complex formed by Cdc28 and Cln3 is responsible for the control of cell size. When the cell has reached the proper dimensions, Cln3-Cdc28 activates transcriptional complexes that induce genes specifically to the G1 phase, which include cyclins *CLN1*, *CLN2*, *CLB5* and *CLB6*. Specific transcription of the G1/S transition also requires the activity of some phosphatases, such as Sit4, Ppz1 or Glc7.

The *S. cerevisiae* gene *SIT4* encodes a Ser/Thr phosphatase related to type 2A enzymes. The Sit4 protein may have been conserved through evolution, as PP6 phosphatase in human or Drosophila PPV are functional homologs. *sit4* mutant cells are viable but display a slow-growth phenotype and defects in bud emergence, characteristic

of a delayed G1/S transition (Sutton *et al.*, 1991; Sutton, Immanuel and Arndt, 1991). For that reason, Sit4 is required in late G1 for progression into S phase for expression of *SWI4*, *CLN1* and *CLN2* cyclins and seems to be required also for bud emergence (Fernandez-Sarabia *et al.*, 1992).

Ppz1 has been related also as a regulatory component of the G1/S transition in the yeast cell cycle, since its regulatory subunit, Hal3 (detailed in section 6), was identified by its capacity, when overexpressed, to recover the growth defect of *sit4* cells (Como *et al.*, 1995). Therefore, overexpression of PPZ1 causes blockage of cell growth, decreased expression level of *CLN2* and *CLB5* cyclins and display an increased number of unbudded cells, all these features characteristics of a delay G1/S transition (Clotet *et al.*, 1999; Merchan *et al.*, 2004). By contrast, deletion of *PPZ1* accelerates the slow growth phenotype of *sit4* mutants and results in an earlier expression of *CNL2* and *CLB5* to favor entry in S phase. The link between the functions of Ppz1 and Sit4 phosphatases evidences that Ppz1 exerts an important effect in the G1/S transition that it is opposed to some of the functions attributed to Sit4 Ser/Thr phosphatase. Specifically, Ppz1 has consequences in a pathway that negatively regulates G1 cyclin transcription, through a mechanism that would not be mediated by Sit4, Bck2, or Cln3. In addition, Ppz1 should negatively regulate certain processes that affect proper budding (Clotet *et al.*, 1999).

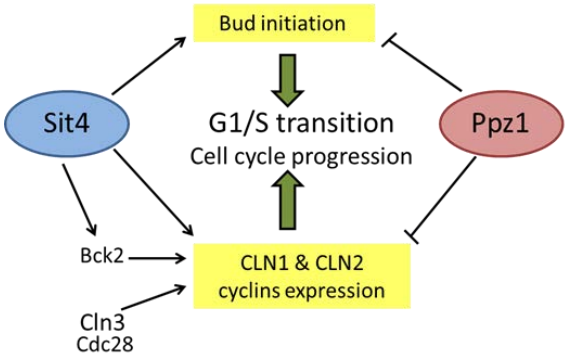

Figure 4. Schematic representation showing the phosphatases Sit4 and Ppz1 role in the regulation of G1/S transition. Adaptation from Clotet 1999 (Clotet *et al.*, 1999).

3.4 Ppz1 involvement in protein translation

Protein translation is the process by which messenger RNA (mRNA) is decoded by ribosomes in the cytoplasm to produce specific polypeptides. The elongation factor 1 (EF1) participates in the GTP-dependent binding of aminoacylated tRNA to the ribosomal A site during elongation of the polypeptide and contributes to proofreading of the codon-anticodon match. In *S. cerevisiae* EF1 consist of different subunits (EF1A, EF1Bα), whose function is critical for an efficient and correct translation. The translation elongation factor 1Bα (Tef5) has been demonstrated to be phosphorylated *in vivo* in the Ser-86 residue. In a previous work, hyperphosphorylated EF1Bα protein was found as a result of deletion of the PPZ genes, suggesting that the Ppz phosphatases could influence the phosphorylation state of the translation elongation factor 1Bα. Moreover, the absence of Ppz1 and Ppz2 increases the tolerance of yeast cells to the protein synthesis inhibitor paromomycin, and alters translational fidelity (Nadal *et al.*, 2001). Recent studies have shown that deletion of *PPZ1* increases efficacy of suppression in the presence of various

nonsense suppression factors (SUP35, SUP45, PSI+ and ISP+) (Ivanov, Radchenko and Mironova, 2010).

4. Cation homeostasis in *Schizosaccharomyces pombe*

Budding and fission yeast rely on different mechanisms for ion transport at the membranes mediating the efflux of cations. The principal difference is related to the exclusion of Na^+ ions. In *S. cerevisiae*, a major determinant for Na^+ efflux is the P-type Na^+-ATPase encoded by *ENA1* (detailed in section 3.1.). On the contrary, in *S. pombe* there is no evidence for the existence of an equivalent Na^+ efflux system. In the fission yeast, the active efflux of Na^+ is mediated by a H^+/Na^+ antiporter encoded by the *sod2* gene (Jia *et al.*, 1992; Dibrov *et al.*, 1997). This system was identified because *S. pombe* is highly sensitive to Na^+ when growing at neutral pH, that is, without a proton gradient (Jia *et al.*, 1992). Moreover, a second H^+ antiporter was identified in *S. pombe*, designated as a Sod22, which efficiently is involved in K^+ efflux (Papouskova and Sychrova, 2007). However, the mechanism of K^+ influx in *S. pombe* could be analogous to *S. cerevisiae*. Fission yeast also encodes a *TRK* gene (SpTRK) (Soldatenkov *et al.*, 1995; Lichtenberg-Fraté *et al.*, 1996), which complements the impaired K^+ uptake of a *trk1 trk2 S. cerevisiae* mutant (Lichtenberg-Fraté *et al.*, 1996).

Despite these differences, a PPZ-like phosphatase, encoded by the *pzh1* gene, was identified in this organism and, similarly to *S. cerevisiae* Ppz1, it was shown to be involved in cation homeostasis. Pzh1 is a protein of 515 amino acids that contains a catalytic C-terminal domain (from the residue 193 to the C-terminal end) which shares 78% identity with Ppz1 and Ppz2, and a shorter N-terminal region that also shows a high number of

phosphorylatable residues (Ser and Thr), and the presence of a consensus site for N-myristoylation (Balcells *et al.*, 1997).

The expression of the *pzh1* ORF in *S. cerevisiae* cells lacking *ppz1* is able to complement the absence of Ppz1, since it produces a decrease in tolerance to high salt and rescues the caffeine-induced lytic phenotype. However, the Pzh1 functions in *S. pombe* are not exactly the same as those Ppz1 in *S. cerevisiae, since* the disruption of *pzh1* in *S. pombe* triggers an increase in Na^+ tolerance, without effects on caffeine sensitivity and, moreover, it produces hypersensitivity to K^+ ions (Balcells *et al.*, 1997, 1998, 1999). Although lack of Pzh1 results in a 2 to 3-fold increase in Sod2 mRNA, the *pzh1* mutation significantly increases salt tolerance in the absence of the *sod2* gene, suggesting that the phosphatase also regulates a Sod2-independent mechanism.

5. Regulatory subunits of Ser/Thr phosphatase type 1 (PP1)

The specificity and regulation of mammalian PP1 is explained because PP1 interacts with more than 200 known regulatory subunits to form a variety of holoenzyme complexes. These regulatory proteins control the activity (inhibitors), the localization (targeting proteins), and substrate specificity of PP1c.

The regulatory subunits share no significant sequence similarity among them and they are structurally unrelated. However, the structures of PP1 in complex with some peptides along with the comparison of subunit sequences has evidenced that most of these subunits bind to PP1 in the same manner. The binding of the regulatory subunits to PP1

is mediated by docking motifs, that is, short sequences of about 4-8 residues present in the regulatory subunits that are combined to create a large interaction surface for PP1. Despite the conservation of motifs during evolution, these motifs are somewhat degenerated, displaying variants of the consensus sequence that differ in affinity for PP1. Moreover, PP1 interacting proteins usually have multiple PP1 binding sites, and different regulatory subunits can compete for a common binding site present on PP1 (Bollen *et al.*, 2010; Heroes *et al.*, 2013).

There are about 10 known distinct PP1-docking motifs present on the regulatory subunits (Table 1). However, most regulatory subunits (70%) bind to PP1 by the identifiable RVxF sequence. The relevance of this short conserved region was revealed by the first X-ray crystallography structures of PP1 with the regulatory subunits G_M and MYPT1 (Myosin phosphatase target subunit 1) (Egloff *et al.*, 1997; Terrak *et al.*, 2004). More recently analysis of the docking peptides refined the consensus sequence to (**R**/**K**/H/N/S) x_1 (**V**/**I**/L) x_2 (**F**/**W**/Y) where x_1 could be absent or any residue except a large hydrophobic amino acid, and x_2 is any amino acid except a large hydrophobic residue or phosphoserine (in bold marked the most frequent residues) (Bollen, 2001; Ceulemans, Stalmans and Bollen, 2002; Meiselbach, Sticht and Enz, 2006; Shi, 2009; Rebelo *et al.*, 2015). In addition, this sequence is commonly preceded by 2-5 basic residues and followed by 1 acidic residue (Zhao and Lee, 1997). This short peptide sequence is sufficient to generate a strong interaction with PP1(Cohen, 2002). As expected, to produce the interaction it is necessary that the regulatory subunit exposes the residues conforming this motif on its surface (Wakula *et al.*, 2003). The diversity of the consensus RVxF sequence-containing regulators may be an evolutionary strategy that dictates the affinity for the phosphatase and allows dynamic physiological regulation of PP1 functions (Gibbons,

Weiser and Shenolikar, 2005). This motif docks within a hydrophobic groove on the surface of the PP1c enzyme near the C-terminus, situated opposite to the active site (Barford, Das and Egloff, 1998; Gibbons, Weiser and Shenolikar, 2005). Interaction with the RVxF motif is relevant for the catalytic activity modulation of PP1. It has been described that modifications of the RVxF-binding pocket in the regulatory subunits such as single amino acid substitutions of the hydrophobic residues (V/I/L) and/or aromatic ones (F/W/Y) severely impaired or abolished its ability to bind and regulate PP1 phosphatase (Dombek *et al.*, 1999; Wu and Tatchell, 2001). Moreover, in PP1 the hydrophobic pocket plays also an important role in the recognition of these regulatory subunits, because substitutions in the C-terminal sequence of PP1 (^{289}LMC^{291} amino acids) which lined the RVXF-binding motif could result in deficits in PP1 inhibition or effects in binding (Gibbons, Weiser and Shenolikar, 2005).

Motif	PP1 interacting proteins	Function
RVxF	G-subunit	PP1 anchoring
SILK	Inhibitor-2	PP1 anchoring
MYphoNE	Mypt1	Substrate selection
SpiDoc	Spinophilin	Substrate selection
IDoHA	Inhibitor-2	Inhibition
BiSTriP	SDS22	Unknown
Pseudosubstrate	Inhibitor-1	Inhibition
AnkCap	Mypt1	Substrate selection

Table 1. PP1 docking motifs. The principal PP1 docking motifs are shown, together with representative examples of interacting subunit and the function attributed to the motif. Adapted from (Heroes *et al.*, 2013).

Despite the importance of the RVxF motif for the interaction of targeting subunits, the docking of the RVXF-motif onto PP1 is not inhibitory itself, but mediates the initial anchoring of regulatory subunits (Wakula *et al.*, 2003). Thereby, this primary regulatory site facilitates the accommodation of additional or secondary binding sites

present in these targeting subunits, that allows to stabilize the binding mediated by the RVxF motif and then to modulate the activity and/or specificity of the phosphatase (Bollen, 2001; Ceulemans *et al.*, 2002; Ceulemans, Stalmans and Bollen, 2002; Cohen, 2002; Gibbons, Weiser and Shenolikar, 2005).

Recent progress in elucidating the structures of PP1 bound to regulatory subunits have identified and functionally characterized additional motifs (Table 1). Among the best studied docking motifs present in the PP1 regulatory subunits are MyPhoNe, SILK, SpiDoc, IDoHA and others (Heroes *et al.*, 2013). MyPhoNE (myosin phosphatase N-terminal element) was determined in PP1 complex with MYPT1, a protein that affects the specificity for substrate. The PP1-MYPT1 complex is formed by the result of interaction with the RVxF motif and, additionally, the N terminus of MYPT1 binds to the base of the catalytic cleft of PP1 and, thereby stabilize its C terminus region. This secondary interaction produces alterations in PP1 that are responsible for the substrate specificity of the enzyme (Roy and Cyert, 2009). SpiDoC (spinophilin) is a docking site for the C-terminal groove that prevents substrate recruitment. The IDoHA motif blocks phosphatase activity by occluding the catalytic site. The SILK interaction site contains the consensus sequence G/SILR/K and it is located opposite to the active site of PP1, below the RVxF motif.

Other region also important for interaction with the regulatory subunits on the surface of the PP1 phosphatase is the β12-β13 loop, which forms a flexible binding site and it is essential for inhibition of PP1 by toxins (acid okadaic and calyculin A) and protein inhibitors (Inh-1, DARPP-32, Inh-2 and NIPP1).

The PP1 interactors better characterized include proteins that act either as targeting subunits and thus they direct PP1 to specific cellular structures, or inhibitors, which block access to the active site and inhibit dephosphorylation activity. Among the targeting subunits, the most relevant and extensively characterized are MYPT1, PNUTS (Phosphatase 1 NUclear Targeting Subunit), NIPP1 (nuclear protein and, also, a potent and specific inhibitor of PP1) and spinophilin (it directs PP1 to substrates in the dendritic spine, such as dopamine receptors). On other hand, PP1 binding subunits acting as potent inhibitors have been studied in order to use the structural information to design new inhibitors of PP1. Some of the inhibitors include a variety of naturally occurring toxins such as okadaic acid and microcystin. The first PP1 inhibitors discovered were Inhibitor-1 and Inhibitor-2, able to instantaneously inhibit the catalytic subunit of PP1 at nanomolar concentrations. Inhibitor-1 requires phosphorylation for the inhibitory activity, whereas inhibitor-2 inhibits PP1 without previous phosphorylation. All members of the Inhibitor-1 family share an RVxF-motif that is C-terminally coupled to an inhibitory module.

Inhibitor-2 binds to the PP1c RVxF-docking groove through a related KSQKW sequence, in a site some distance from the catalytic center of PP1c and facilitates the additional interactions. Moreover, Inhibitor-2 contains a SILK motif, that associates residues 12-17 of Inhibitor-2 with PP1c by mean of hydrophobic interactions and hydrogen bonds. These two contacts induce conformational changes of Inhibitor-2, which lacks significant ordered structure and, then, enhances association with PP1c. However, a third region present in the inhibitor-2, called binding site 3, is the responsible for the inhibitory mechanism of the phosphatase. This region corresponds to residues 130-169 of I-2, contacts directly with the catalytic active site of PP1c, and displaces the metal ions for the catalysis, thus inactivating PP1 (Hurley *et al.*, 2007).

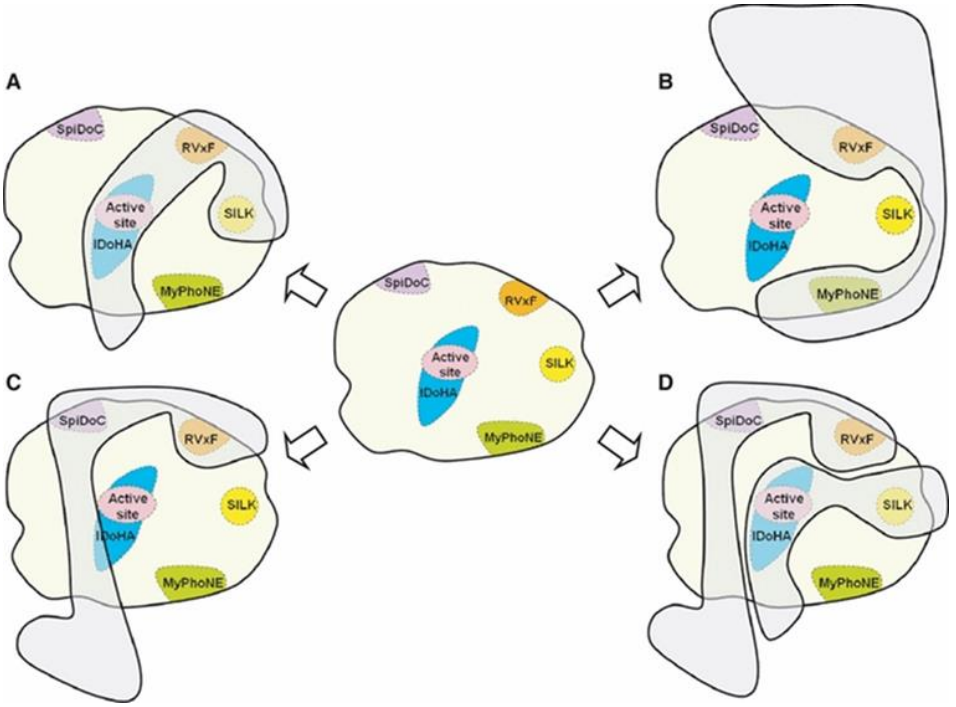

Figure 5. PP1 binding code. Center: PP1 catalytic domain (PP1c), some of the most studied binding sites for specific docking motifs that bind interacting subunits are coloured (RVxF, SILK, MyPhoNe, SpiDoc and IDoHA), and the active site is represented in pink. PP1 holoenzymes are formed by binding of subunits to a combination of docking sites. It is represented based on known structures of PP1 with: A) inhibitor-2; B) Mypt1; C) spinophilin; D) spinophilin plus inhibitor-2 (Heroes *et al.*, 2013).

In yeast, more than a dozen genes that encode PP1-binding proteins have been identified. They include proteins that are required to control intracellular PP1 activity toward specific substrates in different ways (Cannon, 2010). For example, Gac1 is the subunit involved in glycogen metabolism (Stuart *et al.*, 1994), and Reg1 is associated with Glc7 to function in negative regulation of glucose-repressible genes (Tu and Carlson, 1995).

Most yeast PP1 regulatory subunits also possess the RVxF motif (Egloff *et al.*, 1997; Cohen, 2002). The genes *GAC1*, *REG1*, *REG2*, *SCD5*, *GIP1*, *SHP1*, and *GIP2* encode

regulatory subunits of Glc7 that exhibit such motif. However, similar to mammals, there are Glc7 regulatory subunits that bind to PP1 using other motifs. An example is Sds22, which bind through leucine-rich repeats. The first inhibitory subunit of Glc7 identified in *S. cerevisiae* was Ypi1 (Garcia-Gimeno *et al.*, 2003), a homolog of mammalian PP1 inhibitor-3. It is considered an important inhibitor since deletion of *YPI1* is lethal due to the dramatic blockage in the G2/M transition of the cell cycle. Ypi1 is a small hydrophobic protein of 155 amino acids which contains a RVxF-like sequence possibly necessary for binding to Glc7. This subunit interacts in vitro with Glc7 and Ppz1 phosphatase catalytic subunits, but it inhibits only Glc7. Another significant Glc7 regulator is Glc8, although is not required for viability. While Glc8 wears some similarity to the inhibitor-2, it is able to activate Glc7. This protein also binds and activates Ppz1 (Venturi *et al.*, 2000).

6. Regulatory subunits of Ppz phosphatases: Hal3 and Vhs3

In contrast to PP1 phosphatase, for which several regulatory subunits related to different cellular functions have been identified, only two regulatory subunits, Hal3 and Vhs3, have been described for the Ppz phosphatases. As it will be described below, Hal3 and Vhs3 are able to regulate all the functions mediated by the phosphatases.

The gene *HAL3/SIS2* was identified by two laboratories independently, as a multicopy suppressor of the growth defect in a *sit4* mutant, in which normalizes the expression of Cln1 and Cln2 cyclins of G1 phase (Como *et al.*, 1995) and as a gene that confers salt tolerance when overexpressed in wild type cells (Ferrando *et al.*, 1995).

The overexpression of *HAL3* confers tolerance to high concentrations of sodium and lithium cations due to increased *ENA1* expression (Ferrando *et al.*, 1995; De Nadal *et al.*, 1998). Moreover, Hal3 overexpression increases the K^+ influx via Trks, and it allows growth at potassium limiting conditions. These are phenotypes completely opposite to those found in a *ppz1* mutant. Such evidence prompted studies leading to the identification of Hal3 as a regulatory subunit of Ppz1 (De Nadal *et al.*, 1998). These authors demonstrated that the effects of Hal3 on salt tolerance could be explained through the inhibition of Ppz1. It was also demonstrated that Hal3 binds to the C-terminal catalytic moiety of the PPase. In keeping with the negative role of Hal3 on Ppz1, the overexpression of Hal3 aggravates the lytic phenotype of the *slt2* mutant, which requires full osmotic support and is only viable in the presence of sorbitol (De Nadal *et al.*, 1998).

On the other hand, Hal3 overexpression induces synthesis of G1 cyclins that accelerate the exit of a stop in G1 and increases the rate of budding in cells lacking *sit4*, suppressing, at least in part, the characteristic growth defect of *sit4* cells (Como *et al.*, 1995; De Nadal *et al.*, 1998; Clotet *et al.*, 1999). It is known that the *sit4* and *hal3* double mutation is synthetically lethal because of a G_1/S blockade (Como *et al.*, 1995; Simón *et al.*, 2001), and this phenotype is suppressed by deletion of *PPZ1* (Clotet *et al.*, 1999). Finally, cells with excess of Hal3 show an increase in the phosphorylation of Tef5 (elongation factor 1Bα) (Nadal *et al.*, 2001). Therefore, Hal3 appears to negatively regulate all known Ppz1 cellular manifestations (Table 2).

		Ppz1		Hal3	
Cellular process	Strain	*Overexpression*	*Deletion*	*Overexpression*	*Deletion*
saline homeostasis	Wild type	NA	Na^+/Li^+ tolerance	Na^+/Li^+ tolerance	Na^+/Li^+ sensitivity
	ppz1	-	-	Na^+/Li^+ tolerance	NP
	ppz1,2	-	-	NP	NP
Cell cycle progression	Wild type	↓ growth	NP	NP	NP
	sit4	lethal	Improves growth	Improves growth	lethal
Cell integrity	Wild type	NA	Sensitivity to caffeine and ↑T^a	NP	NP
	slt2	Improves growth	lethal	lethal	Improves growth
Protein translation	Wild type	NP	Tolerance to translational inhibitors and ↓ translational fidelity	Tolerance to translational inhibitors and ↓ translational fidelity	Induces allosupression

Table 2. Comparison between the phenotypes resulting from the overexpression or deletion of Ppz phosphatases and their negative regulatory subunit Hal3. The phenotypes are grouped according to the cellular processes involved. NP, no phenotype. NA, not analyzed. In the analyzed conditions, the phenotypes observed by the lack of Ppz1 are similar to those obtained by overexpressing Hal3, and vice versa.

The Hal3 gene is expressed constitutively and its product is found in the cytoplasm (Ferrando *et al.*, 1995). This gene encodes a protein of 562 amino acids, that possess a characteristic acidic C-terminal tail (of approximately 80 amino acids), extremely rich in acid residues, especially in aspartic.

Interestingly, Hal3 does not show a significant degree of similarity with the regulatory subunits of PP1c and it is not able to interact with Glc7 (De Nadal *et al.*, 1998; Garcia-Gimeno *et al.*, 2003). Although it contains a ^{263}KLHVLF^{268} sequence, which resemble the consensus RVxF motif present in most PP1c regulatory subunits (Bollen *et al.*, 2010), previous work in our laboratory, in which the RVxF-like motif was mutated, demonstrated that this element is not critical in the binding and inhibition of Ppz1 by Hal3, suggesting that the mechanism by which Hal3 and Ppz1 interact may be different from those described for the PP1c regulatory subunits in mammals (Muñoz *et al.*, 2004). However, a mutagenesis analysis followed by screen for loss-of-function identified a number of important residues in Hal3 for Ppz1 binding and/or inhibition. Most of them are restricted to a small region (residues from 446 to 480), indicating that this region has a key role in Hal3 functions regarding regulation of Ppz1. Curiously, mutations in Hal3 affecting the ability to inhibit Ppz1 but not to interact with the PPase were found. This suggests that the Hal3 structural elements required for Ppz1 inhibition and binding can be independent (Muñoz *et al.*, 2004).

The second regulatory subunit of Ppz phosphatases is Vhs3 (YOR054c). The YOR054c gene was identified (among others) in our laboratory as a multicopy suppressor of the G1 phase blockage in a *sit4 hal3* conditional mutant, from which its name *VHS3* (**v**iability in **h**al3 **s**it4) derives (Muñoz *et al.*, 2003). *VHS3* encodes a 674 residues protein structurally close to Hal3 (49% identity), and maintains the characteristic rich-acidic tail.

Overexpression of *VHS3* improves the slow growth phenotype in cells lacking *SIT4*; in a *slt2* mutant produces a growth defect and increased sensitivity to caffeine; in terms of cation homeostasis, *VHS3* overexpression also improves salt tolerance, increasing slightly the levels of *ENA1* expression. Then, all the phenotypes resulting from deletion or

excess of *VHS3* are similar to those derived from that of *HAL3*, although the effect is usually less noticeable. This suggested that *VHS3* functionally mimics Hal3. Furthermore, the ability of Vhs3 to bind *in vitro* and *in vivo* to the catalytic domain of Ppz1 was demonstrated and Vhs3 was also able to inhibit the phosphatase activity as successfully as Hal3. Therefore, Vhs3 acts as a negative regulatory subunit of the Ppz phosphatases with lesser effective biological role that the functional homolog Hal3, maybe due to lower levels of mRNA (Ruiz, Muñoz, *et al.*, 2004).

The *hal3 vhs3* double mutation is synthetically lethal, but this phenotype, contrary to that expected, is not caused by excess of Ppz1 phosphatase activity, because deletion of both *PPZ1* and *PPZ2* cannot rescue the lethal phenotype produced by the absence of their regulatory subunits (Ruiz, Muñoz, *et al.*, 2004). This observation suggested for the first time that Vhs3 and/or Hal3 could be acting in other functions, independently to their inhibitory role of Ppz phosphatases.

However, the characterization of the synthetic lethality of the *hal3 vhs3* mutant allowed to detect another phenotype related to Ppz function. Cells depleted for the regulatory subunits of Ppz1 showed a flocculation phenotype (Ruiz, Muñoz, *et al.*, 2004). Flocculation is an asexual and reversible process in which cells adhere through formation of filaments to form multicellular structures (flocs) that sediment from liquid medium. This aggregation is important in adaptive mechanisms such as invasive growth for fungal virulence or formation of biofilms (Gimeno *et al.*, 1992; Guo *et al.*, 2000; Reynolds and Fink, 2001), as well as in industrial processes to separate the cells from the fermented product. In *S. cerevisiae* this process requires lectin-type proteins, called flocculins, which are located in cell walls and interact in a Ca^{2+}-dependent way with mannose residues of adjacent cells (Verstrepen *et al.*, 2003). Flocculins are encoded by the FLO gene family, in

which *FLO11* is the only one not silenced in most laboratory strains. The regulation of *FLO11* is complex since it has a very large promoter (3kbp) that integrates signals from diverse pathways. This gene is required for the flocculation phenotype observed in cells depleted for Hal3 and Vhs3 (Ruiz, Muñoz, *et al.*, 2004). Recent evidences have shown that this effect is Ppz-dependent (González *et al.*, 2013). Cells suffering an increase in Ppz1 activity such as the *hal3* mutant, already showed an increased *FLO11* expression. In contrast, *ppz1* deletion abolished the flocculation phenotype and suppressed the increased expression of *FLO11*. These results proposed a model which establishes a link between potassium homeostasis and flocculation. Activated Ppz1 would inhibit potassium uptake through the Trk-transporters, leading to a decrease in intracellular pH and to an increase in cAMP levels. Increased cAMP results in activation of PKA pathway, which trigger expression of the *FLO11* flocculin gene (González *et al.*, 2013).

7. The family of Hal3-related proteins

In addition to the paralog Vhs3, the genome of *S. cerevisiae* codes for another protein structurally related to Hal3, called Cab3 (Yklo88w). Cab3 is an essential protein and shows a 28% of sequence identity to Hal3. The size of Cab3 is very similar to that of Hal3 and Vhs3 proteins, sharing also the C-terminal acidic tail. However, this protein is not an inhibitor of protein phosphatase Ppz1, indicating that its essential nature must be attributed to another function (Ruiz *et al.*, 2009).

Unexpectedly, unlike fungal-specific Ppz phosphatases, Hal3 is evolutionarily conserved. Homologs of Hal3 can be found in other fungi, but also in plants, and mammals, which seems to indicate a key role in the physiology of the most diverse kind of cells. In

other yeasts, as *Candida tropicalis*, the homologs conserve the acidic carboxi-terminal tail. However, the Hal3 homologs described in higher eukaryotes, as *Arabidopsis thaliana*, *Nicotiana tabacum*, *Caenorhabditis elegans*, *Droshophila melanogaster*, rice, mouse and human (Espinosa-Ruiz A, Bellés JM, Serrano R, 1999), are shorter proteins in which only the central segment of about 180 residues is conserved and, therefore, they lack the N-terminal extension and the acidic C-terminal tail. This conserved segment is related to the DFP family of prokaryotic flavoproteins involved in DNA synthesis and the metabolism of coenzyme A.

Arabidopsis thaliana contains two genes, AtHAL3a and AtHAL3b, which encode similar proteins in function and structure. AtHal3a is the isoform most studied and shares a 52% identity with the central core of ScHal3. Its overexpression slightly complements the salt sensitivity of a *hal3* mutant in *S. cerevisiae* (Espinosa-Ruiz A, Bellés JM, Serrano R, 1999). This suggested the possible existence of conserved functions between this protein and budding yeast Hal3. AtHal3a is a flavoprotein whose three-dimensional structure was resolved by X-ray diffraction, allowing the determination of the biological unit as a trimer (Albert *et al.*, 2000). Importantly, it was described that AtHal3 catalyzes *in vitro* the decarboxylation of 4-phosphopantothenoylcysteine (PPC) to phosphopantetheine (PC), a key step in the biosynthesis of coenzyme A (Kupke *et al.*, 2001) (see also section 8). In this process, the residues Histidine 90 and Cysteine 175 of AtHal3 are essential catalytic components in the active site. Each of them is contributed by one of the monomers, so that the enzyme has three identical active centers.

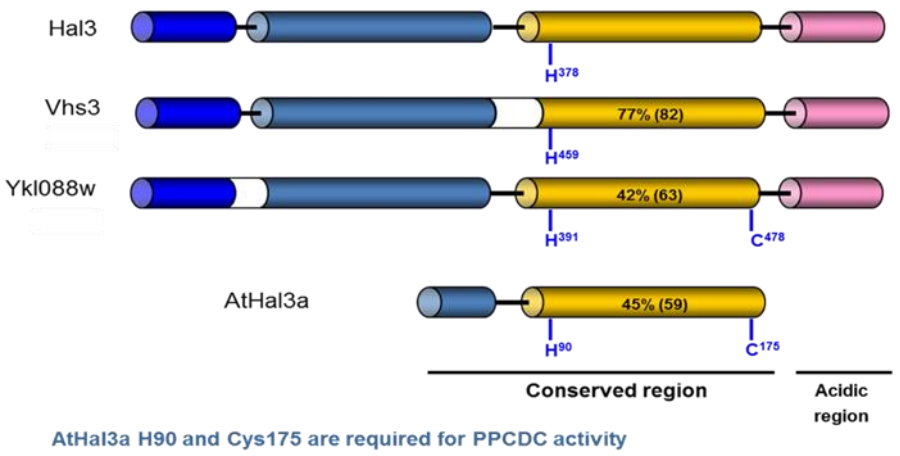

Figure 6. Schematic structure comparison of Hal3, Vhs3, Cab3 and AtHal3a. The percentages indicate the degree of identity (and similarity) of the central core with Hal3. The residues identified in the *Arabidopsis thaliana* protein required for decarboxylation of 4'-phosphopantothenylcysteine are shown in blue.

The high structural similarity between AtHal3, and Hal3, Vhs3 and Cab3 of *S. cerevisiae* suggested that these three yeast proteins could be candidates as putative PPCDC enzymes.

8. PPCDC in *Saccharomyces cerevisiae*

The flavoprotein phosphopantothenoylcysteine decarboxylase (PPCDC) is a key component of the Coenzyme A biosynthetic pathway. Coenzyme A is a common cofactor used by a broad variety of enzymes. The CoA biosynthetic pathway is universal and consists of five enzymatic reactions, where the third step is carried out by PPCDC, which catalyzes the decarboxylation of PPC to PP (Begley, Kinsland and Strauss, 2001; Ye *et al.*, 2005). All PPCDC enzymes share a common mechanism and active site structure (Strauss *et al.*, 2001; Hernández-Acosta *et al.*, 2002). The PPCDC catalytic mechanism occurs in two

steps, for which two conserved His and Cys residues are important. In the first step, in which the histidine residue is involved, decarboxylation of PPC results in a thioaldehyde generating an enethiol intermediate. The second step involves the cysteine residue, here the intermediate is reduced to PP and the FMN cofactor is reoxidized (Strauss, 2010).

Most of characterized PPCDC in bacteria and eukaryotic organisms, such as humans and plants, are monogenic, that is, encoded by a single gene (Albert *et al.*, 2000; Manoj *et al.*, 2003; Steinbacher *et al.*, 2003). The enzyme is formed by three identical protomers that contains the required residues (His and Cys for the catalytic activity as well as an Asn), creating three active sites at the interface of the monomers, where the catalytic essential residues are provided by adjacent monomers.

Ruiz and coworkers (Ruiz *et al.*, 2009) demonstrated that the budding yeast PPCDC enzyme is a heterotrimer, composed of at least one subunit of Cab3 and two subunits of Hal3, Vhs3 or one of each. In this heterotrimer, Cab3 provides the catalytic Cys (Cys^{478}) and the required Asn (Asn^{442}), whereas Hal3 or Vhs3 supply the necessary His (His^{378} and His^{459}, respectively). It was also demonstrated that, although Cab3 contains an (apparently) catalytic His (His^{391}), this residue is not functional (Ruiz *et al.*, 2009). Therefore, none of the polypeptides are individually sufficient to provide PPCDC activity (Figure 7). This anomalous structure, in which the enzyme contains only a single functional active site, also explains the essential nature of *CAB3* and the synthetic lethality phenotype of the *hal3 vhs3* mutations. Therefore, Hal3 and Vhs3 can be defined as moonlighting proteins, since they play two apparently unrelated functional roles: inhibitory subunits of the Ppz1 phosphatase and components of an enzyme involved in CoA biosynthesis.

A moonlighting protein is a single protein that has multiple roles, apparently unrelated, that are not due to gene fusions, multiple RNA splice variants or multiple proteolytic fragments (Jeffery, 2003; Tompa and Sza, 2005). Examples of moonlighting proteins have been described in many species from prokaryotes to animals (Huberts and van der Klei, 2010). A certain number of these proteins have been characterized in yeast (Gancedo and Flores, 2008; Gancedo, Flores and Gancedo, 2016). Many of the currently known moonlighting proteins are highly conserved (ancient) enzymes (Huberts and van der Klei, 2010). Biochemical evidence and bioinformatic predictors demonstrate that these proteins are largely disordered and their structural disorder is crucial for executing disparate effects (Tompa and Sza, 2005). The ability of proteins to moonlight can benefit the cell or organism in several ways, such as to expand functional capabilities that are encoded without expanding the genome (Jeffery, 1999, 2009).

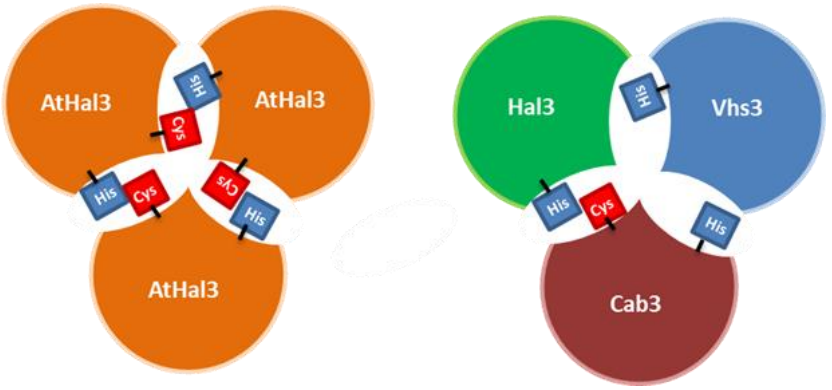

Figure 7. Proposed model for *S. cerevisiae* and *A. thaliana* PPCDC enzyme structure and catalytic sites.

Left, the homotrimeric *A. thaliana* PPCDC showing three active sites containing the conserved residues (His and Cys) at the interfaces of the monomers. Right, the heterotrimer of *S. cerevisiae* formed by Hal3, Vhs3 and Cab3, showing the conserved His residue in all three proteins, and the Cys residue in Cab3, creating a single functional active site. Adapted from (Ruiz *et al.*, 2009).

Therefore, *S. cerevisiae* PPCDC composition is unusual compared to most eukaryotic organisms, in which the PPCDC is formed by a homotrimer. Moreover, the subunits of the enzyme are usually relatively small proteins (<300 residues), lacking the N-terminal extension and the acidic C-terminal tail in comparison to the budding yeast proteins that, therefore, could be considered as divided into three segments. A functional mapping study characterized the structural elements of Hal3 involved in both Ppz1- and CoA-related functions (Abrie *et al.*, 2012). The conserved central domain (PD), similar to the PPCDC enzymes in other organisms, is necessary for the PPCDC activity, whereas neither the N-terminal region nor the acidic tail is required for this function (although the N-terminal fragment might have a role in stabilizing interactions between Hal3 and Cab3). Also, while the ScHal3 PD domain is required for Ppz1 binding and regulation, it is not sufficient to inhibit the phosphatase activity. The highly acidic tail of Hal3 plays an important role for the inhibition of Ppz1, suggesting a possible interaction with the phosphatase. It is worth noting that previous work revealed nine amino acids located at the PD core of Hal3 whose mutation affected the capacity to bind or inhibit Ppz1 (Muñoz *et al.*, 2004). These changes, however, did not interfere with the PPCDC activity of the protein. Therefore, the structural determinants for Ppz1 regulation and PPCDC function are independent.

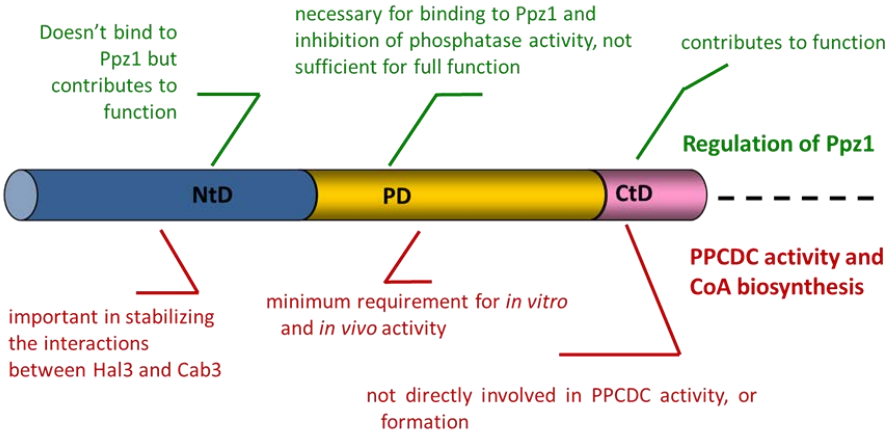

Figure 8. Schematic representation of the functional domains of *S. cerevisiae* Hal3. NtD: N-terminal domain. PD: Core domain, which contains the essential residues for the PPCDC activity. CtD: C-terminal highly acidic domain (Adapted from (Abrie *et al.*, 2012)).

9. Divergence of Hal3 in other yeasts and the unusual ORF of *S. pombe*

The examination of fungal genomes for putative PPCDC enzymes offers an interesting variety of possibilities concerning Hal3, Vhs3 or Cab3 structures, which could be categorized in three different scenarios. In the first one, and similar to *S. cerevisiae*, organisms that consist of three putative PPCDC-encoding genes corresponding to Hal3, Vhs3 and Cab3 are found. The second situation comprises Hemiascomycetes, where only two genes are identified, one Cab3-like that conserves the cysteine residue (and the asparagine), but not the histidine; and the other Hal3/Vhs3-like lacking the cysteine and asparagine, but maintaining the conserved histidine. One relevant example is the case of *Candida albicans*, in which both genes have been recently characterized (Petrenyi *et al.*, 2016). Finally, the last case is found in Archyascomycetes such as *S. pombe*, and most of the

Euascomycetes and Basidiomycetes, which contain only a single putative PPCDC-encoding gene (*Neurospora crassa* and *Cryptococcus neoformans* are exceptional cases because of their genome duplication). In any case, these genes contain all the required elements similarly to AtHal3 and human PPCDC (hsCoaC), suggesting that they encode essential monogenic enzymes (Ruiz *et al.*, 2009).

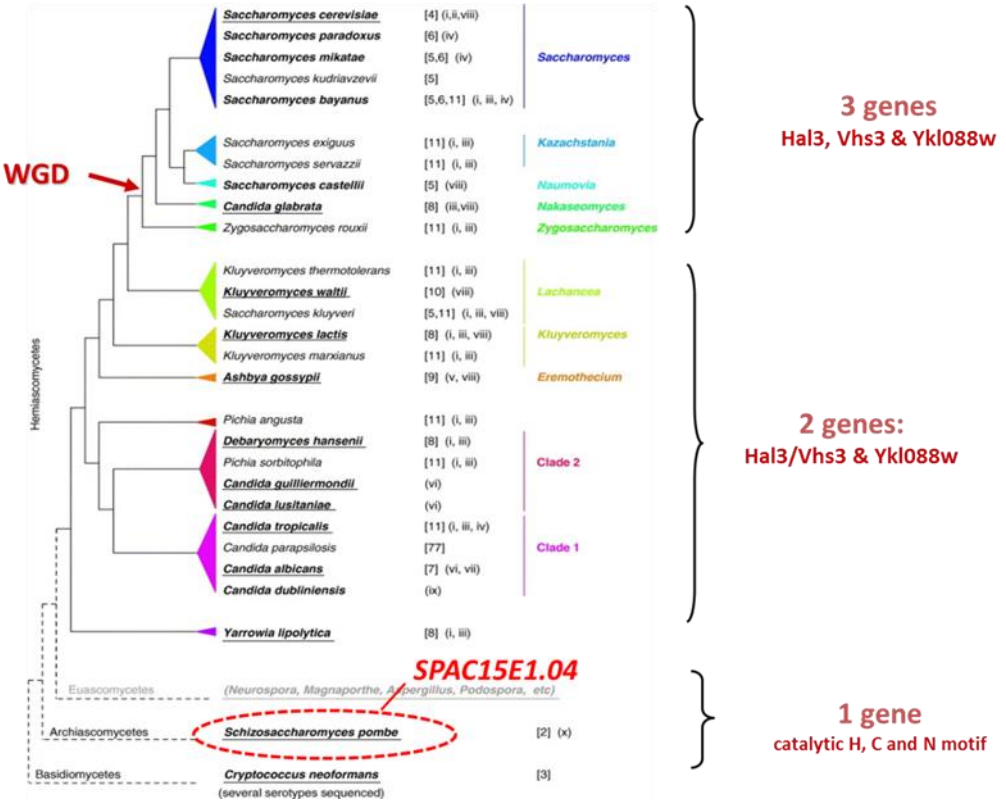

Figure 9. Phylogenetic analysis of putative PPCDC genes in fungi. On the right-hand the number of genes identified in each organism is indicated. Search was performed at NCBI by means of the BLAST algorithm using the sequence of ScHal3 as query. WGD, whole-genome duplication. The ORF SPAC15E1.04 of *S. pombe,* which will be object of study in this work, is highlighted. Adapted from (Dujon, 2006).

Although there has been some controversy about the precise location of *Schizosaccharomyces pombe* (fission yeast) in the fungal evolutionary tree, it is clear that the ancestors of *S. cerevisiae* and *S. pombe* separated quite early, with estimations ranging between 420 and 330 million years ago (Heckman, 2001). In spite of this, fundamental biological processes are preserved and there are numerous orthologous genes between both yeast (Kennedy *et al.*, 2008). However, unlike *S. cerevisiae*, in which there are three similar proteins related to PPCDC, the inspection of the *S. pombe* genome sequence showed only a putative PPCDC -encoding gene (SPAC15E1.04). According to data bases, the sequence of this ORF would encode a protein of 625 residues. Remarkably, while the N-terminal half of the protein showed a putative flavoprotein with a 58% similarity to the core of *S. cerevisiae* Hal3, followed by a short acidic tail, the carboxy terminal half of this gene was highly similar to thymidylate synthase (TS). This unusual structure represents the only instance of these two highly conserved enzymes in the *S. pombe* genome and suggested that the SPAC15E1.04 ORF is the result of a gene fusion event.

10. Thymidylate Synthase activity

Thymidylate synthase is an enzyme crucial to DNA synthesis both in prokaryotic and eukaryotic cells. This enzyme catalyzes the methylation of the pyrimidine ring of deoxyuridine monophosphate (dUMP) to deoxythymidine monophosphate (dTMP), the first step in deoxythymidine triphosphate (dTTP) synthesis (Bisson and Thorner, 1981; Costi *et al.*, 1999; Munro *et al.*, 1999). Inhibition of thymidylate synthase produces an imbalance of deoxynucleotides content because of increased levels of dUMP, that leads to DNA damage (Storms *et al.*, 1984; Taylor *et al.*, 1987). Usually, the enzyme is a homodimer

and its three-dimensional structure is defined by 8 α-helix and 10 β-sheets (Taylor *et al.*, 1982; Carreras, 1995; Munro *et al.*, 1999; Finer-Moore *et al.*, 2005).

Thymidylate synthase is one of the most highly conserved enzymes known, which suggest that TS evolved from an ancestral form by addition of inserts and mutations in the catalytic core (Munro *et al.*, 1999; Abeysinghe *et al.*, 2017). Thymidylate synthase shares a 69% homology between human and yeast. In *Saccharomyces cerevisiae*, as well as in some other fungi, thymidylate synthase provides the exclusive source of dTMP for DNA synthesis because this organism lacks thymidine kinase activity and cells are impermeable to thymine, thymidine and dTMP (Singer *et al.*, 1989; Ahmad, Kirk and Eisenstark, 1998; Vernis, Piskur and Diffley, 2003). For that reason, dTMP can only be synthesized *de novo* and TS is essential for the proliferation of yeast cells.

In the budding yeast, thymidylate synthase is encoded by *CDC21* as a 304 amino acid protein. Conditional mutations produce arrest of the yeast cell cycle in the S phase, and mitochondrial DNA replication is also stopped (Chien, Chou and Su, 2009). dTMP absence is lethal, inducing DNA strand breakage, mitotic crossing-over, gene conversion, and unequal sister chromatid exchange (Taylor *et al.*, 1987; Vernis, Piskur and Diffley, 2003). In *S. cerevisiae,* Thymidylate synthase exhibit differential expression during cell cycle, increasing the mRNA amount during late G1 and early S phase (McIntosh, Ord and Storms, 1988). The enzyme from *S. cerevisiae* was also purified and characterized by Bisson and Thorner (Bisson and Thorner, 1981), who determined that the enzyme is a dimer composed of similar subunits of about 30 - 35 kDa. The enzyme localizes at the nuclear periphery associated with membranes of the nucleus or endoplasmic reticulum (Poon and Storms, 1994).

Surprisingly, according to a large-scale gene disruption study in *S. pombe* (Kim *et al.*, 2010), the SPAC15E1.04 deletion was not reported as lethal. This result was very surprising to us, since this ORF ought to encode a polypeptide containing two likely essential activities: a unique putative PPCDC, at its N-terminal half, and a canonical thymidylate synthase at its C-terminal half. Such incongruence moved us to undertake the study of the *S. pombe* SPAC15E1.04 ORF.

OBJECTIVES

Because Hal3 does not share any of the sequence characteristics that define a protein phosphatase inhibitor and, despite the similarity of Ppz1 to PP1 phosphatases, Hal3 does not inhibit PP1 enzymes, it can be hypothesized that the way Hal3 regulates Ppz1 differs from previously known phosphatase regulatory mechanisms. Therefore, the goal of this work was to contribute to the elucidation of the mechanism of recognition and inhibition of Ppz1 phosphatase by its regulatory subunit Hal3.

This objective has been approached in the following ways.

1.- By a combination of PCR-based mutagenesis and a functional screen to identify mutations in the catalytic region of Ppz1 that result in loss of the capacity to be inhibited by Hal3.

2.- By purification of the Ppz1-Hal3 complex in sufficient amounts to attempt the crystallization of the complex and subsequent determination of its 3D structure by X-ray crystallography.

3.- Through the characterization of the peculiar ORF SPAC15E1.04 found in *Schizosaccharomyces pombe*, focusing in the investigation of the properties and functions of the encoded putative PPCDC subunit.

EXPERIMENTAL PROCEDURES

1. Yeast strains and media

S. cerevisiae cells were grown at 28 °C, unless otherwise stated, in YPD medium (10 g/L yeast extract, 20 g/L peptone, and 20 g/L dextrose). When carrying plasmids, cells were grown in synthetic minimal medium composed of 0.17% yeast nitrogen base (YNB) without ammonium sulfate and amino acids, 0.5% ammonium sulfate, 2% glucose, and 0.13% drop-out mix (lacking the appropriate selection requirements) (Adams and Kaiser, 1997).

S. pombe cells were grown at 32 °C in YE (5 g/L yeast extract, 30 g/L dextrose, supplemented with 40 mg/L adenine and 20 mg/L uracil) or Edinburgh Minimal Medium (EMM, Bio101 Systems-Q Biogene 4018-022), as indicated.

The yeast strains used in this work are listed in table 1 of Annexes.

For sporulation of *S. cerevisiae* diploid strains, cells were transferred for several days to liquid medium containing 10 g/L potassium acetate, 1 g/L yeast extract and 0.5 g/L glucose (pH 7.2).

2. Recombinant DNA techniques

Escherichia coli DH5α cells were used as a plasmid DNA host and were grown at 37 °C in LB (Lysogeny Broth) medium supplemented, if necessary, with antibiotics according to the plasmid-conferred resistance (100 μg/ml ampicillin or 30 μg/ml Kanamycin). Restriction reactions, DNA ligations, and other DNA recombinant techniques were performed as described in (Sambrook, Fritsch and Maniatis, 1989).

DNA fragment purifications, such as PCR products or restriction enzyme digestions, were done isolating the fragments by agarose gel electrophoresis. The bands of interest were purified using the Nucleo-Spin Gel and PCR Clean-Up kit (Macherey-Nagel).

Isolation of plasmids from *S. cerevisiae* cells were carried out as described in (Topal, Karaer and Temizkan, 1997). The plasmid isolations from *E. coli* cells were performed using the QuickLyse Miniprep (Quiagen) or NucleoSpin® Plasmid Macherey-Nagel kits. Purified DNA was quantified by measuring the absorbance at 260 nm and its integrity/size verified by electrophoresis in agarose gels.

E. coli cells were transformed with the standard calcium chloride procedure (Sambrook, Fritsch and Maniatis, 1989), except otherwise stated. *S. cerevisiae* cells were transformed following the lithium acetate method as described in (Ito *et al.*, 1983).

3. Plasmids

-pRS316: YC-type centromeric vector containing the *URA3* gene for marker selection (Sikorski and Hieter, 1989).

-pRS316-PPZ1: pRS316 plasmid (AmpR, *URA3*) containing the *PPZ1* gene (2750 bp) that was extracted from the plasmid YCp33-PPZ1 (Aksenova *et al.*, 2007) and cloned at BamHI/HindIII sites.

-**pGEX6P-1:** plasmid for bacterial expression of GST (glutathione transferase)-fusion proteins with a PreScission protease site (Amersham Biosciences).

-**pGEX-6P1-Ppz1WT:** plasmid for expression as recombinant protein of the coding region of Ppz1 (Ruiz, Muñoz, *et al.*, 2004).

-**pGEX-6P1-Ppz1 (mutated variants from screen):** All of the mutated versions of *PPZ1* were removed from pRS316-Ppz1 by digestion with BsrGI and BspEI, and the resulting 1.2 kbp fragments were cloned into the same site of plasmid pGEX-6P1-Ppz1WT.

-**pGEX-6P1-Ppz1Cter:** plasmid for recombinant expression of the catalytic domain of Ppz1 (Δ1-344) fused to GST (Ruiz, Muñoz, *et al.*, 2004)**.**

-**pGEX-6P1-Hal3:** plasmid for expression of the Hal3 coding region in *E. coli* as a recombinant protein fused to GST (Ruiz, Muñoz, *et al.*, 2004).

-**pGEX-6P1-Vhs3:** plasmid containing Vhs3 for recombinant protein expression in *E. coli* fused to GST (Ruiz, Muñoz, *et al.*, 2004).

-**pGEX-6P1-SpHal3:** Plasmid pGEX6P1 for expression of the recombinant protein fused to GST, containing the entire SPAC15E1.04 ORF of *S. pombe* (from +1 to 1878 pb) amplified with the oligonucleotides FwSpHal3-pGEXok and RvSpHal3-XhoI (carrying BglII and XhoI-added sites, respectively) and cloned into BamHI and SalI sites of the plasmid.

-**pGEX-6P1-SpHal3-Nter:** Plasmid for expression as a recombinant protein of the N-terminal ORF of *S. pombe* (Hal3-related fragment) fused to GST. The plasmid was made by PCR amplification of the N-terminal region ORF (from nt +1 to 952 bp) with the oligonucleotides FwSpHal3-pGEXok and RvSpHal3-Nterok (carrying BglII and XhoI-added sites, respectively) and cloned into BamHI and SalI sites of the plasmid.

-pGEX-6P1-Pzh1: plasmid for expression of the *S. pombe* Ppz phospahatase (Pzh1) as a GST fusion. The plasmid was generated by PCR amplification of the *pzh1* gene coding region from genomic DNA of the *S. pombe* strain 972 with the oligonucleotides SpPzh1-EcoRI and SpPzh1-XhoI (which contain EcoRI and XhoI-added sites, respectively) and cloned into these same sites of the pGEX-6P1 vector.

-pWS93: high-copy number plasmid for the expression of proteins with N-terminal 3x-HA (haemagglutinin)-tag in *S. cerevisiae* under the control of a strong *ADH1* promoter (*URA3* marker) (Song and Carlson, 1998).

-pWS93-Hal3: allows expression of *S. cerevisiae HAL3* gene under the *ADH1* promoter, producing protein fused to 3-HA epitope (Ruiz *et al*., 2009).

-**pWS93-SpHal3:** pWS93 plasmid containing the entire SpHAL3 ORF SPAC15E1.04 (fragment Hal3 + TS, nucleotides +1 to 1888). The ORF was amplified with the oligonucleotides FwSpHAL3pWS93ok and RvSpHAL3-Xhol (carrying BglII and XhoI-added sites, respectively), digested with the corresponding enzymes and cloned into BamHI and SalI restriction sites of the plasmid. The amplification fragment contains a mutation (864 A→ G) which do not change amino acid sequence.

-**pWS93-SpHal3-Nter:** pWS93 plasmid containing the amino-terminal fragment of the *S. pombe* ORF SPAC15E1.04 (from +1 to +952 pb) amplified with the oligos FwSpHAL3pWS93ok and RvSpHAL3-NterOK (carrying BglII and XhoI-added sites, respectively), and cloned into the BamHI and SalI restriction sites of the plasmid. The amplification fragment contains a mutation (864 A→ G) which not change amino acid sequence.

-**pWS93-SpHal3-Cter:** plasmid pWS93 containing the TS fragment of the *S. pombe* SPAC15E1.04 ORF fused to 3-HA epitope. It was made by PCR amplification of the ORF (from nt +953 to +1878) with the oligonucleotides FwSpTS-pWS93 y RvSpHAL3-Xhol (carrying BglII and XhoI-added sites, respectively) and cloning into BamHI and SalI sites of the pWS93 plasmid.

-pWS93-YKL088w: plasmid that allows protein expression of the *CAB3* coding region fused to 3-HA epitope (Ruiz *et al.*, 2009).

-pET-Duet-1: Bacterial vector for the co-expression of two genes. The vector contains two multiple cloning sites (MCS), each of which preceded by T7 promoter, *lac* operator and ribosome binding site (Ampicillin resistance) (Novagen).

-pET-Duet-1-Ppz1Cter+Hal3: pETDuet1 plasmid for the co-expression of 6His-tagged Ppz1-Cter and Hal3 as recombinant proteins. (*)

-pET-Duet-1-Ppz1Cter R451L +Hal3: Similar to pET-Duet-1-Ppz1Cter+Hal3 containing the inactive version of Ppz1 (R451L) using as a template the YCplac111-Ppz1R451L (pYPC6Z1) plasmid (Clotet et al., 1996).

-pET-Duet1-Ppz1: pET-Duet1 plasmid for recombinant expression in *E. coli* of Ppz1 coding region with 6His tag. The Ppz1 fragment was amplified with the oligonucleotides pDuet PPZ1full_5a and pDuet_ppz1_T1-3 (which contain BamHI and HindIII-added sites, respectively) and cloned into these same sites of the pET-Duet1 vector.

-plasmid A1: cloning vector pET His TEV LIC, is a transfer vector with the ribosome binding site (RBS) to be used as intermediary for polycistronic destination vector (A2).

-plasmid A2: pET empty polycistronic destination vector (2E). This plasmid can express up to five genes at once. Genes must first be cloned into the transfer vector, and then subcloned into any of the five cassettes of the destination vector thus transfering the RBS with the encoding protein.

-A1-HAL3: cloning vector plasmid containing the Hal3 gene encoding region, which was amplified by PCR with the oligonucleotides A1_Hal3_5 and A1_Hal3_3 (carrying NdeI and AsiSI-added sites), and cloned into these same sites of the vector.

-A1-Ppz1Cter x6His R451L: cloning plasmid vector containing the inactive catalytic domain of Ppz1 (Δ1-344) with a 6His tag. (*)

-A1-Ppz1Cter x12His R451L: cloning plasmid vector containing the inactive C-terminal domain of Ppz1 (Δ1-344) with 12-His tag. The plasmid was made similarly to A1-Ppz1Cter

x6His R451L, except that oligonucleotide 5´was A1_Ppz1Cter_5 12His, thus adding 12 His at the N-terminal of the product protein.

-A2-Ppz1Cter x6His R451L: polycistronic vector containing the inactive version of the C-terminal domain of Ppz1 that comes from A1-Ppz1-Cter x6His R451L cloned with the XbaI and BamHI restriction enzymes in the first cassette of the vector.

-A2-Ppz1Cter x12His R451L: polycistronic vector containing the inactive version of the C-terminal domain of Ppz1 that comes from A1-Ppz1-Cter x12His R451L cloned with the XbaI and BamHI restriction enzymes in the first cassette of the vector.

-polycistronic A2-Ppz1-Cter x6His R451L+Hal3: polycistronic vector derived from A2-Ppz1Cter x6His R451L in which the Hal3 coding region was included. (*)

-polycistronic A2-Ppz1-Cter x6His+Hal3: similar to the polycistronic A2-Ppz1-Cter x6His R451L+Hal3 but containing the active catalytic C-terminal version of Ppz1. The plasmid was made by substitution of the relevant Ppz1 fragment with the restriction enzymes BspTI and SacI from pRS316-Ppz1.

-polycistronic A2-Ppz1-Cter x12His R451L+Hal3: polycistronic vector derived from A2-Ppz1Cter x12His R451L in which the Hal3 ecoding region was included. (*)

-polycistronic A2-Ppz1-Cter x12His+Hal3: similar to the polycistronic A2-Ppz1-Cter x6His R451L+Hal3 but containing the active catalytic C-terminal version of Ppz1. The plasmid was made by substitution of the Ppz1 fragment with the restriction enzymes BspTI and SacI from pRS316-Ppz1.

-polycistr TEV: plasmid derived from polycistronic A2- Ppz1Cter x12his R451L + Hal3, in which a TEV-cleavage recognition site was inserted after I27 of the Ppz1-Cter present in the construct (that corresponds to residue I361 of the complete sequence of Ppz1). The insertion of the TEV cleavage site was made by PCR using oligonucleotides Ppz1_TEV_R and Ppz1_TEV_F.

-polycistr TEV Hal3 G490Stop: plasmid derived from polycistr TEV, in which Hal3 lacks the acidic C-terminal tail. The plasmid was made by PCR mutagenesis inserting a stop codon after the G489 Hal3 residue with the oligonucleotides Hal3_G490Stop_F and Hal3_G490Stop_R.

(*) The plasmid was constructed as described in section 12.1 of Experimental procedures.

4. Random mutations and screen for deregulated Ppz1 versions

In order to identify relevant residues for regulation of Ppz1, we developed an approach based on PCR-error prone random mutagenesis followed by a genetic screen that allows identifying hyperactive Ppz1 versions. To this end, a library of mutated catalytic C-terminal domain of the Ppz1 phosphatase was generated by random PCR mutagenesis using the plasmid pRS316-Ppz1 as a template. The method was essentially as described in (Fromant, Blanquet and Plateau, 1995), using $MgCl_2$ at a final concentration of 5.5 mM to minimize the occurrence of insertions and/or deletions. For amplification of the catalytic domain, oligonucleotides 5´-PPZ1_BspEI and 3´-PPZ1_BsrGI were used

because sites BspEI (located at nt 1042 of the ORF) and BsrGI (located 59 nt downstream the stop codon) encompass the *PPZ1* C-terminal half, producing a fragment of 1.2 Kbp. The PCR reaction was made in four different dNTPs conditions, the concentration of the forcing dNTP being 3.4 mM, whereas the others were at 0.2 mM. Then, the four independent PCR products were pooled and purified by phenol/chloroform/isoamyl alcohol extraction, followed by ethanol precipitation. Afterwards, the amplification fragments were digested with BsrGI and BspEI, and cloned into the same sites of the gapped plasmid pRS316-PPZ1. The ligation reaction was performed at 25 °C. Ligation products were introduced into *E. coli* DH5α host cells by electroporation (Inoue, Nojima and Okayama, 1990), using 1-1.5 μg of the ligation to obtain around 1000 – 1500 colonies per plate. Various plasmids were extracted from colonies and subjected to restriction mapping to verify the presence of the insert and it was observed that a large proportion of the library plasmids carried inserts with the correct size. Approximately 25,000 independent colonies were recovered from the plates with a total volume of 3 ml of LB medium, mixed, and stored at -80 as a glycerol stock to create the PCR-based library.

To set up the functional screen in yeast, plasmid DNA from the library (3 ml at 160 ng/μl) was prepared by DNA extraction from *E. coli* (Midiprep kit, Eppendorf) and utilized to transform strain JC010 (*slt2*Δ). One μg of DNA was used for each transformation to yield around 3000 transformants per plate, as determined using control CM plates lacking uracil (CM-uracil). The transformation mixture was plated on Ura^- plates containing 4 mM caffeine (non-permissive conditions). Based on these amounts, around 25000 transformants were finally plated on CM-uracil medium containing 4 mM caffeine and plates were incubated at 28 °C. On the average, around 10-20 clones per plate were able to grow in this condition, generating macroscopic colonies after 48-72 h. These

colonies (180 independent clones) were picked out and grown in CM-uracil liquid medium for an additional 3–6 h in sterile 96-well plates, and they were then spotted for initial characterization (as described in section 5) on CM-uracil plates and in the same plates containing 3, 4 or 5 mM caffeine. The clones that showed a strong phenotype (able to grow at 4-5 mM caffeine), were selected for subsequent analysis. To this end, their plasmids were recovered and amplified in *E. coli*. The constructs were reintroduced into strain JC010, and growth tests were performed (described in section 5) to reconfirm the caffeine-tolerant phenotypes. Clones showing a consistent behavior were considered positives and subsequently subjected to sequencing in search of mutations producing changes in the amino acid sequence of the protein.

5. Growth tests

The sensitivity of different yeast strains to several stresses such as saline (NaCl, LiCl), caffeine, Hygromycin B, Spermine or TMA (tetramethylammonium) was assayed by drop test on freshly prepared YPD or synthetic minimal medium lacking uracil (Ura^-) plates containing different concentrations of the compounds (Posas, Camps and Arino, 1995). Yeast saturated cultures were diluted to an OD_{600} of 0.05 and 3 µl were spotted (plus, in most cases, a 1/10 dilution). Plates were then incubated at 28 °C, except when otherwise specified, for various periods of time. Details about concentrations of the compounds tested and time of incubation are given on the corresponding figure legends.

Tolerance to caffeine was also evaluated by growth test in liquid media performed in plates. Yeast cultures (300 µl) at an initial OD_{600} of 0.05 were grown for 24 hours at 28

°C in synthetic minimal medium lacking uracil supplemented with 4 mM caffeine. Growth was monitored by measuring OD_{600} every 30 min with previous shaking in a Bioscreen C equipment (Labsystems).

Growth under limiting external potassium concentrations was performed using a YNB (yeast nitrogen base)-based medium (Translucent K-free medium; CYN7505-Formedium) formulated so that potassium content in the final medium is negligible (15 μM approx) (Navarrete *et al.*, 2010). Yeast proliferation was evaluated by growth tests in liquid media using 96-well plates. Yeast cultures (300 μl) at an initial A_{600} of 0.004 or 0.008 were grown without shaking for 16-20 h at 28 °C in the Translucent K-free medium supplemented with 1 mM or 50 mM KCl (Barreto *et al.*, 2011). Growth was monitored in a MultiSkan Ascent (*Thermo Scientific*) at 600 nm.

Flocculation measurement was performed as in (Bony, Barre and Blondin, 1998) with some variations. Saturated yeast cultures were deflocculated by two washes in 50 mM Na-citrate pH 3.0, 5 mM EDTA buffer and the cells were resuspended in 5 ml of the same buffer. The optical density was measured at OD_{600}. Afterwards, calcium chloride (at 20 mM final concentration) was added to induce flocculation. Tubes were incubated at 28 °C with shaking for 5 min and left standing vertically for 5 min. A 0.2 ml sample of the suspension was taken (just on the culture surface) and mixed with 1 ml of 0.25 M EDTA pH 8.0 to measure the OD_{600}. The flocculation index represents the ratio between the OD_{600} measured in the fully deflocculated cell suspension and the EDTA-treated supernatant sample after 5 min of settling.

6. Spore analysis

For sporulation, diploid cells containing plasmids were grown in selective medium at 28 °C shaking until saturation. The cultures were centrifuged at 3000 rpm for 5 min at RT, and the pellets were washed twice with H_2O. Then, cells were transferred to liquid sporulation medium and were incubated at 28 °C in a shaker for 5-7 days. The cultures were examined periodically by optical microscopy to monitor the presence of asci.

The analysis of meiotic products was performed by tetrad dissection or random spore analysis. For random spore analysis, 1 ml of sporulated culture was resuspended in 5 ml of H_2O with 10 U of Zymolyase (Arthrobacter luteus, MP Biomedicals) and 10 µl of β-Mercaptoethanol, and was incubated at 28 °C shaking o/n. The culture was centrifuged at 3000 rpm for 5 min, the pellet was resuspended in 1 ml of H_2O and 100 µl of Zirconia/Silica 0.5 mm beads (BioSpec) were added. Two vortex - ice cycles of 1 min were performed and 4 ml of H_2O were added. 1/10 and 1/50 dilutions were plated on plasmid-selective medium and the plates were incubated at 28 °C for 3 days. Then, the colonies were replicated on selective medium plates for the appropriate genetic markers and conjugated with mating type tester strains. To analyze spores by tetrad dissection a standard protocol was followed (Sherman and Hicks, 1991). Fifty µl of sporulated culture was washed with H_2O, and cells were resuspended in 250 µl of H_2O with 12 µl Zymolyase 10 U/ml (from Arthrobacter luteus, MP Biomedicals) and incubated for 10 min at RT. A small volume of the culture was spread as a thin line on YPD-agar. Asci were dissected using a MSM 300 Yeast Dissection Microscope (Singer Instruments). The plates containing the dissected tetrads were incubated at 28 °C for 3 days and to determine the genotype of each spore, haploid colonies were replicated to the appropriate plates for selection.

7. Protein immunodetection

7.1. Sample collection and extracts preparation

Yeast protein extracts for immunodetection were prepared as follows. For *S. cerevisiae* strain AGS9 (*ppz1*) expressing the different versions of Ppz1 (and its corresponding controls), 10 ml of cells were grown at 28 °C in synthetic minimal medium lacking uracil until OD_{600} reached 0.8-0.9 and cells were collected by centrifugation (5 min at 1,228 xg). Protein extracts were prepared as described in (Abrie *et al.*, 2012). Briefly, the cell pellets were resuspended in 100 µl of buffer extraction containing 50 mM Tris-HCl pH 7.5, 150 mM NaCl, 10% Glycerol, 0.1% Triton X-100, 2mM dithiothreitol (DTT), and Complete™ protease inhibitor mixture (Roche Applied Science), and 100 µl of Zirconia/Silica 0.5 mm beads (BioSpec) were added. Cell lysis was accomplished by vigorous vortex (five cycles of 1 minute vortex and 1 minute on ice), and then 50 µl of extraction buffer were added. Samples were centrifuged at 750 xg for 10 min at 4 °C and the cleared supernatants were transferred to new tubes. Protein quantification was performed by the Bradford method (Sigma Chemical Co.) and 40 µg of total protein were used to immunoblotting analysis.

Yeast protein extracts for *S. cerevisiae* strain IM021 (*ppz1 hal3*) expressing the pWS93 multicopy plasmid with the different HA-tagged Hal3 versions were performed following the protocol described above, except that cells were growth in 60 ml of YPD medium. Thus, the volume of extraction buffer was increased to 800 µl and 400 µl of Zirconia/Silica 0.5 mm beads were used.

For *S. pombe* cultures, cells were inoculated at initial OD_{600} of 0.5 in 60 ml of YE medium modified according to the different condition tested (salt stress, H_2O_2, menadione,

t-butyl hydroperoxide, $CdCl_2$, nocodazole, low glucose, low adenine, etc). The optical density was measured to take a sample equivalent to 5 OD_{600} at different times (1h, 3h, 6h. The extracts were prepared following a TCA-based method (Sansó *et al.*, 2008). TCA 100% up to 10% final concentration was added to the collected sample and this was centrifuged for 1 min at 4 ºC at 1500 xg. The supernatant was removed and the pellet was resuspended in 1 ml of TCA 20%, transferred to an Eppendorf tube and centrifuged for 0.5 min at 4 ºC at 16000 xg. The pellet was resuspended in 100 µl TCA 12.5% by pipetting, 100 µl of Zirconia/Silica 0.5 mm beads (BioSpec) were added, and the mixture vortexed for 5 min. The eppendorf was then punched at the bottom to recover the liquid into a new eppendorf by mean of a quick spin. The samples were centrifuged for 20 min at 4 ºC at 16000 xg and the pellet was disaggregated in 1 ml of acetone by physical stirring. After that, it was centrifuged for 5 min at 4 ºC at 16000 xg, the supernatant was removed and the pellet was let dry at 55 ºC for 10 min. Finally, the pellet was resuspended in 50 µl Alkylating buffer (0.1 M Tris-HCl pH 8.0; 1 mM EDTA; 1% SDS) for immunoblot analysis.

7.2. SDS-PAGE and immunoblotting

Protein extracts were mixed with 4xSDS-PAGE loading buffer (125 mM Tris-HCl pH 6.8, 40% Glycerol, 8% SDS, 0.2% Bromophenol blue, 0.1 M DTT), boiled for 5 min at 95 ºC, and resolved by SDS-PAGE. Subsequently, proteins were transferred onto polyvinylidene difluoride (PVDF) membranes (Immobilon-P, Millipore). Membranes were blocked with TBS-Tween 20 (20 mM Tris-HCl pH 7.6, 150 mM NaCl, 0.1% Tween-20) plus 5% of fat-free powdered milk for 1h with gentle agitation. Incubation with the primary antibody (Anti-HA, Covance (MMS-101P-500) or anti-GST-Ppz1 (Clotet *et al.*, 1996)) was performed overnight at 4ºC with mild shaking. The monoclonal anti-HA

antibody was used at 1:1000 dilution in TBS-Tween 20 plus 5% fat-free powdered milk, and anti-GST-Ppz1 polyclonal antibodies were used at 1:250 dilution prepared in the same conditions. Afterwards, membranes were washed three times with TBS-Tween 20 for 10 min and incubated with the secondary antibody for 1h at room temperature and gentle agitation. Finally, membranes were washed three times with TBS-Tween 20 for 10 min. The appropriate secondary anti-mouse or anti-rabbit IgG-horseradish peroxidase (GE Healthcare) were used at a 1:20000 dilution in TBS-Tween 20 plus 5% fat-free powdered milk. Immunoreactive proteins were visualized with ECL Prime Western blotting detection kit (GE Healthcare) and chemiluminescence was detected by an Imaging-System – VersaDoc 4000 MP (BioRad). Levels of specific proteins were quantitated by analyzing the signals in the images using QuantityOne (Bio-rad) or GelAnalyzer softwares after background subtraction. Membranes were stained with Ponceau Red (prior of after antibody incubation) or Coomassie Brilliant Blue (after antibody incubation) to evaluate the amount of charge.

8. Expression and purification of GST-fused recombinants proteins

BL21 DE3 RIL *E. coli* cells (Stratagene), used to express GST-proteins from the plasmid pGEX-6P-1, were grown in LB medium supplemented with 100 μg/ml ampicillin and 34 μg/ml chloramphenicol at 37 °C. Five ml cultures, inoculated from single cell colonies or glycerinated stock, were grown overnight. A dilution 1:10 of these saturated cultures was used to inoculate the appropriate volume for large cultures in the same media. Bacterial cultures were grown in a shaker at 37 °C to an optical density of OD_{600} 0.6-0.8.

At this point, gene expression was induced by addition of isopropyl-β-D-thiogalactopyranoside (IPTG), with different induction conditions depending on each protein. The entire *S. cerevisiae* Ppz1 (also its mutated variants) and its C-terminal domain (Ppz1-Cter), as well as ScHal3, were expressed and purified as previously described (Garcia-Gimeno *et al.*, 2003; Ruiz, Muñoz, *et al.*, 2004; Ruiz *et al.*, 2009) except that induction was carried out, in all the cases, with 0.1 mM IPTG followed by overnight expression at 21 ºC. For Ppz1 and Ppz1-Cter expression the medium was supplemented with 0.5 mM $MnCl_2$. Conditions for *S. pombe* Pzh1 were similar (Balcells *et al.*, 1997), except that the induction was optimized and carried out with 0.1 mM IPTG, overnight and at 25 ºC. Expression of *S. pombe* ORF SPAC15E1.04, and its N-terminal domain (SpHal3-Nter) was achieved with 0.1 mM IPTG and resuming growth overnight at 25 ºC and 21 ºC, respectively, before collection of the cells.

Upon induction, cultures were centrifuged at 6500 xg for 20 min at 4 ºC and pellets were resuspended in Lysis Buffer (20 ml/liter of culture, approximately) that contained 50 mM Tris-HCl pH 7.5, 150 mM NaCl, 10% Glycerol, 0.1% Triton X-100, 2 mM dithiothreitol (DTT), 0.5 mM phenylmethylsulfonyl fluoride (PMSF) and protease inhibitor cocktail (Roche). Cells were then sonicated and centrifuged at 7800 xg at 4 ºC for 10 min, and the supernatant was collected. To purify GST fusion proteins, the bacterial crude lysates were incubated with Glutathione Sepharose 4B beads (GE) for 3-4 h at 4 ºC with mild rotation (300 µl beads for 1L culture approximately). Afterwards, the beads were spun down by centrifugation (750 xg, 5 min) at 4 ºC and were washed 8 times with 500 µl of Lysis Buffer (the two last were made in the same buffer but without Triton X-100). In the case that removal of the GST moiety was necessary, beads containing bound recombinant proteins were resuspended in PreScission Buffer (50 mM Tris-HCl pH 7, 150

mM NaCl, 1 mM EDTA, 1 mM DTT) and treated with PreScission protease (GE Healthcare) according to manufacturer's instructions. Incubation was performed at 4ºC for 16 h in a rotating wheel (Abrie *et al.*, 2012). Subsequently, the samples were centrifuged at 750 xg for 3 min at 4 °C in a Multi Screen 96-well filter plate (Millipore) to recover the eluate, which was made 10% glycerol and stored at -80º C. The amounts of recombinant protein were determined by SDS-PAGE followed by Coomassie staining using different amounts of bovine serum albumin (BSA) as standards (Laemmli, 1970). The gels were scanned with EPSON PERFECTION V500 PHOTO Scan and the protein concentration of the specific proteins was estimated with Gel Analyzer software.

9. In vitro enzyme assays

9.1. Phosphatase activity

Saccharomyces cerevisiae Ppz1 activity assays were performed in 96-well plates essentially as reported previously (Muñoz *et al.*, 2004; Abrie *et al.*, 2012) using *p*-nitrophenylphosphate (pNPP, Sigma) as substrate with buffer 50 mM Tris-HCl pH 7.5, 2 mM $MnCl_2$, 1 mM DTT in a final volume of 300 µl mixture. The amount of catalytic proteins in the assays was 0.6 µg Ppz1 (7.79 pmol) in experiments with the different variants of Ppz1 isolated from the screen; or 1 µg Ppz1 (13.5 pmol) to test the inhibition capacity of the different constructs of SpHal3. In the case of *S. pombe* Pzh1 phosphatase activity determination, 9 pmol of the recombinant protein were used and $MnCl_2$ in the mixture buffer was raised from 2 to 10 mM $MnCl_2$ (Adám et al., 2012). Different amounts of the inhibitors; *S. cerevisiae* ScHal3, *S. pombe* SpHal3 or SpHal3-Nter (indicated in each experiment) were added to the assay mixture and incubated at 30 °C for 5 min. The

reaction started when 10 mM pNPP was added and the assay was carried out for 20 min measuring the absorbance at 405 nm in a UV MultiSkan Ascent (Thermo Scientific). The absorbance of the mixture lacking the enzyme was measured as reference and the value was subtracted from the assay measurements.

9.2. PPCDC activity

In vitro PPCDC assays, based on the formation of the 4 ´-phosphopantheine product were performed by the laboratory of Professor Erick Strauss at Stellenbosch University (South Africa) as described in (Ruiz et al., 2009).

10. Pull-down experiments

To determine the ability of wild type *S. cerevisiae* Ppz1 and its variants derived from the screen, or that of *S. pombe* Pzh1, to interact with ScHal3 or the *S. pombe* related proteins, aliquots of 50 µl of the glutathione agarose beads containing ~4 µg of bound GST-Ppz1, GST-Ppz1Cter or GST-Pzh1 were incubated with protein extracts prepared from strain IM021 (*ppz1 hal3*) expressing HA-tagged Hal3 as described above. The amount of extracts used depended on the expression levels of the relevant proteins. In the case of the bindings to Ppz1 variants, 0.2 mg of protein extracts expressing *S. cerevisiae* HA-ScHal3 were used. For experiments of binding capacity of fission yeast SpHal3 and SpHal3-Nter in comparison to ScHal3, the amount of extracts required was different, to equalize them according to the previously determined specific level of expression. Then, 0.15 mg of

protein extracts from cells expressing ScHal3 were used for binding to GST-Ppz1 (in the case of GST-Ppz1Cter only 0.075 mg was used); for cells expressing *S. pombe* SpHal3 and SpHal3-Nter, 1 and 2 mg were required, respectively. Negative controls were prepared using extracts containing 2.0 mg of proteins prepared from cells carrying the empty vector pWS93.

In all the experiments, the pull-down conditions and analysis were as in (Abrie et al., 2012). Fifty µl of the glutathione agarose beads containing the GST-bound phosphatases were mixed with the appropriated protein extracts and then the volume of the samples was adjusted to the highest volume with extraction buffer without protease inhibitors (50 mM Tris-HCl pH 7.5, 150 mM NaCl, 10% glycerol, 0.1% Triton X-100, 2 mM DTT). The samples were incubated for 1h at 4 °C with gentle rotation and subsequently were centrifuged at 750 xg for 5 min at 4ºC to recover the beads. The beads were then washed 3 times by addition of 200 µl of washing buffer (extraction buffer without Triton-X100) and centrifuged again. The beads recovered were resuspended in 100 µl of washing buffer and 33 µl of 4X Laemmli buffer was added. Samples were boiled for 5 min, centrifuged at 750 xg for 2 min at 4ºC and the supernatant was recovered for SDS-PAGE analysis and immunodetection.

The stoichiometry of the Ppz1-Hal3 complex was evaluated by pull-down experiments using Ppz1 and Hal3 both as recombinant proteins. To this end, glutathione-agarose beads containing 6 µg of GST-Ppz1Cter were mixed with increasing amounts of Hal3 devoid of the GST moiety (0.5- to 6-fold ratio) and then the volume of the samples was adjusted to the same volume with binding buffer (50 mM Tris-HCl pH 7.5, 150 mM NaCl, 10% glycerol, 0.1% Triton X-100, 2 mM DTT and protease inhibitor cocktail (Roche)). The samples were incubated for 1 h at 24 °C with gentle rotation and

subsequently were centrifuged at 750 xg for 5 min at 4ºC to recover the beads with the bound proteins. The supernatants were also recovered to analyze the amount of unbound Hal3. Afterwards, the beads were washed 3 times with 200 µl of washing buffer as described above. Finally, the beads were resuspended in 100 µl of washing buffer, 33 µl of 4X Laemmli buffer was added. Then samples were boiled for 5 min, centrifuged at 750 xg for 2 min at 4ºC and the supernatant was recovered for analysis by 8% SDS-PAGE and stained with Coomassie Brilliant Blue.

11. Cross-linking assays

The ability of Hal3-related proteins to oligomerize was tested by chemical crosslinking with glutaraldehyde as follows. GST-tagged recombinant ScHal3, SpHal3 or SpHal3-Nter were expressed and purified following removal of the GST tag as described above, except that buffers contained 50 mM NaH_2PO_4 (pH7.0) instead of Tris-HCl (which cannot be used for crosslinking experiments). For glutaraldehyde treatment, 50 µl of sample containing 2 µg ScHal3, 3.6 µg of SpHal3, or 10 µg of SpHal3-Nter were treated with 5 µl of 0.2% (for ScHal3) or 0.4% (for SpHal3 and SpHal3-Nter) freshly prepared solution of glutaraldehyde for 20-25 min at 24 °C. The reaction was terminated by addition of 2 µl of 1 M Tris-HCl (pH 7.5) and incubation for 5 min at 24 °C. Cross-linked proteins were solubilized by addition of the appropriate volume of sample buffer (4X) and heated at 95 °C for 5 min. Samples were analyzed on 6% SDS-Polyacrylamide gels and stained with Coomassie Brilliant Blue.

12. Protein preparation and crystallization for X-ray analysis of the Ppz1-Hal3 complex

12.1. Construction of co-expression plasmids.

pET-Duet1-based

Plasmid pET-Duet1 was used for co-expression of Ppz1-Cter (N-terminally fused to a 6-His tag) and of untagged Hal3. The rationale behind this strategy was to affinity-purify Ppz1-Cter by metal affinity chromatography and recover Hal3 by its ability to bind to the phosphatase. The construct was made by PCR amplification of the relevant ORFs. Ppz1-Cter (1.2 kbp) was amplified, using as a template the plasmid pGEX6P1-Ppz1, with the oligonucleotides pDuet_ppz1Cter-5 and pDuet_ppz1_T1-3, which have added AscI and HindIII restriction sites, respectively). A Hal3 fragment (1.6 kbp) was amplified from pWS93-ScHal3 with oligonucleotides pDuet_Hal3_5 and pDuet_Hal3_3 (carrying BglII and XhoI-added sites). The fragments were purified and digested with appropriate enzymes. Ligation in the pETDuet1 vector was performed step-wise: firstly Hal3 was introduced into the BglII and XhoI restriction sites of the MCS2, and subsequently the Ppz1-Cter fragment, digested with AscI and HindIII, was cloned into the pETDuet-1 vector containing Hal3 in these same restriction sites present in the MCS1. The steps of cloning were made in that specific sequence to avoid the inconvenient introduction of restriction sites present in the newly inserted material. The obtained construct, named pETDuet1-Ppz1Cter+Hal3, was first introduced in *E. coli* DH5α host strain from amplification and sequence confirmation. For protein expression, the plasmid was introduced in the BL21 DE3 RIL *E. coli* strain.

Polycistronic vectors

A polycistronic vector for expression of the Ppz1-Cter–Hal3 complex was generated by cloning Ppz1-Cter and Hal3 into the multiple cloning sites of the pET empty polycistronic destination vector (2E) (Addgene), designated A2. This vector allows simultaneous expression of different proteins under the control of a single T7 promoter. Then a single large mRNA is transcribed, and subsequently translated into proteins. However, the vector does not include any ribosome binding site (RBS), so these need to be inserted prior the final cloning step. This is done by using a transfer vector, pET His TEV LIC cloning vector (2B-T) (Addgene), designated A1, which contains a set of restriction sites similar to those present in the A2 polycistronic vector.

The individual genes for A1 construction of Ppz1-Cter and Hal3 were obtained by polymerase chain reaction (PCR) amplification of the relevant DNA. Plasmid pGEX6P1-Ppz1 and oligonucleotides A1_Cter_5_6His or A1_Cter_5_12His and A1_Cter_3 were used to amplify the 1.1 kbp fragment corresponding to the inactive version of the catalytic domain of Ppz1 from YCplac111-Ppz1R451L (Clotet *et al.*, 1996), resulting in the addition of N-terminal 6-His or 12-His fusion tags, respectively. PCR products were digested with NdeI and BamHI (restriction sites added with the oligonucleotides) and then ligated into the NdeI/BamHI sites of A1 vector to produce the A1-Ppz1-Cter_x6His and A1-Ppz1-Cter_x12His plasmids. In all cases the digested DNA was isolated by 0.8% agarose gel electrophoresis, eluted from the gel using a PCR clean-up Gel extraction (Macherey-Nagel) and ligated with Rapid DNA Ligation Kit (Thermo Scientific) following the manufacturer's instructions.

In the same way, pGEX6P1-Hal3 was used as template with oligonucleotides A1_Hal3_5 and A1_Hal3_3, which introduce NdeI and AsiSI restriction sites, to amplify the 1.7 kbp product corresponding to the full length ScHal3, which was cloned into the

corresponding sites of A1 vector, creating A1-Hal3 plasmid. The final polycistronic expression plasmid, polycistronic A2-Ppz1Cter_x6His+Hal3 and polycistronic A2-Ppz1Cter_x12His+Hal3 (both carrying the inactive R451L version of the phosphatase), were created in several steps (Figure 10). Ppz1-Cter N-terminally fused to a 6-His tag or 12-His tag carrying the RBS were subcloned from A1-Ppz1-Cter_x6His and A1-Ppz1-Cter_x12His into the cassette 1 of the A2 vector using the XbaI/BamHI restriction sites. Subsequently, Hal3 was subcloned from A1-Hal3 plasmid as a PspXI/AsiSI fragment into the cassette 2 of the A2 vector containing Ppz1-Cter digested with the same restriction enzymes. This specific sequence of procedures was forced by the appropriate combination of restriction enzymes. The final products (named: polycistronic A2-Ppz1-Cter x6His R451L+Hal3 and polycistronic A2-Ppz1-Cter x12His R451L+Hal3) were used to transform DH5α competent cells. Positive colonies grown in LB/agar plates 30 mg/ml Kanamycin were analyzed by restriction and sequenced to verify the absence of unwanted mutations.

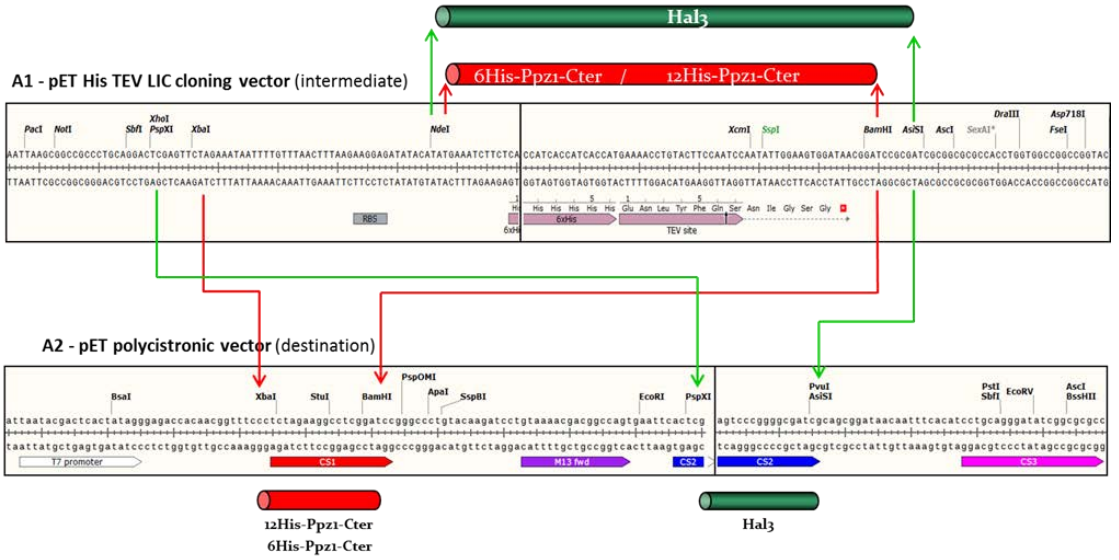

Figure 10. Strategy for His-tagged Ppz1-Cter and Hal3 cloning into the polycistronic vector.

The plasmids were introduced into BL21-CodonPlus-(DE3)-RIL (Stratagene), C41 (DE3), BL21 (DE3) and Rosetta competent cells for expression of the protein complex.

12.2. Protein expression

Expression of recombinant proteins from pETDue1-Ppz1CterR451L+Hal3

Initial tests for protein expression were carried out with 50 ml cultures of BL21 (DE3) transformed with the plasmid (grown from a single colony o glycerol stock) in order to optimize induction conditions. Cultures were grown in LB supplemented with 100 μg/ml ampicillin (vector resistance) at 37 °C until the culture reached a OD_{600} of 0.6-0.8 approximately), at which point IPTG was added to induce expression. The initial variables tested were IPTG concentration and incubation temperature. Conditions varied from 0.05

M IPTG followed by overnight incubation at 37 °C, 25 °C or 18 °C to overnight incubations at 22 °C or 18 °C using 0.01 mM IPTG.

Following small-scale induction optimization, the conditions that yielded best expression were scaled-up. Five ml of LB, supplemented with selection antibiotic (ampicillin), were inoculated from plates or from glycerinated stock and cultures were grown overnight at 37 °C overnight. Ten ml of this culture was used to inoculate 1 L of LB medium supplemented with ampicillin. Growth was continued at 37 °C until an OD_{600} of 0.6-0.8 and gene expression was induced using 0.1 mM IPTG. The culture was then incubated overnight at 18 °C, cells were pelleted at 3642 xg for 1h at 4 °C, and were stored at -80 °C.

Protein expression of polycistronic A2-Ppz1-Cter x12His R451L+Hal3

Preliminary small scale protein expression tests were carried out following an auto-induction method in fifty ml cultures, and three different *E. coli* cell lines were used, BL21 DE3 RIL (Y), C41 (DE3) and Rosetta DE3 to test protein expression. In the case of BL21 DE3 RIL or Rosetta cells an additional selection antibiotic (34 μg/ml chloramphenicol) was used added to ensure the maintenance of the helper plasmids (pRARE and pLysS, respectively).

For large scale protein expression, 50 ml of LB containing 1% glucose were inoculated from plates or from glycerinated stock, supplemented with selection antibiotic (30 μg/ml kanamycin). These primary cultures were grown for 16-18 h in a shaker at 230 rpm at 37 °C and then utilized to inoculate 400 ml of autoinduction medium. The

autoinduction media was prepared with 12 g/l Tryptone and 24 g/l Yeast Extract, supplemented with a mix of salts to yield a final concentration of 25 mM KH_2PO_4, 25 mM Na_2HPO_4, 50 mM NH_4Cl, 5 mM Na_2SO_4 and 40 μM $CaCl_2$. Just prior inoculation this medium was made 0.2 mM $MgSO_4$, 0.5 % Glycerol, 0.05% Glucose and 0.2 % Lactose. A cell density of OD_{600} 0.05 (at least) was the initial inoculum of 400 ml of auto-induction media supplemented, in this case, with 100 μg/ml kanamycin, and the culture was growth with vigorous shaking (230 rpm) at 37 °C to a density of OD_{600} = 0.6-1.2 (approximately 3h). Thereafter, temperature was decreased to 20 °C for additional 48 h. Afterwards, cells were collected by centrifugation at 6500 xg for 20 min at 4 °C and the supernatant was discarded. The cell pellets were washed by resuspending in ice-cold binding buffer (50 mM Tris-HCl pH 8, 100 mM NaCl, 10 mM Imidazole) followed by centrifugation at 4000 xg for 1h at 4 °C. Cell pellets were stored at -80ºC for future use.

12.3. Cell disruption

The cell pellets obtained from pET-Duet1-based expression were resuspended with 30 ml of Lysis buffer (50 mM Tris-HCl pH 7.5, 300 mM NaCl, 10 mM Imidazole, 0,1% Triton X-100) containing Complete EDTA-free cocktail (Roche) and 2 mM PMSF as protease inhibitors, unless otherwise stated. The samples were then sonicated on ice using a Vibra-cell (Sonics and Materials Inc.) equipment for 5-6 minutes (10 seconds on, 10 seconds off) at up to 30% amplitude. The insoluble fraction was then removed by centrifugation at 12400 xg for 30 min at 4 °C to recover the soluble fraction (crude lysate).

The cell pellets from auto-induction expression of polycistronic vectors were diluted with Lysis buffer containing 50 mM Tris-HCl pH 8.0, 100 mM NaCl, 10 mM

imidazole, 0.1% Triton X-100, Complete EDTA-free cocktail (Roche), 1 mM DTT, and Benzonase® Nuclease (Sigma) (1 μl/10 ml) in a volume approximately three times the cell wet weight (i.e. 3 ml/g), resuspended and disrupted at room temperature with a French Press at 1000 psi pressure with the cell homogenizer. The French Press step was conducted thrice for each sample. The cell debris was pelleted by centrifugation in a Beckman J-26 XP Avanti centrifuge at 17000 rpm for 1 hour at 4 °C in a JA 30.50 Ti rotor. The cleared crude lysate was carefully recovered and filtered through 0.45 μm PVDF filters (Millipore).

12.4. Purification of proteins

Purification of pETDue1-Ppz1CterR451L+Hal3

The purification of Ppz1Cter-Hal3 complex expressed from pET-Duet1 plasmid was first attempted using a liquid chromatography system (ÄKTA chromatography system) to optimize the purification procedure. The lysate was loaded on a Ni Sepharose HisTrap HP 1ml column (GE Healthcare). Different buffers with variations in salt concentration, imidazole, etc. were used, and elution was carried out using a gradient running from the starting buffer to 100% buffer elution, in order to monitor imidazol concentrations leading to elution of the complex. The optimized purification protocol was as follows. The sample loaded into a loop was injected at a flow-rate of 0.5 ml/min to a HisTrap column previously equilibrated with binding buffer (50 mM Tris-HCl pH 7.5, 300 mM NaCl, 10 mM imidazole). Afterwards, the column was washed with 20-30 ml of binding buffer at 1 ml/min, and then increasing amounts of imidazole were used to remove non-specific binding proteins. These washes were performed with 8-10 ml of binding buffer containing 30 mM imidazole, followed by 6-8 ml of the same buffer plus 60

mM imidazole and, finally, a wash with 2 ml of buffer plus 80 mM imidazole. Elution of the complex was carried out using 100% buffer elution (50 mM TrisHCl pH 7.5, 300 mM NaCl, 500 mM imidazole) at 1ml/min flow rate. About 15 fractions of 1 ml were collected and 5 mM EDTA and 2 mM DTT were added to each fraction (to avoid aggregation through intermolecular His-nickel coordination due to the His-tag). Occasionally, after this step, samples were stored at 4 °C overnight.

Finally, fractions containing the proteins of interest were pooled and concentrated in a 6 Vivaspin centrifugal concentrators (30 kDa MWCO, Sartorius, GE Healthcare) for subsequent purification steps.

Ion exchange chromatography (IEX)

Protein samples for ion exchange chromatography were concentrated in Vivaspin 6 centrifugal concentrators (Sartorious, GE Healthcare) down to 5-6 ml and then diluted into 40 ml of low ionic strength binding buffer (desalting) to allow binding to the resin.

For Mono Q chromatography purification, 20 mM Tris-HCl pH 7.5, 2 mM DTT, 2 mM EDTA was used as binding buffer. The sample was applied to a Mono Q 5/50 anion exchange column (GE Healthcare) onto an ÄKTApurifier with a flow rate of 1 ml/min. Unbound proteins were removed using 10 Column Volume (CV) of binding buffer. The salt concentration was then linearly increased up to 100% high salt buffer (binding buffer with 500 mM NaCl) in 20 min at 1ml/min flow-rate and 1 ml fractions were collected. After the gradient, the Mono Q column was washed with 5 CV of 2 M NaCl. Samples corresponding to the desired protein peaks were analyzed in 10% SDS-PAGE.

Cation exchange using Mono S 5/50 (GE Healthcare) was performed similarly to Mono Q, except that binding buffer contained 20 mM MES pH 5.5, 2 mM DTT, 2 mM EDTA, and the elution was carried out in the same buffer with 500 mM NaCl.

Size-exclusion chromatography (SEC)

Protein samples for size exclusion chromatography (SEC) were first concentrated to a low volume (500 µl) using Vivaspin 6 concentrator (50 kDa MWCO, to ensure that the complex of ~100 kDa is recovered). Five hundred µl of the concentrated sample were loaded into a loop and injected onto on a Superdex 200 10/300 GL column (GE Healthcare) previously equilibrated with GF buffer (50 mM Tris-HCl pH 7.5, 200 mM NaCl, 2 mM EDTA, 2 mM DTT). Size exclusion separation was carried out at flow rate of 0.5 ml/min, collecting 1 ml elution fractions. Fractions corresponding to the protein peak were pooled and concentrated. Samples homogeneous enough and at sufficient concentration (> 5 mg/ml) were considered suitable for crystallization experiments.

Purification of polycistronic A2-Ppz1-Cter x12His R451L+Hal3 and derived polypeptides

Purification of polycistronic 12His tag-containing constructs was carried out by immobilized-metal affinity chromatography. Gravity flow was used unless stated otherwise. The stationary phase was a sepharose nickel-charged resin (Ni-NTA agarose, Quiagen). Two to three ml of Ni-NTA agarose resin were packed into a plastic column and washed using 5-10 column volumes of milliQ water and equilibrated with 5 CV of binding buffer. Binding buffer contained 50 mM Tris-HCl pH 8.0, 100 mM NaCl, 10 mM Imidazole (equal concentrations that in the lysis buffer). The filtered lysate was then

applied to the Ni-NTA resin and the flow-through collected. Five to ten CV of binding buffer was then applied, followed by 5 CV of wash buffer (binding buffer with 50 mM imidazole) to decrease non-specific binding. Bound proteins were then eluted using 10 ml of elution buffer (50 mM Tris-HCl pH 8.0, 100 mM NaCl, 0.5 M imidazole), with incubation on a roller for 1h and then the eluate was collected. Elution was completed by adding 5 ml of elution buffer and the first and second eluates were combined.

In order to separate the recombinant proteins from its fusion tags, 0.5 mg TEV was added to the combined eluates and the sample was dialyzed for 2 hours at 4 °C with gentle mixing against 2 L of dialysis buffer (50 mM Tris-HCl pH 8.0, 100 mM NaCl). Then, the dialysis buffer was replaced by 2 L of 50 mM Tris-HCl pH 8.0, 100 mM NaCl, 10 mM imidazole and dialysis continued overnight at 4 °C. During the dialysis step, the TEV protease removes the 12-His-tag from the recombinant protein. The residual, uncleaved recombinant protein and the protease were removed by a second passage through a Ni-NTA column, recovering the flow-through in which the proteins without tag are found.

After concentration to 4 ml using Vivaspin 6 concentrator (30 kDa MWCO), the sample was applied to a HiLoad 16/600 Superdex-200 (GE Healthcare) gel filtration column equilibrated in low-salt buffer (50 mM Tris-HCl pH 8.0, 100 mM NaCl; 2 mM DTT, 2 mM EDTA). This step was carried out at 1 ml/min flow-rate in an ÄKTAprime chromatography system, collecting 2 ml fractions. The fractions containing the protein complex were pooled and concentrated as before to a volume of 300 µl to repeat a size exclusion chromatography step on a Superdex 200 10/300 GL column (GE Healthcare). This step was run at 0.5 ml/min flow rate, collecting 1 ml elution fractions. The peak containing the complex protein was concentrated for crystallization trials (section 12.6).

12.5. Concentration measurements

The protein concentration of the eluates was monitored during purification as well as the final concentrations of the purified proteins were determined from the UV absorption at 280 nm with a NanoDrop® ND-1000 Spectrophotometer. Concentration was then calculated using the equation $A_{280}=\varepsilon cl$. Molar extinction coefficients (ε) of proteins were calculated considering their amino acid compositions using "ProtParam" (www. expasy.ch/tools/protparam.html)

To assess the purity of samples, SDS-PAGE (usually 10% polyacrylamide) was used after each purification step, and gels were stained with Coomassie Blue (InstantBlue, Expedeon).

12.6. Crystallization trials

Purified protein SEC eluates were adjusted to 6-14 mg/ml for Ppz1-Cter/Hal3 complex protein using the Vivaspin 6 and 500 concentrators (Sartorius) with a 10 kDa MWCO. The vapour diffusion technique was the main method used for crystallization. Preliminary high-throughput crystallography trials were carried out in sitting drop vapour diffusion 96-well plates in combination with commercially available screen kits. These kits included Crystal Screen PEG/Ion, pEG/Ion 2, and Salt Rx Screen (Hampton Research), JCSG-plus HT-96, PACT-premier HT-96, SG1 screen, Structure Screen 1, ProPlex, Morpheus I, and Morpheus II (Molecular Dimensions), all of them containing 96 different buffer conditions. The reservoir was filled with 200 µl of the screen solution while the

crystallization drop was made by mixing from 200-300 nl protein and 200-300 nl reservoir solution. The Mosquito robot (TTP Labtech) was utilized to create the drops. There are three clefts in each of the 96 compartments of the plate preset for the crystallization drop so up to three ratios protein:precipitant ratios (1:1, 1:2, 1:3; 2:1) could be screened simultaneously if enough material was purified. The plates were immediately sealed with plastic film (3M Hampton Research) or ClearVue covers (Molecular Dimensions) and incubated at 4 °C or 18 °C.

For optimization of crystallization conditions derived from initial screens, 24-well plates for hanging drop vapour diffusion were used to manually set up the selected conditions. The reservoir was filed with 500-600 µl of screening solution and the crystallization drop was made by mixing from 1 to 3 µl of protein and 1-3 µl of reservoir solution. The crystallization drop was placed on a siliconized glass cover slide placed over the reservoir with the drop facing downwards. In some cases, the Mosquito robot was used for producing drops with the optimized conditions. For this, the reservoir was filled with 200 µl of the screening solution, while the crystallization drop contained a mix from different amounts of protein, crystal seeds and reservoir solution to a final volume of 1200 nl. The plates were sealed and incubated at 4 °C or 18 °C.

All plates were inspected immediately after preparation, in order to identify dust particles and to monitor how the proteins react upon the addition of precipitants. These inspections were repeated after 2-3 days and then weekly, under a light microscope. All conditions and changes in the crystallization drops were logged.

In order to obtain better diffracting crystals, the resulting tiny, needle-shaped crystals from the screens were used as seeding material. The micro-seeding method

separates the process of nucleation from that of crystal growth, as the best conditions for each of these processes may differ. In this method, formed fresh crystals are crushed with a small tool and then the seeds (microscopic debris of the crystal) transferred to a pre-equilibrated solution with precipitant concentration just below saturation. The seeding was performed as follows. Firstly 200 µl of the solution of condition to be seeded (in which crystals appeared) was added to a Seed Bead (Hamptom Research) tube. Thirty µl of the same solution was then added directly to the drop containing the crystals and the entire drop was taken by pippeting and added to the Seed Bead tube. This tube was heavily vortex for 90 seconds to break the crystals into tiny nuclei. A dilution series of seeds were performed at 10^{-6}, 10^{-9} and 10^{-12} and diluted and undiluted seed stocks were then applied to the screening plates.

12.7. Diffraction

Crystals large enough to be picked from drops were analyzed. Crystals were harvested and cryo protected prior to plunge freezing in liquid nitrogen. All samples were subsequently analysed at the national synchrotron facility (Diamond Light Source) in the UK. X-Ray analysis revealed that cryo protection in PEG 200 resulted in optimal diffraction.

RESULTS AND DISCUSSION

I) Mutagenesis analysis of the catalytic domain of Ppz1 in search specific residues required for inhibition or binding by Hal3

The Ser/Thr phosphatase Ppz1 is regulated by its subunit Hal3, which binds to the catalytic C-terminal domain of the phosphatase and inhibits its activity. Despite the similarity of Ppz1 with PP1, the regulatory subunit Hal3 is not similar in structure to PP1 inhibitors characterized so far. Although Hal3 contains a sequence that resembles the RVxF motif, typical in many regulators of PP1, previous work demonstrated that this motif in Hal3 is not relevant for the interaction with the phosphatase (Muñoz *et al.*, 2004). Moreover, Hal3 doesn ŧ bind to or inhibit yeast PP1c (Glc7). This indicates a strong specificity and suggests a particular regulatory mechanism towards Ppz1.

1.1. Screening of a random mutagenesis library for deregulated Ppz1 phosphatase versions

With the aim of identify Ppz1 residues involved in the regulation by Hal3, we developed an approach based in a genetic screen in search of deregulated Ppz1 versions, caused by loss of ability to be inhibited by Hal3, and thus resulting in a more active phosphatase in vivo. The strategy is based on the previous observation that *PPZ1* overexpression suppresses the lytic phenotype associated with disruption of *SLT2* (Hughes *et al.*, 1993; Lee, Hines and Levin, 1993; Posas, Casamayor and Ariño, 1993). The *slt2* strain, which is defective in the construction of the cell wall, is prone to lysis under certain stress

conditions, such as the presence of caffeine. Conversely, the absence of Hal3 increases the tolerance to caffeine of these mutant cells. This is caused because increased Ppz1 activity blocks influx of potassium through the Trk transporters, thus decreasing intracellular turgor pressure, which is beneficial cell wall-weakened cells such as the *slt2* mutant (Yenush *et al.*, 2002; Merchan *et al.*, 2004). On the contrary, deletion of *PPZ1* increased sensitivity to caffeine that aggravates the lytic phenotype of a *slt2* MAP kinase mutant (Hughes *et al.*, 1993; Posas, Casamayor and Ariño, 1993).

For this reason, it was considered that *slt2* cells expressing a deregulated Ppz1 phosphatase, due to either being unable to bind to Hal3 or to be inhibited by its regulator, should be able to grow at higher concentrations of caffeine, mimicking the behavior of cells lacking Hal3. Therefore, a PCR-error prone random-mutagenesis of the C-terminal domain approach was devised in a way that a subsequent screen in the presence of caffeine would provide a positive selection for deregulated Ppz1 variants. We anticipated that mutations leading to a selectable phenotype could affect the ability of Ppz1 to bind Hal3 (leading to non-inhibited Ppz1), the ability of bound Hal3 to inhibit Ppz1, or even result in a constitutively hyperactive form of Ppz1, unable to be sufficiently inhibited in vivo by Hal3.

Firstly, the appropriate conditions for the screening, such as the plasmid for construction of the mutant library or the caffeine concentration range to be used, were determined using a *hal3* mutant as test strain. Both centromeric and 2-micron (multicopy) vectors were considered and tested. Finally, the centromeric pRS316 plasmid was used to generate the library, thus avoiding the negative effect in growth caused by high-copy number expression of Ppz1 (Clotet *et al.*, 1996; De Nadal *et al.*, 1998). Different caffeine

concentrations were also examined, ranging from the tolerance of a normal (WT) Ppz1 version (in the *slt2* background) to a hyperactive one (a *slt2 hal3* mutant), which would provide the upper limit tolerance.

The library was created by random mutagenesis PCR of the catalytic C-terminal domain, from residue 351 to the end of Ppz1 (including 59 nt after stop codon of the coding sequence) and inserted in the pRS316 vector. Twenty-five thousand independent clones carrying copies of Ppz1 with increased chance of mutations were recovered to be introduced in yeast cells for functional screening.

The strain JC010 (*slt2*) was transformed with the mutant library (36000 clones approximately) and plated on synthetic medium lacking uracil and containing 4 mM caffeine. At this concentration, *slt2* cells with the native version of Ppz1 cannot grow. However, mutated versions of Ppz1 with enhanced activity will be able to grow, as it is observed for *slt2* cells lacking *HAL3* and expressing the Ppz1 wild type version. Clones able to grow as macroscopic colonies after 72h were selected, and the phenotype of caffeine tolerance of 180 clones was evaluated by drop test on plates with 3, 4 or 5 mM caffeine. Clones that showed strong growth at higher caffeine concentrations (4 or 5 mM) were selected for plasmid isolation, transformation of *E. coli* host and sequencing of the catalytic region of Ppz1 in search of possible mutations. Finally, 36 sequenced clones contained one or more changes affecting the encoded amino acid (table 3 of Annexes). All clones containing a single amino acid change, or those containing two amino acid changes and showing a strong phenotype in this initial screen were selected for further characterization. It must be noted that truncation of the protein by mutations producing

premature stop codons are not expected to be recovered, since the screen is based in a gain-of-function, for which the full size protein should be required.

1.2. Phenotypic characterization of selected mutants

Initially, versions of Ppz1 with single amino acid mutations obtained from the screen were subjected to study, in order to identify important residues involved in the regulatory mechanism of the phosphatase by Hal3. These selected clones and their correspondent nucleotide and amino acid changes are summarized in table 3.

Clone	Nt position	Nt change	AA change			Residue
136	1165	GAA → AAA	Glu	→	Lys	389
99	1282	TTA → GTA	Leu	→	Val	428
125, 126	1504	AAG → CAG	Lys	→	Gln	502
132	1538	ACA → GCA	Thr	→	Ala	513
116	1556	ATC → AGC	Ile	→	Ser	519
124, 139, 143	1724	GAA → GGA	Glu	→	Gly	575
151	1735	AGT → GGT	Ser	→	Gly	579
97, 141	1889	GAA → GGA	Glu	→	Gly	630
149	2053	ACA → CCA	Thr	→	Pro	685

Table 3. Clones containing a single amino acid change in the catalytic domain of Ppz1 selected for characterization. The nucleotide (nt) position in which the mutations are produced are indicated, with the corresponding change of amino acid. At the right-hand the position of the affected residue in the protein is shown.

Phenotypic characterization of these Ppz1 mutated versions was carried out by testing the tolerance to caffeine. All plasmids carrying single amino acid changes, along

with the native Ppz1, were used to transform in a *slt2* strain and compared with the *slt2 hal3* strain in a range of caffeine concentrations (Figure 11).

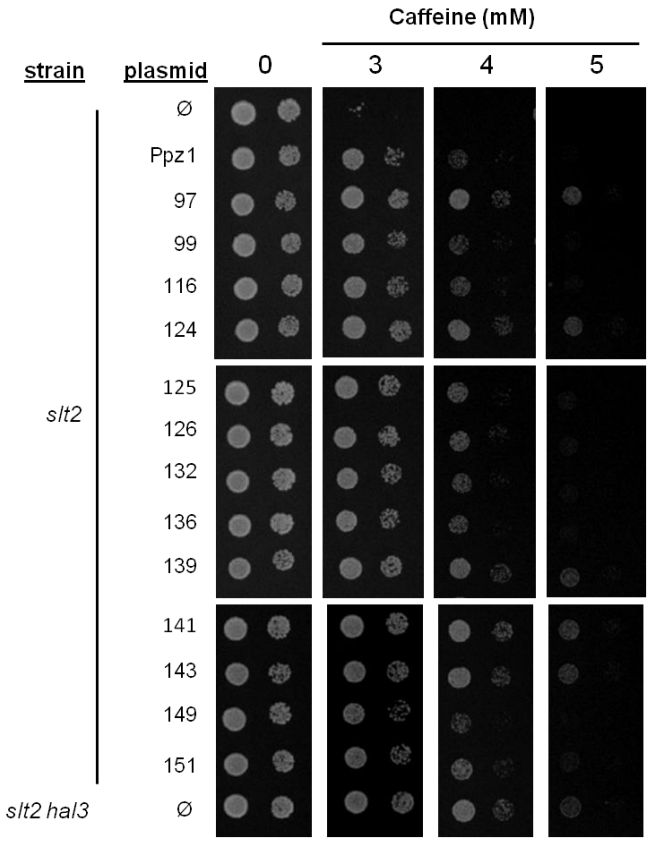

Figure 11. Caffeine tolerance conferred by expression of different mutated versions of Ppz1 carrying single amino acid mutations. The strains *slt2* and *slt2 hal3* were transformed with pRS316 plasmids containing the indicated versions of Ppz1, wild type (Ppz1) or the empty plasmid (Ø) and spotted at OD_{600}=0.05 and at 1/10 dilution, on synthetic media plates lacking uracil containing the indicated caffeine concentration. Growth was monitored after 72 h at 28ºC.

As it can be observed in Figure 11, the potency of the phenotype exhibited by the

different Ppz1 versions was not identical when tested in the *slt2* background. Clone 97 and its equivalent 141, and clone 124 (with its equivalents 139 and 143) displayed a vigorous growth, with a tolerance to caffeine higher than the wild type version of Ppz1 and comparable to that of the cells lacking Hal3 (*slt2 hal3*). Clone 97 carries a substitution of Glu for Gly, at residue 630, whereas clone 124 presents the same change at residue 575. Clones 116 (Ile^{519} to Ser), 125 and its equivalent 126 (Lys^{502} to Gln), 132 (Thr^{513} to Ala), 136 (Glu^{389} to Lys), and 151 (Ser^{579} to Gly) also presented an increase in caffeine tolerance, stronger than that of cells transformed with the native Ppz1, although the phenotype was less noticeable. Clones 99 and 149 did not show an apparent increase to caffeine tolerance in comparison to the wild type phosphatase, despite that they were selected in previous assays.

In addition, growth in liquid cultures in the presence of 4 mM caffeine was carried out to corroborate the behavior of the different clones (Figure 12). The growth pattern was consistent with the plate tests, showing clones 97 and 124 a similar growth rate compared to cells lacking *hal3*. Clones 125, 132, and 151 also showed increase growth rate than cells expressing the wild type Ppz1.

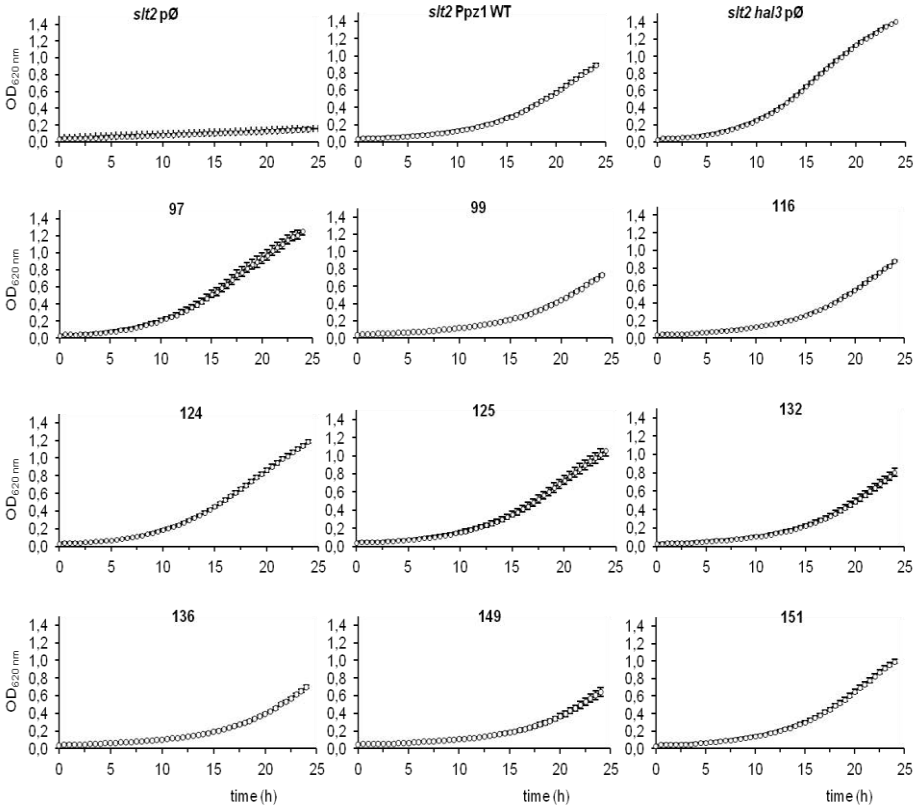

Figure 12. Time-course of growth in liquid medium of *slt2* cells carrying the single mutant variants of Ppz1. The medium (SD lacking uracil) was supplemented with 4 mM caffeine. Growth was assessed over 24 hour at 28 °C by measuring OD_{600} every 30 min in a Bioscreen C equipment (Labsystems). pØ, empty plasmid; WT, wild type.

Taking together these results indicated that in most cases the behavior of these clones for caffeine tolerance was consistent with its selection during the screen.

The *slt2* cells carrying the diverse Ppz1 versions were also submitted to high temperature (37 °C). Under this stress condition, cells lacking MAP-kinase Slt2 are prone

to lysis. However, expression of PPZ1 could relieve the temperature-dependent cell lysis defect of this mutant, similarly as it happens under to caffeine stress (Hughes *et al.*, 1993; Posas, Casamayor and Ariño, 1993). After 48 hours at 37 °C clones 97 and 124 displayed a vigorous growth, while cells containing the Ppz1 wild type version required 65 hours of incubation to present a slight growth. At this time, also clones 125 and 151 were able to grow (data not shown). The behavior observed under this stress condition correlated well with the phenotypes shown in test for tolerance to caffeine.

Ppz1 plays an important role in salt tolerance, since it regulates negatively the efflux of cations such as sodium and lithium by repression of the *ENA1* gene (Posas, Camps and Arino, 1995; Ruiz, Yenush and Ariño, 2003). The absence of regulation of Ppz1, as can be found in the *hal3* mutant, produces cells sensitive to high salt. On the contrary, overexpression of Hal3 confers tolerance to these cations (Ferrando *et al.*, 1995).

The fact that Ppz1 activity has a negative effect on the cells exposed to cations prompted us to consider up to what extent the diverse variants of the phosphatase found in this work could mimic the salt sensitivity of a *hal3* mutant. To test this, the growth of cells carrying the mutated Ppz1 versions and exposed to high concentrations of Li^+ cations was tested. As shown in Figure 13, most of the selected clones presented a tolerant phenotype to this cation below the level of wild type cells. Particularly, expression of clones 97 and 124 presented the strongest phenotype, being these cells even more sensitive to Li^+ than the *hal3* mutant. Also, clone 151 exhibited a noticeable sensitivity to this cation. Clone 125 displayed sensitivity to lithium resembling to that of the *hal3* strain.

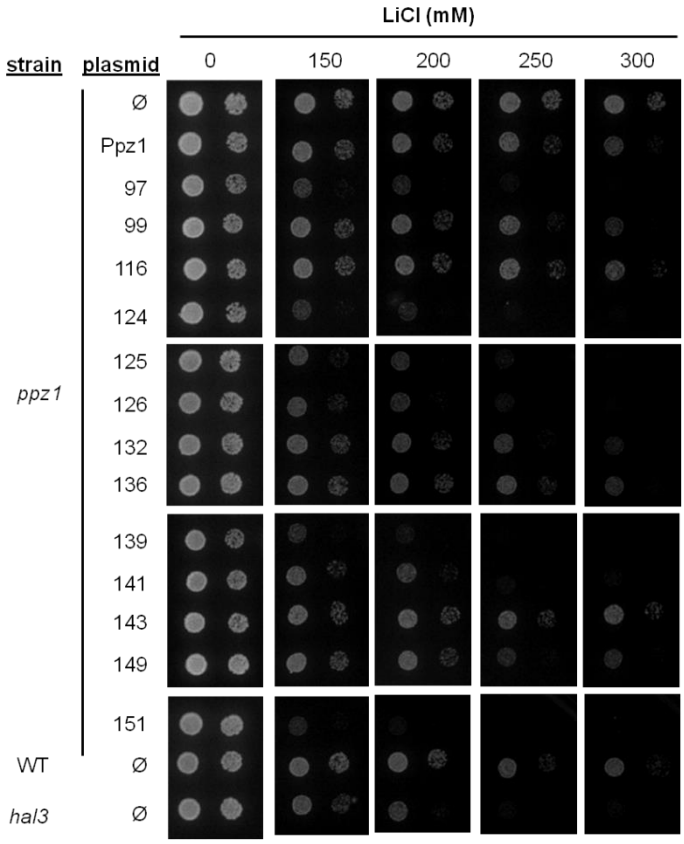

Figure 13. Analysis of salt sensitivity conferred by expression of different Ppz1 versions containing a single mutation. The indicated strains were transformed with the plasmid pRS316 harboring the diverse versions of Ppz1 or an empty plasmid (Ø). Cultures at OD_{600} of 0.05, plus a 10-fold dilution were spotted on synthetic medium lacking uracil agar plates, supplemented with the indicated concentrations of LiCl and incubated at 28 °C. Growth was monitored after 3 days.

All these phenotypes demonstrated that cells bearing the majority of mutant Ppz1 versions behaved as cells devoid Hal3. Then, this observation allows speculating that these Ppz1 variants might be unregulated in the cell, despite Hal3 is present. The variability of the phenotypes observed across the diverse Ppz1 versions studied could be attributed not

only to differences in their regulatory properties *vs* Hal3, but it could be the result of variations in the expression levels of these versions. Therefore, these levels were evaluated by immunoblot experiments in cells lacking native Ppz1. To this end, protein extracts from cultures of the different clones were prepared and analysed using a polyclonal antibody anti-GST-Ppz1 to detect the phosphatase. As shown in Figure 14, all the expressed variants of Ppz1 displayed similar level of protein, which also did not differ from that of the wild type version of Ppz1. Importantly, the levels of Ppz1 expressed from plasmid constructs were quite similar to those obtained from chromosomal expression of native Ppz1 (WT strain). This was not unexpected because the conditions to carry out the functional screen were defined using a centromeric plasmid in which Ppz1 expression is driven by its own gene promoter.

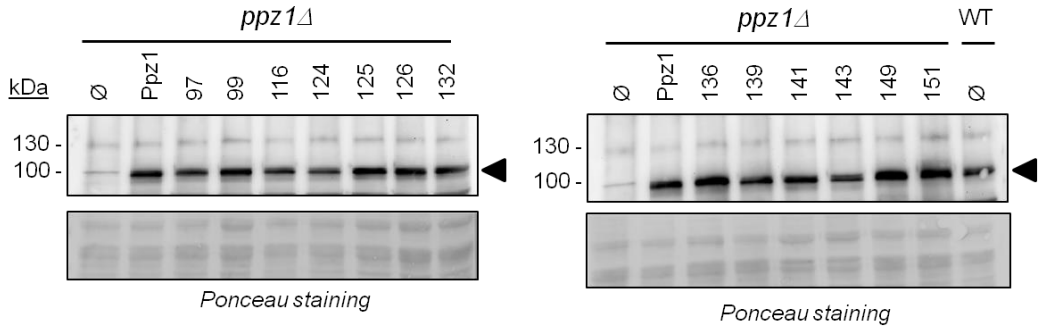

Figure 14. Expression levels of putative deregulated Ppz1 versions in *ppz1* mutant cells. Forty μg of total protein extracts from the indicated strains were resolved by SDS-PAGE (10% polyacrylamide gels), transferred to membranes and proteins were probed with a polyclonal anti-GST-Ppz1 antibody. Ø, empty plasmid; WT, wild type.

These results demonstrated that the different cellular properties conferred by

expression of each of the Ppz1 variants, as deduced from the phenotypes tested, were not caused by variations in the amount of the protein phosphatase, supporting the notion that they were likely due to intrinsic properties of each Ppz1 mutant version.

During the course of the phenotypic assays we observed in *slt2* cells growing in liquid medium a tendency to aggregate when certain Ppz1 versions were expressed. These cultures were analysed by optical microscopy and it was observed that some of them formed large clusters of cells (data not shown). This observation was relevant since hyperactivation of Ppz1 was related to the appearance of a flocculent phenotype that was reminiscent of that observed upon potassium deprivation (González *et al.*, 2013). This is an important feature related to Ppz phosphatases, since the ortholog in *Candida albicans*, CaPpz1, hasd been related to hyphal growth, and therefore with virulence of this pathogen (Adám et. al, 2012). Since Ppz1 inhibits potassium influx, it was reasonable to assume that deregulated forms of the phosphatase could lead to a similar phenotype.

To test this possibility, a quantitative flocculation test was carried out. The ability to flocculate of the *slt2* cells carrying the diverse Ppz1 single-mutation variants was monitored and the flocculation index calculated.

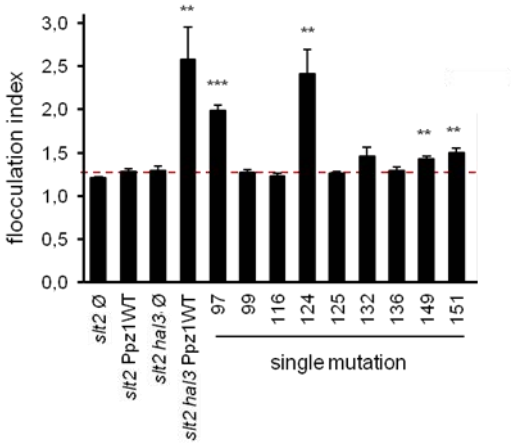

Figure 15. Deregulated versions of Ppz1 induce flocculation in a *Slt2*-deficient background. The indicated strains were transformed with the empty plasmid (Ø), with the wild type version of *PPZ1* (WT), or with the indicated *PPZ1* alleles carrying single mutations, as stated. The flocculation index of the cultures was determined as the ratio of the OD_{600} between the fully deflocculated cell suspension and the EDTA-treated supernatant measured as described in Experimental procedures section 5. Data is presented as the mean ± S.E. from 4-5 independent determinations. Statistical significance was determined by unpaired Student test. (*) $p < 0.05$, (**) $p > 0.01$, (***) $p < 0.001$.

As shown in Figure 15, the expression of the wild type version of Ppz1 in *slt2* cells had no effect on flocculation. However, when the natural inhibitor Hal3 was deleted (*slt2 hal3*), a readily detectable flocculation phenotype was observed, yielding the highest flocculation index. Interestingly, clones 97 and 124 also exhibited a strong tendency to flocculate with an index close to that of the strain that lacks Hal3. The mutated versions 149 and 151 also displayed a statistically significant increase in the flocculation phenotype with respect to the expression of wild type Ppz1, although this effect was less apparent. These results demonstrated that, despite the presence of the chromosomal native Hal3,

some of the mutated versions of Ppz1 can trigger flocculation, suggesting again that Hal3 could no longer inhibit them.

In summary, the functional characterization of these mutated Ppz1 versions in *S. cerevisiae* have shown that the majority of mutations that carried these variants affected the function of the Ppz1 *in vivo*, leading to greater cellular activity in comparison to the wild type phosphatase. The possible increase in Ppz1 activity caused by the mutations was reflected in the function of the PPase on cations homeostasis, either by negative regulation of the expression of *Ena1*- mediated Na^+ extrusion, or by the regulation on the Trk transporters-mediated K^+ influx. This last effect would explain the phenotypes observed in caffeine in absence of *SLT2*, which were the basis of our functional screen.

Nevertheless, the potency of the observed phenotypes was not identical and depended on the carried mutation. Specifically, clones 97 and 124 showed a remarkable behaviour throughout these phenotypic analyses, similar to cells lacking Hal3. These results suggest that these phosphatase versions have lost the ability to be inhibited by Hal3, although it is not excluded that the mutation can produce a phosphatase with a higher-than-normal catalytic activity, in a way that cellular Hal3 would be insufficient to reduce Ppz1 activity to normal levels.

1.3. Determination of the Hal3 inhibitory capacity for Ppz1 mutated versions

Once characterized phenotypically, our purpose was to characterize biochemically the Ppz1 variants, through production of the recombinant protein in *E. coli*. This was an

important issue because, as mentioned above, in addition to an interference with the regulatory Hal3 protein, the observed phenotypes could be attributed to a positive effect of the mutation on the catalytic activity of the phosphatase. To test this possibility the first goal was to evaluate the activity of these Ppz1 versions *in vitro*, in order to compare whether the intrinsic phosphatase activity itself presented differences between these versions.

To that end, purified recombinant proteins of the different Ppz1 variants were used to develop phosphatase activity assays in comparison to wild type Ppz1 using pNPP as substrate (Experimental procedures, section 9). The results showed that none of the mutated forms of Ppz1 displayed significant alterations in the specific activity of Ppz1 (data not shown). Only slight differences were found in the clones 116, 124 and 151, whose activity was even lesser than that of the native protein. These slight variations in the activity displayed by different Ppz1 versions could be due, at least in part, to the fact that the level of purity of the samples precluded an accurate determination of the amount of purified recombinant phosphatase. These slight variations suggested that none of the mutation increased intrinsic Ppz1 activity, therefore discarding that the observed phenotypic effects could derive from the expression of hyperactive forms of the phosphatase.

To assess the capacity of these Ppz1 variants to be inhibited by its regulatory subunits, the phosphatase activity was determined by incubation of stoichiometrically increasing amounts of Hal3 previously to carry out the activity assay. All the Ppz1 variants carrying single mutations were tested and, since clones with identical mutation had a similar behaviour, Figure 16 only shows a representative clone for each different mutation,

(for instance, only 97 is represented, although141 gave equivalent results). As shown in Figure 16, recombinant Hal3 was able to produce a strong inhibition of the wild type Ppz1 phosphatase activity (up to 25-30% of the initial activity) in a dose-dependent manner, as was previously reported (De Nadal *et al.*, 1998). Remarkably, phosphatases present in clones 97 and 124 were largely refractory to Hal3 inhibition. This profile was in agreement with the behavior displayed in the *in vivo* characterization experiments, in which they showed the strongest phenotypic effects. Clone 151 also demonstrated to be refractory to inhibition by Hal3. In the case of Ppz1 proteins from clones 125, 136 and, up to some extent, from clone 149, Hal3 was not able to inhibit their phosphatase activity as effectively as that of the wild type version, although the effect was much weaker compared to clones 97 and 124. Moreover, the same assay was developed using Vhs3 recombinant protein. Vhs3 has been shown to inhibit the phosphatase activity *in vitro* with efficiency similar to that of Hal3 (Ruiz, Muñoz, *et al.*, 2004). Indeed, all Ppz1 tested behaved similarly with Vhs3 than with Hal3 (Figure 1 Annexes). The consistency of the inhibitory pattern of Hal3 and Vhs3 on the different Ppz1 variants suggests that both natural inhibitors share a similar inhibitory mechanism on the phosphatase.

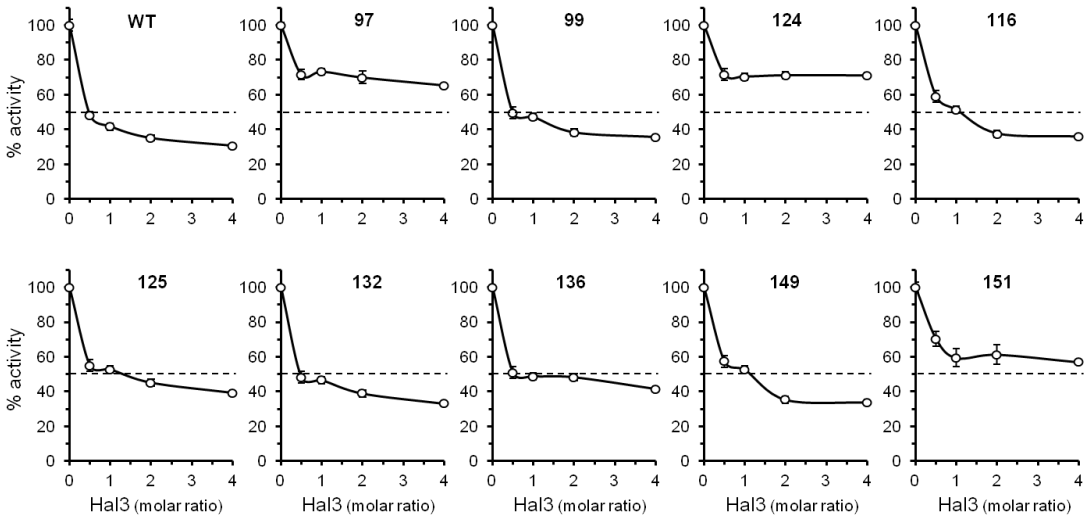

Figure 16. Ppz1 mutated versions show differences in their capacity to be inhibited *in vitro* by Hal3.

Six hundred ng of recombinant Ppz1 versions were incubated in the presence of increasing concentrations of Hal3, and the phosphatase activity was tested using p-nitrophenyl phosphate (pNPP). Data is presented as the mean ± S.E. from 4 to 12 independent experiments and the values are expressed as the percentage of phosphatase activity relative to control without inhibitor. The dashed line at 50% activity is included to facilitate comparisons between panels.

In conclusion, these results demonstrated that the increase in Ppz1 activity was due to mutations that caused a loss in the capacity to be inhibited by Hal3. It is worth noting that there is a good correlation between the in vitro inhibition pattern of the different Ppz1 variants and their behavior in vivo.

1.4. The ability of Ppz1 variants to interact with Hal3

After demonstrating the inability of Hal3 to inhibit efficiently the mutated Ppz1 versions compared to the wild type phosphatase, the possibility that the loss of inhibitory capacity could be due to loss of interaction between these proteins was tested. Two different approaches were used to evaluate the ability of Hal3 to bind to the different phosphatases variants.

First, pull-down experiments were performed by immobilization of recombinant versions of GST-Ppz1 to Glutathione-agarose resin, followed by incubation with HA-tagged Hal3 from a yeast protein extract. Hal3 bound to the affinity system was then detected by mean of SDS-PAGE and immunoblot with a HA specific antibody. Figure 17a demonstrates that Hal3 was immunodetected in equivalent amounts for all the Ppz1 versions tested. The interaction of Hal3 with the catalytic domain of Ppz1 was more effective than the interaction with the entire protein, as it has been reported in previous works (De Nadal *et al.*, 1998; Abrie *et al.*, 2012). Quantification of the Hal3/Ppz1 signal ratio from 3 independent experiments was performed and confirmed that Ppz1 versions bound Hal3 with quite similar efficiency. Therefore, this experiment showed that any of the mutations seemed to significantly alter Hal3 and Ppz1 interaction in vitro and suggested that the effect of the mutations was related to the direct impairment of the inhibitory capacity of Ppz1-bound Hal3.

In order to confirm these findings, a second approach was carried out based in the co-expression of selected His-tagged catalytic Ppz1-Cter variants, together with Hal3, using a polycistronic vector (see section 12 Experimental procedures for details). After affinity purification of Ppz1-Cter using Ni^{+}-based resin, the untagged Hal3 could be only recovered if it was efficiently bound to the phosphatase. The experiment was carried out

using some of the mutant variants, such as 97 and 124, which showed a considerable loss of inhibiting capacity and the strongest phenotypes, together with clones, as 116 and 132, which had weaker phenotypes, and were compared with the wild type version of Ppz1-Cter. The results of the experiment are shown in Figure 17b and confirmed that Hal3 is recovered basically in the same amounts in all cases, independently of the Ppz1-Cter version present in the assay.

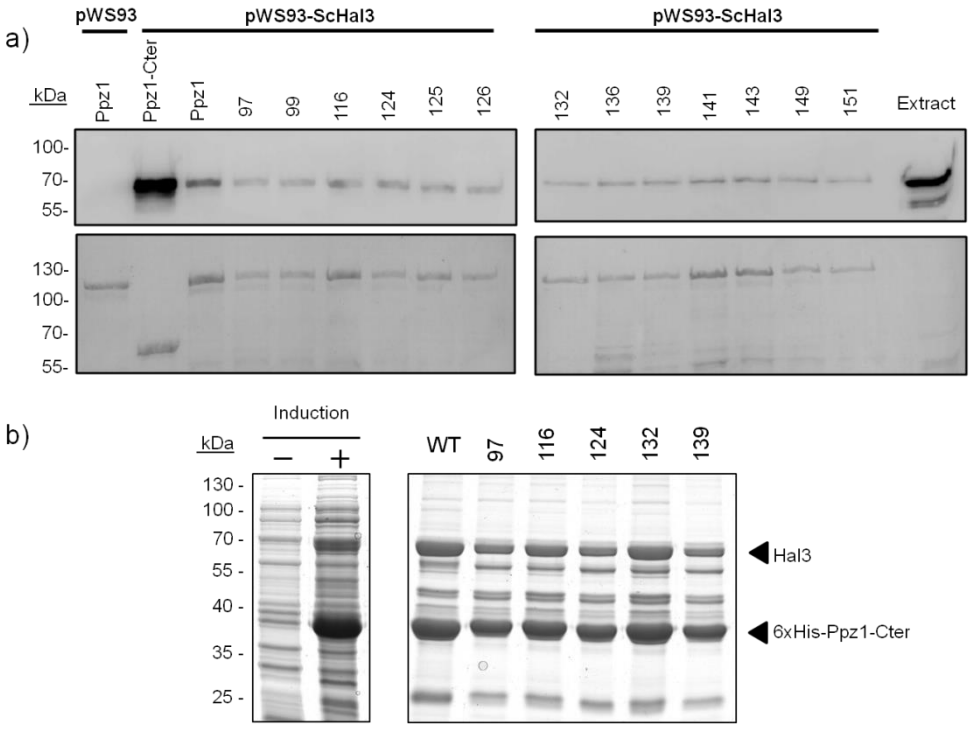

Figure 17. Physical interaction between different mutated Ppz1 versions and Hal3. **a)** Cell extracts (strain IM021, *ppz1 hal3*) carrying 3xHA-Hal3 were incubated with equal amounts of the indicated variants of GST-Ppz1 bound to glutathione-agarose beads. Pull-down assays were performed as described in Experimental procedures (section 10). After washing, the protein content of the beads was analyzed by 8% SDS-PAGE followed by immunoblot using anti-HA antibodies. The lower panel corresponds

to the Ponceau-stained membranes, to reveal the amount of Ppz1. Quantification of the Hal3/Ppz1 signal ratio from three independent experiments yielded values ranging from 0.79 ± 0.09 (clone 116) to 1.22 ± 0.22 (clone 136), with a ratio for native Ppz1 of 1.14 ± 0.14. **b)** Co-expression and co-purification of selected Ppz1-Cter variants and Hal3 in *E. coli*. The 6xHis-tagged Ppz1-Cter versions were co-expressed with untagged Hal3 in a polycistronic vector under the T7 promoter. The left panel shows bacterial extracts corresponding to the wild type version of Ppz1-Cter as an example of expression (-, non-induced; +, induced). The 6xHis-tagged Ppz1-Cter proteins were purified by Ni-NTA agarose affinity chromatography and the protein complex subsequently eluted with buffer containing 500 mM imidazole. Fifteen µl of samples were analyzed by 10% SDS-PAGE and revealed with BlueSafe protein stain.

From these results, collectively, was concluded that the Ppz1 variants harboring the studied mutations did not have affected their ability to interact with Hal3. Interestingly, despite its capacity to bind Hal3 similarly to the wild type Ppz1, most of them were less effectively inhibited. This suggests that the mutated residues are involved specifically in the mechanism of inhibition by Hal3 and allow concluding there are specific structural determinants related to binding to Hal3 and others involved in the inhibitory mechanism. This situation is reminiscent of that observed in a previous functional screen in Hal3, in which independent residues were involved in the mechanism of inhibition and Ppz1 binding (Muñoz *et al.*, 2004).

1.5. Analysis of additional Ppz1 mutated versions

Because numerous alleles found in our screen carried more than one mutation involving changes in amino acid (Table 3 of Annexes), we considered expanding the work by selecting and characterizing four clones containing two mutation that showed a strong

phenotype. Clones 75 and 120 were chosen because they shared a common mutation, the exchange of Val^{605} to Ala (the mutations in clone 75 were also found in 144, and the modifications of clone 120 were present in clones 85, 100 and 140). Another selected double mutant was clone 121, which contained the changes of both Phe^{436} and Phe^{631} to Leu, (identical mutations were found in clones 138, 153, and 168). Moreover, Phe^{631} was the residue following the single Glu^{630} to Gly mutation found in clone 97, which also displayed a strong phenotype. Similarly, clone 129 harboring the mutations Glu^{365} to Gly and Asn^{574} to Ser was also selected, since the modification affecting position 574 preceded the single change characterized in clone 124, also with a strong phenotype (Table 4).

Clone	Nt position	Nt change	AA change			Residue
75, 144	1331	TTC → TCC	Phe	→	Ser	444
	1814	GTT → GCT	Val	→	Ala	605
120, 85,100,140	1070	TTC → TCC	Phe	→	Ser	357
	1814	GTT → GCT	Val	→	Ala	605
121, 138, 153, 168	1306	TTC → CTC	Phe	→	Leu	436
	1893	TTT → TTG	Phe	→	Leu	631
129	1094	GAA → GGA	Glu	→	Gly	365
	1721	AAC → AGC	Asn	→	Ser	574

Table 4. Selected clones with mutations resulting in two amino acid changes. The nucleotide (nt) positions affected by the mutations are indicated, with the corresponding change of amino acid. On the right, the affected residue is shown.

All four clones (75, 120, 121 and 129) were subjected to verification and evaluation for tolerance to caffeine in the *slt2* background. Similarly to versions with single amino acid mutation, these clones were examined by growing in plates with a range of caffeine concentrations as well as by continuous monitoring of growth for 24 hours in liquid

cultures (synthetic minimal medium without uracil supplemented with 4 mM caffeine). The results presented in Figure 18 showed that all four selected clones had a strong phenotype, since were able to grow at least at the same caffeine concentration that cells lacking the inhibitor Hal3 (strain *slt2 hal3*). In fact, clones 75 and 120 presented even a more vigorous growth that this strain at 5 mM caffeine (Figure 18a). Growth in liquid culture confirmed the tolerance to caffeine (Figure 18b).

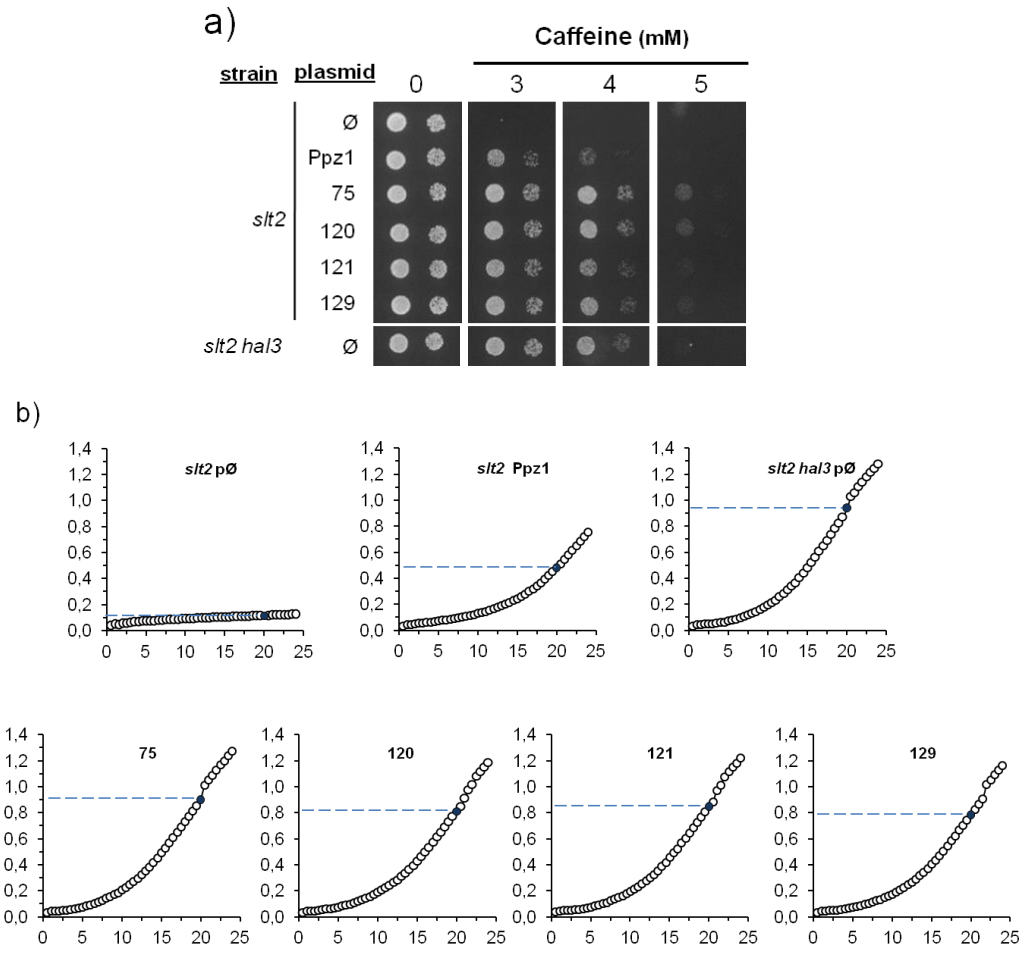

Figure 18. Caffeine tolerance provided by the expression of Ppz1 versions carrying two amino acid mutations. a) Growth on caffeine plates. The indicated strains were transformed with pRS316-based plasmids carrying the indicated versions of Ppz1. Cultures were spotted on plates containing the indicated caffeine concentrations. Growth was monitored after 72 h at 28 °C. **b)** Growth curves of *slt2* cells carrying alleles of Ppz1 harboring two amino acid mutations. Strain JC010 (*slt2*) was transformed with the indicated pRS316-based Ppz1 variants and growth in liquid synthetic medium lacking uracil supplemented with 4 mM caffeine was monitored up to 24 h at 28 °C by measuring OD_{600} every 30 min in a Bioscreen C equipment (Labsystems). pØ, empty plasmid; WT, wild type. For comparison, the absorbance after 20 h of growth is denoted by a blue discontinuous line.

Cells expressing Ppz1 variants carrying two amino acid mutations were also tested for sensitivity to salt. To that end, *ppz1* cells transformed with the plasmids were examined by drop test in presence of LiCl. As shown in Figure 19a, exposure of these clones to high LiCl concentrations resulted in decreased cell growth in all four variants compared to wild type Ppz1. Remarkably, except for clone 121, the sensitivity to lithium was even slight higher than that of the *hal3* mutant.

We also observed that *slt2* cells carrying all four variants when grown in liquid media exhibited clear tendency to aggregation. After quantitative evaluation of the flocculation phenotype (Figure 19b), it was confirmed that all these double mutants showed higher tendency to flocculate than that produced by expression of native Ppz1.

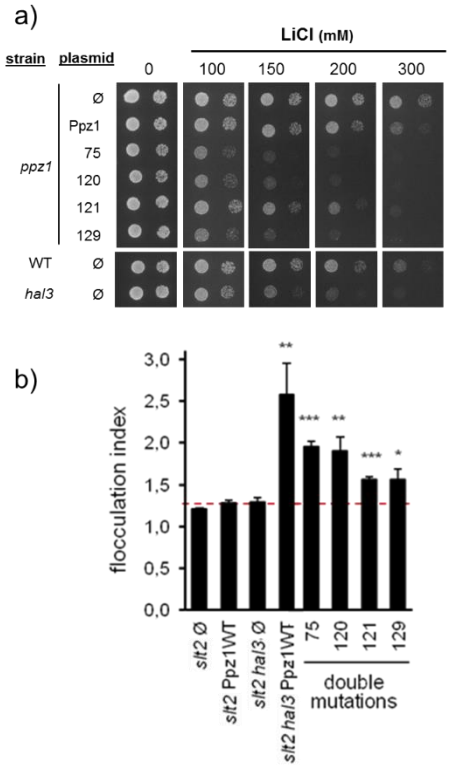

Figure 19. Lithium tolerance and flocculation index of cells carrying selected Ppz1 versions with two amino acid changes. a) The indicated yeast strains were transformed with the diverse versions of Ppz1 or with the empty plasmid (Ø) and cultures were spotted in the presence of various concentrations of LiCl. Growth was monitored after 72 h. **b)** Flocculation index of *Slt2*-deficient cells carrying the indicated Ppz1 versions. The strains were transformed with the empty plasmid (Ø), with the wild type version of *PPZ1* (WT), or with the *PPZ1* alleles carrying two mutations. The flocculation index of the cultures was determined as the ratio of the OD_{600} between the fully deflocculated cell suspension and the EDTA-treated supernatant measured as described in Experimental procedures section 5. Data is presented as the mean ± S.E. from 4-5 independent determinations. Statistical significance was determined by unpaired Student test. (*) $p < 0.05$, (**) $p > 0.01$, (***) $p < 0.001$.

The amount of expressed protein was also examined in order to determine if the phenotypes showed were caused by differences in expression levels respect to the wild type version. Protein extracts from cells expressing the Ppz1 plasmids harbouring the two mutations were prepared and analysed by immunoblot using a polyclonal antibody developed against recombinant Ppz1 (Posas, Camps and Arino, 1995). As shown in Figure 20, no significant variations were found in the amount of expressed protein when the different plasmid-borne mutants, plasmid-borne wild type Ppz1 or the native Ppz1 expressed from its chromosomal locus were compared. Therefore, as previously evidenced for the single mutants (Figure 14), it must be assumed that the different cellular phenotypes observed are due to the intrinsic cellular activity of the Ppz1 versions and not to variations in the levels of the proteins.

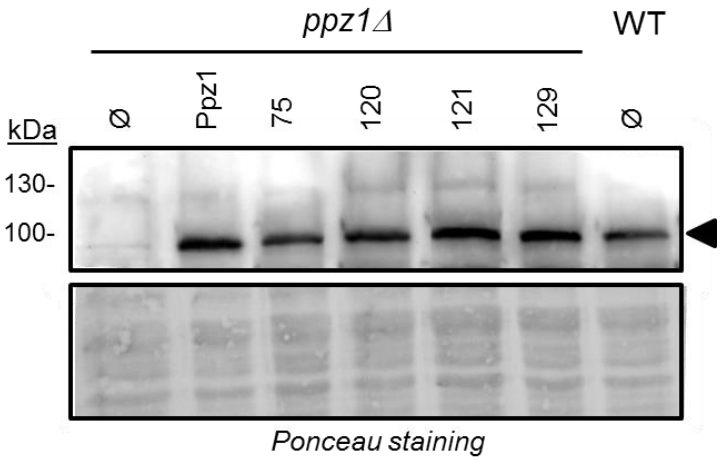

Figure 20. Expression levels of Ppz1 versions containing two mutations. Protein extracts (40 μg) prepared the indicated strains were resolved by SDS-PAGE (10% polyacrylamide gels), transferred to

membranes and proteins were probed with a polyclonal anti-GST-Ppz1 antibody. Ø, empty plasmid; WT, wild type.

In summary, the functional characterization of these mutated versions in *S. cerevisiae*, based on sensitivity to lithium, tolerance to caffeine and increased tendency to flocculation pointed out that the Ppz1 versions containing two mutations were more active in the cell. In fact, expression of these alleles conferred cells phenotypes similar to those of the *hal3* strain.

The ability of Hal3 to inhibit the Ppz1 versions carrying two amino acid changes was evaluated by activity assays with purified recombinant proteins without GST-tag, using pNPP as a substrate. It should be noted that we were not able to perform inhibition experiments with clone 75 since all the attemps to rescue the protein in a soluble form from the glutathione-agarose beads after removing the GST-tag failed. Identical results were obtained when purification of the protein derived from clone 144, which contain the same two mutations, was attempted. Because clones 75 and 120 share a common mutation (Val^{605} to Ala) and clone 120 was successfully purified and active, it is reasonable to assume that the mutation Phe^{444} to Ser specifically present in clone 75 could be responsible for the inestability of the bacterially expressed protein . As Figure 21a shows, the phosphatase activity measured after incubation of these Ppz1 versions with stoichometric amounts of the inhibitor (Hal3) was not inhibited as it was in the case of the wild type version. The Ppz1 version from, clone 120 was not inhibited at all by Hal3, whereas that of clone 121 was clearly refractory to inhibition compared with the native Ppz1. These patterns of inhibition were generally in agreement with the intensity of the

phenotypes observed *in vivo*, with the exception of clone 129, wich was only slightly less prone to inhibition by Hal3 than wild type Ppz1. This was surprising because the phenotypes produced for the expression of the clone 129 in yeast were not too different from those of clone 121.

To test whether the inability of these four Ppz1 versions to be fully inhibited by Hal3 could be caused by loss of binding, pull-down experiments were carried out. Figure 21b showed that all clones containing two mutations had a similar interaction pattern, not distinguishable from that of native Ppz1. Therefore, the presence of these specific two amino acid changes, albeit markedly affected the sensitivity of the phosphatases to the regulator, did not affect their interaction with its inhibitor.

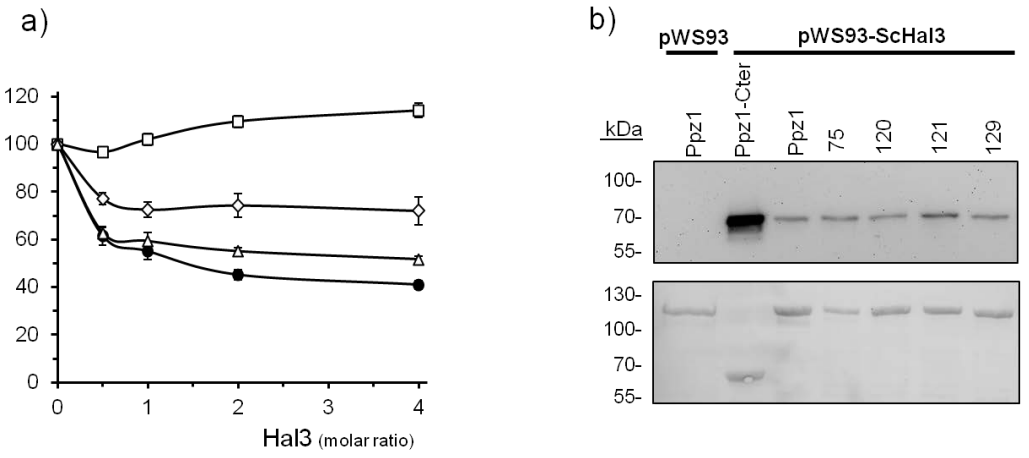

Figure 21. Inhibition profile of Ppz1 phosphatase activity and Hal3 interaction capacity. **a)** Activity assays were carried out using PNPP as substrate as described in Figure 16. Wild type Ppz1 (-●-); clone 120 (-□-); clone 121 (-◊-); clone 129 (-Δ-). Values are means ± SEM for 6 to 10 different assays. **b)** The indicated versions of GST-Ppz1 were immobilized on glutathione-agarose beads and incubated with yeast protein

extracts expressing 3xHA-tagged Hal3. After pull-down, proteins were analyzed by 8% SDS-PAGE followed by immunoblotting using anti-HA antibodies. The lower panel correspond to the Ponceau-stained membrane, to show the amount of Ppz1.

Moreover, these results indicated that, similarly to that observed for Ppz1 variants affected in a single amino acid, the residues in Ppz1 involved in the inhibition were independent of those required for binding. This fact was not surprising, as previous work indicated specific residues in Hal3 required for binding or inhibition (Muñoz *et al.*, 2004).

1.6. Mapping the mutations in Ppz1 and PP1c sequences

The catalytic C-terminal half of Ppz-like phosphatases and type1 protein phosphatase (PP1c) exhibit high sequence identity, and the residues that coordinate the active site are conserved. For that reason, the sequences corresponding to the Ppz1 C-terminal halves of *S. cerevisiae* and *C. albicans* were aligned with the entire PP1 catalytic subunits of *S. cerevisiae* (Glc7) and human PP1c in order to identify the positions of the mutations found in this work and compare them between the different phosphatases. The diverse mutations characterized in this work were mapped in the sequence of *S. cerevisiae* Ppz1 and distinguished in the alignment (Figure 22). Also, residues that define the regulatory motifs in mammalian PP1c, identified as described (Chen *et al.*, 2016) were annotated in the alignment.

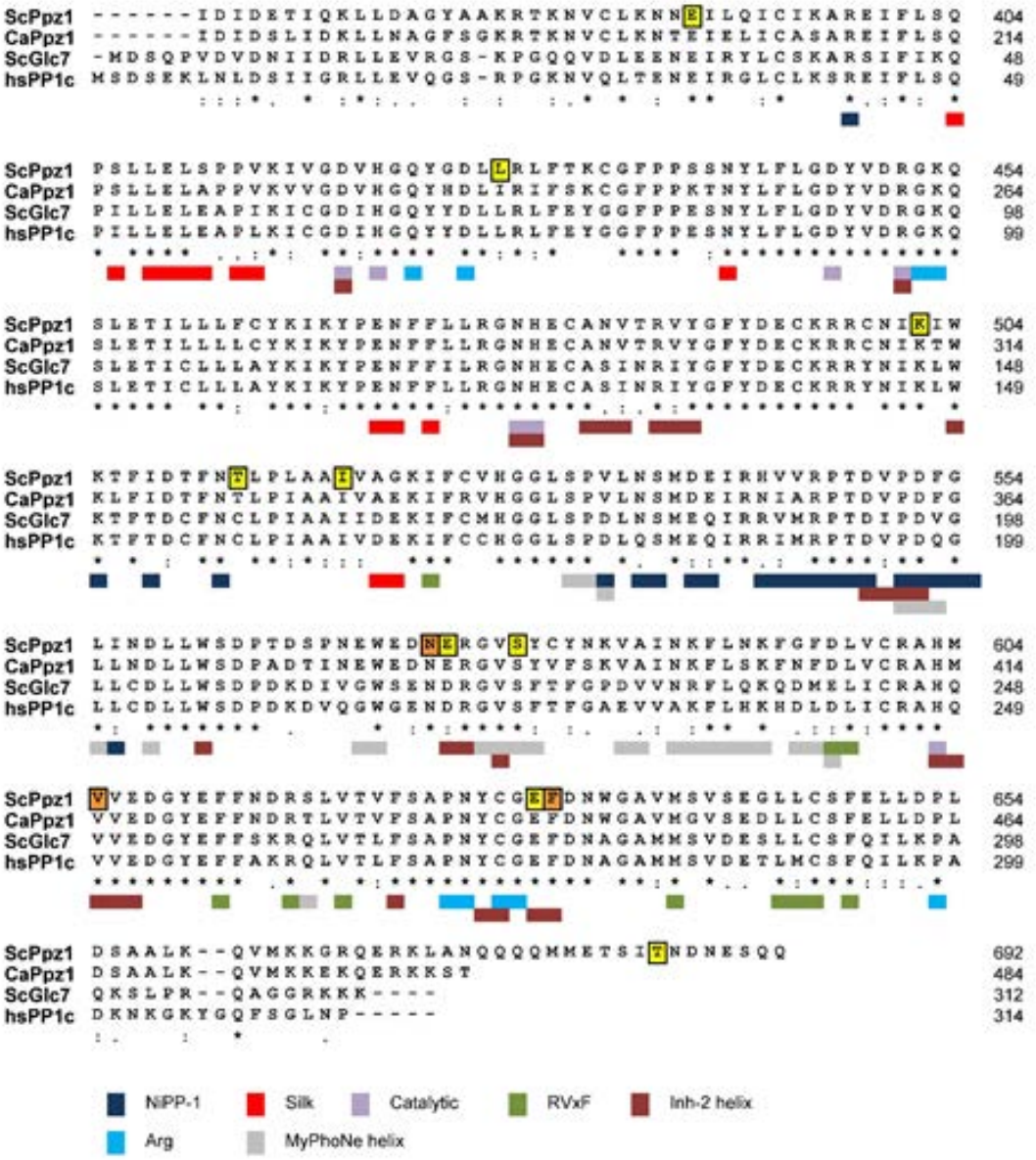

Figure 22. Alignment of the catalytic domains of Ppz1 from *S. cerevisiae* (ScPpz1) and *C. albicans* (CaPpz1), with the yeast (ScGlc7) and human (HsPP1c) catalytic subunit of type 1 protein phosphatase. The positions of the single mutations described in this work are denoted in yellow background, whereas the three relevant mutations found in clones 75, 121 and 129 are in orange. The positions of residues

relevant for interaction with diverse regions of regulators of mammalian PP1c or forming the catalytic site are indicated at the bottom of the sequences using a color code system. Numbering corresponds to the full length proteins.

The most significant docking motif was the RVxF pocket since the interaction residues of this motif are highly conserved between Ppz1 and PP1c, and also, the majority of PP1c regulators contains the RVxF motif (Bollen *et al.*, 2010; Chen *et al.*, 2016). The conserved RVxF-binding motif in Ppz1 has been reported to be functional, since Glc7 regulatory subunits such as Glc8 and Ypi1 displaying an RVxF motif interacted in vivo with Ppz1 (Venturi *et al.*, 2000). Moreover, mutations in the RVxF-like sequence present in Ypi1 abolished the binding to both Glc7 and Ppz1 phosphatases (Garcia-Gimeno *et al.*, 2003). Nevertheless, none of the mutations recovered in the screen affected the hydrophobic surface involved in the binding to RVxF motifs. This was not unexpected, since it was previously reported that mutations in the ^{263}KLHVLF^{268} sequence present in Hal3 (affecting H^{265} or F$^{268)}$, which resembles a RVxF motif, did not affected the ability of the regulator to bind to or inhibit Ppz1, thus suggesting that this sequence was not relevant for interaction with Ppz1 (Muñoz *et al.*, 2004). Moreover, there is evidence that Hal3 does not bind or inhibit in vitro Glc7 (De Nadal *et al.*, 1998; Garcia-Gimeno *et al.*, 2003). According to these observations, Hal3 must interact with Ppz1 by means of other structural elements, likely highly specific for this phosphatase, different of the RVxF motif.

Another binding motifs are rather conserved between PP1c and Ppz1 phosphatases, although to a lesser extent, such as SILK and MyPhoNE binding pockets (Chen *et al.*, 2016) and were also represented in Figure 22. The most different was the ϕϕ

interaction site, suggesting that PP1 regulators that contain a ϕϕ motif should bind Ppz1 with lower affinity than PP1c, or do not bind at all.

Sequence comparison of the mutated residues that produced Ppz1 versions refractory to inhibition by Hal3 indicates that, in general, the affected residues did not coincide with known PP1c regulatory motifs. Notably, the exceptions were Glu^{575}, Val^{605}, Glu^{630}, and Phe^{631}, which corresponded to PP1c residues (Glu^{575} being an Asp residue in PP1c) known to interact with the Inhibitor-2 helix. Interestingly, these mutations were found in clones 97, 124, 75, 120 and 121 (Table 3 and Table 4) which exhibited the strongest phenotypes for a Ppz1 function *in vivo* and were clearly refractory to inhibition by Hal3.

Inhibitor-2 was the first protein phosphatase regulator identified. The molecular basis by which Inhibitor-2 modulates the function of PP1 were established by resolution of the 3D structure through co-crystallization (Hurley *et al.*, 2007). This regulatory subunit is a disordered protein (as many PP1c interactors are), which seems to acquire structure when forms a complex. It has been reported that Inhibitor-2 establishes interaction with PP1 at three different sites. The first site comprises the characterized binding motif SILK, although the sequence is degenerated. This motif binds primarily to a surface in the PP1c subunit and can promote other interactions. A second interaction with PP1 is mediated by the typical RVxF motif present in most PP1c regulators. This docking site is located at some distance from the catalytic center. Remarkably, a third interaction region occurs between the residues 130 – 169 of Inhibitor-2 and the region surrounding the active site of PP1c. This interaction appears to be the responsible for the inhibition of PP1c since results in the displacement of the metal ions required for the catalytic activity.

The observation that Ppz1 mutations that abolished the capacity of Hal3 to inhibit the phosphatase lied in the equivalent region of PP1c that interacts with the third motif of Inhibitor-2 suggests that the inhibitory mechanism could be similar. This is in agreement with the observation that Ppz1 phosphatases activity could be affected in vitro by Inhibitor-2, although Ppz1 enzymes were clearly less sensitive to Inhibbitor-2 than PP1c (Posas *et al.*, 1995; Chen *et al.*, 2016).

In order to place the relative position of the mutations characterized in this work in a 3D-structure of the protein, a tridimensional model of the *S. cerevisiae* Ppz1 C-terminal domain was created based in the recently solved 3D structure of the catalytic domain of the *C. albicans* homolog. As shown in Figure 23, all the functional relevant mutations were located at the surface and on the same side of the phosphatase, which corresponds to the access to the catalytic site.

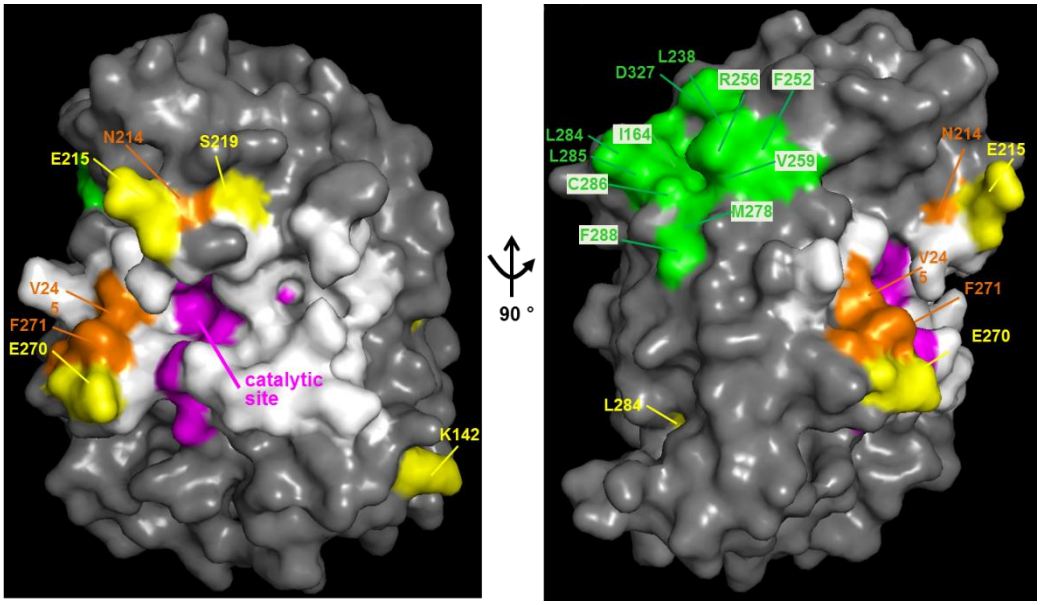

Figure 23. Mapping mutations and functional elements on a structural model of the C-terminal catalytic domain of ScPpz1. The relevant mutations described in this work are highlighted in yellow and orange. Residues involved in the catalytic mechanisms are pink, and the conserved hydrophobic groove implicated in binding to RVxF-containing regulatory subunits is denoted in green. Residues identical or similar to those involved in the interaction of mammalian PP1c with Inhibitor-2 α-helix described in the text are highlighted in white. The first residue in the model corresponds to residue 361 of the full length Ppz1 protein. Note that E215, V245, E270, and F271, as well as diverse residues in the catalytic site, although not depicted in white, are also involved in PP1c interaction with Inhibitor-2.

The location of the mutated residues is in close vicinity to the catalytic site could explain why they were relevant in the modulation of the phosphatase activity by the inhibitor Hal3. It must be noted that the PP1c binding channel where Inhibitor-2 helix binds is strongly conserved in fungal Ppz1 proteins. Therefore, it could be hypothesized that the inhibitory strategy of Hal3 on Ppz1 might mimic that for Inhibitor-2 on PP1c, where Hal3 would occlud the catalytic active site of the phosphatase and then cause the inactivation of Ppz1. However, the recognition of the Ppz1 phosphatase must differ from that of PP1c, since Hal3 is not interacting through a RVxF motif. It should be noted that the presence of the unstructured N-terminal domain in the Ppz1 phosphatase, which is absent in PP1c, could represent a significant difference, as this domain might block certain interactions with existing binding sites, as has been recently suggested (Chen *et al.*, 2016).

The knowledge of the inhibitory mechanism of the Ppz phosphatases becomes particularly relevant, since Ppz-like phosphatases are also found in pathogenic fungi, such as *Candida albicans*, with a high degree of conservation as far as the catalytic moiety is concerned. Taking into account that the 3D structure of this phosphatase domain has been resolved and that the residues involved in the inhibitory mechanism are conserved, this

could provide the foundation for the design of peptides or small moleculaes that could target this region in order to modulate its activity. Similar studies have been carried out in the past with PP1 phosphatases (Guergnon *et al.*, 2006; Tappan and Chamberlin, 2008; Bollen *et al.*, 2010; Chatterjee *et al.*, 2012; Chatterjee and Köhn, 2013). One approach could be the design of small molecules that prevent Hal3 from blocking these residues near the active site without occluding the active site, then providing an active Ppz phosphatase. Should the increase of Ppz1 activity be detrimental for yeast cell growth in fungal pathogens as it is in *S. cerevisiae* (Clotet *et al.*, 1996; Makanae *et al.*, 2013) such intervention might have antifungal properties. An alternative strategy would be the design of small molecules that, when bound to these residues, would block the phosphatase activity. In should be stressed that the case of *C. albicans* it has been demonstrated that the absence of Ppz1 activity resulted in reduction of virulence (Adám et. al, 2012). In conclusion, gaining insight into the regulatory mechanism of Ppz1 should be a relevant step to in the evaluation of Ppz phosphatases as possible relevant antifungal targets.

CONCLUSIONS

1) A mutant library was generated by random PCR-mutagenesis of the catalytic C-terminal domain of Ppz1 that, in conjunction with a functional screen carried out in the *slt2* background allowed to select versions that were, putatively, incapable to be regulated by Hal3.

2) The *in vitro* characterization of 13 Ppz1 variants found in this work demonstrated that these mutations affected the capacity of Ppz1 to be inhibited by Hal3, but not the interaction with the regulatory protein.

3) Mapping of the mutations in a ScPpz1 3D structural model revealed that those with the highest effect on Ppz1 function lay in the surface of the phosphatase and correspond to the region in PP1c that interact with the docking site 3 of Inhibitor-2 and is responsible for the inhibition of the phosphatase.

4) None of the mutated residues are located in the region of the phosphatase that interacts with the RVxF motif found in many PP1c regulatory subunits, in agreement with the previous observation that the RVxF-like motif found in Hal3 is not relevant for its inhibitory function.

5) We postulate that the mechanism of inhibition of Ppz1 by Hal3 mimics in part the strategy by which Inhibitor-2 acts on PP1, that is, by occluding the active site of the phosphatase. However, the mechanism of recognition of Ppz1 by Hal3 differs from that of Inhibitor-2 (and most PP1 regulatory subunits), being the interacting elements still unknown.

II) Purification and crystallization of the Ppz1/Hal3 complex for X-ray crystallography

Visualization of the three-dimensional structure of biological macromolecules provides information to understand how the proteins operate at the molecular level. The Ppz1 phosphatase shares homology in its catalytic domain with PP1c, which structure has been defined, often in combination with regulatory polypeptides. Therefore, models of Ppz1 C-terminal domain can be made based on PP1c or, more recently, using the structure of the C-terminal domain of *Candida albicans* Ppz1, which has been resolved a few months ago (Chen *et al.*, 2016). However, Hal3 does not structurally resemble to any PP1 regulatory subunit. Moreover, the structure of the Hal3 homolog in *Arabidopsis thaliana*, resolved more than a decade ago (Albert *et al.*, 2000), is not useful to develop a model of the whole budding yeast Hal3 protein, since ScHal3 contains an N-terminal extension of about 250 residues and an acidic C-terminal tail that is not conserved in higher eukaryotes. The absence of similarity between Hal3 and regulatory subunits of phosphatases, together with the fact that Hal3 does not bind or inhibit in vitro yeast PP1c (Garcia-Gimeno *et al.*, 2003), suggest that the mechanism of Ppz1 regulation by Hal3 could be specific and different from that of PP1c enzymes. Despite that residues in Hal3 relevant for the inhibitory capacity or involved in the interaction with Ppz1 have been identified (Muñoz *et al.*, 2004), and that several residues in Ppz1 relevant to the inhibition by Hal3 have been recognized in this work, the molecular bases of this regulation are still unknown. Therefore, we considered that the determination at atomic resolution of the three-dimensional structure of the Ppz1/Hal3 complex should yield novel insight into the interaction between both proteins and highlight the basis of the inhibition mechanism.

X-ray crystallography is the prevailing biophysical method for determining the detailed three-dimensional structure of proteins and protein complexes, as a key step to elucidate the mechanisms of action and determine interactions between proteins or substrates. The method is based on the diffraction of a beam of electro-magnetic radiation (X-rays) caused by a crystal consisting of an orderly, repeating pattern of many identical molecules. The principle is to grow suitable well-ordered and homogenous protein crystals that are big enough without impurities and shoot them with an intense X-ray beam (Nobbmann and Bergfors, 2009). The resulting intensities and directions of the diffracted beams (scattering) is recorded and the resulting data can be used in molecular modeling.

The structural analysis by X-ray crystallography requires extensive preparations, ranging from protein expression to purification and, finally, crystallization. Hence, the main goal of this work was to obtain samples of highly homogeneous and concentrated Ppz1 and Hal3 purified proteins forming a complex. To this end, different co-expression methods were chosen for production of recombinant proteins in *E. coli*. Co-expression is widely used for proteins that form a complex, because it allows in vivo assembling of the complex and offers the possibility of co-folding together with their protein partners that would otherwise be insoluble if expressed alone. (Romier *et al.*, 2006; Stefan *et al.*, 2015). In our case, co-expression was an interesting option, since Hal3 presents large predicted unstructured regions, which were considered that might be stabilized by the interaction with Ppz1. The strategy for purification was the expression of His-tagged Ppz1 and recovering of the expressed Hal3 (untagged) on the basis of its capability to bind to the phosphatase. Because previous observations demonstrated that Hal3 binds more intensely to the C-terminal domain of Ppz1 when the phosphatase lacks its N-terminal segment (De Nadal *et al.*, 1998; Abrie *et al.*, 2012), only the catalytic C-terminal domain was used for

cloning into the expression vectors, Moreover, the large unstructured N-terminal half of the phosphatase could compromise the stability of the protein and make the protein less likely to self-organize into a crystal (Deller, Kong and Rupp, 2016).

2.1 Optimisation of expression and purification of the Ppz1-Cter/Hal3 complex from *E. coli*

Both Ppz1-Cter and Hal3 were cloned into two different MCS of the pET-Duet1 vector for expression in *E. coli*. This vector encodes a N-terminal His-tag sequence with no cleavage site that preceded the Ppz1-Cter encoding sequence. The conditions for induction were investigated to maximize production of the recombinant proteins. To that end, initial tests were carried out in small cultures and induction initiated by addition of IPTG. Several induction conditions (varying temperature and IPTG concentration) were tested to improve the level of expression. Successful co-expression of Ppz1-Cter and Hal3 from the pET-Duet1 construct in BL21 cells was attained in cultures induced overnight with 0.1 mM IPTG at 18 °C, as bands at the expected MW for His-Ppz1 (~40 kDa) and for Hal3 (~70 kDa) that were not present in non-induced cultures were detected by SDS-PAGE upon induction (data not shown).

The optimized conditions for the co-expression of the Ppz1Cter/Hal3 complex were applied to scaled-up cultures of 1 L. Cells pellets were lysed in Tris-based buffer containing 300 mM NaCl and 10 mM Imidazole for purification by IMAC. Optimization of the purification was carried out in packed IMAC resin columns (HisTrap 1ml FF) using the AKTA purification system. Once the supernatant had been applied to the column, two wash steps were done to remove non-specific bound proteins, followed by elution using

an imidazole gradient (up to 0.5 M). Figure 24 shows the SDS-PAGE analysis of the IMAC purification. His-tag Ppz1 was efficiently bound to the IMAC resin and allowed recovering the interacting Hal3, although elution of the complex started at 250 mM imidazole and continued until the end of the gradient. It should be noted that even though the wash with 50 mM imidazole removed some unspecific band, the desired proteins were still accompanied by significant amounts of contaminating proteins, likely proteolytic fragments of the recombinant polypeptides or interacting *E. coli* proteins. The observation that the recombinant proteins eluted along the imidazole gradient and none of the eluted fractions contained lesser amounts of contaminants determined to perform a direct elution step with 500 mM imidazole for future purifications.

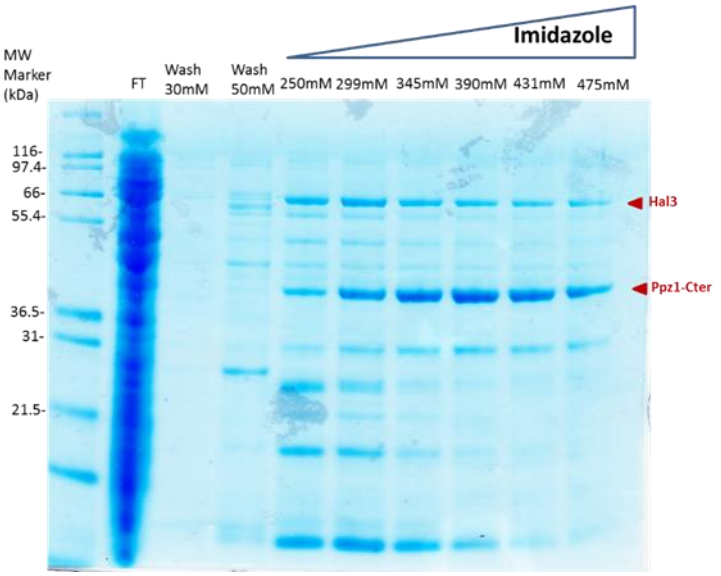

Figure 24. IMAC purification of the His-tagged Ppz1-Cter/Hal3 complex. 1 litre of culture expressing pET-Duet1-Ppz1-Cter/Hal3 was recovered, and cells were lysed and the sample purified using a HisTrap column and an AKTA system. After loading in binding buffer (50 mM Tris-HCl pH 7.5; 300 mM NaCl; 10 mM Imidazole), the samples were washed with binding buffer containing 30 and 50 mM imidazole. Arrows indicate the position of the recombinant His-tagged Ppz1-Cter and co-purified Hal3.

Because the presence of numerous contaminant bands present in the samples recovered from IMAC, the first steps in the study were focused on establishing protocols that would allow improving the purification of the Ppz1-Cter/Hal3 complex to a level suitable for crystallization.

A problem associated to the use of polyhistidine affinity tags is nonspecific binding of untagged proteins, due to the fact that some cellular proteins contain two or more adjacent histidine residues. Because of their affinity for the IMAC matrix, these proteins may coelute with the protein of interest, resulting in significant contamination of the final product. The addition of salt (up to 500 mM NaCl) can reduce nonspecific protein interactions. Then, one approach was to increase the NaCl concentration, in order to avoid weak electrostatic interactions of other proteins with the protein of interest or the column. Moreover, to reach higher purity, additional purification techniques such as ion/size exclusion chromatography could be considered.

Taking this into account, the next approach was a IMAC purification procedure followed by SEC including 500 mM NaCl in all buffers. The elution fractions of the His-tag purification are shown in Figure 25A. The presence of 0.5 M NaCl in the binding and elution buffers did not improve purity of the proteins samples. In fact, more unspecific bands were detected in SDS-PAGE analysis. Some of these could correspond to chaperone interactions since these common contaminants such as DnaK (70 kDa) or DnaJ (40 kDa) interact and co-elute during Ni-affinity chromatography in high salt concentration. A second purification step, size exclusion chromatography, was utilized to remove unspecific contaminants on the basis of their size. The column was also equilibrated with buffer containing high salt concentration to reduce electrostatic interactions and the sample

(pooled elution fractions from IMAC) was run (Kamberi *et al.*, 2004). As it can be observed in Figure 25B, the chromatogram showed two major peaks, indicatives of heterogeneity in the samples. Both peaks were analyzed by SDS-PAGE and it became evident that Peak 1 contained Hal3 and Peak 2 was enriched in 6His-Ppz1-Cter. Therefore, it was apparent that during the purification process the complex dissociated, which correlated with the volume of elution in the gel filtration, according to the size of each individual protein. In conclusion, increasing salt concentration to 0.5 M NaCl in the purification steps not only did not improve the purity of the samples, but dissociated the complex yielding Hal3 and Ppz1-Cter as individual proteins, probably due to the fact that the increase of ionic strength reduces important electrostatic interactions between both proteins.

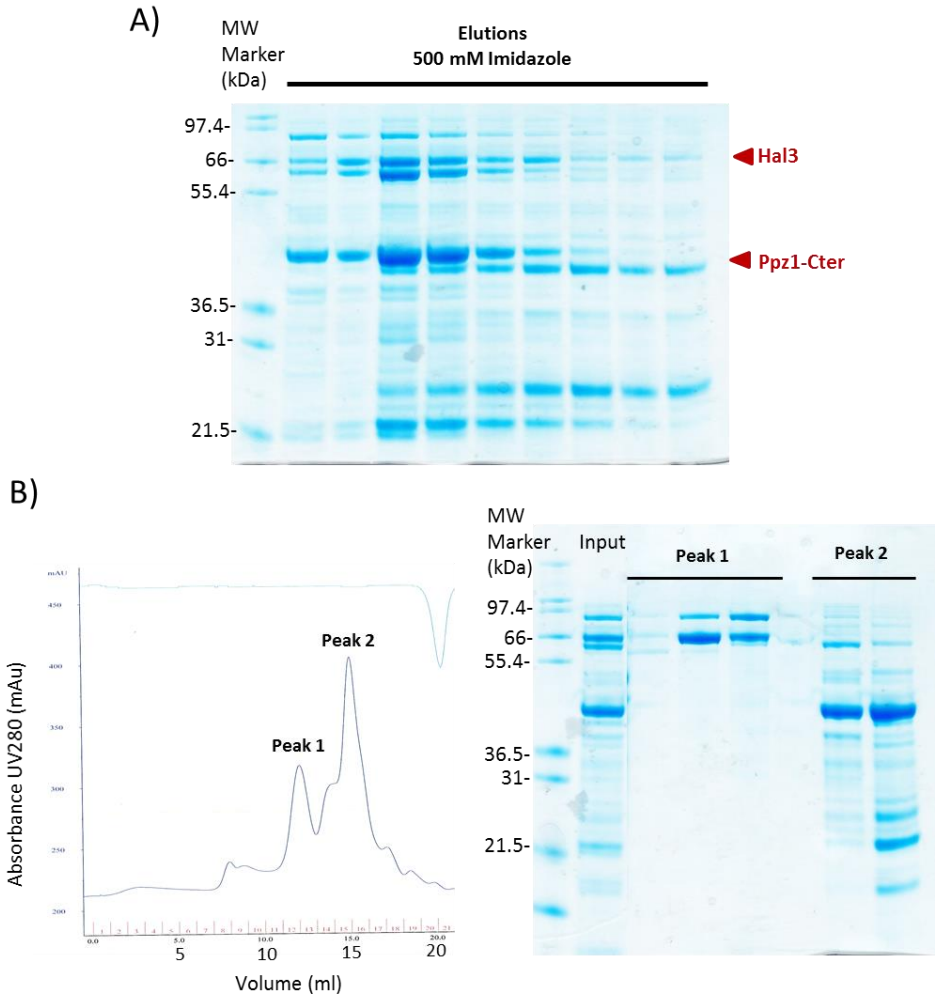

Figure 25. Two-step purification of the Ppz1-Cter/Hal3 complex. A) Eluted protein fractions (1 ml) from the Ni-affinity chromatography with Elution buffer containing 50 mM TrisHCl pH 7.5; 500 mM NaCl; 500 mM Imidazole **B)** SEC of the combined IMAC fractions equilibrated in buffer 50 mM Tris-HCl pH7.5; 0.5 M NaCl; 2 mM DTT; 2 mM EDTA. Left: chromatogram of the Superdex 200 column (Fraction size = 1 ml). Right: SDS-PAGE analysis of Peaks 1 and 2. Hal3 is detected in Peak 1 and Peak 2 contains 6xHis-Ppz1-Cter.

In order to optimize conditions for purifying Ppz1-Cter/Hal3 diverse changes were introduced in the composition of the buffers. For instance, the pH was increased to 8.0, the concentration of imidazol in the binding buffer was raised from 10 to 20 mM and the amount of NaCl was modified in the range of 150 to 500 mM. However, none of the changes improved recovery or purity of the complex and, consequently, the conditions for the IMAC step were kept as in Figure 26A.

Furthermore, an ion exchange (IEX) step was implement after IMAC to isolate recombinant Ppz1-Cter/Hal3 complex from contaminating proteins on the basis of the ionic charge. To carry out IEX, the IMAC elution fractions were pooled and buffer exchanged with buffers without salt to reduce the NaCl concentration. In the first approach an anion exchange column (Mono Q) was used with Tris buffers at pH 7.5. Bound samples were eluted with stepwise increments of NaCl (Figure 26B). In the chromatogram, 4-5 peaks were detected during the progressive increase in salt concentration. Peaks with high UV absorption were analysed by SDS-PAGE. Ppz1-Cter and Hal3 proteins were identified in peaks 2 and 3, respectively, indicating that the complex formed by these proteins had dissociated, similarly to that observed when 0.5 M NaCl was introduced in the buffers. It should be noted that the peak corresponding to Hal3 eluted at 500 mM NaCl, indicating that this protein was tightly bound to the Mono Q column and required high ionic strength to be released, in contrast to Ppz1-Cter, which required less NaCl concentration. This difference was not surprising if the pI of each protein is considered. Hal3 has a pI around 4.5 due to the abundant negative charges in its C-terminal acidic tail, whereas the pI of the expressed Ppz1-Cter polypeptide is almost 2 units higher (6.42).

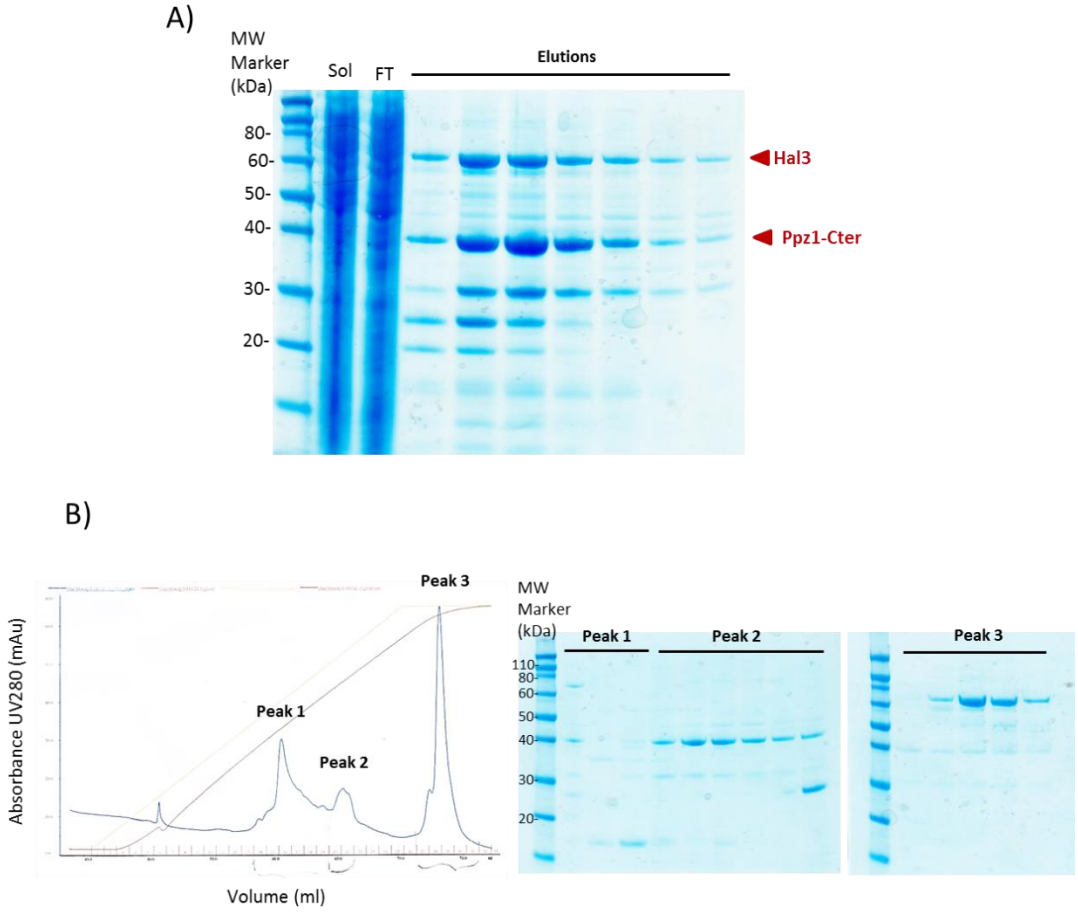

Figure 26. IEX fractionation of Ppz1-Cter/Hal3 at pH 7.5. A) His-tag purification of the Ppz1-Cter/Hal3 complex using Ni-affinity chromatography. The cleared lysate from pET-Duet1-Ppz1-Cter+Hal3 in *E. coli* BL21 was loaded on a HisTrap™ column (1 mL), the protein was eluted with buffer containing 50 mM TrisHCl pH 7.5; 300 mM NaCl; 500 mM imidazole and collected in 1 mL fractions. The arrows indicate the position of the recombinant His-tagged Ppz1-Cter and Hal3. Sol: soluble fraction of lysate; FT: flow-through. **B)** Ion exchange chromatography of eluted fractions on Mono Q column. The column was initially equilibrated with 20 mM Tris-HCl pH7.5; 2 mM DTT; 2 mM EDTA buffer and proteins eluted with a linear NaCl concentration (0–0.5 M) in 20 mM Tris-HCl pH7.5; 0.5 M NaCl; 2 mM DTT; 2 mM

EDTA. Left: A280 profile of the chromatogram. Right: SDS-PAGE analysis. Peaks 2 and 3 reveal the elution of Ppz1-Cter and Hal3, respectively.

The observation that Ppz1-Cter and Hal3 had been dissociated, prompted us to consider the possibility of reconstituting the complex from the isolated proteins. Classically, techniques such as in vitro reconstitution from separately expressed and purified components had been used to study small or mid-size assemblies. Although these techniques facilitate the purification, however the major drawback is that could require refolding steps (in many cases, proteins that form complexes in cells are unfolded without their cellular partners in a heterologous expression system). In our case, the analysis of Peak 1 suggest that the Mono Q step allowed removing some unspecific contaminants and could thus contribute to the generation of complex samples of higher purity.

To reconstitute the complex from previously dissociated components, an overnight incubation of the pooled fractions corresponding peak 2 and peak 3 from the Mono Q eluates was carried out. To facilitate the binding, the buffer was changed to reproduce the one established for pull-down experiments with these two proteins, thus decreasing the concentration of NaCl. After incubation (4 h to o/n) of the recombinant proteins, the sample was concentrated and a SEC step was performed using no more than 300 mM NaCl in the buffer, to avoid possible dissociation of the putatively reconstituted complex. Gel filtration results are shown in Figure 27. The chromatogram showed a single peak indicating a homogeneous population in terms of size and the elution volume suggested a size bigger than the corresponding to individual proteins (compare with Figure 25). The peak was analyzed by SDS-PAGE (Figure 27) and the result was surprising, since although the SEC input sample seemed to contain both components of the complex in comparable amount; the eluted fractions contained both proteins but the amount of

Hal3 was clearly higher. This observation could be explained if one considers that Hal3 can form trimers in solution (Ruiz *et al.*, 2009). Therefore, Peak 1 might be composed of both Hal3 trimers (Mw ~ 187 kDa) and Ppz1-Cter / Hal3 complexes (Mw ~ 103 kDa) which would be difficult to resolve in our working conditions (note that Peak 1 is relatively broad). The appearance of a second peak around 15 ml, which corresponds to the elution position of isolated Ppz1-Cter (see Fig. 25B) would be in agreement with this hypothesis. Taking this into account, the option of reconstituting the complex from the isolated proteins was discarded.

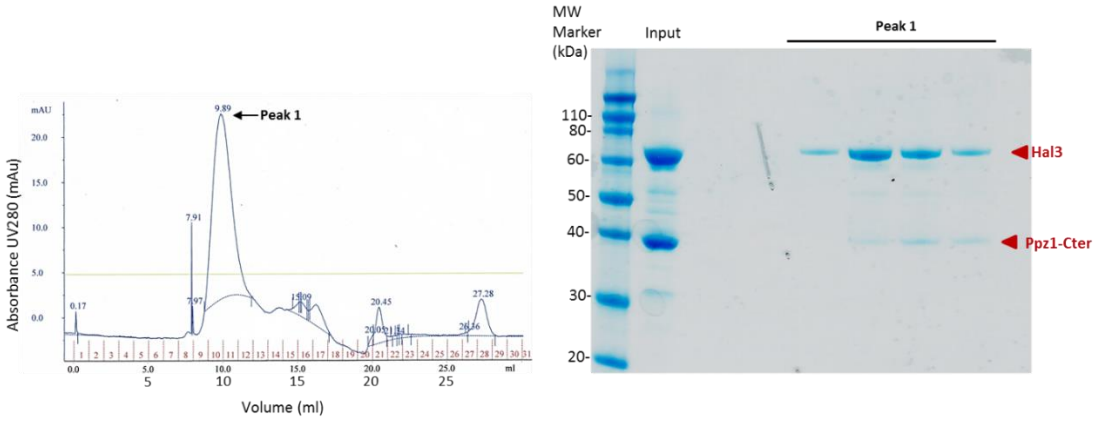

Figure 27. SEC analysis of reconstituted Ppz1-Cter/Hal3 complex after Mono Q chromatography.

Left: Gel filtration profile on Superdex 200 column with buffer 50 mM Tris-HCl pH7.5; 300 mM NaCl; 2mM DTT; 2 mM EDTA (Fraction size = 1 ml). SDS-PAGE analysis of peak 1.

In spite of the failure to isolate recombinant Ppz1-Cter/Hal3 by anion exchange chromatography, and based on the theorical pI of Hal3 (4.56) and the predicted pI for the complex (4.92), we considered the use of a strong cation exchange chromatography as alternative approach. To that end, pooled IMAC elution fractions similar to those described in the precedent experiment were desalted by ultrafiltration, resuspended in

MES buffer at pH 5.5 and applied to a Mono S column. Proteins bound to the column were also eluted using stepwise increments of NaCl. The result is showed in Figure 28. In the chromatogram, only two peaks showed appreciable UV absorption and they were analysed by SDS-PAGE. Peak 1 was detected at the initial phase of the salt gradient. This peak clearly corresponded to the Hal3 protein. Remarkably, peak 2 did not contain Ppz1-Cter, as could be expected, but just contaminant proteins. The possibility that Ppz1-Cter did not bind to this column and was lost in the flow through was considered. In any case, this technique did not allow to obtain both proteins together forming a complex and was considered as not suitable for our purpose.

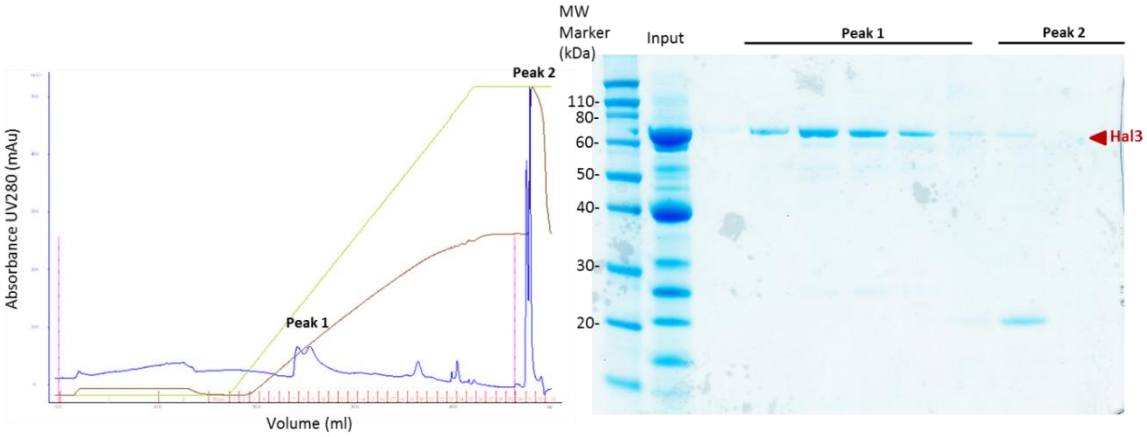

Figure 28. Cation exchange chromatography of Ppz1-Cter/Hal3 at pH 5.5. Left: The Mono S column was initially equilibrated with 20 mM MES pH5.5; 2 mM DTT; 2 mM EDTA buffer and eluted with a linear NaCl concentration (0–0.5 M, green line) in 20 mM MES pH5.5; 0.5 M NaCl; 2mM DTT; 2 mM EDTA. Right: SDS-PAGE analysis of Peak 1 and 2. Peaks 1 contains eluted Hal3.

An alternative approach to remove unwanted protein contaminants is to treat the samples with proteases to produce proteolytic cleavages. After the purification step by Ni^{+} affinity chromatography, the eluted samples were incubated with a variety of proteases

(Proti-Ace kit, Hampton Research) followed by SDS-PAGE analysis (Figure 2 of Annexes). An initial, small scale test, showed that subtilisin produced degradation of Hal3 and some proteolysis of Ppz1-Cter. Incubation with endoproteinase Glu-C did not produce any benefit. Although the incubation with elastase seemed to improve the elimination of some contaminants, when the same protease was used in a large scale experiment no positive effect was detected.

From these results, collectively, none of the approaches to isolate Ppz1-Cter together with Hal3 forming a complex removing contaminant proteins was successful. All the observations suggested that high NaCl concentrations produced the dissociation of the complex, whereas the complex is stable under conditions of low ionic strength. This was indicative that electrostatic charges should be participating in the interaction of Hal3 with the phosphatase. It is remarkable that the RVxF motif present in most of the regulatory subunits of PP1c generate a strong interaction with the phosphatase that can persist at 0.5 M salt concentration (Cohen, 2002). This observation fits with the idea that Hal3 does not bind to Ppz1 through a RVxF-like motif and, consequently, that the interaction of these two proteins likely differs from other known phosphatase-regulator interactions.

2.2 Two-step purification of the Ppz1-Cter/Hal3 complex

The optimization process lead us to establish a two-step purification protocol based on IMAC followed by SEC. Ppz1-Cter/Hal3 proteins from pET-Duet were expressed and initially extracted, as described in Experimental procedures (section 12), according to the optimized protocol. The bacterial lysate was subjected to Ni^{+} affinity chromatography on His-Trap column (GE Healthcare) using an AKTA system. After three

washing steps (up to 80 mM imidazole) the bound proteins were eluted with 500 mM imidazole and approximately 15 fractions of 1 ml were recovered. Different steps of the protein purification process were analyzed in 10% SDS-PAGE (Figure 29A). Afterwards, gel filtration was performed in a Superdex 200 column with 200 mM NaCl in the buffer (a concentration that allows maintenance of a stable Ppz1-Cter/Hal3 complex). SEC produced the purified Ppz1-Cter/Hal3 complex as shown in Figure 29B. The UV_{280} trace showed a main peak (9-10 ml retention volume, Figure 29B, Left), that was consistently observed in different experiments. The SEC eluted fractions were analysed by SDS-PAGE and it was confirmed that this peak contained both expected proteins (Figure 29B, Right).

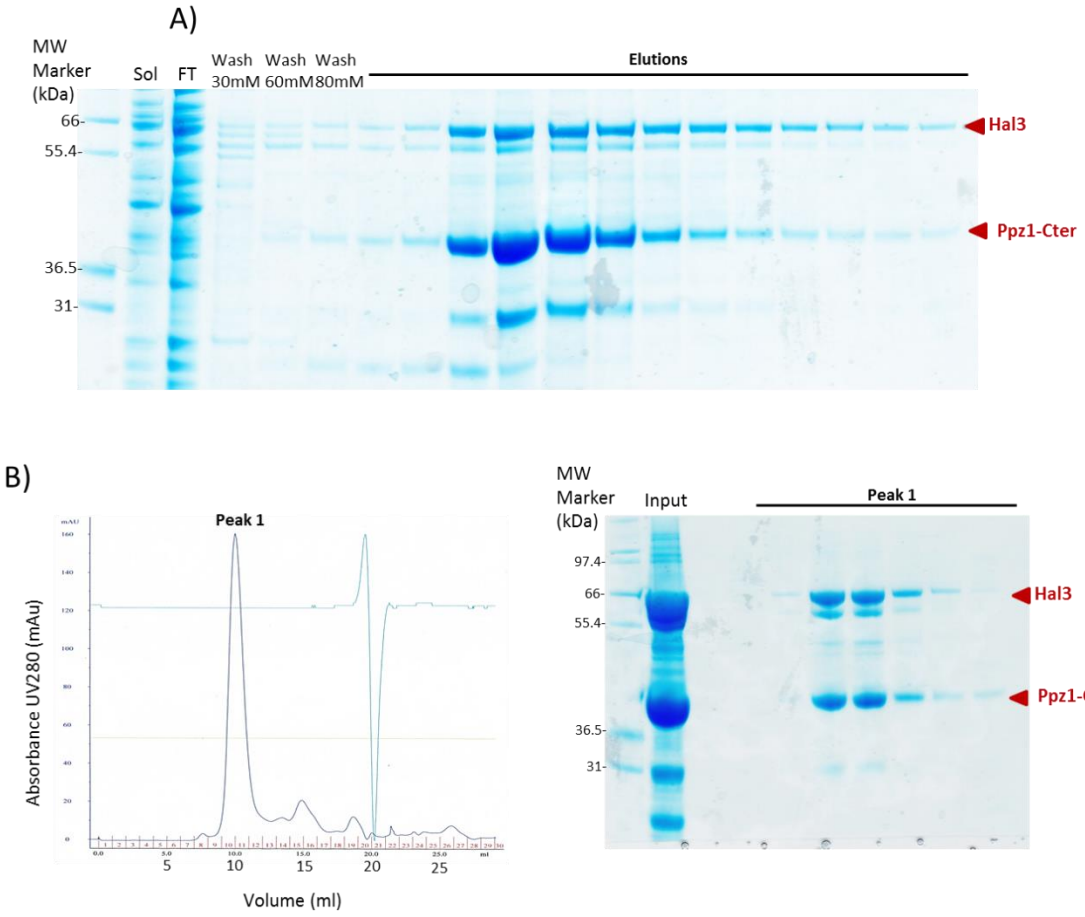

Figure 29. Two-Step purification of Ppz1-Cter/Hal3 complex in low salt. A) Purification of Ppz1-Cter/Hal3 complex using Ni-affinity chromatography. The cleared lysate from pET-Duet1-Ppz1-Cter+Hal3 in *E. coli* BL21 was loaded on a HisTrap™ column (1 mL), Proteins were eluted with buffer containing 50 mM TrisHCl pH 7.5; 300 mM NaCl; 500 mM imidazole and collected in 1 mL fractions. Arrows indicate the position of the recombinant His-tagged Ppz1-Cter and Hal3. Sol: soluble fraction of lysate; FT: flow-through. **B)** SEC of the Ppz1-Cter/Hal3 complex equilibrated in buffer 50 mM Tris-HCl pH7.5; 200 mM NaCl; 2 mM DTT; 2 mM EDTA Left: chromatogram of the Superdex 200 column (Fraction size = 1 ml). Right: SDS-PAGE analysis of Peak 1, containing Ppz1-Cter and Hal3.

Samples from gel filtration showed a single peak corresponding to both proteins that appeared roughly in equivalent amounts, likely forming a complex, which was a main goal of the procedure. However, despite minor contaminants were removed by SEC, this purification protocol did not produce samples of high purity. Also, even the protein concentration of the final samples was enough (8-12 mg/ml), the amount of protein recovered was not sufficient to carry out a large number of crystallization trials. We tried to solve this problem by combining various (4-6) purifications in parallel up to the elution step from the SEC column, pooling the relevant SEC fractions and, after concentration, subjecting the combined samples to gel filtration chromatography again. Following this strategy, a single, main peak of protein was obtained, composed mainly of the desired protein complex (Figure 30), and the final amount of protein recovered increased up to three-fold, yielding up to 600 µl of sample with a protein concentration of 14 mg/ml. These amounts were sufficient to carry out high-throughput crystallography trials.

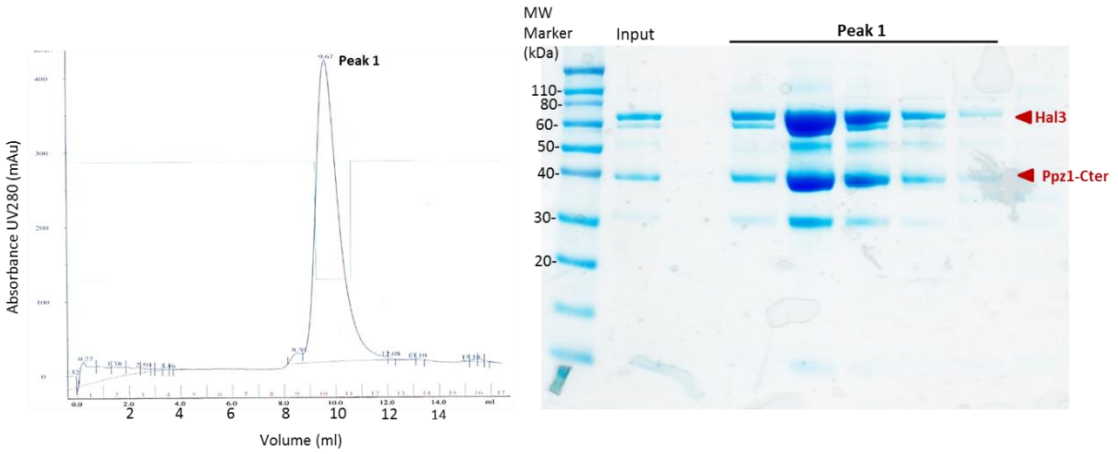

Figure 30. Second SEC of pooled samples from independent purifications. Left: chromatogram of Superdex 200 column from various previous SEC, equilibrated in buffer 50 mM Tris-HCl pH7.5; 200 mM NaCl; 2 mM DTT; 2 mM EDTA (Fraction size = 1 ml). Right: SDS-PAGE analysis of Peak 1.

2.3 Crystallization trials of Ppz1-Cter/Hal3 complex

The typical crystallization process is a time-consuming task and consists of screening hundreds of potential crystallizing conditions and optimizing the conditions with subtle changes. The most commonly used methods for protein crystallization are hanging- and sitting-drop vapour diffusion, in which a droplet containing the purified protein, buffer and precipitant are equilibrated with a reservoir containing similar buffers and precipitants in higher concentrations and a much larger volume. The equilibration reaction is progressing and then gradual changes in concentration of protein and precipitant occurs, allowing a level suitable for growth of crystals (Weber, 1997; Chayen and Saridakis, 2008). The initial crystals are usually tiny, needle-shaped and unsuitable for X-ray diffraction experiments, therefore when crystallization is observed, the size and quality of the crystals can be improved with modifications in the protein concentration, buffer or precipitant concentration, pH range, etc., until sufficiently large crystals are obtained (Bergfors, 2007). Also, small crystals of good quality can be used as seeds (after they have been mechanically crushed) to promote larger ones (Bergfors, 2003). The protein purity and its concentration, pH, temperature and precipitant composition are the most important factors that influence production of high quality diffracting crystals (Qiagen, 2010; McPherson and Gavira, 2014). Protein crystals are usually between 0.1 and 0.3 mm. Moreover, protein crystals are very fragile due to weak non-covalent bonds and higher water content. A given protein can crystallize in more than one form. These different forms provoke variations in diffraction quality, then the form with the best

diffraction should be chosen. Generally, the resolution has to be 3 Å or higher to detect amino acid chains in the electron density map.

Samples of purified recombinant Ppz1-Cter/Hal3 protein complex were employed for crystallization trials using the high-throughput screening capability of the Macromolecular Crystallography Facility at The University of Manchester. Screening was carried out using 96-well crystallization plates and nl-scale sample volumes. The screens provide a wide variety of crystallization conditions, to cover different parameters such as pH, PEG, salts and buffers. Protein concentration is a critical variable in crystallization screening, because the metastable zone for crystal growth is a function of protein concentration and precipitant concentration (Asherie, 2004). Proteins concentration between 5 and 15 mg/ml were tested in this work. At 8 mg/ml the crystallization screens showed the best variation in drop phase (clear, precipitated and denatured), thus this optimal concentration was used for further screening trials. The first indications of crystal formation were obtained in Hampton Research Crystal Screen PEG/Ion2 in a condition 0.1 M Ammoniun Citrate tribasic pH 7.0, 12% PEG 3350 by incubation at 18 °C. Other few protein crystals hits were obtained from SG1 screen or Morpheus I (Molecular Dimensions) at 4 °C (Table 5). To complement the high-throughput screening a number of conditions were screened manually. Primarily, the effects of pH and PEG concentration on crystallogenesis were tested based on conditions that generated small crystals. For instance, for the successful condition of 0.1 M Ammoniun Citrate tribasic pH 7.0, 12% PEG 3350, changes in the relationship between pH (6.5 to 9.0) and in PEG 3350 were assayed in hanging-drop plates. Other successful conditions were also explored by manual tests on individual plates and crystallogenesis was reproducible using different batch preparations of purified proteins and a range of protein concentrations between 8-12

mg/ml. The observation that crystals were reproduced in the same conditions suggested that crystal formation was the result of suitable conditions for nucleation and growth. These nucleation clumps were still too small to be mounted in the X-ray beam, but offered a good starting point for further refinement of crystallization conditions. More crystals could be reproducibly grown with variation of the precipitant:protein ratio and drop size. Also, crystals obtained during screening trials were used as seeding material for further screens. The use of protein crystals seeds can improve the "hit-rate" for crystallization in subsequent screens. Seeding introduces small nuclei to each condition, thus providing a suitable template to start an ordered protein layer and leading to the nucleation of a crystal. This allow to improve crystal quality and size and at the same time it controls crystallization by avoiding the nucleation zone.

	Ligand/Buffer	Precipitant
PEG/Ion 2 Screen	0.2 M Ammonium dihydrogen phosphate 0.1M Tris 8.5	50% v/v MPD
	0.2 M Sodium malonate pH 7.0	20% w/v PEG 3350
	0.1 M Sodium malonate pH 7.0	12% w/v PEG 3350
	0.1 M Sodium malonate pH 6.0	12% w/v PEG 3350
	0.1 M Ammonium tartrate dibasic pH 7.0	12% w/v PEG 3350
	0.2 M Ammonium tartrate dibasic pH 7.0	20% w/v PEG 3350
	0.1 M Sodium acetate trihydrate pH 7.0	12% w/v PEG 3350
	4% v/v Tacsimate pH 7.0	12% w/v PEG 3350
	0.2 M Succinic acid pH 7.0	20% w/v PEG 3350
	0.2M Potassium PO4 dibasic pH 9.2	20% w/v PEG 3350
	0.1 M Sodium acetate trihydrate pH 7.0	12% w/v PEG 3350

Morpheus I screen	0.06 M Divalents 0.1 M buffer 3 pH 8.5	GOL_PK4 30%
	0.09 M Halogens 0.1 M buffer 1 pH 6.5	EDO_P8K 30%
	0.09 M Halogens 0.1 M buffer 3 pH 8.5	GOL_PK4 30%
	0.09 M NPS 0.1 M buffer 1 pH 6.5	EDO_P8K 30%
	0.09 M NPS 0.1 M buffer 2 pH 7.5	EDO_P8K 30%
	0.12 M Alcohols 0.1 M buffer 2 pH 7.5	EDO_P8K 30%
	0.12 M Alcohols 0.1 M buffer 3 pH 8.5	GOL_PK4 30%
	0.1 M Carboxylic acids 0.1 M buffer 3 pH 8.5	GOL_PK4 30%

Table 5. Some of the successful conditions that produced small crystals from Screen PEG/Ion 2 (Hampton Research) and Morpheus I (Molecular dimensions).

The crystallization experiments yielded very thin and small crystals, although they were used for the experiments at the synchrotron radiation source. The best crystals were obtained with the Alcohols 0.12 M; Buffer 3 0.1 M; pH 8.5; GOL_P4K 30% condition from Morpheus I screen using seeds in a ratio 2:1 protein/precipitant. However, crystals grown in this condition were small and the diffraction pattern was of low resolution, collecting diffraction data sets to the resolution of 6.8 Å that was insufficient and not interpretable for structure determination.

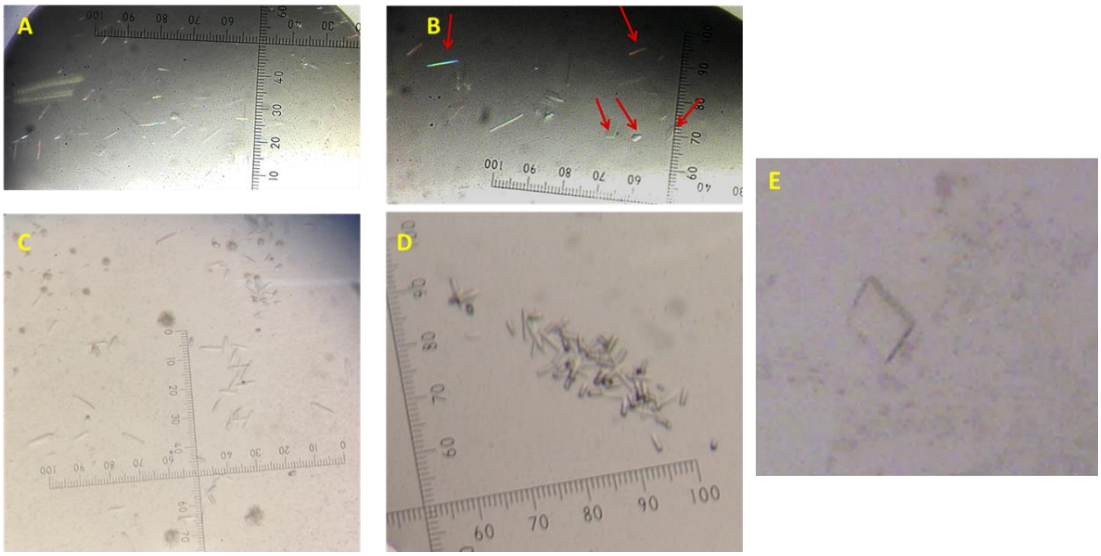

Figure 31. Development of crystallization conditions for the Ppz1-Cter/Hal3 complex. A-D) Potential crystals hits in 0.1 M Ammoniun Citrate tribasic pH 7.0, 12% PEG 33500. **A and C)** Different purified samples giving tiny crystals as needles after 24 hours incubation at 18 °C. **B)** Same conditions after one week **D)** Bigger crystals with two surface after one week incubation at 18 °C dropped with 20 nl seeds. **E)** Crystal selected to exposure to X-ray grown in condition: Alcohols 0.12M, Buffer 3 0.1M pH 8.5, GOL_P4K 30% (Morpheus screen) using 100 nl precipitant, 20 nl seeds and 200 nl protein for the drop and incubated at 4ºC.

2.4 Purification of the Ppz1-Cter/Hal3 complex from a polycistronic vector

To improve the co-purification process and to obtain suitable crystals of high quality for optimal diffraction an alternative strategy was implemented by preparation of new constructs and modification of the induction step. In this approach, a polycistronic

co-expression vector was used, which generates a single mRNA that encodes both proteins. The use of polycistronic vectors for co-expression has been used successfully to purifications of protein complexes, since it allows in vivo reconstitution and proper folding of the individual components together into a complex in a cellular environment (Tan, 2001). Despite this advantage is also provided by the pET-Duet system, the polycistronic vector offers an equal expression level of the components of the protein complex because they are encoded in the same mRNA. It should be noted that creation of the final construct from the polycistronic vector requires multiple subcloning steps and to place particular emphasis on formulating a subcloning scheme that takes into account potential complications such as internal restriction sites. To facilitate the creation of the polycistronic vector, the PET 2-series vector available in Addgene (Plasmid #29665 and Plasmid #29775) were used (see Experimental procedures, section 12.1). On the other hand, in order to increase the amount of recombinant protein produced in *E. coli*, expression was performed by the auto-induction method, which allow higher production of the recombinant proteins under the T7 promoter. This method has been established for massive production of proteins, that are required for structural studies (Blommel *et al.*, 2007). It has been reported that 'auto-induction' media (Studier, 2005) allows *E. coli* cultures to reach considerably higher cell densities (typically five to ten times more than LB medium) in flasks. Moreover, the auto-induction method has been considered to avoid possible proteolysis of the proteins during its production, since improves the folding.

To optimize the expression of polycistronic plasmids containing Ppz1-Cter (with 12His-tag or 6His-tag) and Hal3, expression from the constructs was previously tested in three different *E. coli* strain hosts, BL21 DE3 RIL, C41 or Rosetta DE3 in small-volume cultures. The expression in C41 cells produced the higher level of expression of Ppz1-Cter

and Hal3 and, consequently, this strain was used in subsequent experiments. The A2-Ppz1-Cter x12His R451L+Hal3 polycistronic plasmid was selected to carry out the purification of the complex. The use of 12His-tag construct was based on the idea that it could allow stronger interaction with the Ni^{+} column, and washing steps could be carried out with higher imidazole concentrations to remove unspecific proteins, and still retain the tagged protein bound to the column.

The large-volume cultures using the auto-induction method reached a cell density of OD_{600} ~ 20 and were successful for the expression of Ppz1-Cter and Hal3 from the polycistronic vector. The pellets were lysated using French-Press, due to the large volume of cells obtained. To purify the recombinant proteins, a protocol was developed based on the previous purifications of the Ppz1-Cter/Hal3 as protein complex (i.e., taking into account the maintenance of low salt concentration). The bacterial lysates were subjected to IMAC purification by His-Trap FF column in an AKTA system. All the buffers for Ni^{+} affinity purification contained 100 mM NaCl. The stages of the IMAC purification process were analysed by SDS-PAGE (Figure 32). The wash step with 100 mM imidazole resulted in some loss of the Hal3 protein, but also eliminated a diversity of contaminants. The eluted fractions (10 ml each) contained a large amount of protein (between 30-40 mg/ml total) in comparison with the produced by pET-Duet system induced with IPTG (no more than 15 mg/ml). The elution fractions, however, still showed contaminant proteins, thus requiring a second purification step to isolate highly purified proteins for future analysis.

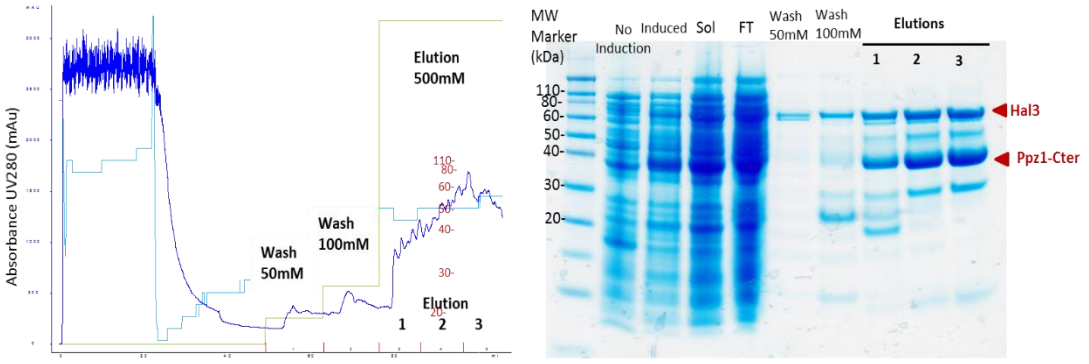

Figure 32. Protein expression and purification of His-Ppz1-Cter/Hal3 complex from the polycistronic vector using the auto-induction method. Four hundred ml culture of cells bearing A2-Ppz1-Cter x12His R451L+Hal3 were lysed and the sample purified using IMAC (HisTrap column). After loading in Binding buffer (50 mM TrisHCl pH 8.0; 100 mM NaCl; 10 mM Imidazole), the samples were washed with binding buffer containing 50 and 100 mM imidazole. The proteins were eluted with 500 mM imidazole and collected in 10 ml fractions. Sol: Soluble fraction of lysate; FT: flow-through. The arrows indicate the position of the recombinant His-tagged Ppz1-Cter and Hal3.

The use of various additives ($MnCl_2$, FMN) in the buffers to improve the purification of the proteins forming a complex was explored, although none of them seemed to improve the process and, consequently, were not included in subsequent experiments.

As previously demonstrated, gel filtration was the only method that allowed isolating purified Ppz1-Cter bound to Hal3. Therefore, this method was continued after IMAC purification, although two steps of SEC were performed to improve the purity of the samples. Firstly, the proteins eluted from the IMAC were concentrated at SEC was carried out in a High-load 16/60 Superdex 200 column. Then, the eluted fractions containing the Ppz1-Cter/Hal3 complex were pooled and concentrated to perform a

second SEC step in a 10/30 Superdex 200 column. The buffer for gel filtration was 50 mM Tris-HCl pH 8.0, 100 mM NaCl, 2 mM DTT, and 2 mM EDTA, which was stablished after testing diverse variations (NaCl concentrations from 100-200 mM, or addition of 10 mM $MnCl_2$). Since the use of 200 mM NaCl did not improve the quality of the proteins, and taking into account that crystals screens also contain salts, the concentration of 100 mM NaCl was selected. An example of the output from the second SEC in Superdex 200 with the buffer optimized is shown in Figure 33.

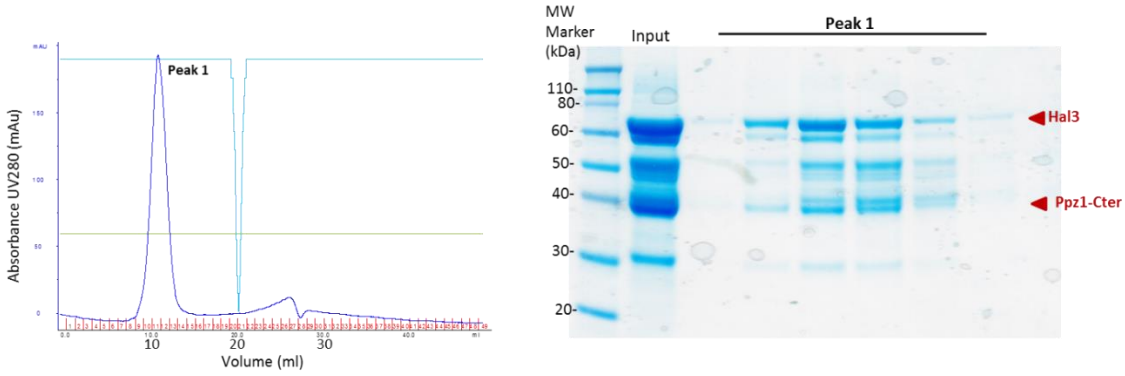

Figure 33. Second SEC of Ppz1-Cter/Hal3 complex after IMAC purification expressed from polycistronic vector. Gel Filtration SEC using Superdex 200 column equilibrated in buffer 50 mM Tris-HCl pH 8.0; 100 mM NaCl; 2 mM DTT; 2mM EDTA Left: chromatogram (Fraction size = 0.1 ml). Right: analysed by SDS-PAGE. The main peak corresponding to the SEC eluates contained Ppz1-Cter and Hal3.

The eluted SEC fractions were concentrated to attempt crystallization of this samples and reproduce, at least, crystals as the previous ones obtained from pET-Duet expression and purification. The advantage of these new samples was that the amount of protein obtained was much higher, allowing sufficient concentration and larger volumes to carried out a variety of crystallization experiments. The protein sample was subjected to the same high-throughput screening procedure using JCSG-plus HT-96, PACT-

premier HT-96, SG1 screen, Morpheus I, Morpheus II (Molecular Dimensions) screens. Despite the development of improved protein preparation procedures and extensive screening, no successful conditions could be obtained to produce 12His-Ppz1Cter+Hal3 crystals suitable for structural determination. Nevertheless, few tiny small crystals emerged in some conditions and they were analyzed at the synchrotron. Only very weak diffraction could be obtained, so data could not be collected for structural determination; however, the diffraction pattern showed that those were protein, and not salt crystals. This result offered a good starting point for further refinement of crystals production, with sufficient size for structural determination.

2.5 Derived constructs of Ppz1-Cter/Hal3 complex from a 12His-Ppz1-Cter Hal3 polycistronic vector

In order to improve the protein samples for crystallization, structural analysis of the protein sequences were carried out using RONN, Jpred and XtalPred. The idea was basically to design a construct in which the expressed protein would start a couple of residues before the first secondary structure and/or at the limit of the disordered regions. As can be observed in Figure 34, the two ends of the catalytic domain of Ppz1 showed a high level of disorder. The Hal3 protein exhibited basically unstructured sequence, except the considered central domain of the protein (core). Taking this into account, two new constructs were generated using the A2-Ppz1-Cter x12His R451L+Hal3 polycistronic vector as starting point. A first modification was to introduce a TEV cleavage site at the N-terminal of Ppz1-Cter, after the Ile^{27} of the fragment expressed in the polycistronic construct (corresponding to Ile^{361} of the full length protein) which would leave, after

cleaving the tag, only the residues from which the protein begins to show secondary structure (Figure 34). Moreover, removal of the tag could be more favourable for crystallography studies, because the 12His-tag conforms a larger unstructured segment than the 6His-tag does. This construct was designate "polycistr TEV". On top of this, a second modification was introduced, removing the C-terminal end of Hal3, corresponding to the acidic tail, since it appears highly disordered. To that end, a stop codon after the residue G489 was inserted by mutation, resulting in the "polycistr TEV Hal3 G490Stop" plasmid.

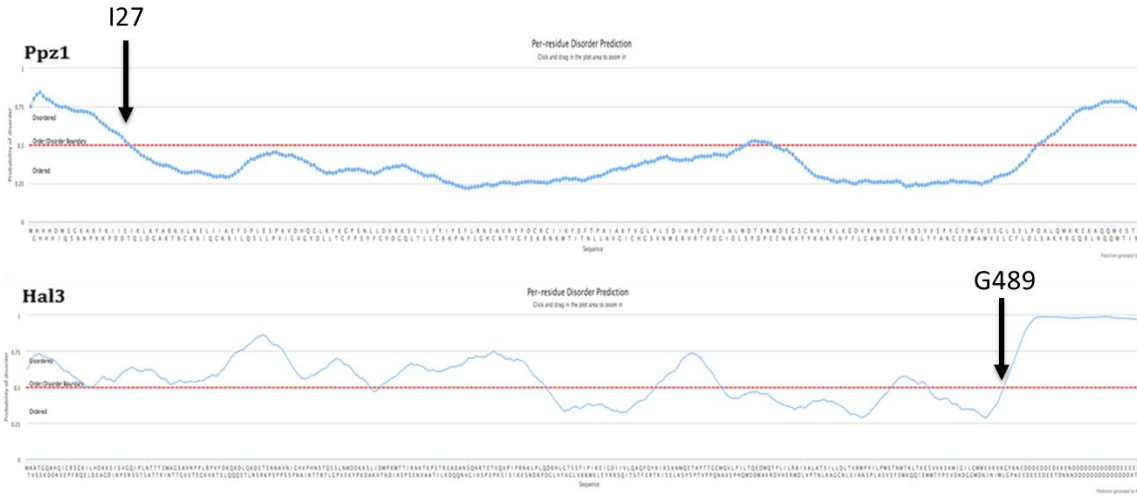

Figure 34. Prediction of disordered regions using RONN v3.2 for the C-ter half of Ppz1 and the entire Hal3 (https://www.strubi.ox.ac.uk/RONN). Arrows indicates where modifications were introduced to generate new constructs.

Different parameters such as EP (Expert Pool) and RF (Random Forest) that predict chance of crystallization improved when disorder regions were avoided. Despite that Hal3 presented more unstructured regions, specifically the entire N-terminal

extension, this region was not removed since previous work demonstrated that this domains of Hal3 was relevant for the interaction with Ppz1 (Abrie *et al.*, 2012).

Both new constructs, polycistr TEV and polycistr TEV Hal3 G490Stop, were expressed in C41 *E. coli* cells following auto-induction, similarly to the protocol used for the previous polycistronic A2-Ppz1-Cter x12His R451L+Hal3 plasmid. In terms of purification, the method was modified and the Ni^{+} affinity purification step was carried out in batch instead of using packed His-Trap columns in order to maximize the binding of the large amount of proteins expressed. Thus, the soluble fraction of the lysate was incubated with 2-3 ml of equilibrated Ni-NTA resin followed by washing and elution by flow gravity. The buffers were the same that used for initial purification of Ppz1-Cter/Hal3 from the polycistronic vector (as shown in Figure 32), but the wash step was made with only 50 mM imidazole. The elution step was performed with 500 mM imidazol by incubation with gently mixing for 1h to allow the removal of all the His-tagged proteins from the resin. The method of purification in batch with Ni-NTA resin successfully generated high levels of purified recombinant proteins. The insertion of the TEV cleavage site in the new constructs would allow to remove the His-tag from the Ppz1-Cter and the short N-terminal disordered region, thus starting the protein at residue 361 of the full lenght Ppz1 sequence. After digestion with the TEV protease during the dialysis step, the samples were applied again to a IMAC resin. After SDS-PAGE analysis of the samples (Figure 35A and Figure 36A) it became evident that after TEV digestion only about 50% of the input complex protein was recovered, and considerable amounts of fusion proteins were still retained in the resin (eluted at 500 mM imidazole). Despite that only a small fraction of the Ppz1-Cter/Hal3 proteins was recovered from the second IMAC purification, the samples were subjected to SEC. Similarly to the original polycistronic

protocol, first a gel filtration was run in a Superdex 16/60 and the eluted fractions containing the desired proteins were subjected to a second gel filtration in a Superdex 200 column. The complex protein successfully eluted after at the expected time retention (9-10 ml of volume), as demonstrated the SDS-PAGE analysis of the relevant peak. (Figure 35B and Figure 36B).

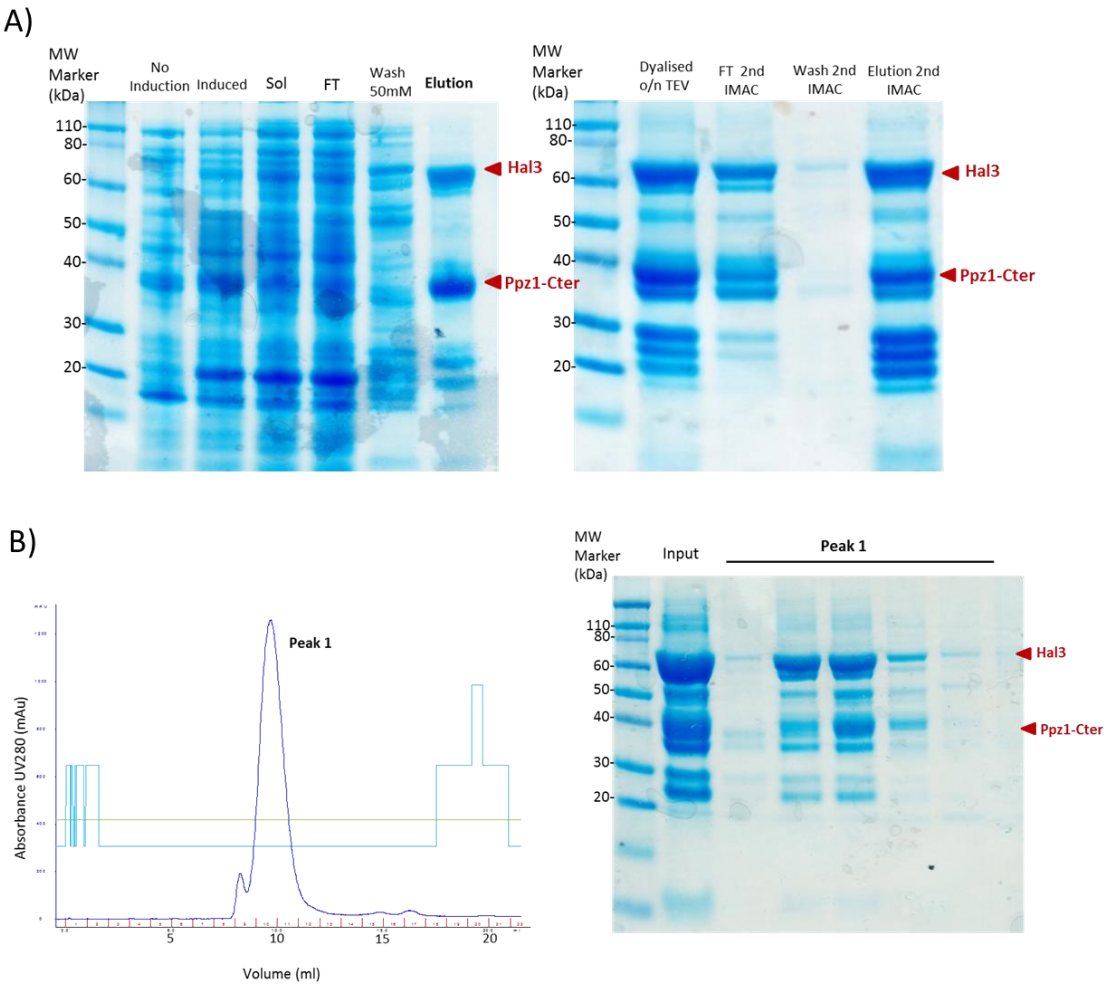

Figure 35. Two-step strategy of purification of Ppz1-Cter/Hal3 from polycistr TEV. A) Batch

purification of Ppz1-Cter/Hal3 complex using Ni-affinity chromatography. The cleared lysate from *E. coli* C41 expressing "polycistr TEV" was loaded on packed Ni-NTA beads, the protein was eluted by incubation for 1 hour by gently mixing with buffer containing 50 mM Tris-HCl pH 8.0; 100 mM NaCl; 500 mM imidazole. The sample was dialysed and digested with TEV protease by incubation o/n. Afterwards, a second IMAC was performed to remove undigested, tagged proteins. Arrows indicate the position of the recombinant Ppz1-Cter and Hal3. Sol: soluble fraction of lysate; FT: flow-through **B)** Left: chromatogram (Fraction size = 0.1 ml) of the SEC using a Superdex 200 column equilibrated in buffer 50 mM Tris-HCl pH 8.0; 100 mM NaCl; 2 mM DTT; 2 mM EDTA Right: SDS-PAGE analysis of peak 1.

The SDS-PAGE analysis (Figure 35A) showed that the Ppz1Cter/Hal3 complex was successfully purified using this method. The wash step removed many contaminants and the eluted fraction contained large amount of the proteins of interest. However, after the TEV cleavage, only a small amount was recovered (FT 2nd IMAC), despite that buffer without EDTA was maintained for optimal digestion. Moreover, the appearance of a faster migrating band just below Ppz1-Cter, suggested a possible degradation that was already observed in the sample taken from the dialysis bag.

Although the chromatogram of the second gel filtration showed only a mayor peak, suggesting that major contaminants were removed, the samples (Figure 35B) exhibited an increase of unspecific bands in comparison with the output of the first IMAC step, mainly between the MW of Ppz1-Cter and Hal3. The observation that during TEV treatment the sample displayed some tendency to precipitation suggested that protein was unstable and probably during dialysis and size exclusion chromatography the sample was being degraded. The fact that the hypothetical degradation product still stick together to other components of the protein complex, eluting in same peak in SEC suggest that they might derive from the Hal3 of Ppz1-Cter polypeptides. This hypothesis was corroborated

by mass spectrometry analysis of several bands migrating on the gel at different MW, which allowed identifying them as derived from Ppz1-Cter or Hal3.

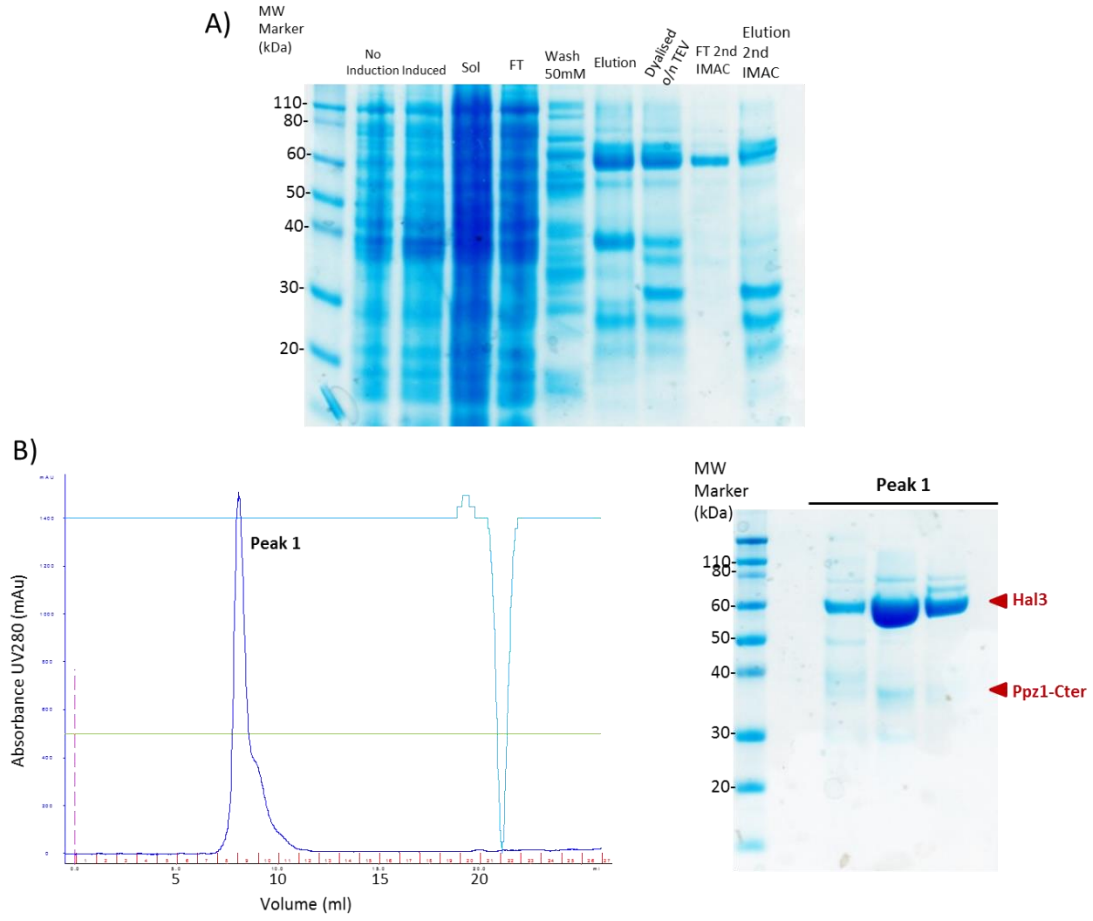

Figure 36. Two-step strategy for purification of Ppz1-Cter+Hal3 without acidic tail (from polycistr TEV Hal3 Stop vector). A) Batch purification of Ppz1-Cter/Hal3 complex using Ni-affinity chromatography, as described in Figure 35A. Sol: soluble fraction of lysate; FT: flow-through **B)** Left: chromatogram (Fraction size = 1 ml) of SEC as described in Figure 35B. Right: analysed by SDS-PAGE analysis of Peak 1. Arrows indicate the position of the recombinant Ppz1-Cter and Hal3.

The purification of recombinant proteins from polycistr TEV Hal3 Stop to isolate Ppz1-Cter without His-tag and Hal3 without the unstructured C-terminal tail also yielded large amount of purified proteins after Ni^{+} affinity chromatography (Figure 36a). However, the first difference from the previous purification (containing the entire Hal3) was observed after the dialysis and TEV overnight digestion. A strong precipitation was observed in the dialysis bag and SDS-PAGE revealed that the amount of Ppz1-Cter was decreased in comparison to that of Hal3. This fact was even more evident during the next steps of purification. In consequence, the result of the SEC showed a large amount of Hal3 in the sample and only a slight quantity of Ppz1-Cter. This behaviour was not entirely surprising, since it has been demonstrated that removal of the Hal3 acidic tail , although has little effect in vitro on the efficiency of the interaction, it affects negatively the ability of Hal3 to inhibit Ppz1-Cter (Abrie *et al.*, 2012) and disrupts Hal3 function in vivo (Ferrando *et al.*, 1995). It could be speculated that a Hal3 polypeptide lacking this region might not properly bind to the phosphatase, facilitating the natural tendency of Hal3 to trimerize and thus releasing free Ppz1-Cter protein, which would be unstable and prone to degradation.

2.6 Crystallization of the Ppz1-Cter/Hal3 complex without His-tag

The isolated proteins produced by these newly engineered constructs were likewise subjected to crystallography trials, since the amount of proteins obtained was enough and the variations introduced (inclusion of a TEV cleavage site and removal of the C-terminal tail of Hal3), based on computer predictions aiming to remove disordered

regions, were expected to improve the crystallization potential of the recombinant Ppz1Cter/Hal3 complex produced.

Extensive investigation and screening of several precipitants, buffers with pH range 4-9, detergents, divalent cations and cryoprotectants, as well as temperature (4 ºC or 18 ºC) were carried out. The number of crystals hits improved using the constructs which allow the TEV cleavage, suggesting that removing the 12His-tag along with the few unstructured residues of Ppz1-Cter enhanced crystallogenesis. Almost five hundred conditions were tested. However, crystalline material was only observed in common conditions, such as Ammonium sulfate with low concentration of precipitant. Various small microcrystals were often observed, and even crystals able to grow in two-three dimensions in some cases, although crystals of diffraction quality could not be obtained. This led us to investigate similar conditions but increasing the drop size and varying ratios proteins:precipitant to yield better crystals.

Large and irregularly shaped crystals with largest dimensions were obtained from diverse conditions, described in Figure 37, after 7-10 days at 4 ºC. They were mounted and frozen with liquid nitrogen together with cryoprotectans to prevent cracking of crystals during freezing for X-ray data acquisition.

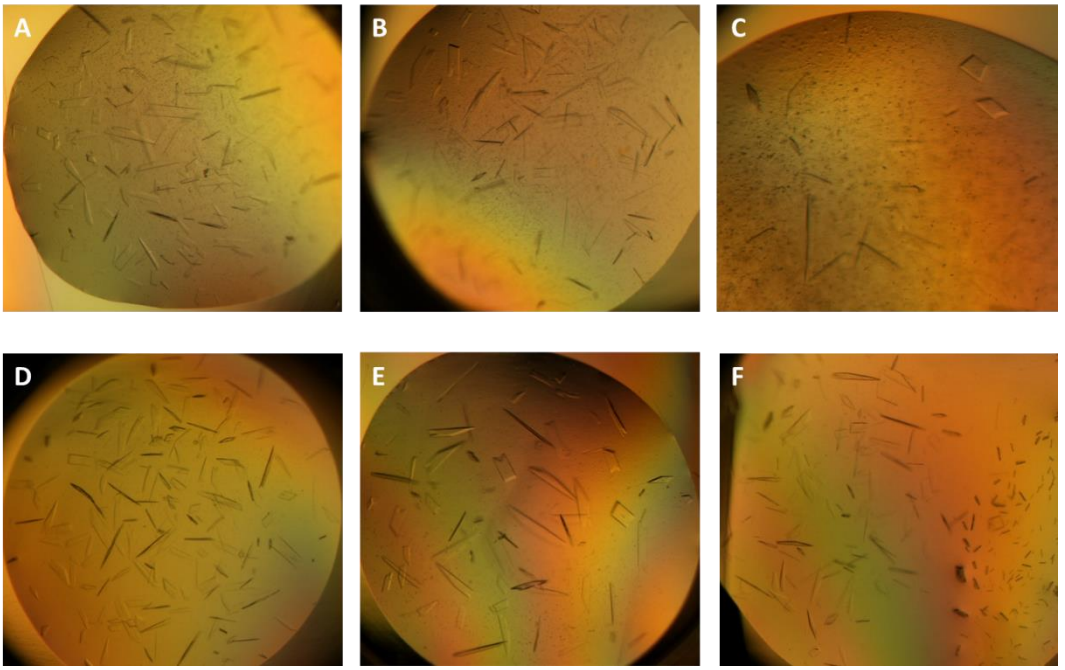

Figure 37. Optical microscope images of Ppz1-Cter/Hal3 crystals obtained from polycistr TEV at 10 mg/ml concentration in different conditions. A-C) 0.2 M Sodium malonate dibasic monohydrate pH 7 20% w/v PEG 3350 with protein:precipitant ratios of 2:1 (A;B) and 3:1 (C) **D)** 0.2 M Sodium sulfate 20% w/v PEG 3350, ratio 3:1 protein:precipitant **E)** 0.2 M Sodium tartrate dibasic dihydrate 20% w/v PEG 3350, ratio 2:1 protein: precipitant **F)** 0.2 M Sodium sulfate 20% w/v PEG 3350, ratio 2:1 protein: precipitant.

Unfortunately, the crystals were extremely susceptible to X-Ray induced radiation damage with resolution rapidly dropping off from an initial high of ~ 3.5Å to nearer 5-6Å over the duration of a data collection period.

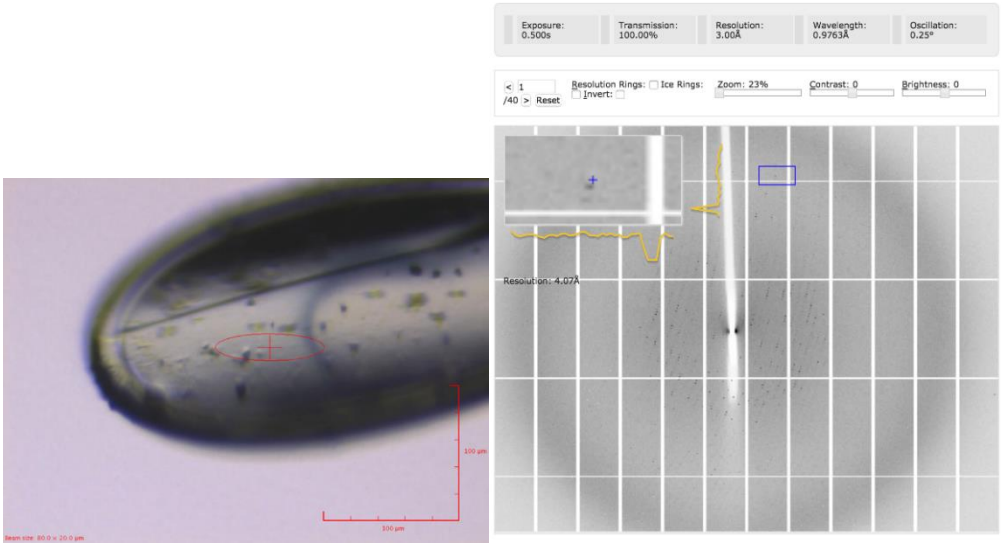

Figure 38. A typical crystal, the maximum resolution observed in this initial image is ~ 4Å. Diffraction image collected on i03 Diamond.

```
Wavelength:  0.97626 A
Run number:    1 consists of batches          1 to        400
   Resolution range for run:   194.95    5.64
   Phi range:                45.00 to              145.00
   Closest reciprocal axis to spindle: a*   (angle   40.5 degrees)
```

	Overall	InnerShell	OuterShell
Low resolution limit	194.955	194.955	5.657
High resolution limit	5.638	26.150	5.638
Rmerge (all I+ & I-)	0.143	0.054	0.799
Rmerge (within I+/I-)	0.136	0.062	0.785
Rmeas (within I+/I-)	0.174	0.078	0.991
Rmeas (all I+ & I-)	0.164	0.063	0.911
Rpim (within I+/I-)	0.106	0.047	0.597
Rpim (all I+ & I-)	0.078	0.031	0.423
Total number of observations	116127	1161	1174
Total number unique	28997	314	293
Mean(I)/sd(I)	7.9	15.4	2.0
Completeness	90.0	79.7	89.6
Multiplicity	4.0	3.7	4.0
CC(1/2)	0.996	0.999	0.674
Anomalous completeness	80.5	79.8	79.4
Anomalous multiplicity	2.3	2.4	2.3
CC(ano)	0.032	-0.597	0.064
|DANO|/sd(DANO)	0.815	0.791	0.770

Table 6. Xia2 Auto processing results from i03 data collection resultant from diffraction.

A large degree of unit cell (unit of volume that allows the construction of the total volume of a crystal by the three lattice vectors) variation was also observed, both between crystals and indeed within single crystals when data were collected using a small beam at multiple sites along a single crystal. This lack of isomorphism prevented the merging of multiple partial data sets to produce a single composite data set minimizing the impact of

radiation damage. Several attempts to determine the structure by molecular replacement failed to provide a solution.

In summary, the experimental work reported in this project has shown that the purification of Ppz1-Cter and Hal3 proteins forming a complex is highly problematic, being the major problem the generation of samples of high purity, in part becasue of the limitations in the purification steps derived from the necessity to avoid conditions leading to the dissociation of the complex (i.e. IEX chromatography). A large variety of constructs, host cells, induction protocols, etc, were tested. After optimization, large amount of proteins was obtained after the first purification step by Ni^{+} affinity chromatography. However, downstream purification presented some difficulties, since Ppz1-Cter/Hal3 co-purified with too high levels of contaminating proteins and samples were, therefore, a heterogeneous population. In addition, the strategy of removing the His-tag together with a few residues at the N-terminal of Ppz1-Cter (based on algorithm predictions) was not successful since the cleavage of the His-tag from Ppz1-Cter led to aggregation. Finally, a two-step purification method (IMAC and SEC) was devised to generate protein samples of sufficient purity and homogeneity for initial crystallization and reproducible crystal growth. The establishment of this protocol yielded protein crystals with size enough for X-ray diffraction, although their quality needs be improved. It should be noted that the macromolecular crystallization process is still empirical and mainly based on trial and error and, in many cases, a very difficult procedure because of the weak nature of protein crystals and irregularity shaped surfaces. Therefore, exploration of further methodological approaches for the generation of crystals appears necessary to produce diffraction quality crystals for structural determination of the Ppz1Cter+Hal3 complex. In any case, although our final goal of producing crystals suitable for successful X-ray diffraction and structure

solving has not been achieved, we have set the basis for experience-guided future attempts. Alternatively, methods not requiring the generation of crystals, such as SAXS or Cryo Electronic Microscopy, would be worth considering.

CONCLUSIONS

1. A purification protocol for the Ppz1-Cter/Hal3 complex that avoided conditions leading to the dissociation of the complex, and provided enough material for structural analysis approaches has been established.

2. Crystallization conditions favorable for crystal growth of the Ppz1-Cter/Hal3 complex were defined. The obtained crystals diffracted up to 3.5Å resolution. However, radiation-induced damage and the nature of the crystals (very thin plates) resulted in their physical alteration that prevented the generation of useful sets of data.

III) Cloning, expression and functional characterization of the *SPAC15E1.04 ORF* from *Schizosaccharomyces pombe*

3.1. Verification and characterization of the ORF SPAC15E1.04

Search of the *S. pombe* genome identified the locus SPAC15E1.04 as the only one able to encode a protein with significant identity to the *S. cerevisiae* Hal3, Vhs3 and Cab3 proteins and compatible with a putative PPCDC. Remarkably, this identity was restricted to the N-terminal half of the *S. pombe* predicted protein, whereas the C-terminal one was strikingly similar to known thymidylate synthases (TS). The anomalous structure of this ORF was subject to verification, since it could be the result of annotation or sequence errors. For this, genomic DNA from *S. pombe* (strain L972 h^-) was isolated and the fragment of approximately 2.6 kbp encompassing the entire ORF was amplified by PCR. The fragment was then sequenced and aligned with the ORF reported in the database. Only a single nucleotide, located at position 864, was found different, and this change produced a synonym codon. Consequently, our sequencing results confirmed the anomalous nature of *S. pombe* SPAC15E1.04 as an ORF of 1878 bp encoding a 625-residue protein in which a Hal3-like polypeptide was fused to a putative thymidylate synthase. The same anomalous structure was experimentally confirmed by sequencing the relevant locus in the *S. japonicus* genome. Sequence searches reveals that such anomalous structure can be also be found in

S. cryophilus and *S. octosporus*, concluding that this possible gene fusion event is likely restricted to the genome of Schizosaccharomycetales.

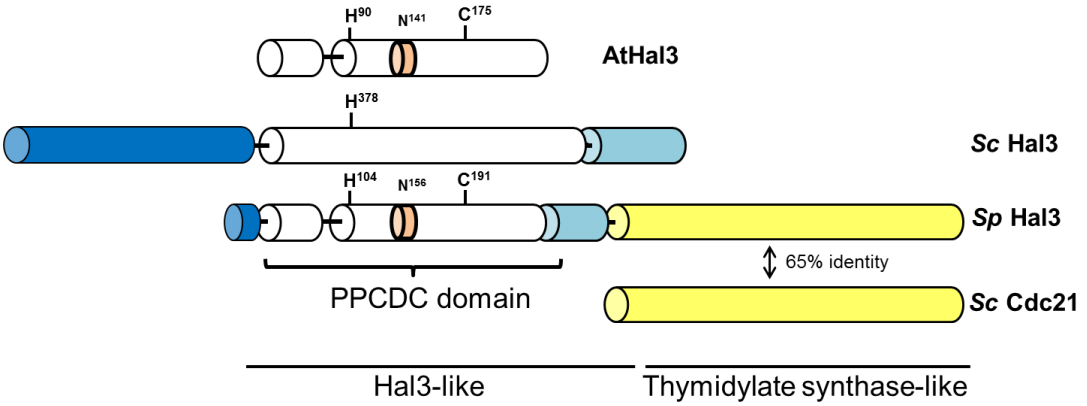

Figure 39. A comparison of the protein encoded by the SPAC15E1.04 ORF (SpHal3), with Hal3 from *Arabidopsis thaliana* (AtHal3), Hal3 from *S. cerevisiae* (ScHal3) and thymidylate synthase from *S. cerevisiae* (ScCdc21). Residues relevant for PPCDC catalytic activity are indicated. The N-terminal extension of Schal3 is shown in dark blue, the acidic segment in light blue, and TS is in yellow.

3.2. Functional analysis of the SPAC15E1.04 gene product as Ppz1 regulator in *S. cerevisiae*

Comparison of the amino acid sequence of the Hal3, Vhs3 and Cab3 proteins of *S. cerevisiae* with that of the *S. pombe* SPAC15E1.04 encoding-gene revealed the existence of a high similarity with respect to the Hal3-like region, showing 35-45% of identity in the Hal3 core domain (Figure 39). This resemblance in sequence suggested the possibility that the *S. pombe* protein could have a mimetic role to ScHal3 in budding yeast. If so, the protein

encoded by SPAC15E1.04 could perform as an inhibitory subunit of Ppz1 phosphatase in *S. cerevisiae*.

First of all, the entire *S. pombe* ORF (from now on, SpHal3), as well as the N-terminal region (similar to ScHal3 central core), were cloned into the pWS93 expression vector, a high copy plasmid with a 3x-HA epitope for N-terminal tagging. Protein extracts from a *hal3* strain transformed with these constructs were prepared and the expression of the proteins was analyzed by SDS-PAGE followed by immunobloting with anti-HA antibodies. As shown in Figure 40, expression of the complete ORF of *S. pombe* produced in *S. cerevisiae* a protein whose molecular mass, estimated from its electrophoretic mobility, was around 70 kDa. This was indicative that the protein was expressed as a single polypeptide, implying that it was not proteolytically processed in budding yeast. The amino terminal region (SpHal3-Nter) generated a polypeptide of approximately 48 kDa. This molecular mass was slightly higher than expected (~42 kDa) for the tagged protein, but it should be considered that Hal3 from *S. cerevisiae* also migrates slowly on SDS-polyacrylamide gels. The expression of SpHal3-Nter seemed to occur in lesser amounts compared to the entire protein.

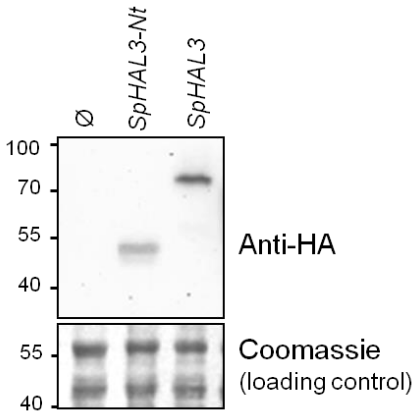

Figure 40. Expression of *S. pombe* SPAC15E1.04 in budding yeast. The entire protein (SpHal3) and the N-terminal part, similar to the Hal3 central core from *S. cerevisiae* (SpHal3-Nter) were expressed from plasmid pWS93 as 3x-HA tagged proteins in a *hal3* mutant. Extracts were prepared and 40 µg of total yeast proteins were analyzed by SDS-PAGE (10% polyacrylamide gel), transferred to membrane and immunoreactive proteins were visualized with anti-HA antibody (Covance). Coomassie Blue staining of the membrane is shown as loading reference.

Part of the functions of Hal3 in *S. cerevisiae* are mediated by Ppz1, as a result of the inhibition of the phosphatase. The entire *S. pombe* protein or its N-terminal half was subjected to analysis to determine if they could replace functionally ScHal3 as a Ppz1 inhibitory subunit. The pWS93-based constructs expressing *S. pombe* SpHal3 and SpHal3-Nter, as well as ScHal3 (as positive control) were introduced in budding yeast cells and different Ppz1-related phenotypes were analyzed.

Since overexpression of *HAL3* in *S. cerevisiae* improves growth of cells exposed to high toxic concentrations of lithium or sodium (Ferrando *et al.*, 1995), we first tested whether expression of the *S. pombe* proteins was able to confer a salt tolerance phenotype.

To this end, pWS93-constructs expressing different Hal3 were introduced in wild type and *hal3* mutant strains and growth in medium containing diverse amounts of NaCl and LiCl was monitored. As reported in Figure 41A, expression of the entire SpHal3 had no effect on tolerance to LiCl. However, expression of the SpHal3-Nter domain showed a modest increase in LiCl tolerance, which was more noticeable in cells lacking *HAL3*. This is interesting on the light of reported evidence, showing that AtHal3, whose structure is largely similar to the product of SpHal3-Nter (Figure 39), also partially complements the LiCl sensitivity of a Hal3-deficiente *S. cerevisiae* strain (Espinosa-Ruiz A, Bellés JM, Serrano R, 1999; Kupke *et al.*, 2001). When tolerance to other toxic cations (which is influenced by the membrane potential) was analyzed, the presence of the N-terminal segment of *S. pombe* increased tolerance to spermine and had a marginal effect on tetramethylammonium (TMA) tolerance. Such effects were only evident in *hal3* mutant cells (Figure 41B). In contrast, no change in NaCl or Hygromycin B tolerance was observed. In collaboration with the laboratory of Dr. Jose Ramos (Universidad de Córdoba) the capacity to extrude Li^+ in these cells was assayed. As shown in Figure 41C, Li^+ extrusion in *hal3* cells containing the full length protein from *S. pombe* was similar to that of cells with the empty plasmid. In contrast, *hal3* cells that expressed SpHal3-Nter improved lithium efflux nearly as expression of Hal3 from *S. cerevisiae* did.

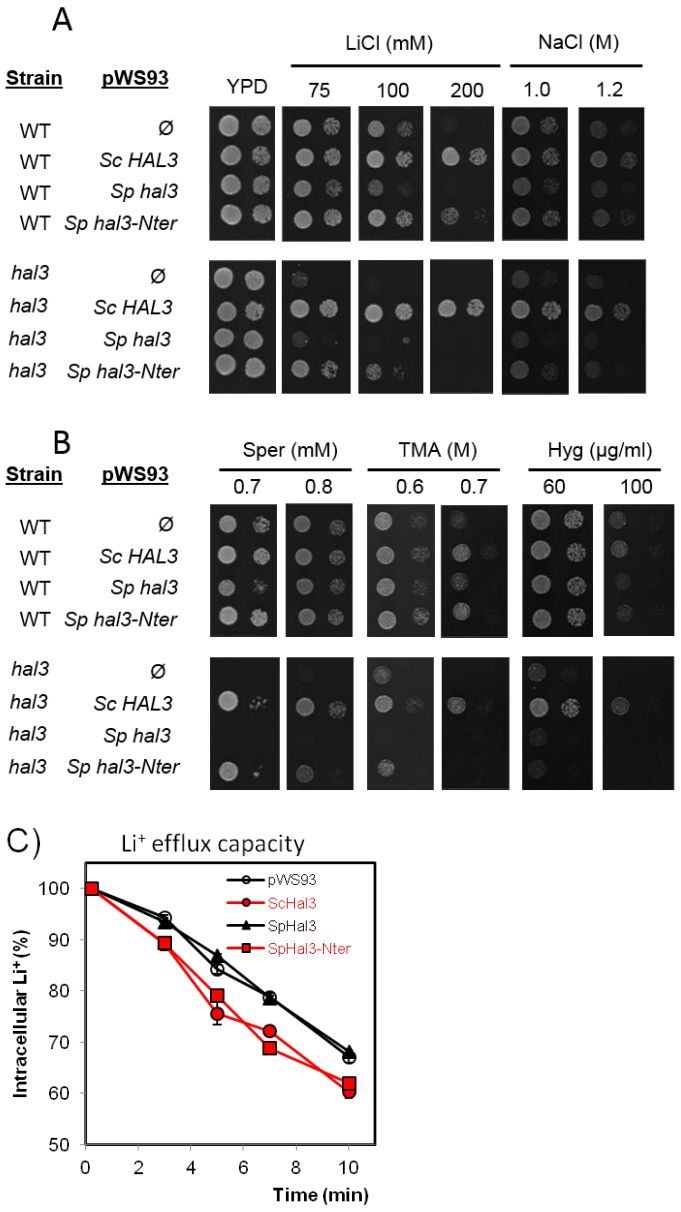

Figure 41. Functional analyses related to cation homeostasis of budding yeast *expressing S. pombe* SPAC15E1.04. A) Wild type strain BY4741 (WT) and the *hal3* mutant derivative were transformed with the pWS93 plasmids containing the different versions of Hal3 from *S. pombe* and *S. cerevisiae* and were spotted on

YPD plates containing different concentrations of LiCl and NaCl. Growth was monitored after 3 days of incubation at 28 °C. **B)** WT and *hal3* strains transformed with the indicated plasmids and grown on YPD plates with different concentrations of the toxic cations Spermine (Sper), TetraMethylAmmonium (TMA) and Hygromicin (Hyg) for 3 days at 28ºC. **C)** *hal3* mutants growing in synthetic medium were loaded with 300 mM LiCl for 1 h and transferred to Li^+-free medium. Samples were taken periodically and the intracellular lithium concentration was determined. Data are represented as percentage of the initial lithium content and correspond to the mean ± SEM from 3 different experiments.

It was known that overexpression of *HAL3* produces an increase of cytoplasmic K^+ (Ferrando *et al.*, 1995). This effect was explained by the consequent inhibition of Ppz1, which improves the influx of potassium to the cell through the high-affinity Trk transporters (Merchan *et al.*, 2004). This situation is reflected in improved growth under potassium limiting conditions (1 mM KCl). To test if the overexpression of *S. pombe* Hal3 could exert a similar effect in K^+ influx, growth under limiting concentrations of potassium was tested using cells expressing the different Hal3 constructs. The growth of wild type and *hal3* strains was reduced under limiting potassium conditions respect to those grown at a concentration of 50 mM KCl in the medium, being more pronounced in the *hal3* mutant. As expected, overexpression of ScHal3 improved the growth of cells under limiting K^+ concentration in both strains (Yenush *et al.*, 2002; Merchan *et al.*, 2004). However, cells overexpressing the entire SpHal3 as well as the SpHal3-Nter did not show a positive effect compared with the empty plasmid (Figure 42). These results suggest that neither the entire *S. pombe* protein nor the N-terminal half, produce an increase in potassium influx and therefore, that these proteins do not influence the activity of the high-affinity Trk transporters.

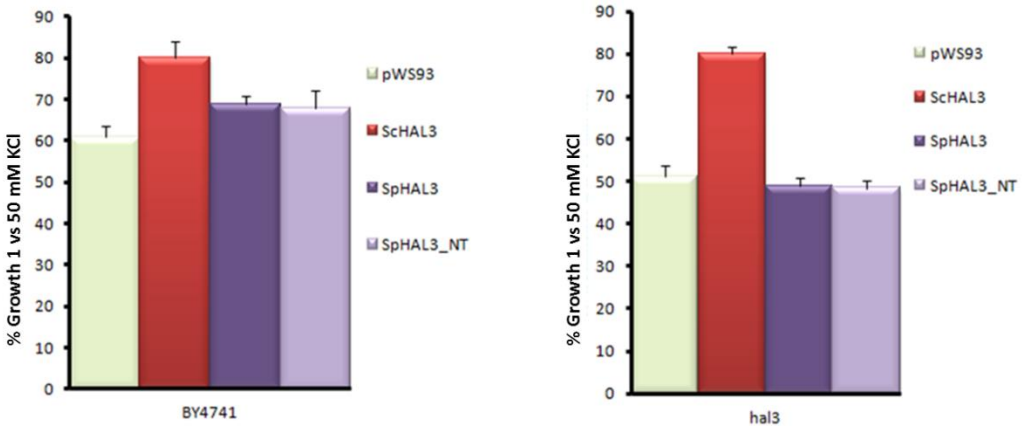

Figure 42. Effect of *S. pombe* SPAC15E1.04 expression in wild type and *hal3 S. cerevisiae* cells under potassium limiting conditions. Wild type (WT) strain BY4741 and the *hal3* derivative carrying the indicated plasmids were inoculated at OD_{660} of 0.005 in Translucent medium containing 1 mM KCl. The growth was measured after 16 hours of incubation. Data are represented as percentage of growth with respect to the strains grown in the same medium supplemented with 50 mM KCl, and correspond to the mean ± SEM from 6 independent experiments.

The previous observation that expression of *S. pombe* Hal3 did not confer general tolerance to toxic cations, along with the incapacity to improve the growth under potassium limiting conditions suggest that these proteins have little effect (if any) on the regulation of K^+ influx. These results cast doubts about the capacity of these *S. pombe* proteins to influence the function of the Trk transporters and, perhaps, to regulate ScPpz1.

Sensitivity to caffeine, a compound that negatively affects the integrity of the cell wall, is another phenotype related to overexpression of Hal3. It has been proposed that the increase in potassium influx produced by inactivation of Ppz1 results in an increase of turgor pressure, leading to cell wall stress. Since the Slt2 kinase plays an essential role for normal cell wall construction, overexpression of *HAL3* leads to a lytic phenotype in the absence of Slt2. The lytic phenotype can be rescued by addition of 1 M Sorbitol in the medium, which acts as an osmotic stabilizer (Posas, Casamayor and Ariño, 1993; Merchan *et al.*, 2004). Conversely, lack of *HAL3* improves growth of a *slt2* strain (De Nadal *et al.*, 1998; Ruiz *et al.*, 2009; Abrie *et al.*, 2012).

To analyze up to what extent the *S. pombe* Hal3 proteins might inhibit Ppz1 function, the sensitivity to caffeine in the *slt2* background was tested. The growth of *slt2* strain carrying the plasmids for the different Hal3 constructs is showed in the Figure 43A. Overexpression of both SpHal3 and SpHal3-Nter did not cause a negative effect in the growth of the *slt2* mutant under normal growth conditions or exposed to caffeine. These results suggested again that expression of the *S. pombe* proteins was not enough to affect the functions of the Ppz1 phosphatase on the input of K^+ through the Trk transporters. Remarkably, *S. pombe* Hal3 even conferred some tolerance to caffeine, allowing to growth at higher concentrations that cells carrying the empty plasmid. This "anti-Hal3" effect was also described for *CAB3* overexpression (Ruiz *et al.*, 2009), and could be explained by assuming that the *S. pombe* protein could be able to interact with Ppz1 (and thus, would compete with native Hal3), but not to capable of inhibiting the phosphatase activity (see section 3.3).

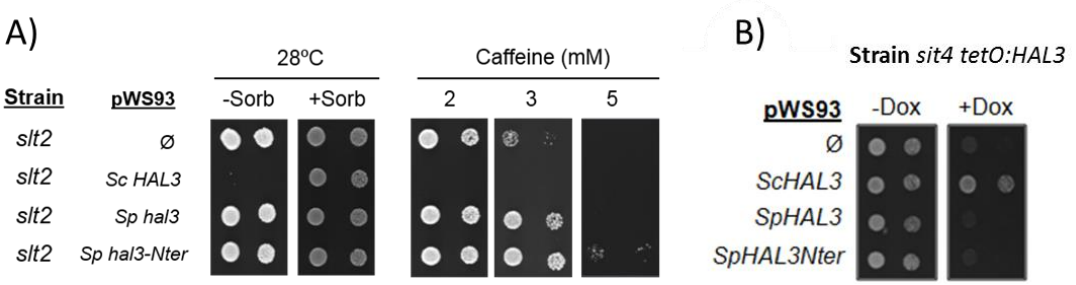

Figure 43. Functional analysis of *S. pombe* SPAC15E1.04 in physiological effects related to Hal3 overexpression. A) Strain JC010 (*slt2*) was transformed with the different Hal3 constructs and growth of the cells monitored on synthetic minimal medium lacking uracil at the permissive temperature (28ºC) in the presence or absence of 1 M sorbitol, and at the same temperature in the presence of different concentrations of caffeine. Plates were incubated for 3 days. **B)** Strain JC002 (*sit4 tetO:hal3*) was transformed with the indicated constructs and plated on YPD plates in the absence or the presence of 20 μg/ml doxycycline incubated for 3days at 28ºC.

On the other hand, overexpression of *HAL3* (named *SIS2*) was reported to recover, at least in part, the growth defect resulting from *SIT4* deletion (Di Como, Chang and Arndt, 1995). Conversely, the *sit4* and *hal3* mutations display synthetic lethality, due to G1 blockade. These effects are explained by the inhibitory role of Hal3 on Ppz1 and its effect on G1 cyclin expression (Clotet *et al.*, 1999; Simón *et al.*, 2001; Muñoz *et al.*, 2003). Therefore, we tested the effect of overexpression of both SpHal3 and SpHal3-Nter in a conditionally lethal mutant (strain JC002, *tetO:HAL3 sit4*). This strain has the *HAL3* promoter replaced by a doxycycline (Dox)-regulatable promoter. When strain JC002 is plated in the presence of 20–100 μg/ml Dox, the expression of endogenous *HAL3* is silenced and growth is blocked. As shown the Figure 43B, overexpression of both versions of *S. pombe* Hal3 did not rescue the lethal phenotype of a conditional *hal3 sit4* mutant under non-permissive conditions, whereas high-copy expression of ScHal3 did (Clotet *et al.*,

1999). Therefore, these results suggest that *S. pombe* Hal3 proteins cannot inhibit Ppz1 as to release the arrest of the cells and allow entry into cell cycle.

In summary, the effects of the overexpression of *S. pombe* Hal3 on the phenotypes related to physiological processes regulated by Ppz1 in *S. cerevisiae* demonstrated that this protein did not behave as native ScHal3. The entire *S. pombe* protein (SpHal3) was not able to replace the role of *S. cerevisiae* Hal3 in any of the phenotypes tested. The expression of the N-terminal half (Hal3-like domain) in *S. cerevisiae* was ineffective in the phenotypes related to potassium influx such as potassium requirements, tolerance to the toxic cations Hygromycin B and TMA or effect on growth in a *slt2* mutant. Moreover, expression of SpHal3-Ner did not rescued the lethality of a conditional *sit4 hal3* mutant. However, the expression of SpHal3-Nter exhibited some effect related to cation homeostasis in the absence of the chromosomal copy of Hal3, although the effect produced was less efficient that those of *S. cerevisiae* Hal3. This was reflected in an increased Li^+ tolerance and improvement of the efflux of this cation, despite the SpHal3-Nter construct was expressed in less amount that the full length SpHal3. The apparent contradiction of the *S. pombe* protein being able to control some Ppz1-related functions, but not others, can be explained if it is considered that Ppz1 has two main roles: inhibition of *ENA1* expression and negative regulation of Trk transporters. For instance, it could be hypothesized that SpHal3-Nter is able to decrease Ppz1 activity in *S. cerevisiae* to a level that allows releasing repression on *ENA1* expression (Posas, Camps and Arino, 1995; Ruiz, Yenush and Ariño, 2003), thus supporting up to some extent efficient extrusion of Li^+ cations (Figure 41A). In contrast, this regulatory effect would be insufficient to improve influx of K^+, thus explain the failure of the *S. pombe* protein to mimic budding yeast Hal3 when potassium-related phenotypes

are tested. It is worth noting that the role of Ppz1 on the regulation of *ENA1* expression has been demonstrated to be independent of the effects on potassium transport associated to Trks (Ruiz, Yenush and Ariño, 2003).

3.3. I*n vitro* Binding and inhibition of Ppz1 and Pzh1 phosphatases by *S. pombe* Hal3

Previous work demonstrated that ScHal3 binds to the C-terminal catalytic domain of Ppz1 (De Nadal *et al.*, 1998). Since overexpression of the entire *S. pombe* ORF as well as its Hal3-like N-terminal half in *S. cerevisiae* resulted in very limited effects, the possibility that these polypeptides could not recognize the phosphatase Ppz1 was considered. To that end, protein extracts from *S. cerevisiae* cells expressing HA-tagged versions of the SpHal3 and SpHal3-Nter, as well as of *S. cerevisiae* Hal3 (as a positive control) were prepared. After normalization for the amount of the expressed proteins, these extracts were tested for binding with the recombinant Ppz1 protein as well as its catalytic domain Ppz1-Cter by mixing with GST-tagged Ppz1 and Ppz1-Cter bound to glutathione-agarose beads. After incubation and washing, the proteins retained by the beads were analyzed in SDS-PAGE followed by immunoblot to detect HA epitopes. The result is showed in Figure 44A, and it was noticeable that both SpHal3 and SpHal3-Nter did bound to the entire Ppz1 as well as to the catalytic domain (Ppz1-Cter). However, the interaction of the *S. pombe* proteins was less intense than that observed for *S. cerevisiae* Hal3 (in fact, the amount of the sample loaded in the gel for SpHal3 was 3-fold higher, to allow detection of the protein).

Once the interaction was demonstrated, our purpose was to determine whether the interacting proteins could affect the phosphatase activity *in vitro*. In order to test the ability of *S. pombe* Hal3 to inhibit the activity of *S. cerevisiae* Ppz1, in vitro assays were performed using pNPP substrate to measure phosphatase activity by incubation of recombinant protein Ppz1 and its catalytic domain (both with the GST-tag removed) with increasing amounts of the different Hal3 versions. As shown in Figure 44B, neither the entire *S. pombe* Hal3 nor the N-terminal polypeptide were effective inhibiting Ppz1 activity, at concentrations that allowed almost full inhibition by *S. cerevisiae* Hal3. Notably, both versions of *S. pombe* Hal3 could inhibit, up to some extent, the phosphatase activity of Ppz1-Cter, although clearly less potently than ScHal3 It was remarkable that the entire SpHal3 seemed to be a slightly more potent inhibitor than Hal3-Nter, despite the observation that SpHal3 displayed slightly less binding capacity.

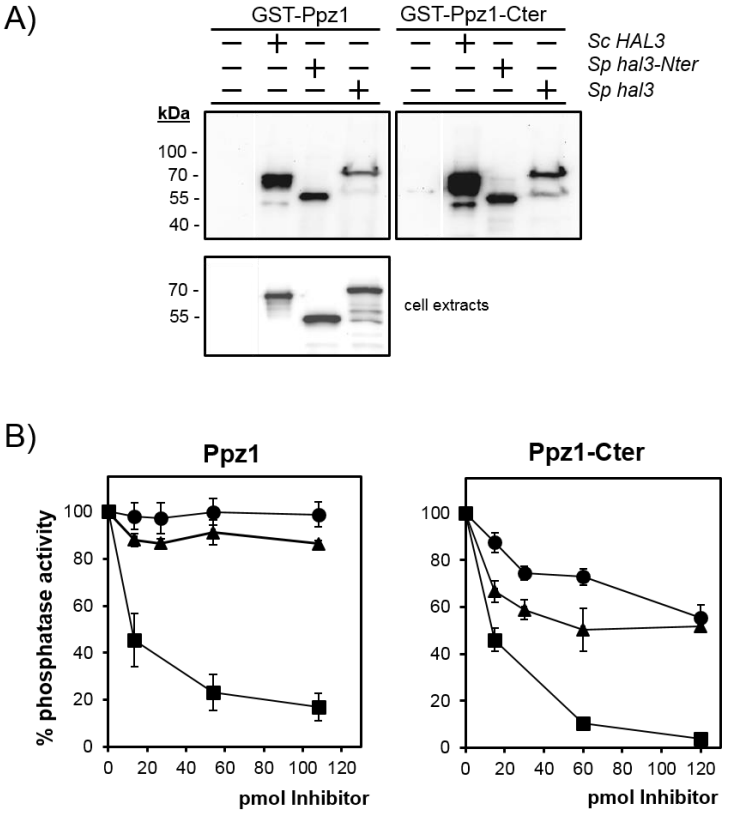

Figure 44. Binding to Ppz1 and inhibition of Ppz1 phosphatase activity by *S. pombe* Hal3 proteins.

A) The entire *S. cerevisiae* Ppz1 and its catalytic C-terminal half (Ppz1-Cter) were expressed in *E. coli* and bound to gluthathione–agarose beads (4 µg of each protein). Extracts of yeast IM021 cells (*ppz1 hal3*) expressing the different pWS93-based, HA-tagged constructs were prepared and binding tests performed as indicated in Experimental procedures. Due to the different expression levels of the Hal3 versions, the amounts of total protein used were adjusted to provide similar quantities of the expressed proteins (lower panel). Resins were washed and processed as in (Abrie et al., 2012). Twenty µl corresponding to 20% of the final sample (60 µl for SpHal3) were electrophoresed in 12% SDS-polyacrylamide gels and immunoblots obtained using anti-HA antibodies. **B)** Recombinant Ppz1 or its C-terminal catalytic moiety (13.5 and 15 pmols, respectively) were incubated with increasing amounts of recombinant Hal3 from *S. cerevisiae* (■), entire SpHal3 (▲) or the N-ter SpHal3 moiety (●). Protein phosphatase activity was determined with pNPP substrate in the absence or in the

presence of increasing concentrations of inhibitors. Data is represented as percentage of the activity of the enzyme preparation in the absence of inhibitors and correspond to the mean ± SEM from 3 to 5 independent determinations.

From these results, collectively, it could be concluded that SpHal3 and SpHal3-Nter displayed a weak in vitro inhibitory capacity on Ppz1-Cter, but were completely unable to inhibit the full length Ppz1 protein. This failure cannot be attributed to the inability of the *S. pombe* proteins to interact with both versions of Ppz1 (although the binding capacity was less intense for the entire *S. pombe* Hal3). The failure of both *S. pombe* proteins to inhibit full length (native) Ppz1 is in agreement with the phenotypes observed in vivo, which show weak or no capacity for these proteins to mimic native Hal3 functions. The observation that SpHal3 or its N-terminal half have some effect inhibiting Ppz1-Cter is interesting. It has been proposed that the N-terminal half of Ppz1 might have a protective effect against excessive in vivo inhibition by Hal3 (Clotet *et al.*, 1996; De Nadal *et al.*, 1998). Therefore, one could hypothesize that SpHal3 (or SpHal3-Nter) would be less effective Ppz1 inhibitors, unable to counteract the effect due to the presence of the N-terminal half of Ppz1. In this regard, it must be noted that SpHal3 not only lacks the N-terminal segment present in ScHal3, but also that the highly acidic region that in ScHal3 follows the PPCDC core is much shorter in SpHal3. Both regions have been shown to be relevant for ScHal3 as far as its Ppz1 inhibitory capacity is concerned (Abrie *et al.*, 2012).

In addition, our results show that *S. pombe* Hal3, despite its inability to inhibit Ppz1, retains the capacity to interact with the C-terminal domain of Ppz1 and, up to some extent, to inhibit its phosphatase activity. Some years ago, nine residues in the core domain

of *S. cerevisiae* Hal3 were identified as important for Ppz1 binding or inhibition (Muñoz *et al.*, 2004). Interestingly, sequence comparison reveals that *S. pombe* Hal3 maintains several, but not all, of these residues. ScHal3 residues I446 (relevant for binding), E460, V462 (both involved in the inhibition) and I480 are conserved in SpHal3, corresponding to I172, E186, V188 and I205 residues. This suggests that the absence of certain residues with functional relevance for the interaction with Ppz1 may be the cause of the limited inhibition observed.

Schizosaccharomyces pombe Pzh1, the homolog of S. cerevisiae Ppz1, is also involved in cation homeostasis, although likely through different regulatory mechanisms. Once the capacity of regulation of Ppz1 by *S. pombe* Hal3 was assayed, we decided to determine if *S. pombe* Hal3 binds and inhibits to its own phosphatase Pzh1, just as their budding yeast orthologs do. This possibility was tested carried out similar experiments using recombinant Pzh1.

The interaction between both *S. cerevisiae* and *S. pombe* Hal3 proteins (entire SpHal3 and its N-terminal region) with Pzh1 is showed in the Figure 45A. Surprisingly, *S. cerevisiae* Hal3 exhibited an interaction with the matrix-bound GST-Pzh1 that was even stronger than to the own budding yeast Ppz1 phosphatase. This result suggests that *S. cerevisiae* Hal3 is a powerful regulator of Ppz-like phosphatases and that Pzh1 fully retain structural elements required for the regulation by Hal3. Testing of both *S. pombe* Hal3 constructs indicated that they could bind to Pzh1 moderately, although the entire SpHal3 gave much weaker interaction (the sample load in this case was also increased three-fold). Therefore, *S. pombe* Hal3 recognized the fission yeast phosphatase, and the pattern of binding was similar to that observed for Ppz1.

The ability of *S. pombe* and *S. cerevisiae* Hal3 to inhibit Pzh1 phosphatase activity was evaluated as for Ppz1. The results (Figure 45B) showed a clear differentiation in the inhibitory effect between *S. pombe* constructs. The entire SpHal3 was a poor *in vitro* inhibitor of Pzh1. Nevertheless, the N-terminal half showed a higher inhibitory capacity. Again, the *S. cerevisiae* Hal3 was the most effective inhibitor of the fission yeast phosphatase, with a pronounced decrease in activity similar as the one observed for *S. cerevisiae* Ppz1.

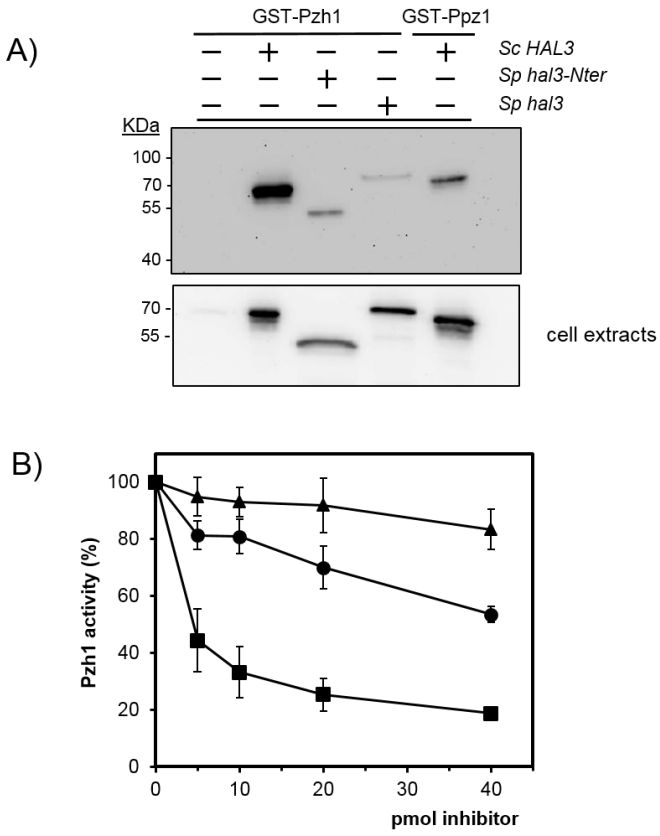

Figure 45. Binding to Pzh1 and inhibition of Pzh1 phosphatase activity. A) The *S. pombe* Pzh1

phosphatase was expressed in *E. coli* and bound to gluthathione–agarose beads (4 μg of protein). *S. cerevisiae* extracts expressing the indicated proteins were used for binding tests as described in the legend of Figure 46A. Note that a 3-fold volume of sample was run in the lane corresponding to SpHal3 to allow better visualization of the band. A binding experiment involving *S. cerevisiae* Ppz1 and Hal3 proteins is included for comparison. **B)** Nine pmol of recombinant Pzh1 was incubated with increasing amounts of recombinant Hal3 from *S. cerevisiae* (■), entire SpHal3 (▲) or the N-ter SpHal3 moiety (●). Data are represented as in Figure 46B and correspond to the mean ± SEM from 3 independent experiments.

In summary, all the results concerning regulation of Pzh1 indicate that full length *S. pombe* Hal3 might not be relevant in the control of the phosphatase Pzh1 in fission yeast. Yet, this cannot be attributed to the fact that fission yeast Pzh1 lacks structural determinants required for inhibition by Hal3-like proteins, since this phosphatase interacts with and is potently inhibited by *S. cerevisiae* Hal3. As mentioned above, the absence in SpHal3 of an N-terminal extension and a long acidic tail, together with the presence of the C-terminally fused TS domain could be detrimental for its inhibitory capacity. Such inefficient regulatory component would fit with the presence in Pzh1 of an N-terminal extension much shorter than that of ScPpz1. It is worth to note that the precise targets for Pzh1 in *S. pombe* could differ from the ones identified in *S. cerevisiae* for Ppz1 (Balcells *et al.*, 1997, 1998, 1999).

3.4. The role of *S. pombe* Hal3 in PPCDC function

The N-terminal region of ORF SPAC15E1.04 mimics the structure of known PPCDC enzymes. On the basis of the AtHal3a protein structure, the sequence of the N-terminal domain of the *S. pombe* Hal3 conserves the histidine, cysteine and asparagine

residues (His^{104}, Asn^{156}, Cys^{191}) known to be necessary for PPCDC function, and this is the only occurrence of such kind of structure in the *S. pombe* genome. This allow speculating that the ORF SPAC15E1.04 should encode a monogenic PPCDC, in contrast to the heteromeric enzyme present in *S. cerevisiae*. In order to investigate whether the *S. pombe* Hal3 exhibit PPCDC activity, genetic tests were performed in budding yeast. It is known that the *hal3 vhs3* deletion mutant is synthetically lethal due to the essential role that these proteins play in the formation of the active PPCDC, where they contribute with a histidine residue to the active site. The other component that forms part of the atypical heterotrimeric enzyme in *S. cerevisiae* is *CAB3* (YKL088w), which provide the cysteine residue required to complete the PPCDC reaction (Ruiz *et al.*, 2009).

Therefore, the ability to rescue the synthetically lethal phenotype of the double *hal3 vhs3* mutant and the lethality of the *cab3* mutation was tested. To this end, diploid strains heterozygous for the *hal3 vhs3* or the *cab3* mutations were transformed with the entire SpHal3 and its N-terminal region, as well as with *S. cerevisiae* Hal3. After sporulation, the meiotic products were assessed by a combination of random spore (sixty spores were analyzed for each expressed plasmid) and tetrad analysis (twenty-five tetrads dissected for each plasmid) to test the viability of the haploid derivates. As shown in Figure 46, and as it was previously demonstrated (Ruiz *et al.*, 2009), ScHal3 recued the synthetic lethality of the *hal3 vhs3* mutation, allowing growth of all four spores in each tetrad, but did not complement the *cab3* mutant. Interestingly, the expression of the entire SpHal3, as well as that of its N-terminal region (SpHal3-Nter) supported growth of all four spores in each tetrad derived from the *CAB3*/*cab3* heterozygous diploid and allowed recovering of haploids harboring deletions of both *HAL3* and *VHS3* genes. This indicates that both *S.*

pombe proteins were able to rescue the lethal effect due to the absence of Hal3 and Vhs3, as well as that of the *cab3* mutation.

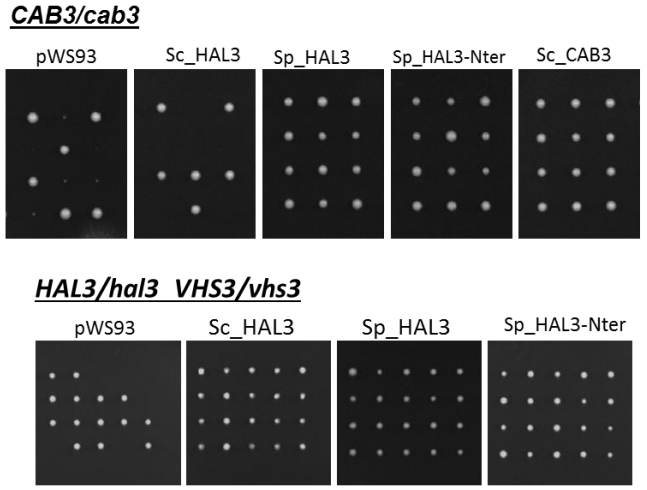

	Strain	
Plasmid	*hal3 vhs3*	*cab3*
pWS93	-	-
ScHAL3	+	-
SpHAL3	+	+
SpHAL3-Nter	+	+
ScCAB3	*nd*	+

Figure 46. Complementation of PPCDC function in *S. cerevisiae* by *S. pombe* Hal3. The diploid strain heterozygous for the *cab3* mutation (MAR25) and the heterozygous diploid strain *hal3 vhs3* (AGS4) were transformed with plasmid pWS93 containing the diverse Hal3 versions and the correspondent controls (empty plasmid as negative, or Cab3 when is required as positive), sporulation was induced and the resulting tetrads were analyzed. Twenty-five tetrads were dissected for each strain containing the different plasmids. The pictures shown the results of three or five dissected tetrads only. In all the cases the auxotrophic markers of the colonies from spores were analyzed. The table at the right summarizes the ability to recover viable haploid cells containing the mutations from random spore and tetrad dissection combined experiments; +, rescues, -, do not rescue; nd, not determined.

The observation that both *S. pombe* Hal3 versions were able to replace all three *S. cerevisiae* proteins demonstrates that the ORF SPAC15E1.04 provide the essential PPCDC function and confirms that in the *S. pombe* Hal3 all the specific structural requirements for

catalysis (His104, Asn166, Cys190) are functional. It must be noted that the presence of the C-terminal TS domain did not affect the ability of the protein to act as a PPCDC, since the entire *S. pombe* Hal3 was also able to rescue all relevant *S. cerevisiae* gene deletions.

The fact that the ORF SPAC15E1.04 appears to be the only PPCDC encoded by the genome of *S. pombe*, together with the evidence that all known PPCDCs build their active sites at the interface between adjacent monomers, allow to postulate that in *S. pombe* the enzyme should have a homotrimeric structure, as it occurs in plants and animals. Consequently, the ability of the fission yeast proteins to form trimers was investigated *in vitro*. To this end, recombinant SpHal3 and SpHal3-Nter proteins (with their GST-tag removed) were used for cross-linking experiments using glutaraldehyde and the products analyzed by SDS-PAGE (Figure 47A). The results showed that treatment with glutaraldehyde resulted in the disappearance of the corresponding monomers (70 kDa in the case of the entire protein and 40 kDa for SpHal3-Nter) and in the presence of bands with higher molecular mass that could be attributed to trimers. ScHal3 was included as positive control since was described that is able to form homomeric trimers (Ruiz *et al.*, 2009). Therefore, the cross-linking experiments confirm that the PPCDC enzyme in *S. pombe* should be formed by three monomers of the same protein, and indicate that besides the residues required for the catalytic reaction, also maintain structural determinants for trimerization. Therefore, the PPCDC enzyme of *S. pombe* is reminiscent to the PPCDC found in plants or animals. Because in these proteins the presence of the flavin coenzyme FMN is also required for the PPCDC activity, we carried out a spectrophotometric scanning of a preparation of recombinant SpHal3. As shown in Figure 47B, two peaks at 382 and 452 nm were detected, which are compatible with the presence of oxidized flavin in the sample.

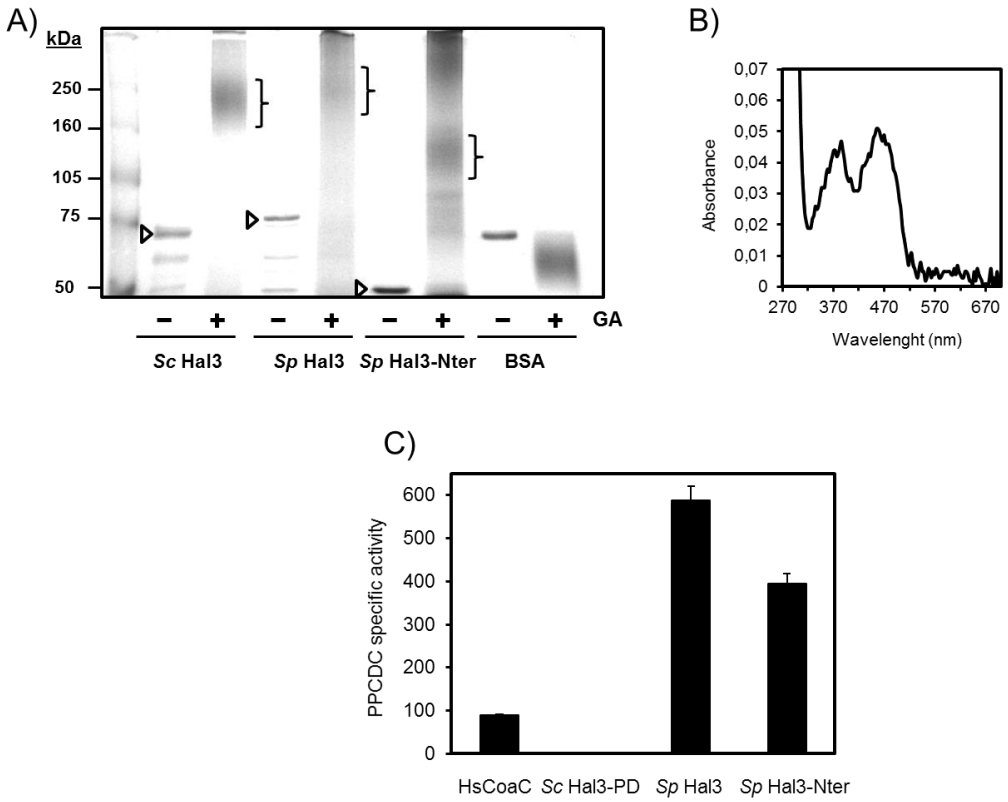

Figure 47. PPCDC activity of *S. pombe* Hal3. A) Analysis of trimerization ability. Samples of the indicated proteins (1 μg) were incubated in the presence (GA, +) or the absence (-) of glutaraldehyde. Samples were resolved by SDS-PAGE (6% polyacrylamide gel) and proteins were visualized by staining with Coomassie Brilliant Blue. Arrowheads point to the monomeric proteins. **B)** UV-Visible spectra of the *Sp* Hal3-Nter preparation showing the peaks at 382 and 452 nm, which are compatible with the presence of oxidized flavin in the molecule. **C)** Recombinant human PPCDC (HsCoaC), S. cerevisiae Hal3 core (Sc Hal3-PD), entire SpHal3 and its N-terminal domain were tested for in vitro PPCDC activity at a concentration of 60 nM. Results are mean ± SD from three independents experiments.

Afterwards, to further confirm the ability of *S. pombe* Hal3 to perform as functional PPCDC, the PPCDC activity of this protein was evaluated *in vitro*. These experiments were carried out in collaboration with the group of Dr. Erick Strauss (Univ. Stellenbosch, South Africa) because the substrate used, 4-PP, is not commercial. As shown in Figure 47C, the

catalytic core of *S. cerevisiae* Hal3 did not exhibit activity, in agreement to previous observations (Ruiz *et al.*, 2009; Abrie *et al.*, 2012). However, both the entire SpHal3 and its N-terminal half (SpHal3-Nter) of *S. pombe* displayed strong PPCDC activities, which were even considerably higher than that shown by an equivalent amount of the human PPCDC enzyme. This is in contrast with the reported observation that the activity of the *S. cerevisiae* heterotrimeric enzyme composed of Hal3/Vhs3/Cab3 was only around 35-40% of the human enzyme (Ruiz *et al.*, 2009). Hence, the enzyme of the fission yeast exhibited a PPCDC activity comparatively much higher, which suggest that the evolution in *S. pombe* had led SpHal3 to specialize in forming a more effective PPCDC enzyme (an essential function), likely in detriment of its ability to perform a role in Pzh1 regulation. Conversely, the ability of ScHal3 to moonlight could have caused adverse effects on the capacity of the protein to perform what would possibly be its primary function (Gancedo and Flores, 2008; Gancedo, Flores and Gancedo, 2016).

3.5. The C-terminal half of *S. pombe* SPAC15E1.04 provides thymidylate synthase activity

The C-terminal of SPAC15E1.04, which presumably encodes a thymidylate synthase, was also subjected to study in this work. Therefore, taking advantage of the fact that TS is an essential enzyme encoded by a single gene (*CDC21*) in *S. cerevisiae*, a *cdc21* mutant was used to test whether the C-terminal half of the ORF could replace and provide the TS function. To this end, the diploid strain heterozygous for *cdc21* deletion (in the BY4743 background) was transformed with the multicopy plasmids pWS93 expressing the

entire SpHal3 as well as the two halves of the *S. pombe* protein (SpHal3-Nter and SpHal3-Cter), *S. cerevisiae* Hal3, or the empty plasmid (included as reference). These cells were induced to sporulate and the ability of the haploids to survive was assessed by tetrad and random spore analyses. After testing for the presence of relevant genetic markers in the meiotic products, the results, shown in Figure 48, indicate that overexpression of both the entire SpHal3 and its C-terminal half allowed rescue of haploid cells containing the *cdc21* mutation. Nevertheless, as it was expected, neither overexpression of *S. cerevisiae* Hal3 nor that of the N-terminal half of *S. pombe* did complement the *cdc21* mutation.

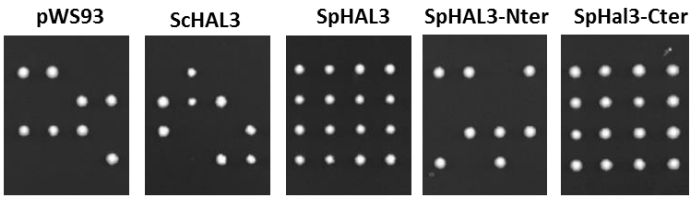

	Strain
Plasmid	*cdc21*
pWS93	-
ScHAL3	-
SpHAL3	+
SpHAL3-Nter	-
SpHAL3-Cter	+

Figure 48. Rescue of thymidylate synthase mutation in *S. cerevisiae* by *S. pombe* Hal3. Diploid strain heterozygous for *cdc21* mutation transformed with the *S. pombe* constructs (SpHal3, SpHal3-Cter and SpHal3-Nter) and negative controls (empty plasmid and ScHal3), was induced to sporulate and the tetrads were dissected. The pictures shown the results of four dissected tetrads. In all the cases the markers of the colonies derived from each spore were analyzed. The table at the right shows in summary the ability to recover viable haploid cells containing the mutation as deduced from the combination of 60 spores analyzed by random spore and 25 tetrads dissected (for each plasmid); +, did rescue; -, did not rescue.

The complementation of the *cdc21* mutant demonstrated that the C-terminal domain of the *S. pombe* protein was able to provide TS function in budding yeast, strongly

suggesting that it performs this specific role in *S. pombe* and that, apparently, the presence of the N-terminal half did not affect this activity. It is noteworthy that TS activity exhibits differential expression during cell cycle in most eukaryotic cells (Storms *et al.*, 1984; Taylor *et al.*, 1987). Commonly, the regulation of thymidylate synthase occurs at the level of transcription, as TS mRNA amounts increase during late G1 and early S phase (Taylor *et al.*, 1987; McIntosh, Ord and Storms, 1988; Vernis, Piskur and Diffley, 2003). In contrast, the mRNA levels of the *S. pombe* SPAC15E1.04 ORF are usually constant along the different phases of cell cycle (Carpy *et al.*, 2014). The evidence that this gene does not show a differential expression along the cell cycle allows to speculate that the PPCDC function imposes to a constant level of transcription, since PPCDC activity is likely required at all times. Still, an additional level of regulation could be envisaged: the proteolytic processing of the full length polypeptide to release free TS when this enzyme would be required.

In conclusion, the entire *S. pombe* ORF was functionally competent, encoding both PPCDC and TS enzymes. These activities are essential for cell survival, as it has been demonstrated in this work. However, this was in contrast with a previous report claiming that the SPAC15E1.04 deletion mutant was viable (Kim *et al.*, 2010). For that reason, we decided to reinvestigate the essential nature of the ORF. To this end, a diploid strain (MC71) heterozygous for the *SPAC15E1.04* deletion was constructed and induced to sporulate. Upon germination of the spores, we were unable to recover haploid progeny carrying the mutation, indicating that the gene is essential. Tetrad analysis of the heterozygous diploid confirmed the lethality of the gene deletion.

3.6. The SPAC15E1.04 gene product is an unprocessed multifunctional protein

Our previous experiments demonstrated that each half of the SPAC15E1.04 gene product is able to perform a specific functional role. Therefore, we considered relevant to explore whether the SPAC15E1.04 gene product is expressed as a hybrid protein or two independent protein products are post-translationally generated in *S. pombe*. In order to detect the polypeptide and to monitor a possible proteolytic process, the ORF was tagged with the HA epitope in its C-terminus and integrated in the same locus (yielding strain MC70). Cells were then grown under standard conditions as well as subjected to diverse kinds of stress, considering the possibility that processing might occur only under particular circumstances. Stress conditions investigated were high temperature, osmotic shock (sorbitol), saline (NaCl and KCl), and oxidative stress (hydrogen peroxide, menadione and t-butyl hydroperoxide). Cells were collected after one and three hours of treatment and protein extracts were tested by immunoblotting (Figure 49). Similar experiments were carried out using 12 mM hydroxyurea or 50 μg/ml nocodazole, which interfere with cell cycle progression at S and G2/M phase respectively; and also in medium with low glucose (1% and 0.5% glucose) and low adenine (7,5 mg/ml and 30 mg/ml adenine) (data not shown).

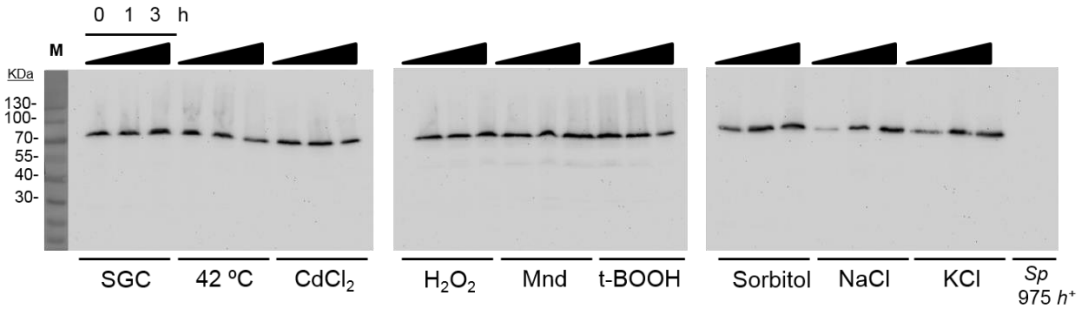

Figure 49. The SpHal3 polypeptide is unprocessed in *S. pombe*. After exposing MC70 strain and 975 h+ (WT) to different stresses, cells were collected at the indicated times and processed for protein extract preparation as indicated in Experimental Procedures. Equivalent amounts were subject to SDS-PAGE (8% Polyacrylamide gels) followed by immunoblot using anti-HA antibodies to reveal HA-tagged SpHal3.

As shown in Figure 49, a single polypeptide with the expected molecular weight of ~ 70 kDa was detected in all the conditions tested. Therefore, the SpHal3 product was neither processed under normal conditions nor in response to the different stresses that were explored. Therefore, it must be assumed that SpHal3 encodes a multifunctional polypeptide, likely as a result of a gene fusion event, in which the different functions can be assigned to specific domains of the protein that do not seem to functionally interfere each other.

Gene fusion events are relatively rare and occur at a low frequency (Snel, Bork and Huynen, 2000; Kummerfeld and Teichmann, 2005; Leonard and Richards, 2012). Gene fusions persist only if they provide an evolutionary advantage and usually they are also functionally related, constituting parts of the same complex or being involved in the same metabolic pathway (Snel, Bork and Huynen, 2000; Yanai, Derti and DeLisi, 2001). It should be noted that genes encoding enzymes that catalyse folate biosynthesis have been

identify as fusion events in many organisms (Stechmann, 2002; Krupenko, 2009). In the *S. pombe* genome 12 gene fusions have been identified, such as thiamine diphosphokinase (Tnr3), various cytochrome c oxidase, or dihydrofolate reductase Dfr1 (Molero *et al.*, 2013). Curiously, the thymidylate synthase coding region is found in plants and many protozoan species as a gene fusion with the functionally related enzyme dihydrofolate reductase (Stechmann, 2002). In contrast, in the case of the ORF SPAC15E1.04, one might assume that the multidomain protein assembles two enzyme activities with unrelated roles. Nevertheless, several reports allow establishing a tight connection between DNA synthesis or DNA integrity with CoA levels. One example is the *E. coli* CoaBC gene, which encodes two enzymes, PPCDC and phosphopantothenoycysteine synthase, which catalyze consecutive reactions in CoA biosynthesis (Kupke *et al.*, 2000; Strauss *et al.*, 2001). A specific mutation affecting the PPCDC domain of this gene caused slow cessation of DNA synthesis (Spitzer and Weiss, 1985; Spitzer, Jimenez-Billini and Weiss, 1988; Kupke, 2001). Other recent works have reported that defective CoA biosynthesis results in increased levels of DNA damage and compromised DNA integrity in Drosophila (Bosveld *et al.*, 2008) and, remarkably, in fission yeast (Nakamura *et al.*, 2012). On the other hand, the thymidylate synthase activity provides the exclusive dTMP source for DNA synthesis is many fungi because these organisms lacks thymidine kinase activity (Singer *et al.*, 1989; Ahmad, Kirk and Eisenstark, 1998; Vernis, Piskur and Diffley, 2003). It has been reported that conditional mutations of TS gene in *S. cerevisiae* produce arrest of the yeast cell cycle in the S phase, and mitochondrial DNA replication is also stopped (Chien, Chou and Su, 2009). In addition, inhibition of TS and consequent dTMP starvation results in loss of DNA integrity because induces DNA strand breakage, mitotic crossing-over, gene conversion, and unequal sister chromatid exchange (Taylor *et al.*, 1987; Vernis, Piskur and

Diffley, 2003). In conclusion, taking into account the adverse effects caused by failures in PPCDC or TS, it allows to speculate that the two essential enzyme activities contained in SPAC15E1.05 ORF could have common functional link to the maintenance of DNA integrity.

CONCLUSIONS

1) Re-sequencing of the ORF SPAC15E1.04 of *S. pombe* and *S. japonicus* confirmed that these organisms contain a sequence related to Hal3-like proteins in its N-terminal half and a sequence likely encoding a thymidylate synthase enzyme in its C-terminal half.

2) The SPAC15E1.04 gene product was expressed in *S. cerevisiae* as a single polypeptide under normal conditions.

3) The phenotypic effects related to Ppz1 regulation indicated that although expression of the N-terminal region (SpHal3-Nter) conferred a slightly increase in salt tolerance, in most cases neither the overexpression of the entire ORF of *S. pombe* (SpHal3) nor SpHal3-Nter could functionally replace the *S. cerevisiae* Hal3.

4) SpHal3 and SpHal3-Nter are able to bind in vitro to Ppz1, although weaker than ScHal3. Despite the interaction, SpHal3 and SpHal3-Nter are unable to inhibit *in vitro* the phosphatase activity of Ppz1. Nevertheless, the putative regulators show a weak inhibitory effect when tested with ScPpz1 devoid of its N-terminal half.

5) Both *S. pombe* Hal3 versions are able to interact with the phosphatase of *S. pombe*, Pzh1. However, the ability of these *S. pombe* Hal3 to inhibit Pzh1 *in vitro* is only exhibited by the SpHal3-Nter polypeptide, suggesting that *S. pombe* Hal3 might have no relevance in the control of the phosphatase in fission yeast.

6) Both the entire SpHal3 and the N-terminal version (SpHal3-Nter) exhibited a very high PPCDC activity *in vitro* and were able to provide PPCDC function in *S. cerevisiae* by rescuing the double deletion *hal3 vhs3* as well as the lethal mutation *cab3*. Moreover, both proteins showed the ability to form trimers. These data evidence that the N-terminal half

of the *S. pombe* protein is able to perform as a PPCDC and that the presence of the C-terminal TS-like domain does not affect this function, allowing proposing a monogenic homotrimeric model of PPCDC enzyme in *S. pombe*.

7) SPAC15E1.04 encodes a functional thymidylate synthase in its C-terminal region, as demonstrated by the fact that overexpression of SpHal3 rescued the lethality of *cdc21* mutant in *S. cerevisiae*.

8) The SPAC15E1.04 ORF is the result of a gene fusion event and it is expressed as a single, unprocessed polypeptide, encoding two essential enzymes.

REFERENCES

Abeysinghe, T., Hong, B., Wang, Z. and Kohen, A. (2017) 'Preserved hydride transfer mechanism in evolutionarily divergent thymidylate synthases', pp. 19–30.

Abrie, J. A., González, A., Strauss, E. and Ariño, J. (2012) 'Functional mapping of the disparate activities of the yeast moonlighting protein Hal3', *Biochemical Journal*, 442(2), pp. 357–368.

Adám C, Erdei E, Casado C, Kovács L, González A, Majoros L, Petrényi K, Bagossi P, Farkas I, Molnar M, Pócsi I, Ariño J, D. V. (2012) 'Protein phosphatase CaPpz1 is involved in cation homeostasis, cell wall integrity and virulence of Candida albicans', *Microbiology*, 158(5), pp. 1258–1267.

Adams, A. and Kaiser, C. (1997) *Methods in yeast genetics : a Cold Spring Harbor Laboratory course manual*. Cold Spring Harbor Laboratory Press.

Ahmad, S. I., Kirk, S. H. and Eisenstark, A. (1998) 'Thymine Metabolism and Thymineless Death in Prokaryotes and Eukaryotes', *Annual Review of Microbiology*, 52(1), pp. 591–625.

Aksenova, A., Muñoz, I., Volkov, K., Ariño, J. and Mironova, L. (2007) 'The HAL3-PPZ1 dependent regulation of nonsense suppression efficiency in yeast and its influence on manifestation of the yeast prion-like determinant [ISP+]', *Genes to Cells*, 12(4), pp. 435–445.

Albert, A., Martínez-Ripoll, M., Espinosa-Ruiz, A., Yenush, L., Culiáñez-Macià, F. A. and Serrano, R. (2000) 'The X-ray structure of the FMN-binding protein atHal3 provides the structural basis for the activity of a regulatory subunit involved in signal transduction', *Structure*, 8(9), pp. 961–969.

Alepuz, P. M., Cunningham, K. W. and Estruch, F. (1997) 'Glucose repression affects ion homeostasis in yeast through the regulation of the stress-activated ENA1 gene.', *Mol Microbiol*, 26(1), pp. 91–98.

Andrews, P. D. and Stark, M. J. (2000) 'Type 1 protein phosphatase is required for maintenance of cell wall integrity, morphogenesis and cell cycle progression in Saccharomyces cerevisiae 1', *J.Cell*

Sci., 113 (Pt 3(0021–9533), pp. 507–520.

Ansai, T., Dupuy, L. C. and Barik, S. (1996) 'Interactions between a minimal protein serine/threonine phosphatase and its phosphopeptide substrate sequence', *Journal of Biological Chemistry*, 271(40), pp. 24401–24407.

Arino, J., Ramos, J. and Sychrova, H. (2010) 'Alkali Metal Cation Transport and Homeostasis in Yeasts', *Microbiology and Molecular Biology Reviews*, 74(1), pp. 95–120.

Ariño, J. (2002) 'Novel protein phosphatases in yeast.', *European journal of biochemistry / FEBS*, 269(4), pp. 1072–7.

Asherie, N. (2004) 'Protein crystallization and phase diagrams', *Methods*, 34(3), pp. 266–272.

Balcells, Â., Calero, F., Arin, Â. and Biochem, J. E. J. (1999) 'The Schizosaccharomyces pombe Pzh1 protein phosphatase regulates Na + ion influx in a Trk1-independent fashion', 37, pp. 31–37.

Balcells, L., Gómez, N., Casamayor, a, Clotet, J. and Ariño, J. (1997) 'Regulation of salt tolerance in fission yeast by a protein-phosphatase-Z-like Ser/Thr protein phosphatase.', *European journal of biochemistry / FEBS*, 250(2), pp. 476–483.

Balcells, L., Martin, R., Ruiz, M. C., Gomez, N., Ramos, J. and Arino, J. (1998) 'The Pzh1 protein phosphatase and the Spm1 protein kinase are involved in the regulation of the plasma membrane H+-ATPase in fission yeast', *FEBS letters*, 435(14-5793–3), pp. 241–244.

Barford, D. (1996) 'Molecular mechanisms of the protein serine/threonine phosphatases.', *Trends in biochemical sciences*, 21(11), pp. 407–12.

Barford, D., Das, A. K. and Egloff, M.-P. (1998) 'THE STRUCTURE AND MECHANISM OF PROTEIN PHOSPHATASES: Insights into Catalysis and Regulation', *Annual Review of Biophysics and Biomolecular Structure*, 27(1), pp. 133–164.

Barreto, L., Canadell, D., Petrezsélyová, S., Navarrete, C., Marešová, L., Peréz-Valle, J., Herrera, R., Olier, I., Giraldo, J., Sychrová, H., Yenush, L., Ramos, J. and Ariño, J. (2011) 'A genomewide screen for tolerance to cationic drugs reveals genes important for potassium homeostasis in Saccharomyces cerevisiae', *Eukaryotic Cell*, 10(9), pp. 1241–1250.

Barton, G. J., Cohen, P. T. W. and Barford, D. (1994) 'Conservation analysis and structure prediction of the protein serine/threonine phosphatases. Sequence similarity with diadenosine tetraphosphatase from Escherichia coli suggests homology to the protein phosphatases', *European Journal of Biochemistry*. Blackwell Publishing Ltd, 220(1), pp. 225–237.

Begley, T. P., Kinsland, C. and Strauss, E. (2001) 'The biosynthesis of coenzyme A in bacteria.', *Vitamins and hormones*, 61, pp. 157–171.

Benito, B., Garciadeblás, B. and Rodríguez-Navarro, A. (2002) 'Potassium- or sodium-efflux ATPase, a key enzyme in the evolution of fungi', *Microbiology*, 148(4), pp.

Bergfors, T. (2003) 'Seeds to crystals', *Journal of Structural Biology*, 142(1), pp. 66–76.

Bergfors, T. (2007) 'Screening and Optimization Methods for Nonautomated Crystallization Laboratories', in *Methods in Molecular Biology*, pp. 131–151.

Bisson, L. F. and Thorner, J. (1981) 'Thymidylate synthetase from Saccharomyces cerevisiae. Purification and enzymic properties', *Journal of Biological Chemistry*, 256(23), pp. 12456–12462.

Bloecher, A. and Tatchell, K. (1999) 'Defects in Saccharomyces cerevisiae protein phosphatase type I activate the spindle/kinetochore checkpoint', *Genes and Development*, 13(5), pp. 517–522.

Blommel, P. G., Becker, K. J., Duvnjak, P. and Fox, B. G. (2007) 'Enhanced bacterial protein expression during auto-induction obtained by alteration of lac repressor dosage and medium composition', *Biotechnology Progress*, 23(3), pp. 585–598.

Bollen, M. (2001) 'Combinatorial control of protein phosphatase-1.', *Trends in biochemical sciences*, 26(7), pp. 426–431.

Bollen, M., Peti, W., Ragusa, M. J. and Beullens, M. (2010) 'The extended PP1 toolkit: Designed to create specificity', *Trends in Biochemical Sciences*, pp. 450–458.

Bony, M., Barre, P. and Blondin, B. (1998) 'Distribution of the flocculation protein flop, at the cell surface during yeast growth: The availability of flop determines the flocculation level', *Yeast*, 14(1), pp. 25–35.

Bosveld, F., Rana, A., Van Der Wouden, P. E., Lemstra, W., Ritsema, M., Kampinga, H. H. and Sibon, O. C. M. (2008) 'De novo CoA biosynthesis is required to maintain DNA integrity during development of the Drosophila nervous system', *Human Molecular Genetics*, 17(13), pp. 2058–2069.

Canadell, D., González, A., Casado, C. and Ariño, J. (2015) 'Functional interactions between potassium and phosphate homeostasis in Saccharomyces cerevisiae', *Molecular Microbiology*, 95(3), pp. 555–572.

Cannon, J. F. (2010) 'Function of Protein Phosphatase-1, Glc7, in Saccharomyces cerevisiae', *Advances in Applied Microbiology*, 73(C), pp. 27–59.

Carpy, A., Krug, K., Graf, S., Koch, A., Popic, S., Hauf, S. and Macek, B. (2014) 'Absolute proteome and phosphoproteome dynamics during the cell cycle of fission yeast.', *Molecular & Cellular Proteomics*, pp. 1925–1936.

Carreras, C. W. (1995) 'The Catalytic Mechanism and Structure of Thymidylate Synthase', *Annual Review of Biochemistry*, 64(1), pp. 721–762.

Ceulemans, H., Stalmans, W. and Bollen, M. (2002) 'Regulator-driven functional diversification of protein phosphatase-1 in eukaryotic evolution', *BioEssays*, 24(4), pp. 371–381.

Ceulemans, H., Vulsteke, V., Maeyer, M. De, Tatchell, K., Stalmans, W. and Bollen, M. (2002)

'Binding of the Concave Surface of the Sds22 Superhelix to the 4 / 5 / 6-Triangle of Protein Phosphatase-1 *', 277(49), pp. 47331–47337.

Chang, J. S., Henry, K., Wolf, B. L., Geli, M. and Lemmon, S. K. (2002) 'Protein phosphatase-1 binding to Scd5p is important for regulation of actin organization and endocytosis in yeast', *Journal of Biological Chemistry*, 277(50), pp. 48002–48008.

Chatterjee, J., Beullens, M., Sukackaite, R., Qian, J., Lesage, B., Hart, D. J., Bollen, M. and Köhn, M. (2012) 'Development of a peptide that selectively activates protein phosphatase-1 in living cells', *Angewandte Chemie - International Edition*, 51(40), pp. 10054–10059.

Chatterjee, J. and Köhn, M. (2013) 'Targeting the untargetable: Recent advances in the selective chemical modulation of protein phosphatase-1 activity', *Current Opinion in Chemical Biology*, pp. 361–368.

Chayen, N. E. and Saridakis, E. (2008) 'Protein crystallization: from purified protein to diffraction-quality crystal.', *Nature methods*, 5(2), pp. 147–153.

Chen, E., Choy, M. S., Petrényi, K., Kónya, Z., Erdődi, F., Dombrádi, V., Peti, W. and Page, R. (2016) 'Molecular insights into the fungus-specific serine/threonine protein phosphatase Z1 in Candida albicans', *mBio*, 7(4).

Chien, C. Y., Chou, C. K. and Su, J. Y. (2009) 'Ung1p-mediated uracil-base excision repair in mitochondria is responsible for the petite formation in thymidylate deficient yeast', *FEBS Letters*. Federation of European Biochemical Societies, 583(9), pp. 1499–1504.

Choy, M. S., Page, R. and Peti, W. (2012) 'Regulation of protein phosphatase 1 by intrinsically disordered proteins.', *Biochemical Society transactions*, 40(5), pp. 969–74.

Clark, C. D., Palzkill, T. and Botstein, D. (1994) 'Systematic mutagenesis of the yeast mating pheromone receptor third intracellular loop', *Journal of Biological Chemistry*, 269(12), pp. 8831–8841.

Clotet, J., Garí, E., Aldea, M., Ariño, J. and Arin, N. (1999) 'The yeast ser/thr phosphatases sit4 and ppz1 play opposite roles in regulation of the cell cycle.', *Molecular and cellular biology*, 19(3), pp. 2408–15.

Clotet, J., Posas, F., Casamayor, A., Schaaff-Gerstenschläger, I. and Arinõ, J. (1991) 'The gene DIS2S1 is essential in Saccharomyces cerevisiae and is involved in glycogen phosphorylase activation', *Current Genetics*, 19(5), pp. 339–342.

Clotet, J., Posas, F., de Nadal, E. and Ariño, J. (1996) 'The NH2-terminal extension of protein phosphatase PPZ1 has an essential functional role.', *The Journal of biological chemistry*, 271(42), pp. 26349–55.

Cohen, P. (1989) 'The structure and regulation of protein phosphatases.', *Annual review of biochemistry*, 58, pp. 453–508.

Cohen, P. T. W. (2002) 'Protein phosphatase 1--targeted in many directions.', *Journal of cell science*, 115(Pt 2), pp. 241–256.

Cohen, P. T. W., Brewis, N. D., Hughes, V. and Mann, D. J. (1990) 'Protein serine/threonine phosphatases; an expanding family', *FEBS Letters*, pp. 355–359.

Como, C. J. Di, Bose, R., Amdt, K. T. and Saccharomyces, H. E. (1995) 'Overexpression of SIS2, Which Contains an Extremely Acidic Region, Increases the Expression of', (1993).

Di Como, C. J., Chang, H. and Arndt, K. T. (1995) 'Activation of CLN1 and CLN2 G1 cyclin gene expression by BCK2.', *Molecular and Cellular Biology*, 15(4), pp. 1835–1846.

Costi, P. M., Rinaldi, M., Tondi, D., Pecorari, P., Barlocco, D., Ghelli, S., Stroud, R. M., Santi, D. V, Stout, T. J., Musiu, C., Marangiu, E. M., Pani, A., Congiu, D., Loi, G. A. and La Colla, P. (1999) 'Phthalein derivatives as a new tool for selectivity in thymidylate synthase inhibition.', *Journal of medicinal chemistry*, 42(Figure 1), pp. 2112–2124.

Cullen, P. J. and Sprague, G. F. (2002) 'The Glc7p-interacting protein bud14p attenuates polarized growth, pheromone response, and filamentous growth in Saccharomyces cerevisiae', *Eukaryotic Cell*, 1(6), pp. 884–894.

Deller, M. C., Kong, L. and Rupp, B. (2016) 'Protein stability: A crystallographer's perspective', *Acta Crystallographica Section:F Structural Biology Communications*, pp. 72–95.

Dibrov, P., Smith, J. J., Young, P. G. and Fliegel, L. (1997) 'Identification and localization of the sod2 gene product in fission yeast', *FEBS Letters*, 405(1), pp. 119–124.

Dichtl, B., Stevens, a and Tollervey, D. (1997) 'Lithium toxicity in yeast is due to the inhibition of RNA processing enzymes.', *The EMBO journal*, 16(23), pp. 7184–7195.

Dombek, K. M., Voronkova, V., Raney, A. and Young, E. T. (1999) 'Functional analysis of the yeast Glc7-binding protein Reg1 identifies a protein phosphatase type 1-binding motif as essential for repression of ADH2 expression.', *Molecular and cellular biology*, 19(9), pp. 6029–40.

Egloff, M. P., Cohen, P. T., Reinemer, P. and Barford, D. (1995) 'Crystal structure of the catalytic subunit of human protein phosphatase 1 and its complex with tungstate', *J Mol Biol*, 254(5), pp. 942–959.

Egloff, M. P., Johnson, D. F., Moorhead, G., Cohen, P. T., Cohen, P. and Barford, D. (1997) 'Structural basis for the recognition of regulatory subunits by the catalytic subunit of protein phosphatase 1.', *The EMBO journal*, 16(8), pp. 1876–87.

Espinosa-Ruiz A, Bellés JM, Serrano R, C.-M. F. (1999) 'Arabidopsis thaliana AtHAL3 : a flavoprotein related to salt and osmotic tolerance and plant growth', 20(August).

Feng, Z., Wilson, S. E., Peng, Z. Y., Schlender, K. K., Reimann, E. M. and Trumbly, R. J. (1991) 'The yeast GLC7 gene required for glycogen accumulation encodes a type 1 protein phosphatase', *Journal of Biological Chemistry*, 266(35), pp. 23796–23801.

Fernandez-Sarabia, M. J., Sutton, A., Zhong, T. and Arndt, K. T. (1992) 'SIT4 protein phosphatase is required for the normal accumulation of S WI4, CLN1, CLN2, and HCS26 RNAs during late G1', *Genes and Development*, 6(12), pp. 2417–2428.

Ferrando, A., Kron, S. J., Rios, G., Fink, G. R. and Serrano, R. (1995) 'Regulation of Cation Transport in Saccharomyces cerevisiae by the Salt Tolerance Gene HAL3', 15(10), pp. 5470–5481.

Finer-Moore, J. S., Anderson, A. C., O'Neil, R. H., Costi, M. P., Ferrari, S., Krucinski, J. and Stroud, R. M. (2005) 'The structure of Cryptococcus neoformans thymidylate synthase suggests strategies for using target dynamics for species-specific inhibition', *Acta Crystallographica Section D: Biological Crystallography*. International Union of Crystallography, 61(10), pp. 1320–1334.

Fromant, M., Blanquet, S. and Plateau, P. (1995) 'Direct Random Mutagenesis of Gene-Sized DNA Fragments Using Polymerase Chain Reaction', *Analytical Biochemistry*, 224(1), pp. 347–353.

Gaber, R. F., Styles, C. A. and Fink, G. R. (1988) 'TRK1 Encodes a Plasma Membrane Protein Required for High-Affinity Potassium Transport in Saccharomyces cerevisiae', *MOLECULAR AND CELLULAR BIOLOGY*, 8(7), pp. 2848–2859.

Gancedo, C. and Flores, C. (2008) 'Moonlighting Proteins in Yeasts', 72(1), pp. 197–210.

Gancedo, C., Flores, C. and Gancedo, J. M. (2016) 'The Expanding Landscape of Moonlighting Proteins in Yeasts', 80(3), pp. 765–777.

Garcia-Gimeno, M. A., Munoz, I., Arino, J. and Sanz, P. (2003) 'Molecular Characterization of Ypi1, a Novel Saccharomyces cerevisiae Type 1 Protein Phosphatase Inhibitor', *J.Biol.Chem.*, 278(48), pp. 47744–47752.

Garciadeblas, B., Rubio, F., Quintero, F. J., Bañuelos, M. A., Haro, R. and Rodríguez-Navarro, A. (1993) 'Differential expression of two genes encoding isoforms of the ATPase involved in sodium efflux in Saccharomyces cerevisiae', *MGG Molecular & General Genetics*, 236(2–3), pp. 363–368.

Gibbons, J. A., Weiser, D. C. and Shenolikar, S. (2005) 'Importance of a surface hydrophobic pocket on protein phosphatase-1 catalytic subunit in recognizing cellular regulators', *Journal of Biological Chemistry*, 280(16), pp. 15903–15911.

Gimeno, C. J., Ljungdahl, P. O., Styles, C. a. and Fink, G. R. (1992) 'Unipolar cell divisions in the yeast S. cerevisiae lead to filamentous growth: Regulation by starvation and RAS', *Cell*, 68(6), pp. 1077–1090.

Goffeau, A., Barrell, B. G., Bussey, H., Davis, R. W., Dujon, B., Feldmann, H., Galibert, F., Hoheisel, J. D., Jacq, C., Johnston, M., Louis, E. J., Mewes, H. W., Murakami, Y., Philippsen, P., Tettelin, H. and Oliver, S. G. (1996) 'Life with 6000 Genes', *Science*, 274(October), pp. 546–567.

Goldberg, J., Huang, H. B., Kwon, Y. G., Greengard, P., Nairn, a C. and Kuriyan, J. (1995) 'Three-dimensional structure of the catalytic subunit of protein serine/threonine phosphatase-1.', *Nature*, pp. 745–53.

Gómez, M. J., Luyten, K. and Ramos, J. (1996) 'The capacity to transport potassium influences sodium tolerance in Saccharomyces cerevisiae', *FEMS Microbiology Letters*, 135(2–3), pp. 157–160.

González, A., Casado, C., Petrezsélyová, S., Ruiz, A. and Ariño, J. (2013) 'Molecular analysis of a conditional hal3 vhs3 yeast mutant links potassium homeostasis with flocculation and invasiveness', *Fungal Genetics and Biology*, 53, pp. 1–9.

Griffith, J. P., Kim, J. L., Kim, E. E., Sintchak, M. D., Thomson, J. A., Fitzgibbon, M. J., Fleming, M. A., Caron, P. R., Hsiao, K. and Navia, M. A. (1995) 'X-ray structure of calcineurin inhibited by the immunophilin-immunosuppressant FKBP12-FK506 complex', *Cell*, 82(3), pp. 507–522.

Guergnon, J., Dessauge, F., Dominguez, V., Viallet, J., Bonnefoy, S., Yuste, V. J., Mercereau-Puijalon, O., Cayla, X., Rebollo, A., Susin, S. A., Bost, P. and Garcia, A. (2006) 'Use of penetrating peptides interacting with PP1/PP2A proteins as a general approach for a drug phosphatase

technology.', *Molecular pharmacology*, 69(4), pp. 1115–24.

Guo, B., Styles, C. a, Feng, Q. and Fink, G. R. (2000) 'A Saccharomyces gene family involved in invasive growth, cell-cell adhesion, and mating.', *Proceedings of the National Academy of Sciences of the United States of America*, 97(22), pp. 12158–12163.

Haro, R., Garciadeblas, B. and Rodriguez-Navarro, A. (1991) 'A novel P-type ATPase from yeast involved in sodium transport', *FEBS Letters*, 291(2), pp. 189–191.

Heckman, D. S. (2001) 'Molecular Evidence for the Early Colonization of Land by Fungi and Plants', *Science*, 293(5532), pp. 1129–1133.

Helbig, A. O., Rosati, S., Pijnappel, P. W. W. M., van Breukelen, B., Timmers, M. H. T. H., Mohammed, S., Slijper, M. and Heck, A. J. R. (2010) 'Perturbation of the yeast N-acetyltransferase NatB induces elevation of protein phosphorylation levels.', *BMC genomics*, 11(1), p. 685.

Hernández-Acosta, P., Schmid, D. G., Jung, G., Culiáñez-Macià, F. A. and Kupke, T. (2002) 'Molecular characterization of the Arabidopsis thaliana flavoprotein AtHAL3a reveals the general reaction mechanism of 4′-phosphopantothenoylcysteine decarboxylases', *Journal of Biological Chemistry*, 277(23), pp. 20490–20498.

Heroes, E., Lesage, B., Görnemann, J., Beullens, M., Van Meervelt, L. and Bollen, M. (2013) 'The PP1 binding code: A molecular-lego strategy that governs specificity', *FEBS Journal*, pp. 584–595.

Hisamoto, N., Sugimoto, K. and Matsumoto, K. (1994) 'The Glc7 type 1 protein phosphatase of Saccharomyces cerevisiae is required for cell cycle progression in G2/M.', *Molecular and cellular biology*, 14(5), pp. 3158–3165.

Holt, L. J., Tuch, B. B., Villén, J., Johnson, A. D., Gygi, S. P. and Morgan, D. O. (2009) 'Global analysis of Cdk1 substrate phosphorylation sites provides insights into evolution.', *Science (New York, N.Y.)*, 325(5948), pp. 1682–6.

Huberts, D. H. E. W. and van der Klei, I. J. (2010) 'Moonlighting proteins: An intriguing mode of multitasking', *Biochimica et Biophysica Acta - Molecular Cell Research*. Elsevier B.V., 1803(4), pp. 520–525.

Hughes, V., Müller, A., Stark, M. J. and Cohen, P. T. (1993) 'Both isoforms of protein phosphatase Z are essential for the maintenance of cell size and integrity in Saccharomyces cerevisiae in response to osmotic stress.', *European journal of biochemistry*, 216(1), pp. 269–79.

Hurley, T. D., Yang, J., Zhang, L., Goodwin, K. D., Zou, Q., Cortese, M., Dunker, a K. and DePaoli-Roach, A. a (2007) 'Structural basis for regulation of protein phosphatase 1 by inhibitor-2.', *The Journal of biological chemistry*, 282(39), pp. 28874–83.

Ingebritsen, T. S. and Cohen, P. (1983) 'Protein phosphatases: properties and role in cellular regulation.', *Science (New York, N.Y.)*, 221(4608), pp. 331–8.

Inoue, H., Nojima, H. and Okayama, H. (1990) 'High efficiency transformation of Escherichia coli with plasmids.', *Gene*, 96(1), pp. 23–8.

Ito, H., Fukuda, Y., Murata, K. and Kimura, A. (1983) 'Transformation of intact yeast cells treated with alkali cations', *Journal of Bacteriology*, 153(1), pp. 163–168.

Ivanov, M. S., Radchenko, E. a. and Mironova, L. N. (2010) 'Protein complex Ppz1p/Hal3p and the efficiency of nonsense suppression in yeasts Saccharomyces cerevisiae', *Molecular Biology*, 44(6), pp. 907–914.

Jeffery, C. J. (1999) 'Moonlighting proteins', 4(98), pp. 8–11.

Jeffery, C. J. (2003) 'Moonlighting proteins: Old proteins learning new tricks', *Trends in Genetics*, pp. 415–417.

Jeffery, C. J. (2009) 'Moonlighting proteins--an update.', *Molecular bioSystems*, 5(4), pp. 345–50.

Jia, Z. P., McCullough, N., Martel, R., Hemmingsen, S. and Young, P. G. (1992) 'Gene amplification at a locus encoding a putative Na+/H+ antiporter confers sodium and lithium tolerance in fission yeast', *EMBO J*, 11(4), pp. 1631–1640.

Kamberi, M., Chung, P., Devas, R., Li, L., Li, Z., Sharon, X. M., Fields, S. and Riley, C. M. (2004) 'Analysis of non-covalent aggregation of synthetic hPTH (1-34) by size-exclusion chromatography and the importance of suppression of non-specific interactions for a precise quantitation', *Journal of Chromatography B: Analytical Technologies in the Biomedical and Life Sciences*, 810(1), pp. 151–155.

Kennedy, P. J., Vashisht, A. A., Hoe, K. L., Kim, D. U., Park, H. O., Hayles, J. and Russell, P. (2008) 'A genome-wide screen of genes involved in cadmium tolerance in Schizosaccharomyces pombe', *Toxicological Sciences*, 106(1), pp. 124–139.

Kim, D.-U., Hayles, J., Kim, D., Wood, V., Park, H.-O., Won, M., Yoo, H.-S., Duhig, T., Nam, M., Palmer, G., Han, S., Jeffery, L., Baek, S.-T., Lee, H., Shim, Y. S., Lee, M., Kim, L., Heo, K.-S., Noh, E. J., Lee, A.-R., Jang, Y.-J., Chung, K.-S., Choi, S.-J., Park, J.-Y., Park, Y., Kim, H. M., Park, S.-K., Park, H.-J., Kang, E.-J., Kim, H. B., Kang, H.-S., Park, H.-M., Kim, K., Song, K., Song, K. Bin, Nurse, P. and Hoe, K.-L. (2010) 'Analysis of a genome-wide set of gene deletions in the fission yeast Schizosaccharomyces pombe.', *Nature biotechnology*, 28(6), pp. 617–23.

Kinclova-Zimmermannova, O., Gaskova, D. and Sychrova, H. (2006) 'The Na^+,K^+/H^+-antiporter Nha1 influences the plasma membrane potential of *Saccharomyces cerevisiae*', *FEMS Yeast Research*. Blackwell Publishing Ltd, 6(5), pp. 792–800.

Kinoshita, N., Ohkura, H. and Yanagida, M. (1990) 'Distinct, essential roles of type 1 and 2A protein phosphatases in the control of the fission yeast cell division cycle 1', *Cell*, 63(0092–8674; 2), pp. 405–415.

Kita, A., Matsunaga, S., Takai, A., Kataiwa, H., Wakimoto, T., Fusetani, N., Isobe, M. and Miki, K. (2002) 'Crystal structure of the complex between calyculin A and the catalytic subunit protein

phosphatase 1. [Erratum to document cited in CA137:121557]', *Structure (Cambridge, MA, United States)*, 10(8), p. 71149.

Klis, F. M., Boorsma, A. and De Groot, P. W. J. (2006) 'Cell wall construction in Saccharomyces cerevisiae', *Yeast*, pp. 185–202.

Ko, C. H., Buckley, A. M. and Gaber, R. F. (1990) 'TRK2 is required for low affinity K+ transport in Saccharomyces cerevisiae', *Genetics*, 125(2), pp. 305–312.

Ko, C. H. and Gaber, R. F. (1991) 'TRK1 and TRK2 encode structurally related K+ transporters in Saccharomyces cerevisiae', *Molecular and Cellular Biology*, 11(8), pp. 4266–4273.

Krupenko, S. A. (2009) 'FDH: An aldehyde dehydrogenase fusion enzyme in folate metabolism', *Chemico-Biological Interactions*, pp. 84–93.

Kummerfeld, S. K. and Teichmann, S. A. (2005) 'Relative rates of gene fusion and fission in multi-domain proteins', *Trends in Genetics*, pp. 25–30.

Kupke, T. (2001) 'Molecular characterization of the 4 '-phosphopantothenoylcysteine decarboxylase domain of bacterial Dfp flavoproteins', *Journal of Biological Chemistry*, 276(29), pp. 27597–27604.

Kupke, T., Hernández-Acosta, P., Steinbacher, S. and Culiáñez-Macià, F. A. (2001) 'Arabidopsis thaliana Flavoprotein AtHAL3a Catalyzes the Decarboxylation of 4′-Phosphopantothenoylcysteine to 4′-Phosphopantetheine, a Key Step in Coenzyme A Biosynthesis', *Journal of Biological Chemistry*, 276(22), pp. 19190–19196.

Kupke, T., Uebele, M., Schmid, D., Jung, G., Blaessei, M. and Steinbacher, S. (2000) 'Molecular characterization of lantibiotic-synthesizing enzyme EpiD reveals a function for bacterial Dfp proteins in coenzyme A biosynthesis', *Journal of Biological Chemistry*, 275(41), pp. 31838–31846.

Lee, K. S., Hines, L. K. and Levin, D. E. (1993) 'A pair of functionally redundant yeast genes (PPZ1 and PPZ2) encoding type 1-related protein phosphatases function within the PKC1-mediated pathway.', *Molecular and cellular biology*, 13(9), pp. 5843–53.

Leiter, É., González, A., Erdei, É., Casado, C., Kovács, L., ádám, C., Oláh, J., Miskei, M., Molnar, M., Farkas, I., Hamari, Z., Ariño, J., Pócsi, I. and Dombrádi, V. (2012) 'Protein phosphatase Z modulates oxidative stress response in fungi', *Fungal Genetics and Biology*, 49(9), pp. 708–716.

Leonard, G. and Richards, T. a (2012) 'Genome-scale comparative analysis of gene fusions, genefissions, and the fungal tree of life', *Proceedings of the National Academy of Sciences of the United States of America*, 109(52), pp. 21402–21407.

Levin, D. E. (2005) 'Cell wall integrity signaling in Saccharomyces cerevisiae.', *Microbiology and molecular biology reviews : MMBR*, 69(2), pp. 262–91.

Lichtenberg-Fraté, H., Reid, J. D., Heyer, M. and Höfer, M. (1996) 'The SpTRK gene encodes a potassium-specific transport protein TKH(p) in Schizosaccharomyces pombe', *Journal of Membrane Biology*, 152(2), pp. 169–181.

Madrid, R., G??mez, M. J., Ramos, J. and Rodr??guez-Navarro, A. (1998) 'Ectopic potassium uptake in trk1 trk2 mutants of Saccharomyces cerevisiae correlates with a highly hyperpolarized membrane potential', *Journal of Biological Chemistry*, 273(24), pp. 14838–14844.

Makanae, K., Kintaka, R., Makino, T., Kitano, H. and Moriya, H. (2013) 'Identification of dosage-sensitive genes in Saccharomyces cerevisiae using the genetic tug-of-war method', *Genome Research*, 23(2), pp. 300–311.

Manoj, N., Strauss, E., Begley, T. P. and Ealick, S. E. (2003) 'Structure of human phosphopantothenoylcysteine synthetase at 2.3 ?? resolution', *Structure*, 11(8), pp. 927–936.

Martinez, R., Latreille, M. T. and Mirande, M. (1991) 'A PMR2 tandem repeat with a modified C-

terminus is located downstream from the KRS1 gene encoding lysyl-tRNA synthetase in Saccharomyces cerevisiae', *Molecular {&} general genetics : MGG*, 227(1), pp. 149–154.

McIntosh, E. M., Ord, R. W. and Storms, R. K. (1988) 'Transcriptional regulation of the cell cycle-dependent thymidylate synthase gene of Saccharomyces cerevisiae', *Mol Cell Biol*, 8(11), pp. 4616–4624.

McPherson, A. and Gavira, J. A. (2014) 'Introduction to protein crystallization', *Acta Crystallographica Section F:Structural Biology Communications*, pp. 2–20.

Meiselbach, H., Sticht, H. and Enz, R. (2006) 'Structural analysis of the protein phosphatase 1 docking motif: Molecular description of binding specificities identifies interacting proteins', *Chemistry and Biology*, 13(1), pp. 49–59.

Mendoza, I., Rubio, F., Rodriguez-Navarro, A. and Pardo, J. M. (1994) 'The protein phosphatase calcineurin is essential for NaCl tolerance of Saccharomyces cerevisiae', *Journal of Biological Chemistry*, 269(12), pp. 8792–8796.

Merchan, S., Bernal, D., Serrano, R. and Yenush, L. (2004) 'Response of the Saccharomyces cerevisiae Mpk1 Mitogen-Activated Protein Kinase Pathway to Increases in Internal Turgor Pressure Caused by Loss of Ppz Protein Phosphatases', 3(1), pp. 100–107.

Minhas, A., Sharma, A., Kaur, H., Rawal, Y., Ganesan, K. and Mondal, A. K. (2012) 'Conserved Ser / Arg-rich Motif in PPZ Orthologs from Fungi Is Important for Its Role in Cation Tolerance □', 287(10), pp. 7301–7312.

Molero, C., Petrenyi, K., Gonzalez, A., Carmona, M., Gelis, S., Abrie, J. A., Strauss, E., Ramos, J., Dombradi, V., Hidalgo, E. and Arino, J. (2013) 'The Schizosaccharomyces pombe fusion gene hal3 encodes three distinct activities', *Molecular Microbiology*, 90(2), pp. 367–382.

Moorhead, G. B., De Wever, V., Templeton, G. and Kerk, D. (2009) 'Evolution of protein

phosphatases in plants and animals', *Biochem J*, 417(2), pp. 401–409.

Mulet, J. M., Leube, M. P., Kron, S. J., Rios, G., Fink, G. R. and Serrano, R. (1999) 'A novel mechanism of ion homeostasis and salt tolerance in yeast: the Hal4 and Hal5 protein kinases modulate the Trk1-Trk2 potassium transporter.', *Molecular and cellular biology*, 19(5), pp. 3328–37.

Munro, E. M., Climie, S., Vandenberg, E. and Storms, R. K. (1999) 'Functional assessment of surface loops : deletion of eukaryote-speci ¢ c peptide inserts in thymidylate synthase of Saccharomyces cerevisiae', *Science*, 1430.

Muñoz, I., Ruiz, A., Marquina, M., Barceló, A., Albert, A. and Ariño, J. (2004) 'Functional characterization of the yeast Ppz1 phosphatase inhibitory subunit Hal3: A mutagenesis study', *Journal of Biological Chemistry*, 279(41), pp. 42619–42627.

Muñoz, I., Simón, E., Casals, N., Clotet, J. and Ariño, J. (2003) 'Identification of multicopy suppressors of cell cycle arrest at the G1-S transition in Saccharomyces cerevisiae.', *Yeast (Chichester, England)*, 20(2), pp. 157–169.

Murguía, J. R., Bellés, J. M. and Serrano, R. (1995) 'A salt-sensitive 3'(2'),5'-bisphosphate nucleotidase involved in sulfate activation.', *Science (New York, N.Y.)*, 267(5195), pp. 232–4.

Nadal, D., Fadden, R. P., Ruiz, A. and Haystead, T. (2001) 'A Role for the Ppz Ser / Thr Protein Phosphatases in the Regulation of Translation Elongation Factor 1B *', 276(18), pp. 14829–14834.

De Nadal, E., Clotet, J., Posas, F., Serrano, R., Gomez, N. and Ariño, J. (1998) 'The yeast halotolerance determinant Hal3p is an inhibitory subunit of the Ppz1p Ser/Thr protein phosphatase', *Proceedings of the National Academy of Sciences of the United States of America*, 95(13), p. 7357.

De Nadal, E., Fadden, R. P., Ruiz, A., Haystead, T. and Ariño, J. (2001) 'A Role for the Ppz Ser/Thr Protein Phosphatases in the Regulation of Translation Elongation Factor 1B??', *Journal of Biological*

Chemistry, 276(18), pp. 14829–14834.

Nakamura, T., Pluskal, T., Nakaseko, Y. and Yanagida, M. (2012) 'Impaired coenzyme A synthesis in fission yeast causes defective mitosis, quiescence-exit failure, histone hypoacetylation and fragile DNA', *Open Biology*, 2(9), pp. 120117–120117.

Navarrete, C., Petrezsélyová, S., Barreto, L., Martínez, J. L., Zahrádka, J., Ariño, J., Sychrová, H. and Ramos, J. (2010) 'Lack of main K+ uptake systems in Saccharomyces cerevisiae cells affects yeast performance in both potassium-sufficient and potassium-limiting conditions', *FEMS Yeast Research*, 10(5), pp. 508–517.

Nobbmann, U. and Bergfors, T. (2009) 'Dynamic light scattering', *IUL Biotechnol. Ser.*, 8, pp. 221–245.

Olsen, J. V., Blagoev, B., Gnad, F., Macek, B., Kumar, C., Mortensen, P. and Mann, M. (2006) 'Global, In Vivo, and Site-Specific Phosphorylation Dynamics in Signaling Networks', *Cell*, 127(3), pp. 635–648.

Papouskova, K. and Sychrova, H. (2007) 'Schizosaccharomyces pombe possesses two plasma membrane alkali metal cation/H+ antiporters differing in their substrate specificity', *FEMS Yeast Research*, 7(2), pp. 188–195.

Peng, Z. Y., Trumbly, R. J. and Reimann, E. M. (1990) 'Purification and characterization of glycogen synthase from a glycogen-deficient strain of }I}Saccharomyces}i} }I}cerevisiae}i}', *J Biol Chem*, 265(23), pp. 13871–13877.

Peti, W., Nairn, A. C. and Page, R. (2013) 'Structural basis for protein phosphatase 1 regulation and specificity', *FEBS Journal*, pp. 596–611.

Petrenyi, K., Molero, C., Konya, Z., Erdodi, F., Arino, J. and Dombradi, V. (2016) 'Analysis of two putative Candida albicans phosphopantothenoylcysteine decarboxylase / protein phosphatase Z

regulatory subunits reveals an unexpected distribution of functional roles', *PLoS ONE*, 11(8).

Poon, P. P. and Storms, R. K. (1994) 'Thymidylate synthase is localized to the nuclear periphery in the yeast Saccharomyces cerevisiae', *Journal of Biological Chemistry*, 269(11), pp. 8341–8347.

Posas, F., Bollen, M., Stalmans, W. and Ariño, J. (1995) 'Biochemical characterization of recombinant yeast PPZ1, a protein phosphatase involved in salt tolerance.', *FEBS letters*, 368(1), pp. 39–44.

Posas, F., Camps, M. and Arino, J. (1995) 'The PPZ protein phosphatases are important determinants of salt tolerance in yeast cells', *Journal of Biological Chemistry*, 270(22), pp. 13036–13041.

Posas, F., Casamayor, A. and Ariño, J. (1993) 'The PPZ protein phosphatases are involved in the maintenance of osmotic stability of yeast cells', *FEBS Letters*, 318(3), pp. 282–286.

Posas F, Casamayor A, Morral N, Ariño J (1992) 'Molecular cloning and analysis of a yeast protein phosphatase with an unusual amino-terminal region.', *Journal of Biological Chemistry*, 267(17), pp. 11734–11740.

Prior, C., Potier, S., Souciet, J.-L. and Sychrova, H. (1996) 'Characterization of the *NHA1* gene encoding a Na^+/H^+-antiporter of the yeast *Saccharomyces cerevisiae*', *FEBS Letters*, 387(1), pp. 89–93.

Ptacek, J., Devgan, G., Michaud, G., Zhu, H., Zhu, X., Fasolo, J., Guo, H., Jona, G., Breitkreutz, A., Sopko, R., McCartney, R. R., Schmidt, M. C., Rachidi, N., Lee, S.-J., Mah, A. S., Meng, L., Stark, M. J. R., Stern, D. F., De Virgilio, C., Tyers, M., Andrews, B., Gerstein, M., Schweitzer, B., Predki, P. F. and Snyder, M. (2005) 'Global analysis of protein phosphorylation in yeast.', *Nature*, 438(7068), pp. 679–84.

Qiagen (2010) 'Critical factors for successful protein crystallization', *Design*.

Rebelo, S., Santos, M., Martins, F., da Cruz e Silva, E. F. and da Cruz e Silva, O. A. B. (2015) 'Protein phosphatase 1 is a key player in nuclear events', *Cellular Signalling*, pp. 2589–2598.

Reynolds, T. B. and Fink, G. R. (2001) 'Bakers' yeast, a model for fungal biofilm formation.', *Science (New York, N.Y.)*, 291(5505), pp. 878–81.

Rodríguez-Navarro, A., Quintero, F. J. and Garciadeblás, B. (1994) 'Na+-ATPases and Na+/H+ antiporters in fungi', *Biochimica et Biophysica Acta (BBA) - Bioenergetics*, 1187(2), pp. 203–205.

Rodriguez-Navarro, A. and Ramos, J. (1984) 'Dual system for potassium transport in Saccharomyces cerevisiae', *Journal of Bacteriology*, 159(3), pp. 940–945.

Romier, C., Ben Jelloul, M., Albeck, S., Buchwald, G., Busso, D., Celie, P. H. N., Christodoulou, E., De Marco, V., Van Gerwen, S., Knipscheer, P., Lebbink, J. H., Notenboom, V., Poterszman, A., Rochel, N., Cohen, S. X., Unger, T., Sussman, J. L., Moras, D., Sixma, T. K. and Perrakis, A. (2006) 'Co-expression of protein complexes in prokaryotic and eukaryotic hosts: Experimental procedures, database tracking and case studies', *Acta Crystallographica Section D: Biological Crystallography*, 62(10), pp. 1232–1242.

Roy, J. and Cyert, M. S. (2009) 'Cracking the phosphatase code: docking interactions determine substrate specificity.', *Science signaling*, 2(100), p. re9.

Ruiz, A., del Carmen Ruiz, M., Sánchez-Garrido, M. A., Ariño, J. and Ramos, J. (2004) 'The Ppz protein phosphatases regulate Trk-independent potassium influx in yeast', *FEBS Letters*, 578(1–2), pp. 58–62.

Ruiz, A., González, A., Muñoz, I., Serrano, R., Abrie, J. A., Strauss, E. and Ariño, J. (2009) 'Moonlighting proteins Hal3 and Vhs3 form a heteromeric PPCDC with Ykl088w in yeast CoA biosynthesis.', *Nature chemical biology*, 5(12), pp. 920–928.

Ruiz, A., Muñoz, I., Serrano, R., González, A., Simón, E. and Ariño, J. (2004) 'Functional

characterization of the Saccharomyces cerevisiae VHS3 gene: A regulatory subunit of the Ppz1 protein phosphatase with novel, phosphatase-unrelated functions', *Journal of Biological Chemistry*, 279(33), pp. 34421–34430.

Ruiz, A., Yenush, L. and Ariño, J. (2003) 'Regulation of ENA1 Na+-ATPase gene expression by the Ppz1 protein phosphatase is mediated by the calcineurin pathway', *Eukaryotic Cell*.

Sadowski, I., Breitkreutz, B.-J., Stark, C., Su, T.-C., Dahabieh, M., Raithatha, S., Bernhard, W., Oughtred, R., Dolinski, K., Barreto, K. and Tyers, M. (2013) 'The PhosphoGRID Saccharomyces cerevisiae protein phosphorylation site database: version 2.0 update.', *Database : the journal of biological databases and curation*, 2013, p. bat026.

Sakumoto, N., Mukai, Y., Uchida, K., Kouchi, T., Kuwajima, J., Nakagawa, Y., Sugioka, S., Yamamoto, E., Furuyama, T., Mizubuchi, H., Ohsugi, N., Sakuno, T., Kikuchi, K., Matsuoka, I., Ogawa, N., Kaneko, Y. and Harashima, S. (1999) 'A series of protein phosphatase gene disruptants in Saccharomyces cerevisiae', *Yeast*, 15(15), pp. 1669–1679.

Sambrook, J., Fritsch, E. F. and Maniatis, T. (1989) *Molecular cloning : a laboratory manual*. Cold Spring Harbor Laboratory.

Sangrador, A., Andrés, I., Eguiraun, A., Lorenzo, M. L. and Ortiz, J. M. (1998) 'Growth arrest of Schizosaccharomyces pombe following overexpression of mouse type 1 protein phosphatases', *Molecular and General Genetics*, 259(5), pp. 449–456.

Sansó, M., Gogol, M., Ayté, J., Seidel, C. and Hidalgo, E. (2008) 'Transcription factors Pcr1 and Atf1 have distinct roles in stress- and Sty1-dependent gene regulation', *Eukaryotic Cell*, 7(5), pp. 826–835.

Sassoon, I., Severin, F. F., Andrews, P. D., Taba, M. R., Kaplan, K. B., Ashford, A. J., Stark, M. J. R., Sorger, P. K. and Hyman, A. A. (1999) 'Regulation of Saccharomyces cerevisiae kinetochores by the type 1 phosphatase Glc7p', *Genes and Development*, 13(5), pp. 545–555.

Serrano, R. (1996) 'Salt tolerance in plants and microorganisms: toxicity targets and defense responses.', *International review of cytology*, 165, pp. 1–52.

Shenolikar, S. (1994) 'Protein Serine/Threonine phosphatases - New Avenues for Cell Regulation', *Annu.Rev.Cell Biol.*, 10, pp. 55–86.

Sherman, F. and Hicks, J. (1991) 'Micromanipulation and dissection of asci', *Methods in Enzymology*, pp. 21–37.

Shi, Y. (2009) 'Serine/Threonine Phosphatases: Mechanism through Structure', *Cell*, 139(3), pp. 468–484.

Sikorski, R. S. and Hieter, P. (1989) 'A system of shuttle vectors and yeast host strains designed for efficient manipulation of DNA in Saccharomyces cerevisiae.', *Genetics*, 122(1), pp. 19–27.

Simón, E., Clotet, J., Calero, F., Ramos, J. and Ariño, J. (2001) 'A Screening for High Copy Suppressors of the sit4 hal3 Synthetically Lethal Phenotype Reveals a Role for the Yeast Nha1 Antiporter in Cell Cycle Regulation', *Journal of Biological Chemistry*, 276(32), pp. 29740–29747.

Singer, S. C., Richards, C. A., Ferone, R., Benedict, D. and Ray, P. (1989) 'Cloning, purification, and properties of Candida albicans thymidylate synthase', *Journal of Bacteriology*, 171(3), pp. 1372–1378.

Snel, B., Bork, P. and Huynen, M. (2000) 'Genome evolutiongene fusion versus gene fission', *Trends in Genetics*, 16(1), pp. 9–11.

Soldatenkov, V. A., Velasco, J. A., Avila, M. A., Dritschilo, A. and Notario, V. (1995) 'Isolation and characterization of SpTRK, a gene from schizosaccharomyces pombe predicted to encode a K+ transporter protein', *Gene*, 161(1), pp. 97–101.

Song, W. and Carlson, M. (1998) 'Srb/mediator proteins interact functionally and physically with transcriptional repressor Sfl1', *EMBO Journal*, 17(19), pp. 5757–5765.

Spitzer, E. D., Jimenez-Billini, H. E. and Weiss, B. (1988) 'beta-Alanine auxotrophy associated with dfp, a locus affecting DNA synthesis in Escherichia coli.', *Journal of Bacteriology*, 170(2), pp. 872–876.

Spitzer, E. D. and Weiss, B. (1985) 'dfp Gene of Escherichia coli K-12, a locus affecting DNA synthesis, codes for a flavoprotein', *Journal of Bacteriology*, 164(3), pp. 994–1003.

Stark, M. J. R. (1996) 'Yeast protein serine/threonine phosphatases: Multiple roles and diverse regulation', *Yeast*, 12(16), pp. 1647–1675.

Stechmann, A. (2002) 'Rooting the Eukaryote Tree by Using a Derived Gene Fusion', *Science*, 297(5578), pp. 89–91.

Stefan, A., Ceccarelli, A., Conte, E., Montón Silva, A. and Hochkoeppler, A. (2015) 'The Multifaceted Benefits of Protein Co-expression in <em>Escherichia coli</em&gt';, *Journal of Visualized Experiments*, (96).

Steinbacher, S., Hernández-Acosta, P., Bieseler, B., Blaesse, M., Huber, R., Culiáñez-Macià, F. A. and Kupke, T. (2003) 'Crystal structure of the plant PPC decarboxylase AtHAL3a complexed with an ene-thiol reaction intermediate', *Journal of Molecular Biology*, 327(1), pp. 193–202.

Storms, R. K., Ord, R. W., Greenwood, M. T., Mirdamadi, B., Chu, F. K. and Belfort, M. (1984) 'Cell cycle-dependent expression of thymidylate synthase in Saccharomyces cerevisiae', *Mol Cell Biol*, 4(12), pp. 2858–2864.

Stralfors, P., Hiraga, A. and Cohen, P. (1985) 'The protein phosphatases involved in cellular regulation. Purification and characterisation of the glycogen-bound form of protein phosphatase-1 from rabbit skeletal muscle', *European Journal of Biochemistry*. Blackwell Publishing Ltd, 149(2), pp. 295–303.

Strauss, E. (2010) 'Coenzyme A Biosynthesis and Enzymology', in *Comprehensive Natural Products II*

Chemistry and Biology, pp. 351–410.

Strauss, E., Kinsland, C., Ge, Y., McLafferty, F. W. and Begley, T. P. (2001) 'Phosphopantothenoylcysteine Synthetase from Escherichia coli. Identification and characterization of the last unidentified coenzyme A biosynthetic enzyme in bacteria', *Journal of Biological Chemistry*, 276(17), pp. 13513–13516.

Stuart, J. S., Frederick, D. L., Varner, C. M. and Tatchell, K. (1994) 'The mutant type 1 protein phosphatase encoded by glc7-1 from Saccharomyces cerevisiae fails to interact productively with the GAC1-encoded regulatory subunit', *Molecular and Cellular Biology*, 14(2), pp. 896–905.

Sutton, A., Lin, F., Sarabia, M. J. F. and Arndt, K. T. (1991) 'The SIT4 protein phosphatase is required in late G1 for progression into S phase', in *Cold Spring Harbor Symposia on Quantitative Biology*, pp. 75–82.

Sutton, a, Immanuel, D. and Arndt, K. T. (1991) 'The SIT4 Protein Phosphatase Functions in Late G1 for Progression into S-Phase', *Molecular and Cellular Biology*, 11(4), pp. 2133–2148.

Swaney, D. L., Beltrao, P., Starita, L., Guo, A., Rush, J., Fields, S., Krogan, N. J. and Villén, J. (2013) 'Global analysis of phosphorylation and ubiquitylation cross-talk in protein degradation.', *Nature methods*, 10(7), pp. 676–82.

Szöor, B., Fehér, Z., Zeke, T., Gergely, P., Yatzkan, E., Yarden, O. and Dombrádi, V. (1998) 'pzl-1 encodes a novel protein phosphatase-Z-like Ser/Thr protein phosphatase in Neurospora crassa', *Biochimica et Biophysica Acta - Protein Structure and Molecular Enzymology*, pp. 260–266.

Tachikawa, H., Bloecher, A., Tatchell, K. and Neiman, A. M. (2001) 'A Gip1p-Glc7p phosphatase complex regulates septin organization and spore wall formation', *Journal of Cell Biology*, 155(5), pp. 797–808.

Tan, S. (2001) 'A Modular Polycistronic Expression System for Overexpressing Protein Complexes

in Escherichia coli', *Protein Expression and Purification*, 21(1), pp. 224–234.

Tappan, E. and Chamberlin, A. R. (2008) 'Activation of Protein Phosphatase 1 by a Small Molecule Designed to Bind to the Enzyme's Regulatory Site', *Chemistry and Biology*, 15(2), pp. 167–174.

Taylor, G. R., Barclay, B. J., Storms, R. K., Friesen, J. D. and Haynes, R. H. (1982) 'Isolation of the thymidylate synthetase gene (TMP1) by complementation in Saccharomyces cerevisiae.', *Molecular and cellular biology*, 2(4), pp. 437–442.

Taylor, G. R., T, P. A. L., Stormslj, K. and Haynes, H. (1987) '~ o l e ~ u l Characterization ar of the Cell Cycle-regulated ~ ~ y m i d y l a t e Synthase Gene of Succhuromyces cereuisiae *', pp. 5298–5307.

Terrak, M., Kerff, F., Langsetmo, K., Tao, T. and Dominguez, R. (2004) 'Structural basis of protein phosphatase 1 regulation.', *Nature*, 429(6993), pp. 780–4.

Tompa, P. and Sza, C. (2005) 'Structural disorder throws new light on moonlighting', 30(9).

Topal, A., Karaer, S. and Temizkan, G. (1997) 'A simple method for rescuing autonomous plasmids from fission yeast', *Technical Tips Online*, 2(1), pp. 89–90.

Tu, J. and Carlson, M. (1995) 'REG1 binds to protein phosphatase type 1 and regulates glucose repression in Saccharomyces cerevisiae.', *The EMBO journal*, 14(23), pp. 5939–46.

Tu, J. L., Song, W. J. and Carlson, M. (1996) 'Protein phosphatase type-1 interacts with proteins required for meiosis and other cellular processes in saccharomyces-cerevisiae', *Molecular and Cellular Biology*, 16(N8), pp. 4199–4206.

Tyson, J. J., Csikasz-Nagy, A. and Novak, B. (2002) 'The dynamics of cell cycle regulation', *BioEssays*, pp. 1095–1109.

Venturi, G. M., Bloecher, A., Williams-Hart, T. and Tatchell, K. (2000) 'Genetic interactions

between GLC7, PPZ1 and PPZ2 in Saccharomyces cerevisiae', *Genetics*, 155(1), pp. 69–83.

Vernis, L., Piskur, J. and Diffley, J. F. X. (2003) 'Reconstitution of an efficient thymidine salvage pathway in Saccharomyces cerevisiae', *Nucleic acids research*, 31(19), p. e120.

Verstrepen, K. J., Derdelinckx, G., Verachtert, H. and Delvaux, F. R. (2003) 'Yeast flocculation: what brewers should know.', *Applied microbiology and biotechnology*, 61(3), pp. 197–205.

Vissi1, E., Clotet, J., de Nadal, E., Barceló, A., Bakó, É., Gergely, P., Dombrádi, V. and Ariño, J. (2001) 'Functional analysis of the Neurospora crassa PZL-1 protein phosphatase by expression in budding and fission yeast', *Yeast*, 18(2), pp. 115–124.

Wakula, P., Beullens, M., Ceulemans, H., Stalmans, W. and Bollen, M. (2003) 'Degeneracy and function of the ubiquitous RVXF motif that mediates binding to protein phosphatase-1', *Journal of Biological Chemistry*, 278(21), pp. 18817–18823.

Wang, B., Zhang, P. and Wei, Q. (2008) 'Recent progress on the structure of Ser/Thr protein phosphatases', *Science in China, Series C: Life Sciences*, 51(6), pp. 487–494.

Weber, P. C. (1997) 'Overview of protein crystallization methods', *Methods in Enzymology*, pp. 13–22.

Wieland, J., Nitsche, A. M., Strayle, J., Steiner, H. and Rudolph, H. K. (1995) 'The PMR2 gene cluster encodes functionally distinct isoforms of a putative Na+ pump in the yeast plasma membrane.', *The EMBO journal*, 14(16), pp. 3870–82.

Wood, V., Gwilliam, R., Rajandream, M., Lyne, M., Lyne, R., Stewart, A., Sgouros, J., Peat, N., Hayles, J., Baker, S., Basham, D., Bowman, S., Brooks, K., Brown, D., Brown, S., Chillingworth, T., Churcher, C., Collins, M., Connor, R., Cronin, A., Davis, P., Feltwell, T., Fraser, A., Gentles, S., Goble, A., Hamlin, N., Harris, D., Hidalgo, J., Hodgson, G., Holroyd, S., Hornsby, T., Howarth, S., Huckle, E. J., Hunt, S., Jagels, K., James, K., Jones, L., Jones, M., Leather, S., Mcdonald, S., Mclean,

J., Mooney, P., Moule, S., Mungall, K., Murphy, L., Niblett, D., Odell, C., Oliver, K., Neil, S. O., Pearson, D., Quail, M. A., Rabbinowitsch, E., Rutherford, K., Rutter, S., Saunders, D., Seeger, K., Sharp, S., Skelton, J., Simmonds, M., Squares, R., Squares, S., Stevens, K., Taylor, K., Taylor, R. G., Tivey, A., Walsh, S., Warren, T., Whitehead, S., Woodward, J., Volckaert, G., Aert, R., Robben, J., Grymonprez, B. and Weltjens, I. (2002) 'The genome sequence of Schizosaccharomyces pombe', 415(February).

Wozniak, E., Ołdziej, S. and Ciarkowski, J. (2000) 'Molecular modeling of the catalytic domain of serine/threonine phosphatase-1 with the Zn2+ and Mn2+ di-nuclear ion centers in the active site.', *Computers & chemistry*, 24(3–4), pp. 381–390.

Wu, X. and Tatchell, K. (2001) 'Mutations in yeast protein phosphatase type 1 that affect targeting subunit binding.', *Biochemistry*, 40(25), pp. 7410–7420.

Yanai, I., Derti, A. and DeLisi, C. (2001) 'Genes linked by fusion events are generally of the same functional category: A systematic analysis of 30 microbial genomes', *Proceedings of the National Academy of Sciences*, 98(14), pp. 7940–7945.

Ye, Y., Osterman, A., Overbeek, R. and Godzik, A. (2005) 'Automatic detection of subsystem/pathway variants in genome analysis', *Bioinformatics*, 21(SUPPL. 1).

Yenush, L., Merchan, S., Holmes, J. and Serrano, R. (2005) 'pH-Responsive, posttranslational regulation of the Trk1 potassium transporter by the type 1-related Ppz1 phosphatase.', *Molecular and cellular biology*, 25(19), pp. 8683–92.

Yenush, L., Mulet, J. M., Ariño, J. and Serrano, R. (2002) 'The Ppz protein phosphatases are key regulators of K+ and pH homeostasis: Implications for salt tolerance, cell wall integrity and cell cycle progression', *EMBO Journal*, 21(5), pp. 920–929.

Yonemoto, W., McGlone, M. L. and Taylor, S. S. (1993) 'N-myristylation of the catalytic subunit of cAMP-dependent protein kinase conveys structural stability', *Journal of Biological Chemistry*,

268(4), pp. 2348–2352.

Zhang, S., Guha, S. and Volkert, F. C. (1995) 'The Saccharomyces SHP1 gene, which encodes a regulator of phosphoprotein phosphatase 1 with differential effects on glycogen metabolism, meiotic differentiation, and mitotic cell cycle progression.', *Molecular and cellular biology*, 15(4), pp. 2037–50.

Zhao, S. and Lee, E. Y. (1997) 'A protein phosphatase-1-binding motif identified by the panning of a random peptide display library.', *The Journal of biological chemistry*, 272(45), pp. 28368–72.

ANNEXES

Table 1. Yeast strains used in this study.

Strain	Genotype	Source/reference
JA100	*MATa ura3*-52 *leu2*-3, 112 *his4 trp1*-1 *can*-1r	(De Nadal *et al.*, 1998)
JC010	JA100 *slt2*::*LEU2*	(Vissi1 *et al.*, 2001)
AGS9	JA100 *ppz1*::*LEU2*	(Canadell *et al.*, 2015)
JA104	JA100 *hal3*::*LEU2*	(De Nadal *et al.*, 1998)
CCV186	JA100 *slt2*::*LEU2 hal3*::KAN	(Petrenyi *et al.*, 2016)
IM021	JA100 *ppz1*::KanMX4 *hal3*::*LEU2*	(Muñoz *et al.*, 2004)
BY4741	*MATa his3Δ 1 leu2Δ met15Δ ura3Δ*	Euroscarf
hal3	BY4741 *hal3*::KanMX4	Euroscarf
JC002	JA100 *tetO:HAL3 sit4::TRP1*	(Simón *et al.*, 2001)
JA110	JA100 *sit4::TRP1*	(Clotet *et al.*, 1999)
MAR25	1788 *cab3::KanMX4/CAB3*	(Ruiz *et al.*, 2009)
AGS31	1788 *hal3::LEU2/HAL3 vhs3::nat1/VHS3 cab3::kanMX4/CAB3*	(Ruiz *et al.*, 2009)
AGS4	1788 *hal3::LEU2/HAL3 vhs3::KanMX4/VHS3*	(Ruiz, Muñoz, *et al.*, 2004)
BY4743-cdc21	BY4743 *cdc21::KanMX4/CDC21*	Euroscarf
Fw786	MAT a (mating) *ade8*	(Clark, Palzkill and Botstein, 1994)
Fw787	MAT α (mating) *ade8*	(Clark, Palzkill and Botstein, 1994)
975	h^+	Leupold (1970)
MC70	h^+ SPAC15E1.04::HA::kanMX6	This work

Table 2. Oligonucleotides used in this study.

Oligonucleotide	Sequence
PPZ1_BsrGI	TGTGCATATGTACATCGTTGAG
PPZ1_BspEI	TAATGCAATCTTCCGGAAAC
PPZ1_5'_seq_cat	TGCTATCGTAGCCGGAAAGA
PPZ1_3'_seq_cat	CTACATGTCTGATTTCATCC
PPZ1_5'_cat	CAAGTCGCGATATTTACCCG
PPZ1_3'_cat	CAATACACACGCGAAGGCAG
pGEX 5 Sequencing Primer	GGGCTGGCAAGCCACGTTTGGTG
pGEX 3 Sequencing Primer	CCGGGAGCTGCATGTGTCAGAGG
pDuet_ppz1Cter-5	TTGGCGCGCCTGATAATGCAATCTTCCGGAA
pDuet_ppz1_T1-3	GGG**AAGCTT**CAATACACACGCGAAG
pDuet_Hal3_5	GCA**AGATCT**GACTGCCGTCGCCTCTACT
pDuet_Hal3_3	CCGCTCGAGTTATTGATGCTTATCTATTAT
pDuet_PPZ1full-5´	CAGGATCCGATGGGTAATTCAAGTTCAAAATCT
A1_Hal3_5	ATACATATGACTGCCGTCGCCTCTACT
A1_Hal3_3	GCCGCGATCGCTTATTGATGCTTATCTATTAT
A1_Ppz1Cter_5 6His	ATACATATGGGCCATCACCATCATCACCACGATATAATGCAAT CTTCCGGAAAC
A1_Ppz1Cter_5 12His	ATACATATGGGCCATCACCATCATCACCACCACCATCACCACC ATCATGATATAATGCAATCTTCCGGAAAC
A1_Ppz1Cter_3	GATGGATCCTTACTGTTGAGATTCGTTATC
Ppz1_TEV_R	CTGTACTTCCAATCCATCGATATTGATGAAACTATCCAA
Ppz1_TEV_F	GTTCTCTCCTCCGGAAGATTGCATTATATCGTG

Hal3_G490Stop_F	GTTATGAAATTGGGTTGATACCCAAAAAATAAC
Hal3_G490Stop_R	GTTATTTTTTGGGTATCAACCCAATTTCATAAC
FwSpHAL3-pGEX-ok	GAAGATCTATGTCACAACCTTTGCATGC
FwSpHAL3-pWS93-ok	GAAGATCTGCATGTCACAACCTTTGCATGC
RvSpHAL3-N-ter-X-ok	CCGCTCGAGCAGGAGGTTCGGGTTTGGTAG
RvSpHAL-XhoI	CCGCTCGAGTTAGACACTCATTTTC
FwSpTS-pWS93	GAAGATCTGCTCCTCCGAATATAGAAATAC
SpPzh1-EcoRI	AATAGAATTCATGGGACAGGGGAGCAGTAAA
SpPzh1-XhoI	AATACTCGAGTTACACGCTTTGGGTAACCTG

Table 3. Characterization of selected clones. (+++) strong, (++) medium, (+) weak phenotype. The asterisks denote clones studied in detail in this work.

clone ID	Ident. clones	Nt position	Codon change	AA change	Phenotype
75 (*)	144	1331	TTC → TCC	Phe → Ser	+++
		1814	GTT → GCT	Val → Ala	
81		1066	AAA → GAA	Lys → Glu	+++
		1272	TAT→ TAC	*none*	
		1942	TTT → CTT	Phe → Leu	
		1951	TTA → CTA	*none*	
		2066	GAA → GGA	Glu → Gly	
		2088	(non coding)	*none*	
83		1672	GAT → AAT	Asp → Asn	++
		1137	AGA → AGC	Arg → Ser	
85	100, 120, 140	1070	TTC → TCC	Phe → Ser	+++
		1806	GCT → GCC	*none*	
		1814	GTT → GCT	Val → Ala	
		1845	GAT → GAC	*none*	
97 (*)	141	1889	GAA → GGA	Glu → Gly	+++
99 (*)		1282	TTA → GTA	Leu → Val	+
		2028	CAA → CAG	*none*	
100	85, 120, 140	1070	TTC → TCC	Phe → Ser	+++
		1806	GCT → GCC	*none*	
		1814	GTT → GCT	Val → Ala	
		1845	GAT → GAC	*none*	
113		1055	AAC → ACC	Asn → Thr	+++
		1137	AGA → AGG	*none*	
		1628	CAT → CGT	His → Arg	
		1944	TTT → TTG	Phe → Leu	
		1978	AAG → GAG	Lys → Glu	

clone ID	Ident. clones	Nt position	Codon change	AA change	Phenotype
115		1788	TTT → TTG	Phe → Leu	+
		2075	CAG → CCG	Gln → Pro	
119		1274	GGG → GAG	Gly → Glu	+
		1572	ATT → ATC	*none*	
		1990	AAG → GAG	Lys → Glu	
120 (*)	85, 100, 140	1070	TTC → TCC	Phe → Ser	+++
		1806	GCT → GCC	*none*	
		1814	GTT → GCT	Val → Ala	
		1845	GAT → GAC	*none*	
121 (*)	138, 153, 168	1306	TTC → CTC	Phe → Leu	+++
		1893	TTT → TTG	Phe → Leu	
124 (*)		1724	GAA → GGA	Glu → Gly	+++
125 (*)	126	1504	AAG → CAG	Lys → Gln	++
		1881	TAT → TAC	*none*	
126	125	1504	AAG → CAG	Lys → Gln	++
		1881	TAT → TAC	*none*	
129 (*)		1094	GAA → GGA	Glu → Gly	+++
		1721	AAC → AGC	Asn → Ser	
131		1478	GAT → AAT	Asp → Asn	++
		2021	AAT → AGT	Asn → Ser	

clone ID	Ident. clones	Nt position	Codon change	AA change	Phenotype
132 (*)		1538	ACA →GCA	Thr → Ala	+
133		1065	AAA → AAC	Lys → Asn	+
		1224	TTA → TTG	*none*	
		1810	ATG → CTG	Met → Leu	
136		1165	GAA → AAA	Glu → Lys	+
138	121, 153, 168	1306	TTC → CTC	Phe → Leu	++
		1893	TTT → TTG	Phe → Leu	
139		1296	ACC → ACT	*none*	+++
		1724	GAA →GGA	Glu → Gly	
140	85, 100, 120	1070	TTC → TCC	Phe → Ser	+++
		1806	GCT →GCC	*none*	
		1814	GTT → GCT	Val → Ala	
		1845	GAT →GAC	*none*	
141	97	1889	GAA →GGA	Glu → Gly	+++
143		1296	ACC → ACT	*none*	+++
		1724	GAA →GGA	Glu → Gly	
144	75	1814	GTT → GCT	Val → Ala	+++
		1331	TTC → TCC	Phe → Ser	
145		1924	GAA → CAA	Glu → Gln	
		1955	GAT →GGT	Asp → Gly	+
		2038	ATG → CTG	Met → Leu	

clone ID	Ident. clones	Nt position	Codon change	AA change	Phenotype
148		1143	AAA → AAT	*none*	++
		1144	AAT → GAT	*none*	
		1089	ATT → ATC	*none*	
		1443	GAA →GAG	*none*	
		1763	AAC →AGC	Asn → Ser	
		1830	TAT → TAC	*none*	
		2011	AAA → GAA	Lys → Glu	
149 (*)		1128	GCT →GCC	*none*	+
		2053	ACA → CCA	Thr → Pro	
151 (*)		1278	GAT →GAC	*none*	++
		1735	AGT →GGT	Ser → Gly	
		2111	3'-non coding	*none*	
153	121, 138, 168	1306	TTC → CTC	Phe → Leu	+++
		1893	TTT → TTG	Phe → Leu	
158		1659	TTT → TTA	Phe → Leu	+
		1731	GGT →GGC	*none*	
		1772	TTG → TCG	Leu → Ser	
167		1135	AGA →GGA	Arg → Gly	+
		1148	GTT → GCT	Val → Ala	
		1422	TTT → TTC	*none*	
		1516	ACA → TCA	Thr → Ser	
		1778	AAG →AGG	Lys → Arg	
		1944	TTT → TTC	*none*	
168	121, 138, 153	1306	TTC → CTC	Phe → leu	+
		1893	TTT → TTG	Phe → Leu	
179		2091	3'-non coding	*none*	+

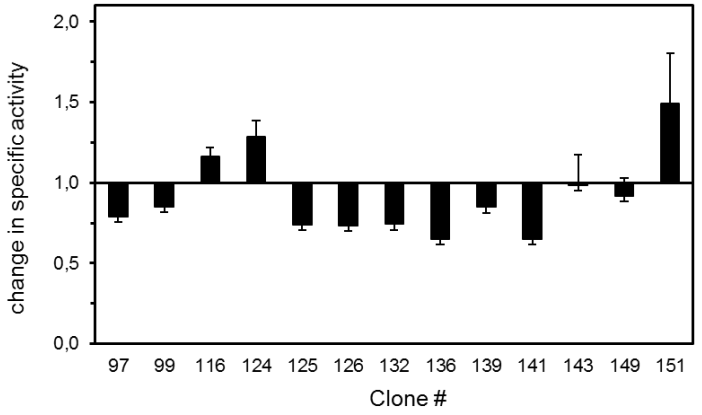

Figure 1. Relative specific activity of diverse Ppz1 alleles. The activity of diverse recombinant Ppz1 variants was determined and compared with that of native Ppz1, which was taken as the unit. The assays were carried out using from 0.5 to 1 μg of recombinant phosphatase preparations. Data is presented as the mean ± S.E. from 5 to 9 determinations from at least five different protein preparations.

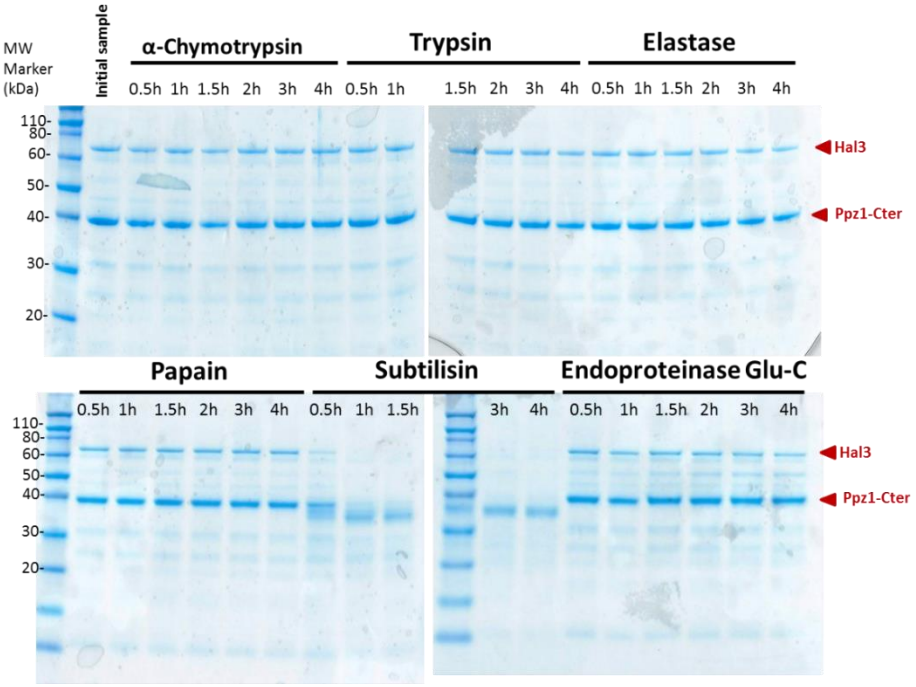

Figure 2. SDS-analysis of protease digestion test. 100 µg of purified 6His-Ppz1-Cter/Hal3 protein complex after Ni^{+} affinity chromatography was incubated with a variety of proteases (Proti-Ace kit, Hampton Research) at 37 °C for four hours. Samples were taken at different times of incubations.